In presenting the dissertation as a partial fulfillment of the requirements for an advanced degree from the Georgia Institute of Technology, I agree that the Library of the Institute shall make it available for inspection and circulation in accordance with its regulations governing materials of this type. I agree that permission to copy from, or to publish from, this dissertation may be granted by the professor under whose direction it was written, or, in his absence, by the Dean of the Graduate Division when such copying or publication is solely for scholarly purposes and does not involve potential financial gain. It is understood that any copying from, or publication of, this dissertation which involves potential financial gain will not be allowed without written permission.

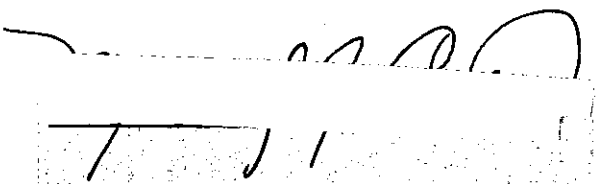

3/17/65
b

# A PRELIMINARY INVESTIGATION OF OXYGEN TRANSFER TO LIQUID DROPS PRODUCED IN A SPRAY IN A GASEOUS MEDIUM

A THESIS

Presented to

The Faculty of the Graduate Division

by

Michael Albert Collins

In Partial Fulfillment

of the Requirements for the Degree

Master of Science in Civil Engineering

Georgia Institute of Technology

December, 1967

# A PRELIMINARY INVESTIGATION OF OXYGEN TRANSFER TO LIQUID DROPS PRODUCED IN A SPRAY IN A GASEOUS MEDIUM

Approved:

Chairman

Date approved by Chairman:

June 26, 1968

TABLE OF CONTENTS

TABLE OF CONTENTS, continued

# ACKNOWLEDGEMENTS

The writer wishes to thank the members of his reading committee, Dr. William Gates and Dr. George Slaughter, for their assistance and cooperation. His appreciation is directed especially to his thesis advisor, Dr. Paul G. Mayer, for his continuing assistance, guidance and patience.

Appreciation is expressed to Bruce Olmstead and Wouter Gulden, Laboratory Assistants, for their help in some of the experimentation.

The writer is also sincerely appreciative of the continuing interest shown by Dr. Fredrick W. Schutz in the writer's efforts in many areas.

The writer acknowledges the assistance of the National Science Foundation, which provided a one year traineeship for his graduate studies at Georgia Institute of Technology.

The writer is also indebted to the School of Civil Engineering, Dr. William M. Sangster, Director, which provided financial assistance for the reproduction of this thesis.

Most importantly, the writer must express his gratitude to his wife without whose encouragement, patience, and untiring assistance this thesis could not have been completed.

# LIST OF TABLES

# LIST OF ILLUSTRATIONS

LIST OF ILLUSTRATIONS, continued

## SUMMARY

A possible method for obtaining water with relatively high concentrations of dissolved oxygen is that of spraying oxygen deficient water into a tank pressurized with nearly pure oxygen. The water spray would fall through the oxygen atmosphere, absorbing oxygen as it did so, and strike a receiving pool from which water could be withdrawn to enrich oxygen deficient waters. A theoretical and experimental investigation is conducted to investigate the feasibility of such a method.

A literature review is made of the basic interphase mass transfer theories with emphasis upon development from fundamentals of mass conservation. Two film, penetration, boundary layer, and turbulence theories are discussed.

Mass transfer in liquid droplets is discussed extensively. The effects of droplet circulation and surface tension are discussed. Theoretical equations for transfer efficiencies, i.e., fractional increases in oxygen absorbed, and film coefficients are reviewed. Stagnant, circulating, turbulent, and oscillating droplet models are discussed.

The experimental study employed a 75 gallon tank into which water was sprayed through 0.082 and 0.125 in. diameter whirl chamber type nozzles. Total operating pressures ranged from zero to approximately 110 psig with

partial pressures of oxygen from approximately 10 to 50 psi. Flow rates varied from one half to one and one half gpm while mean droplet diameters varied between $6 \times 10^{-3}$ and $12 \times 10^{-3}$ cm. Drop Reynolds numbers varied between 526 and 1695.

Oxygen concentrations were measured with galvanic cell oxygen analyzers. Calibration studies attempted to evaluate the analyzer sensitivities not only at normal atmospheric pressure but also at total pressures nearing 110 psig. Unexpected, sudden changes in analyzer sensitivities were observed in some instances when the analyzers were subjected to pressures as low as 20 psig. This behavior, which could not be explained, restricted the range of experimentation.

The measured dissolved oxygen concentrations were used to determine overall transfer characteristics of the system under various operating conditions. Transfer efficiencies were correlated with the dimensionless time parameter, $D_d t_{ct}/a^2$, where $D_d$ is the diffusivity of oxygen in water, $t_{ct}$ is the time of contact of the droplet with the oxygen atmosphere, and a is the mean droplet radius. Overall transfer efficiencies for the smaller diameter nozzle ranged from approximately 2.3 to one, decreasing with increasing values of the dimensionless time parameter, while efficiencies for the larger diameter nozzle increased with increasing values of the time parameter, reaching approxi-

mately one at a dimensionless time of 0.2. For the range of pressures developed, fifteen-fold increases in dissolved oxygen concentrations could be obtained, 120 mg/l concentrations being obtained in some instances.

An effective diffusivity ratio, i.e., basically the ratio of the observed diffusivity to that predicted by the stagnant droplet model, was determined from some of the experimental results after approximate corrections for end effect transfer. The effective diffusivity ratio was found to be 3.3. The asymptotic value of the time average transfer coefficient indicated that the transfer was similar to that predicted by both the circulating and turbulent droplet models.

# CHAPTER I

# INTRODUCTION

## Background

Pollution of natural watercourses is a serious and growing problem in the United States. Each year the quality of many surface waters decreases. The heavy pollutant load continually discharged into this country's rivers and lakes causes increasing deterioration of these surface waters (200)*.

Good quality surface water has dissolved oxygen concentrations near saturation levels (2). Sewage discharged into natural watercourses, because of the oxidation of the organic matter contained in it, causes decreases in dissolved oxygen concentrations, such decreases sometimes becoming so great that anaerobic conditions occur over areas of considerable extent. In a river with adequate aeration and sewage dilution, dissolved oxygen concentrations will eventually return to former levels if the river is not over taxed with additional pollutant loads. Natural purification is never fast, however, and undesirable conditions may exist over long reaches of a river (58). In many lakes, natural circulation and aeration rates may be so low that continual discharge of sewage into

*Numbers in parentheses refer to literature citations in bibliography.

them results in drastically low levels of dissolved oxygen concentrations, particularly in the lower strata of deeper lakes where nearly stagnant conditions may exist.

To overcome the problem of oxygen deficiency in natural watercourses, one obvious solution would be to reduce the pollutant load of sewage through increased sewage treatment prior to discharge. Another method, however, which might prove advantageous in many cases, would be the introduction of water with high concentrations of dissolved oxygen directly into bodies or reaches of oxygen deficient water. The water so introduced could possibly have a dissolved oxygen concentration level above the saturation level normally encountered in the surface strata of natural waters. Introduction of such water would appear to be highly beneficial and effective in returning oxygen concentration levels in a natural watercourse to desirable levels.

Introduction of water with high concentrations of dissolved oxygen directly into oxygen deficient waters seems to offer several advantages. By merely pumping the oxygen concentrated water from its point of production to its point of use, the water could be injected at the exact locale where conditions were the most severe. The problem of oxygen deficiency could be attacked at the point where it exists. Furthermore, the relatively slow and not always predictable natural transport of a river or lake would not have to be relied upon to carry high quality water to regions of low

quality. Transport of this water with high oxygen concentrations to its point of use would be quick, direct, and reliable.

Not only could the oxygen enriched water be introduced at the desirable locale, but it could also be injected directly into the particular water stratum which was most severely deficient in oxygen. Thus even in deep lakes with stagnant lower strata, oxygen levels could be increased. In the lower portions of the pool behind a dam, for instance, in which oxygen deficiency is sometimes severe, this highly concentrated water could be injected. Removal of water from the deeper pool elevations for passage through turbines would not then result in the movement of large quantities of oxygen deficient water downstream. Furthermore, by varying the oxygen concentration in the injected water, saturation levels could be conceivably approached in all levels of a lake, not merely surface strata.

High levels of concentration would also mean that only relatively small quantities of water need be introduced in some instances. A sufficiently high dissolved oxygen content of the injected water would mean that considerable dilution of the injected water could occur while still providing enough oxygen to substantially increase oxygen levels in the river or lake.

Thus this method of increasing dissolved oxygen levels in a natural body of water has advantages which make it worthy of consideration.

## Purpose and Objectives

Given that introduction of water with high levels of dissolved oxygen directly into a natural watercourse appears to offer promise, the question arises as to how these high concentrations could be obtained. One method, the method to be examined here, might be that of spraying water, with relatively low oxygen concentration levels, into a nearly pure oxygen atmosphere under pressure. Since the saturation concentration of a gas in a liquid is a function of the partial pressure of the gas, the use of pure oxygen under a high pressure would mean that the saturation concentration would be high. If the spray operation employed resulted in a high degree of transfer of oxygen to the individual droplets produced by the spray, highly oxygen enriched water could be obtained for injection into a natural watercourse.

A spray operation such as that envisioned has an advantage over that of an apparatus bubbling oxygen or air directly into oxygen deficient water since the absorption of oxygen into the water would take place prior to injection of the water into the oxygen deficient water. Oxygen introduced in previously oxygen enriched water would not be so readily subject to lose from the deficient water. Bubbles, on the other hand, would remain only a short time in any particular stratum in which they were formed.

A spray operation as proposed also might have valuable application in related areas. Rather than spray ordinary

water into the oxygen atmosphere, sewage might be used. Oxidation rates would be considerably enhanced resulting in better sewage treatment. Oxygen enriched water from such a spray operation would seem also to be particularly well suited for use in raising the quality of subsurface ground water. Rather than pumping ordinary water through a recharge well to raise ground water levels, oxygen enriched water might be used in those instances in which the existing ground water was of poor quality as well as being below desired levels.

Proposed here to provide the desired spray operation is a relatively simple apparatus, one which might be considered a crude prototype. Basically, it is proposed to pump water with relatively low dissolved oxygen concentrations into a pressurized tank, the actual injection of water into the tank being through a spray nozzle. Inside the tank would be an atmosphere of essentially pure oxygen. Droplets produced by the spray nozzle would fall through the high pressure oxygen atmosphere onto the surface of a pool of water in the bottom of the tank. Water drawn from this pool, now oxygen enriched, could then be pumped or gravity fed to its point of use.

The practicality and usefulness of this proposed process depends to a considered extent on the amount of oxygen which is absorbed by the water as it passes through the tank. This study will attempt to make a very preliminary evaluation of the proposed spray process.

In addition, essential background material will be presented and discussed in order that there shall exist a broad foundation of considerable depth for future study of a more detailed nature should the proposed process appear promising.

Oxygen absorption by water droplets in a spray is basically a mass transfer process between two phases. Absorption of gases by droplets is merely a special case of the more general field of interphase mass transfer. Thus an understanding of the principles and theories of interphase mass transport is both necessary and desirable before examination of transfer in droplets. Chapter II is devoted exclusively to a discussion of mass transfer between two phases.

In Chapter III attention is focused upon mass transfer in droplet systems. Much theoretical and experimental work has been devoted to the single, idealized, spherical droplet. The discussion reflects this emphasis. Mass transfer inside a droplet and outside a droplet are both discussed. While transfer outside of a droplet is not of direct concern in relation to the proposed process to be examined in this study, since the continuous phase surrounding the water droplets is very nearly pure oxygen, it is of value to examine it in an exploratory study, such as this one, in order that mass transfer inside a droplet be seen in proper relation to the continuous phase transfer in a droplet system. Furthermore,

modification of the proposed process might result in the need for consideration of transfer in the continuous phase.

The experimental work of the study is discussed in Chapter IV. The experimental investigation conducted was of an exploratory nature and thus was of limited extent. The apparatus used was essentially that described in preceding paragraphs. Examination of results from the operation of the experimental apparatus are examined and evaluated in light of providing a preliminary determination of the promise of the proposed process and determining whether or not further study and experimentation seem justified.

# CHAPTER II

# INTERPHASE MASS TRANSPORT THEORY

## Definition of Basic Terms

Absorption can be considered the transfer of mass from one phase to another phase (239) resulting in a spatial dispersion of the transferred mass, termed the solute, within the second phase, the solvent, with such a fine degree of intermingling that the solution becomes homogeneous and the solute becomes optically void (240). Dissolution is another term for absorption, although the term dissolution is generally used only when the solvent is a liquid (177). It can correctly be applied to systems with any type of solvent phase, however, since solutions can exist with a gas, liquid, or solid as either the solute or solvent.

A phase itself can be defined as that portion of a system which has different thermodynamic properties from the remainder of the system even though the entire system is in thermal equilibrium (116). The facts that the zones in near proximity of the transition from one phase to another assume such important roles in the absorption phenomenon and that the physical properties in these surface zones may be substantially different from those in the bulk of the phases (22, 102) has led Harkins (87) to separate the phases in a system into two subdivisions, termed regions. That

portion of a phase which excludes the surface zone constitutes one region, termed the bulk of the phase, while the transition zone or surface zone between the bulk of two phases constitutes the other region. More properly then, the thermodynamic properties of a phase need be constant only in the bulk of the phase and the dispersion of a solute in a solvent becomes homogeneous only necessarily in the bulk of the solvent phase. In the transition region, because of the very nature of the absorption process, the dispersion of the solute, if undergoing active absorption, will not be homogeneous.

The actual transition from one phase to another occurs through what is termed the interface. The interface and the region in which it lies is not completely understood at this time. However, the interface itself has generally been described (1, 24, 80, 86, 171, 179, 226) as being a rather abrupt transition between two phases, on the order of one or two molecules in thickness. Though it is subject to violent kinetic agitation and frequent interchange of molecules between itself and the bulk phase regions, it is assumed to be less than 100 angstroms thick. For the purposes of this study this interfacial description will be adequate.

## Fick's Laws of Diffusion

If one were to fill the lower portion of a tall container with iodine solution and then were to pour water on

top of the iodine solution with such great care so as to cause almost no disturbance of the iodine solution, it would be observed initially that the water immediately above the iodine solution would become darkly colored. With passing time, one would observe the upper portions of the water becoming colored while the lower portions would become gradually less intensely colored. After a sufficient length of time the container would hold colored water of equal intensity throughout. Obviously molecules of iodine are moving from regions of high concentration to regions of low concentration. This classic example (32) serves to illustrate that molecular phenomenon, termed diffusion, by which mass of one species moves through a collection of other species due solely to the difference in concentration of the species. The random motion of the diffusing molecules themselves produces the net transport of the molecules. Consideration of a thin element normal to the net movement of the diffusing substance demonstrates why this is so. If the molecular motion of the diffusing species be purely random, then the same certain percentage of the diffusing molecules at each face of the element will move across the face of the element. A higher concentration at one face will therefore necessarily result in a net movement of the diffusing substance through the element from regions of high to low concentration (33, 167, 170). To distinguish this phenomenon from other types of mass transport which are quite often

described as a particular type of diffusion, such as thermal or pressure diffusion, it is often called molecular (222) or ordinary diffusion (6). As it will be used in this study, the term diffusion will refer only to molecular diffusion unless it is stated otherwise.

Fick's First Law of Diffusion

First (34) to state mathematically the laws which govern mass transport in solutions by diffusion was Adolf Fick (59, 60). Fick, realizing the essence of the diffusion mechanism was the same as that which occurred in the conduction of heat and electricity, stated in 1855 that the time rate of mass transport of component A through component B of a solution per unit area of solution, that is, the mass flux of A, in the x direction due to diffusion is directly proportional to the negative of the concentration gradient of the diffusing component A. Thus

$$J_{Ax} = -D\frac{\partial \rho_A}{\partial x} \tag{2.1}$$

where

$$J_{Ax} = \frac{1}{\text{Area}} \cdot \frac{dM_A}{dt} \tag{2.2}$$

and

$$\rho_A = M_A/(\mathcal{V}_A+\mathcal{V}_B) = M_A/\mathcal{V} \qquad (2.3)$$

and where $J_{Ax}$ = mass diffusive flux of A in the x direction, $M_A$ = mass of A, Area = area normal to the x direction, t = time, $\rho_A$ = the mass concentration of A, $\mathcal{V}_A$ = volume of A in solution, $\mathcal{V}_B$ = volume of B in solution, $\mathcal{V}$ = total volume of solution, D = the coefficient of molecular diffusion, or diffusivity. More generally, component B may be considered to be the collection of all species in the solution other than A, in which case the definition of the mass concentration of A, eq. (2.3), becomes

$$\rho_A = M_A/\left(\sum_{\ell=1}^{n} \mathcal{V}_\ell\right) = M_A/\mathcal{V} \qquad (2.4)$$

where $\mathcal{V}_\ell$ is the volume of component $\ell$ in an n component solution.

From Fick's First Law, as eq. (2.1) or its many similar forms have come to be known, it is seen the mass transport occurs in the direction of decreasing concentration. Thus Fick's First Law can be viewed as a description of a mechanism by which a system attempts to achieve a particular type of equilibrium. A useful concept that has been employed extensively is that of considering the negative of the concentration gradient as a driving potential.

Considering gas A diffusing through gas B in the x direction, $\rho_A$, in eq. (2.1), represents the mass concentration of gas A. If it is assumed that gas A is a perfect gas then

$$\rho_A = (m_A p_A)/(RT) \tag{2.5}$$

where $m_A$ = molecular weight of A, $p_A$ = partial pressure of A, R = universal gas constant, T = absolute temperature. Therefore, as shown by Colburn and Hougen (30) and Eckert (47),

$$J_{Ax} = -(Dm_A/RT)\partial p_A/\partial x \tag{2.6}$$

where the mass flux is now a function of partial pressure rather than concentration.

The more general form of Fick's First Law, allowing for possible nonisotropic diffusive properties of the substance through which the diffusion is occurring, is (36)

$$J_{Ax} = -(D_{xx}\frac{\partial \rho_A}{\partial x} + D_{xy}\frac{\partial \rho_A}{\partial y} + D_{xz}\frac{\partial \rho_A}{\partial z}) \tag{2.7-a}$$

$$J_{Ay} = -(D_{yx}\frac{\partial \rho_A}{\partial x} + D_{yy}\frac{\partial \rho_A}{\partial y} + D_{yz}\frac{\partial \rho_A}{\partial z}) \qquad (2.7\text{-b})$$

$$J_{Az} = -(D_{zx}\frac{\partial \rho_A}{\partial x} + D_{zy}\frac{\partial \rho_A}{\partial y} + D_{zz}\frac{\partial \rho_A}{\partial z}) \qquad (2.7\text{-c})$$

where $J_{Ay}$ = mass diffusive flux of A in the y direction, $J_{Az}$ = mass diffusive flux of A in the z direction, $D_{xy}$ = the diffusivity in the x direction for a concentration gradient existing in the y direction, and similarily for the other diffusivity components, and the other symbols are as previously defined. In liquids and gases diffusive properties are generally considered to be isotropic, in which case eqs. (2.7) reduce to the more general form of Fick's First Law, viz.,

$$\vec{J}_A = -D(\frac{\partial \rho_A}{\partial x}\vec{i} + \frac{\partial \rho_A}{\partial y}\vec{j} + \frac{\partial \rho_A}{\partial z}\vec{k}) \qquad (2.8)$$

where $\vec{J}_A$ = mass diffusive flux vector of A, $\vec{i}$, $\vec{j}$, $\vec{k}$ are unit vectors in the x, y, and z directions, respectively.

Fick's Second Law of Diffusion

Consider a differential control volume, $d\forall$, in rectilinear co-ordinates x, y, and z, with one corner at the point (o, o, o) and which contains an isothermal solution of A dissolved in B where B represents the collection of all the species in the solution except A. Assume no mass transport of A to exist other than that due solely to diffusion. The concentration of A at point (o, o, o) is $\rho_A$ and varies continu-

ously over $d\forall$. By the conservation of mass, therefore,

$$\begin{array}{c}\text{Rate of mass}\\ \text{accumulation}\\ \text{of A in } d\forall\end{array} = \begin{array}{c}\text{Rate of mass}\\ \text{transport of}\\ \text{A into } d\forall\end{array} - \begin{array}{c}\text{Rate of mass}\\ \text{transport of A}\\ \text{out of } d\forall\end{array} \qquad (2.9)$$

The rate of mass transport of A through a face of the control volume is the mass flux of A times the area of the face. Thus in the x direction the

$$\begin{array}{c}\text{Rate of mass}\\ \text{transport of A}\\ \text{into } d\forall\end{array} = J_{Ax}\, dydz \qquad (2.10)$$

and the

$$\begin{array}{c}\text{Rate of mass}\\ \text{transport of A}\\ \text{out of } d\forall\end{array} = \left(J_{Ax}+\frac{\partial J_{Ax}}{\partial x}\, dx\right)dydz \qquad (2.11)$$

The net rate of mass transport in the x direction into the control volume is therefore

$$J_{Ax} \cdot dydz-\left(J_{Ax}+\frac{\partial J_{Ax}}{\partial x}\, dx\right)dydz$$

which reduces to

$$-(\partial J_{Ax}/\partial x)dxdydz \qquad (2.12\text{-a})$$

Similarly for the y and z directions, the net mass transport rates into $d\Psi$ are

$$-(\partial J_{Ay}/\partial y)dydxdz \qquad (2.12\text{-b})$$

and

$$-(\partial J_{Az}/\partial z)dzdxdy \qquad (2.12\text{-c})$$

respectively. Therefore,

$$\text{R.H.S. of eq.(2.9)} = -\left(\frac{\partial J_{Ax}}{\partial x} + \frac{\partial J_{Ay}}{\partial y} + \frac{\partial J_{Az}}{\partial z}\right)dxdydz \qquad (2.13)$$

But

$$\text{L.H.S. of eq.(2.9)} = \frac{\partial \rho_A}{\partial t} \cdot d\Psi \qquad (2.14)$$

Since

$$d\Psi = dxdydz \qquad (2.15)$$

then

$$\partial \rho_A/\partial t = -(\partial J_{Ax}/\partial x + \partial J_{Ay}/\partial y + \partial J_{Az}/\partial z) \qquad (2.16)$$

Substituting eq. (2.7) in eq. (2.16)

$$\frac{\partial \rho_A}{\partial t} = \frac{\partial}{\partial x}\left(D_{xx}\frac{\partial \rho_A}{\partial x} + D_{xy}\frac{\partial \rho_A}{\partial y} + D_{xz}\frac{\partial \rho_A}{\partial z}\right)$$

$$+ \frac{\partial}{\partial y}\left(D_{yx}\frac{\partial \rho_A}{\partial x} + D_{yy}\frac{\partial \rho_A}{\partial y} + D_{yz}\frac{\partial \rho_A}{\partial z}\right)$$

$$+ \frac{\partial}{\partial z}\left(D_{zx}\frac{\partial \rho_A}{\partial x} + D_{zy}\frac{\partial \rho_A}{\partial y} + D_{zz}\frac{\partial \rho_A}{\partial z}\right) \qquad (2.17)$$

This is the most general form of what has come to be known as Fick's Second Law. If the diffusive properties of the solution are isotropic then eq. (2.17) becomes (36)

$$\frac{\partial \rho_A}{\partial t} = \frac{\partial}{\partial x}\left(D\frac{\partial \rho_A}{\partial x}\right) + \frac{\partial}{\partial y}\left(D\frac{\partial \rho_A}{\partial y}\right) + \frac{\partial}{\partial z}\left(D\frac{\partial \rho_A}{\partial z}\right) \qquad (2.18)$$

If the diffusivity is homogeneous the form of Fick's Second Law generally used with gases and liquids is obtained from eq. (2.18), viz.,

$$\frac{\partial \rho_A}{\partial t} = D\left(\frac{\partial^2 \rho_A}{\partial x^2} + \frac{\partial^2 \rho_B}{\partial y^2} + \frac{\partial^2 \rho_C}{\partial z^2}\right) \qquad (2.19)$$

For variation of concentration in the x direction only, eq. (2.19) reduces to the form

$$\frac{\partial \rho_A}{\partial t} = D\frac{\partial^2 \rho_A}{\partial x^2} \qquad (2.20)$$

which Fick proposed in 1855 (157, 158).

Considering the diffusion of gases, Maxwell also derived a form analogous to eq. (2.20) from kinetic theory (168). Using formulations which he originally developed in 1860 (166), Maxwell presented his theory for diffusion in gases (168), as opposed to Fick's theory which arose from the consideration of diffusion in liquids. The pressure gradient required to overcome the resistance to diffusion in a binary gas solution, Maxwell hypothesized, was directly proportional to the number of molecules of each gas and the difference in the mean velocities of each gas. Thus for transport by diffusion in which gas A was diffusing through gas B in the x direction, Maxwell proposed (202)

$$\frac{\partial p_A}{\partial x} = -a' \frac{\rho_A \rho_B}{m_A m_B}(u_{xA} - u_{xB}) \qquad (2.21)$$

where $p_A$ = partial pressure of A, $a'$ = proportionality constant, $m_A$, $m_B$ = molecular weight of A and B, respectively, $u_{xA}$, $u_{xB}$ = velocity of A and B, respectively.

For diffusive transport only, the diffusive flux of A is equal to the negative of the diffusive flux of B. Using this fact in conjunction with eq. (2.9), Sherwood showed (203) that

$$\frac{\partial p_A}{\partial t} = \frac{R^2 T^2}{a' (p_A + p_B)} \frac{\partial^2 \rho_A}{\partial x^2} \qquad (2.22)$$

where $p_B$ is the partial pressure of B and the other notation is as above. If the diffusivity of the solution is defined as

$$D = \frac{R^2 T^2}{a' (p_A + p_B)} \qquad (2.23)$$

then eq. (2.22) reduces directly to eq. (2.20), Fick's Second Law.

A simple approach by which to express eq. (2.20) in terms of partial pressures can be made by using the substitution of eq. (2.5), in which case eq. (2.20) becomes

$$\frac{\partial p_A}{\partial t} = D \frac{\partial^2 \rho_A}{\partial x^2} \qquad (2.24)$$

which is of a similar nature to that of eq. (2.6).

It should be noted, as has been pointed out by Treybal (223), the true diffusive driving force is in all probability the chemical potential or activity rather than the concentration gradient. For many applications, however, the concentration gradient sufficiently approximates the true driving potential. Expressions defining diffusivity in terms of concentration are commonly the form found in applied engineering literature. Furthermore, these forms have occupied a promi-

nent position in the development of mass transfer theory. The emphasis in this study will, likewise, be that of expressing the diffusive driving potential as a concentration gradient.

Equations of Continuity For an Isothermal System

Consideration has thus far been limited to mass transport by diffusion. Mass transport occurs, however, due not only to diffusion but also due to convection. Consider a rectangular differential control volume containing an isothermal solution of A dissolved in n-1 other species. The solution is no longer considered to be stationary as it was, implicitly, in the derivation of Fick's Second Law, eq. (2.17).

The mass concentration of a particular species in a solution is as previously defined in eq. (2.4). Since the mass density of the solution is the total mass of solution per unit volume of solution, it can be seen that

$$\rho = \sum_{\ell=1}^{n} \rho_\ell \tag{2.25}$$

since

$$\sum_{\ell=1}^{n} \rho_\ell = \sum_{\ell=1}^{n} (M_\ell / \mathcal{V}) = M/\mathcal{V} \tag{2.26}$$

where $\rho$ = mass density of the solution, $M_\ell$ = mass of species $\ell$, M = total mass of solution, and the other symbols are as previously defined.

General Equations of Continuity

Defining the mass flux of A into a rectangular control volume, due to any modes of transport, in the x, y, and z directions as $N_{Ax}$, $N_{Ay}$, and $N_{Az}$, respectively, the net rate of mass transport of A into the control volume in the x direction is

$$N_{Ax}dydz - (N_{Ax} + \frac{\partial N_{Ax}}{\partial x} dx)dydz$$

which reduces to

$$-(\frac{\partial}{\partial x}N_{Ax})dxdydz \qquad (2.27\text{-a})$$

Similarly for the y and z directions the net rate of mass transport of A into the control volume is

$$-(\frac{\partial N_{Ay}}{\partial y})dxdydz \qquad (2.27\text{-b})$$

and

$$-(\frac{\partial N_{Az}}{\partial z})dxdydz \qquad (2.27\text{-c})$$

respectively. The net rate of transport of A into the control volume is the sum of eqs. (2.27). In vector notation this becomes

$$-\vec{i}\frac{\partial}{\partial x}(\vec{N}_A)-\vec{j}\frac{\partial}{\partial y}(\vec{N}_A)-\vec{k}\frac{\partial}{\partial z}(\vec{N}_A) \qquad (2.28)$$

where

$$\vec{N}_A = N_{Ax}\vec{i} + N_{Ay}\vec{j} + N_{Az}\vec{k} \qquad (2.29)$$

Since the rate of mass accumulation of A in the control volume is $(\partial\rho_A/\partial t)dxdydz$, then by eq. (2.9), after division by dxdydz,

$$\frac{\partial\rho_A}{\partial t} + \frac{\partial N_{Ax}}{\partial x} + \frac{\partial N_{Ay}}{\partial y} + \frac{\partial N_{Az}}{\partial z} = 0 \qquad (2.30)$$

which is the equation of continuity for component A. Addition of the equations of continuity for each component in the solution, similar to eq. (2.30), results in the equation of continuity

$$\frac{\partial\rho}{\partial t}+\vec{i}\frac{\partial}{\partial x}\left(\sum_{l=1}^{n}\vec{N}_l\right)+\vec{j}\frac{\partial}{\partial y}\left(\sum_{l=1}^{n}\vec{N}_l\right)+\vec{k}\frac{\partial}{\partial z}\left(\sum_{l=1}^{n}\vec{N}_l\right) = 0 \qquad (2.31)$$

where $\vec{N}_\ell$ is the vector mass flux of component $\ell$. A mass average velocity of the solution is defined as

$$\vec{V} = \left( \sum_{\ell=1}^{n} \rho_\ell V_\ell \right) \Big/ \left( \sum_{\ell=1}^{n} \rho_\ell \right) \tag{2.32}$$

where $\vec{V}$ = mass average vector velocity of the solution with components $V_x$, $V_y$, and $V_z$ in the x, y, and z directions, respectively, $\vec{V}_\ell$ = vector velocity of component $\ell$, and the other symbols are as defined earlier. It is to be noted that the velocity of each component is the total velocity resulting from mass transport by both diffusion and convection. The mass flux of A is therefore

$$\vec{N}_A = \rho_A \vec{V}_A \tag{2.33}$$

The mass flux of the solution, due to convection and diffusion is the sum of the fluxes of the components of the solution, viz.,

$$\sum_{\ell=1}^{n} \vec{N}_\ell = \sum_{\ell=1}^{n} \rho_\ell \vec{V}_\ell \tag{2.34}$$

which, from eqs. (2.25) and (2.32) reduces directly to

$$\sum_{\ell=1}^{n} \vec{N}_\ell = \rho \vec{V} \qquad (2.35)$$

The equation of continuity for the solution, eq. (2.31), then becomes

$$\frac{\partial \rho}{\partial t} + \frac{\partial}{\partial x}(\rho V_x) + \frac{\partial}{\partial y}(\rho V_y) + \frac{\partial}{\partial z}(\rho V_z) = 0 \qquad (2.36)$$

which is the same as that for a fluid of only one component.

Considering diffusion and convection as the only two pertinent forms of mass transport mechanisms, the equations of continuity for the components of the solution in terms of the convective and diffusive fluxes can be formulated, after recognition of the following important points. Convective transport of any component of the solution results in a bodily movement of the solution. Therefore the convective velocity of each component is equal to the average velocity of the solution. On the other hand, the diffusion of any component occurs with reference to the motion of the total solution, that is, the diffusive velocity of a species is the difference between the total velocity of the species and the average velocity of the solution (169). In a stagnant solution, the diffusive velocity reduces to the total velocity, as previously considered in the discussion of Fick's Laws of Diffusion. The total mass flux of A is thus

$$\vec{N}_A = \rho_A \vec{V} + \vec{J}_A \tag{2.37}$$

where the first and second terms on the R.H.S. are the mass fluxes of component A due to convection and diffusion, respectively.

Equations of Continuity with Constant Diffusivity and Density

Assuming the diffusive properties of the solution are isotropic, eq. (2.37) becomes, from eq. (2.8),

$$\vec{N}_A = \rho_A \vec{V} - D[\vec{i}\frac{\partial \rho_A}{\partial x} + \vec{j}\frac{\partial \rho_A}{\partial y} + \vec{k}\frac{\partial \rho_A}{\partial z}] \tag{2.38}$$

The equation of continuity for A, eq. (2.30), thus becomes

$$\frac{\partial \rho_A}{\partial t}+\frac{\partial}{\partial x}(\rho_A V_x)+\frac{\partial}{\partial y}(\rho_A V_y)+\frac{\partial}{\partial z}(\rho_A V_z)$$

$$- \frac{\partial}{\partial x}(D\frac{\partial \rho_A}{\partial x})- \frac{\partial}{\partial y}(D\frac{\partial \rho_A}{\partial y})- \frac{\partial}{\partial z}(D\frac{\partial \rho_A}{\partial z}) = 0 \tag{2.39}$$

If the diffusivity is homogeneous, eq. (2.39) becomes

$$\frac{\partial \rho_A}{\partial t}+\frac{\partial}{\partial x}(\rho_A V_x)+\frac{\partial}{\partial y}(\rho_A V_y)+\frac{\partial}{\partial z}(\rho_A V_z) =$$

$$D(\frac{\partial^2 \rho_A}{\partial x^2}+\frac{\partial^2 \rho_A}{\partial y^2}+\frac{\partial^2 \rho_A}{\partial z^2}) \tag{2.40}$$

If the density of the solution, $\rho$, is constant, then eq. (2.36) becomes

$$\frac{\partial V_x}{\partial x} + \frac{\partial V_y}{\partial y} + \frac{\partial V_z}{\partial z} = 0 \qquad (2.41)$$

In this case, using eq. (2.41), eq. (2.40) becomes

$$\frac{\partial \rho_A}{\partial t} + V_x \frac{\partial \rho_A}{\partial x} + V_y \frac{\partial \rho_A}{\partial y} + V_z \frac{\partial \rho_A}{\partial z} =$$

$$D\left(\frac{\partial^2 \rho_A}{\partial x^2} + \frac{\partial^2 \rho_A}{\partial y^2} + \frac{\partial^2 \rho_A}{\partial z^2}\right) \qquad (2.42)$$

The density of the solution is essentially constant for dilute solutions. Therefore for dilute solutions with constant diffusivities the approximate equation of continuity is eq. (2.42).

For the special case in which the convective velocity is zero, eq. (2.43) becomes

$$\partial \rho_A / \partial t = D\left(\frac{\partial^2 \rho_A}{\partial x^2} + \frac{\partial^2 \rho_A}{\partial y^2} + \frac{\partial^2 \rho_A}{\partial z^2}\right) \qquad (2.43)$$

which is seen to be identical to eq. (2.19).

## Interphase Mass Transfer Theories

One of the first to consider the phenomenon of interphase mass transport was Hurter (112, 113, 114). In 1885 Hurter grouped absorption equipment under three basic headings which have continued to adequately categorize much industrial absorption equipment (103). Significantly, he also noted the importance of the contact time between phases and the velocities of the phases in the absorption process.

### Diffusion Layer Theory

Examining the dissolution of solids in liquids Noyes and Whitney in 1897 (38) demonstrated that the rate of dissolution could be expressed as being proportional to the difference between the saturation concentration, which was assumed to exist at the interface between the solid and liquid phases, and the concentration of the solid in solution. Thus for a solid substance A dissolving in a liquid B, the rate of dissolution was hypothesized to be

$$(\partial \rho_A / \partial t) = k_L(\rho_{AB_i} - \rho_{AB_b}) \qquad (2.44)$$

where $\rho_{AB_i}$ = mass concentration of A at the interface in B, $\rho_{AB_b}$ = mass concentration of A in the liquid bulk of B, $k_L$ = mass transfer coefficient, and the other notation is as defined earlier.

Brunner extended Noyes and Whitney's work considerably in 1904 (18, 38) when he measured dissolution rates and deter-

mined the constant $k_L$ in Noyes and Whitney's equation, eq. (2.44), for various solutions.

Extending Noyes and Whitney's concepts even further, Nernst, one of the founders of modern physical chemistry (56), postulated in 1904 (165, 173) that the dissolution mechanism was controlled by diffusion through a thin stationary film or layer of liquid at the interfacial boundary between the liquid and the dissolving substance. The interface itself was assumed, as Whitney and Noyes had assumed, to be saturated. Nernst viewed the liquid film as offering a resistance to the diffusion of the solute. Since diffusion through the liquid layer was postulated to be the controlling dissolution mechanism, the mass flux was approximately equal to the diffusive flux. Nernst expressed the mass flux of a solute A dissolving in a liquid B as

$$J_A = C_D \frac{D}{f_D} \qquad (2.45)$$

where $f_D$ = diffusion layer thickness, $C_D$ = constant of proportionality, and the other symbols are as defined previously. Letting the numeric value of $C_D$ be unity, $C_D$ was used merely to satisfy dimensional homogeneity. The reason that eq. (2.45) may be considered only approximately correct will become apparent in the discussions to follow. The similarity of eq. (2.45) to Fick's First Law, eq. (2.1), is apparent when it is realized that the film thickness $f_D$ is the reciprocal of an

average driving force, namely, the concentration gradient. As such the diffusion film thickness can be viewed as a resistance to the transport of the dissolving substance.

Importantly, Nernst suggested that his theory applied not only to solids dissolving in liquids but also gases and liquids dissolving in liquids (38).

The salient points of Nernst's theory were (1) that dissolution of a substance in a liquid was governed by diffusion through a stationary liquid film at the phase interface, (2) that the resistance to mass transfer could be concentrated in the liquid interfacial film, and (3) the recognition of the similarity in absorption mechanisms in liquid-gas, liquid-liquid, and liquid-solid systems. These concepts became the basis for most absorption studies in the following years.

Two Film Theory

Investigators following Nernst used the basic concepts of Fick and Nernst (46), although in many different forms. The steady state absorption of a gas was considered to be dependent on some type of driving potential, the particular potential varying with the particular investigator.

Some, such as Lewis (151), expressed this driving potential as the difference in partial pressures of the solute in the gaseous phase and the liquid phase, the partial pressure of the solute in the liquid phase being determined from the solute concentration in the liquid phase by use of the solubility relationship. Lewis considered that a stationary

or nearly stationary film in the less viscous phase, the gas phase in a liquid-gas system, formed on the surface of the other phase and the diffusion through this film controlled the absorption process. The partial pressure at the interface itself was considered to be essentially at the equilibrium condition.

Other investigators, such as Donnan and Mason (41) and VanArsdel (237, 238), used a driving potential based on the difference in concentration of solute between the gas phase, converted from a partial pressure by the solubility relationship, and the liquid phase. Here diffusion through a stagnant or nearly stagnant liquid layer or film was the controlling mechanism. Again, at the interface conditions were assumed to be in equilibrium.

Thus two basic forms arose describing the steady state absorption process in gas-liquid systems, each assuming the mass transport from one phase to another was controlled by diffusion in a resisting film. For a substance A being absorbed from a species C by a species B, these two forms could be represented as

$$J_A = k_G(p_{AC_b} - p_{AC_i}) \tag{2.46}$$

and

$$J_A = k_L(\rho_{AB_i} - \rho_{AB_b}) \tag{2.47}$$

where $p_{AC_b}$ = partial pressure of A in the bulk of C, $p_{AC_i}$ = partial pressure of A at the interface in C, $k_G$, $k_L$ = mass transfer coefficients for the gas and liquid phases, respectively, and the other notation is as previously defined. The partial pressures and concentrations at the outer boundaries of the gas and liquid films, respectively, were assumed to be essentially equal to those in the bulk of the phases because of the convective and turbulent mixing occuring there. With the assumption of convective and turbulent mixing in the bulk of the phases the thicknesses of the supposedly stagnant or nearly stationary films were not easily determined directly.

A significant advancement in the understanding of mass transfer between phases was made by Whitman and his colleagues as they attempted to explain the absorption phenomenon in gas-liquid systems. In 1922, using a heat transfer analogy, Whitman in conjunction with Keats (243) stated that the total resistance to the absorption of a gas by a liquid could be considered as the summation of two resistances in series, one resistance being that of a gas film at the interface, the other being a liquid film at the interface. Further amplification of this two film concept came in 1923 when Whitman presented the basics of his two film theory as well as some preliminary experimental verification of his theory (241). Whitman and Lewis provided a more complete elaboration of the two film theory in 1924 (152).

Whitman realized that, in general, the resistance to the dissolution of a gas between a liquid phase and a gas phase was not dependent merely on the gas phase or the liquid phase, as earlier investigators, including Whitman himself, had assumed. Both phases contributed to the total resistance experienced by a solute as it dissolved. As idealized by earlier investigators, adjoining each side of the interface was a thin, practically stagnant, film through which the solute moved only by diffusion. The principle phase resistance, a diffusive resistance, was assumed to be concentrated within these films. At the outer boundary of the films the concentrations and partial pressures were those within the bulk of the phases while at the interface itself equilibrium conditions were assumed to exist, although it was noted by Lewis and Whitman (152) that an accumulation of an impurity at the interface could create an interfacial resistance. Furthermore, since the mass transfer being investigated was assumed to be time independent, it was assumed no accumulation of solute of appreciable magnitude at the interface occurred.

The absorption model idealized by Whitman for a species A, say a gas, undergoing dissolution to a species B from species C, is seen in Fig. 1. A more realistic representation (227), from which Whitman formulated his idealized model, is also seen in Fig. 1. Assuming the absorption of A is occurring in an isothermal system in the x direction as shown in Fig. 1, the mass flux through both films, since the dissolution of A

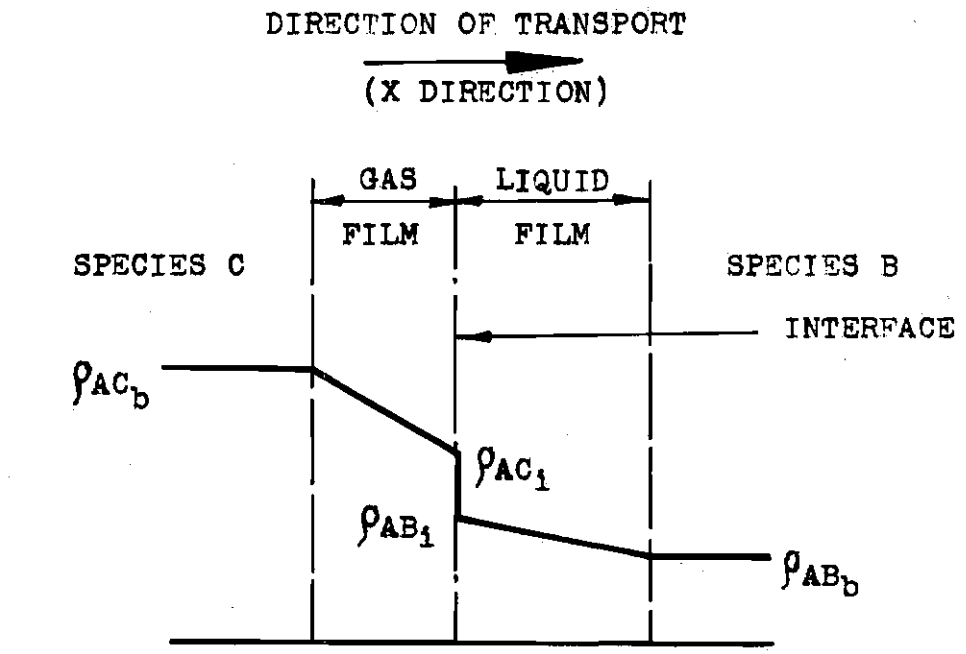


IDEALIZED INTERFACIAL REGION

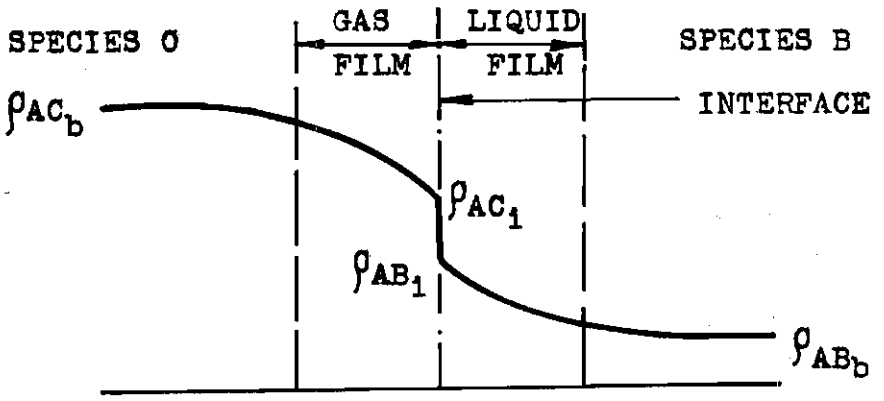


REALISTIC INTERFACIAL REGION

Figure 1. Interfacial Region with Concentration Gradients

is assumed to be steady, is $N_{Ax}$. Therefore in each film, from eq. (2.37)

$$\vec{N}_A = N_{Ax} = \rho_A V_x + J_{Ax} \tag{2.48}$$

where the notation is as defined in earlier sections. Letting $\rho_{AB}$ equal the mass concentration of A in B and $\rho_{AC}$ equal the mass concentration of A in C and defining $\rho_{SB}$ and $\rho_{SC}$ as the mass density of the liquid and gas solutions, respectively, eq. (2.48) is equivalent to, from eq. (2.32),

$$N_{Ax} = (\rho_{AB}/\rho_{SB})(N_{Ax}+N_{Bx}) + J_{Ax} \tag{2.49}$$

in the liquid film and similarly for the gas film. Eq. (2.49) is similar to that given by Bird, Stewart, and Lightfoot (10).

For the case in which $N_{Bx}$ is zero, as would occur if B were insoluble in C, eq. (2.49) reduces directly to

$$N_{Ax} = (J_{Ax})\left(1 - \frac{\rho_{AB}}{\rho_{SB}}\right) \tag{2.50}$$

In general, however, from eq. (2.49)

$$N_{Ax}-(\rho_{AB}/\rho_{SB})(N_{Ax}+N_{Bx}) = J_{Ax} \tag{2.51}$$

Whitman implicitly assumed in his analysis that

$$N_{Ax} = J_{Ax} \tag{2.52}$$

Thus the second term of the L.H.S. of eq. (2.51) must be zero. This condition is satisfied exactly if $N_{Ax} = -N_{Bx}$. On the other hand, if the solute is dilute, $\rho_{AB}/\rho_{SB}$ is approximately zero and eq. (2.52) becomes approximately correct. The present development will be restricted to the situation in which eq. (2.52) is at least approximately true in order that the transfer functions presented by Whitman may be developed. This is desirable since, as has been noted (11), most investigations have proceeded on the basis that the second term of the L.H.S. of eq. (2.51) is essentially zero. Further discussion of this point will be found in the following section.

Assuming that the diffusivity in each phase is constant and that A approximates a perfect gas, from eqs. (2.6) and (2.52),

$$N_{Ax} = -(D_{AC}\, m_A/RT)\, \partial p_{AC}/\partial x \tag{2.53}$$

while for the liquid film, from eqs. (2.1) and (2.52),

$$N_{Ax} = -D_{AB}\, \partial \rho_{AB}/\partial x \tag{2.54}$$

where $D_{AC}$ = diffusivity of A in C, $D_{AB}$ = diffusivity of A in B, $p_{AC}$ = partial pressure of A in C, and the other notation is as defined previously. The assumption that A approximates a perfect gas is not really critical. In the situation in which A does not approximate a perfect gas the term $m_A/RT$ in eq. (2.53) would be replaced by a more complicated function. For the model assumed by Whitman the concentration gradients and partial pressure gradients are linear. Therefore eqs. (2.53) and (2.54) become, for the case of the transfer of A from C to B,

$$N_{Ax} = - \frac{D_{AC} m_A}{RT} \frac{(p_{AC_i} - p_{AC_b})}{f_G} \tag{2.55}$$

and

$$N_{Ax} = -D_{AB} \frac{(\rho_{AB_b} - \rho_{AB_i})}{f_L} \tag{2.56}$$

where $f_G$ and $f_L$ are the thicknesses of the idealized gas and liquid films, respectively, subscripts i and b denote concentrations at the interface and in the bulk of the phase, respectively, and the other notation is as previously defined. The notation is also shown in Fig. 1. Letting

$$k_G = \frac{D m_A}{RT f_G} \tag{2.57}$$

and

$$k_L = D/f_L \tag{2.58}$$

where $k_G$ and $k_L$ are now gas and liquid film coefficients, or mass transfer coefficients for the gas and liquid phases, respectively, then eqs. (2.57) and (2.58) become

$$N_{Ax} = k_G(p_{AC_b} - p_{AC_i}) \tag{2.59}$$

and

$$N_{Ax} = k_L(\rho_{AB_i} - \rho_{AB_b}) \tag{2.60}$$

which are the forms originally presented by Whitman (241).

In general, the equilibrium solubility relationship for each phase can be represented by some function S such that $p_e = S(\rho_e)$ where the subscript e denotes corresponding equilibrium conditions, as shown in Fig. 2. For dilute solutions, S is approximated by a constant, H, in which case S merely becomes Henry's Law. Since the transfer through the interface is assumed to be steady with time, eqs. (2.59) and (2.60) can be equated. Furthermore, using the inverse of the film coefficients results in

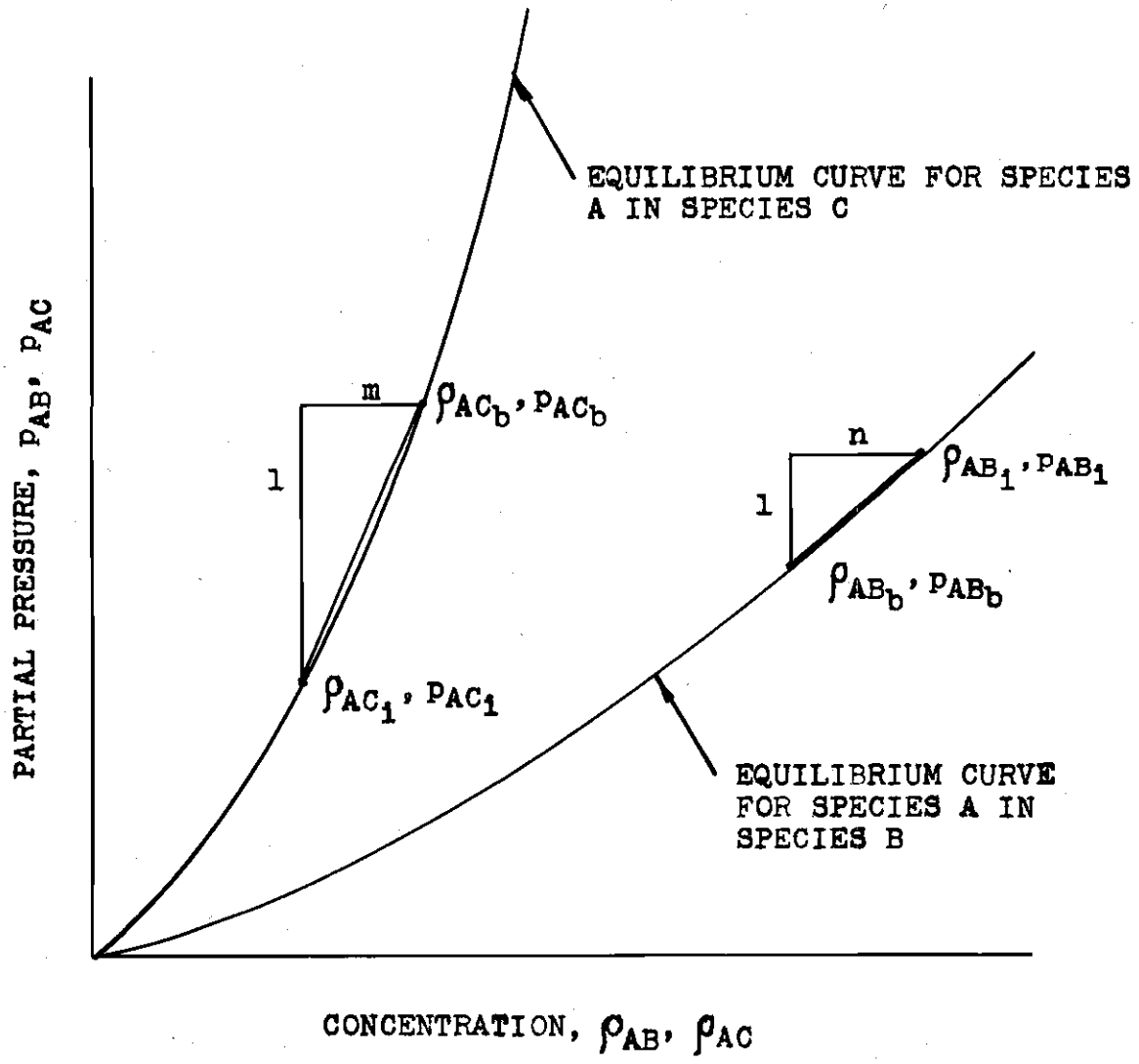


Figure 2. Typical Equilibrium Partial Pressure As Function of Concentration

$$\frac{1}{1/k_G}(p_{AC_b}-p_{AC_i}) = \frac{1}{1/k_L}(\rho_{AB_i}-\rho_{AB_b}) \qquad (2.61)$$

where $1/k_G$ and $1/k_L$ can now be considered film resistances, as originally discussed by Whitman and Keats (243). From Fig. 2 it is seen that the L.H.S. of eq. (2.61) can be put in the form

$$\frac{m}{m/k_G}(p_{AC_b}-p_{AC_i}) = \frac{\rho_{AC_b}-\rho_{AC_i}}{m/k_G} \qquad (2.62)$$

where m is the reciprocal of the slope of the line joining $p_{AC_b}$ and $p_{AC_i}$ and the other notation is as shown in Fig. 2. From eq. (2.62), using eq. (2.59),

$$\frac{m}{k_G}+\frac{1}{k_L} = \frac{1}{k_L}\left(1+\frac{\rho_{AC_b}-\rho_{AC_i}}{\rho_{AB_i}-\rho_{AB_b}}\right) \qquad (2.63)$$

Multiplying the L.H.S. of eq. (2.61) by the fraction formed from the R.H.S. of eq. (2.63) divided by itself, it can be seen that, using eq. (2.59)

$$N_{Ax} = \frac{\rho_{AB_i}-\rho_{AB_b}-\rho_{AC_b}-\rho_{AC_i}}{m/k_G + 1/k_L} \qquad (2.64)$$

The relationship between the equilibrium concentrations of A in the two phases can be represented by some function (13)

$$\rho_{AC_e} = f(\rho_{AB_e}) \tag{2.65}$$

as shown in Fig. 3. Defining r as the reciprocal of the slope of the straight line in Fig. 3 joining the origin to the point $(\rho_{AC_i}, \rho_{AB_i})$, eq. (2.64) becomes

$$N_{G_x} = \frac{\rho_{AB_i}(1-r) + \rho_{AC_b} - \rho_{AB_b}}{m/k_G + 1/k_L} \tag{2.66}$$

where $N_{G_x}$ = mass flux in gas phase in x direction. In a manner similar to which eq. (2.64) was derived, it can easily be shown

$$N_{G_x} = \frac{p_{AC_b} - p_{AC_i} + p_{AB_i} - p_{AB_b}}{\frac{1}{k_L n} + \frac{1}{k_G}} \tag{2.67}$$

where n is the reciprocal of the slope joining $\rho_{AB_b}$ and $\rho_{AB_i}$ and the other notation is as shown in Fig. 2. Thus

$$N_{G_x} = \frac{p_{AC_i}(s-1) + p_{AC_b} - p_{AB_b}}{\frac{1}{k_L n} + \frac{1}{k_G}} \tag{2.68}$$

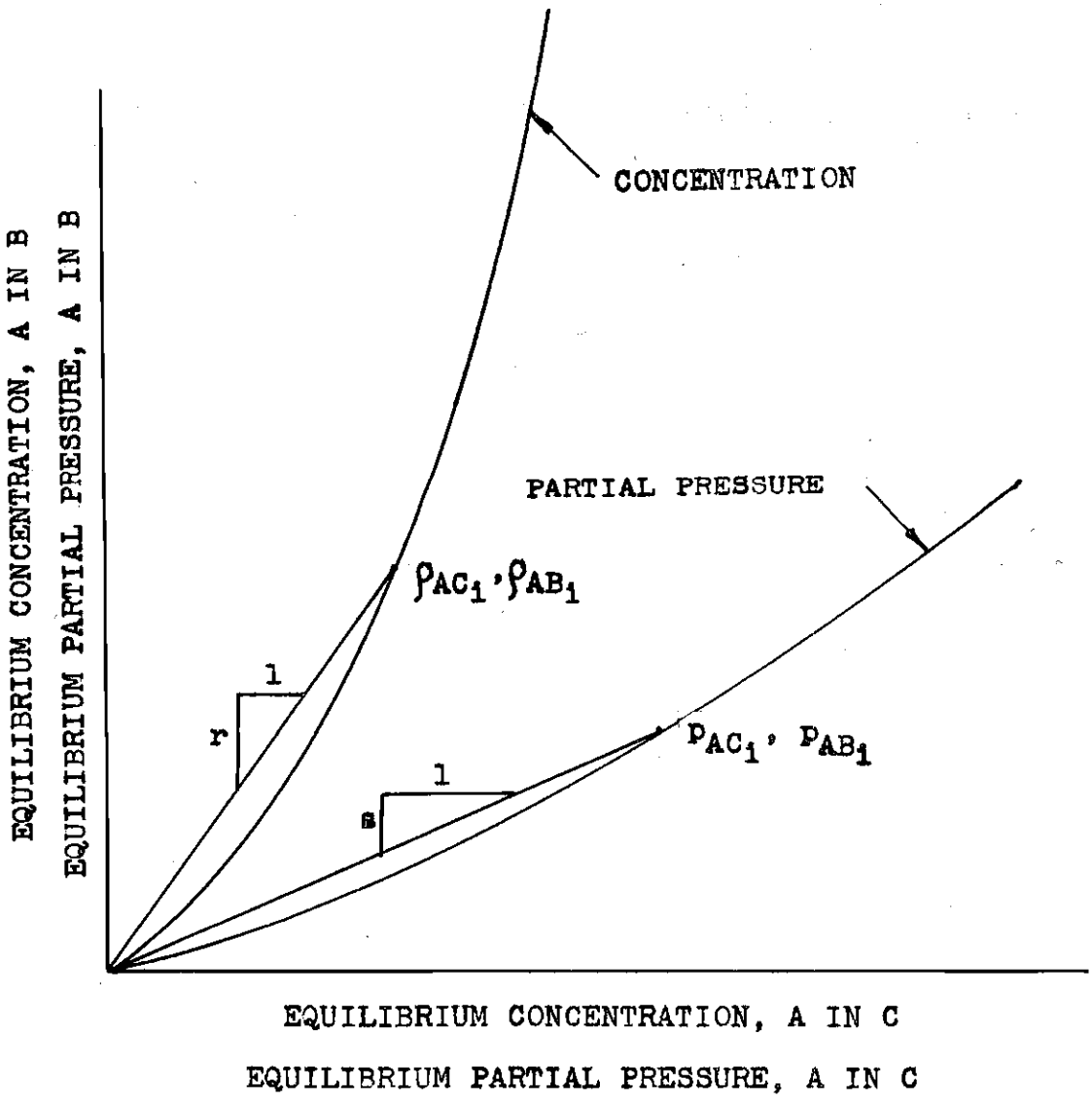


Figure 3. Equilibrium Concentration and Partial Pressure

where s is defined in an analogous manner to r as shown in Fig. 3 which shows the equilibrium partial pressure of A in the two phases.

Examining eqs. (2.66) or (2.68) it is seen why Whitman considered the total resistance to transfer to be the sum of a gas film resistance and a liquid film resistance if it is realized that the total resistance to transfer is just

$$\frac{m}{k_G} + \frac{1}{k_L} \tag{2.69}$$

or

$$\frac{1}{k_L n} + \frac{1}{k_G} \tag{2.70}$$

since the transfer is inversely proportional to either of these sums.

Letting

$$\frac{1}{K_L} = \frac{m}{k_G} + \frac{1}{k_L} \tag{2.71}$$

and

$$\frac{1}{K_G} = \frac{1}{k_G} + \frac{1}{nk_L} \tag{2.72}$$

where $K_G$ and $K_L$ are overall transfer coefficients, eqs. (2.66) and (2.68) become

$$N_{G_x} = K_L[\rho_{AB_i}(1-r) + \rho_{AC_b} - \rho_{AB_b}] \tag{2.73}$$

and

$$N_{G_x} = K_G[p_{AC_i}(s-1) + p_{AC_b} - p_{AB_b}] \tag{2.74}$$

respectively.

For the special case in which component B is the same as component C, eqs. (2.73) and (2.74) reduce to

$$N_{G_x} = K_L(\rho_{AC_b} - \rho_{AB_b}) \tag{2.75}$$

and

$$N_{G_x} = K_G(p_{AC_b} - p_{AB_b}) \tag{2.76}$$

respectively. Eqs. (2.75) and (2.76) are more amenable to experimental evaluation and are similar to those given by Whitman and Lewis (152). If the solution be dilute then n equals H, Henry's constant, and it can easily be shown by equating eqs. (2.75) and (2.76) and using eqs. (2.71) and

(2.72) that

$$K_L = (k_G k_L)/(Hk_L + k_G) \tag{2.77}$$

and

$$K_G = HK_L \tag{2.78}$$

Eqs. (2.77) and (2.78) are those given by Lewis and Whitman as the defining relationships between liquid and gas overall transfer coefficients.

Examining the definitions of $k_G$, $k_L$, $K_G$, and $K_L$ it is apparent that these various transfer coefficients are subject to numerous sources of variation. In order to take into consideration these variables, the transfer coefficients must be considered as average values for a given system and given conditions within this system. To understand that system conditions must be specified when a transfer coefficient is given, if it is to be of the most value, all that need be considered is, for example, that the degree of turbulent and/or convective mixing occurring in the bulk of either phase will have a distinct influence on the thickness of the hypothesized interfacial films. Though the concentration levels may be the same in two similar systems, different transfer coefficients will characterize the two systems if the two systems are subjected to different mixing intensities.

An implicit, but very important, assumption in the above derivation is that the transfer coefficients are independent of the mass transfer rate. For low mass transfer rates, the mass transfer through the films will have negligible effects on the concentration profiles in the films. This in general will not be the case at high transfer rates. Many investigations have dealt with low transfer rates and more information is available for low mass transfer rates. In this study, only low transfer rates are of concern; therefore, high mass transfer rates are not discussed here. For information on high transfer rates, the reader is referred to (3), (29), and similar texts. It should be realized, however, the precision of most data does not warrant concern about the effects of high transfer rates, particularily in liquid-liquid systems (225).

Two special cases of transfer through interfaces should be noted in connection with Whitman's two film theory. They are of interest since they enable the experimental determination of individual film coefficients. Considering the transfer of a gas A to a liquid B from the gas C, the mass flux is given by eqs. (2.64) and (2.67). If the gas has a very low solubility in the liquid then essentially all the transfer resistance is concentrated in the liquid (152, 228). Therefore

$$K_L \simeq k_L \qquad (2.79)$$

and eq. (2.64) becomes

$$N_{A_x} \simeq k_L(\rho_{AC_b} - \rho_{AB_b}) \tag{2.80}$$

If the solute is very soluble, little resistance is encountered in the liquid film (152, 228); therefore

$$K_G \simeq k_G \tag{2.81}$$

and from eq. (2.67)

$$N_{A_x} \simeq k_G(p_{AC_b} - p_{AB_b}) \tag{2.82}$$

A tabulation of some film coefficients as determined by various investigators is presented in Table 1. As has been noted by many investigators, the physical characteristics of the system have a prime influence on transfer coefficients, so, when ascertainable, a brief description of the system in which the various transfer coefficients were determined is also given. Lewis and Whitman (152), as well as Haslam, Hershey, and Keen (97), noted that for systems of similar physical description in which the concentration of the solute was low the liquid film coefficient, $k_L$, is approximately independent of the type of solute for a given solvent (206). It was also pointed out that for similar systems of low so-

lute concentrations and the same solvent, the gas film coefficient was directly proportional to the molecular weight of the solute. The effects of fluid velocity and temperature on film coefficients as determined empirically are summarized in (201).

It should be noted that when effective liquid film thicknesses are calculated, eqs. (2.57) and (2.58) are generally used. Since it is necessarily the total mass flux which is experimentally determined, the film thickness is therefore necessarily approximate even without consideration of other effects as will be apparent from the discussion in the following section.

Definitions of Mass Transfer Coefficients

Examination of the various forms proposed by different investigators to define and describe interphase mass transfer discussed in the preceding paragraphs will show that all take the general form

$$N_A = K \Delta \rho_A \qquad (2.83)$$

where $N_A$ = mass flux of A, K = general mass transfer coefficient, and $\Delta \rho_A$ is some characteristic change in concentration (or partial pressure). The development of this form stems from Fick's First Law, eq. (2.1), since early experimenters considered the controlling transfer mechanism to be a diffusive one. General use of this form continues to be common largely due, perhaps, to the fact it is the basic original

form proposed by Whitman whose work has been widely quoted and whose concepts have and continue to find wide usage (31, 136, 145, 148, 149, 218, 221). Thus the defining equation for a mass transfer coefficient commonly takes the form of eq. (2.83) (10, 16, 224).

As has been briefly alluded to, however, in preceding paragraphs, eq. (2.83) is not absolutely, in general at least, correct. The total mass flux of a substance A is properly given by eq. (2.37) which is equivalent to, from eq. (2.35),

$$\vec{N}_A - (\rho_A/\rho) \sum_{\ell=1}^{n} \vec{N}_\ell = \vec{J}_A \qquad (2.84)$$

for an n component system. Considering one dimensional transfer only, assumed to be in the x direction, eq. (2.84) becomes

$$N_{A_x} - (\rho_A/\rho) \Sigma N_x = J_{A_x} \qquad (2.85)$$

where the second term of the L.H.S. of eq. (2.85) takes the place of the corresponding term in eq. (2.84). If the second term of the L.H.S. of eq. (2.85) is essentially zero then the basic concept which leads to eq. (2.84), that is, the mass flux is a diffusive flux, is essentially correct, for the transfer coefficient then becomes merely a diffusivity per unit thickness of gas or liquid film. More properly, however, if the concept that the right side of eq. (2.83) is

to be a diffusive flux is to be retained, mass transfer coefficients should be defined as

$$K = (1/\Delta\rho_A)[N_A-(\rho_A/\rho)\Sigma N] \qquad (2.86)$$

The awareness of the approximation in eq. (2.83) has not always been present in many investigations (204). Furthermore, proper evaluation of transfer coefficients determined by different experimenters necessitates a knowledge of which form the defining equation for the transfer coefficients has been used, especially in those instances in which transfer rates are high. Both forms are currently found in the literature.

Penetration Theory

A major drawback in Whitman's two film theory is that it assumes transfer through the interfacial region and the concentration profiles in the interfacial region are time independent. That is, the two film theory applies to established conditions with constant, with respect to time, concentration gradients. Examining the dissolution of gases in liquids, Higbie in 1935 (103) realized that in many instances the contact time between two phases was of such short duration that concentration profiles never had sufficient time to even approach the steady state condition. Many instances exist in which two phases are suddenly brought into contact and the time required for the solute, a gas for instance, to penetrate, as Higbie termed it, into the solvent to such a degree

so as to approach the steady state concentration is much greater than the contact time between phases. The first stage in the dissolution of a gas in a liquid could thus be idealized as shown in Fig. 4 where the solid line indicates established profiles, the dashed lines indicate the profiles during the penetration period, and the dotted lines represent the concentration profile at the instant the phases come in contact assuming that they are initially well mixed.

Higbie considered the case of gases of low solubility in which case, as discussed earlier in connection with the two film theory, the resistance of the gas phase could be considered as negligibly small in comparison to the liquid phase resistance. He assumed that the liquid in and near the interfacial region was in laminar flow moving parallel to the gas-liquid interface. The simplifications were made that in and near the interfacial region the velocity was both uniform, as shown in Fig. 4, and time invariant over the time period under consideration. Higbie limited his analysis to low transfer rates with the assumption that the transfer through the liquid did not appreciably affect the velocity profile. The depth of the liquid was considered to be quite large compared to the zone of concentration variation, that is, mathematically the depth of the liquid was assumed to be infinite.

Consider the two dimensional transfer of a gas A through a liquid B under the assumptions in the preceding paragraph. The gas is assumed to be dissolving in the x di-

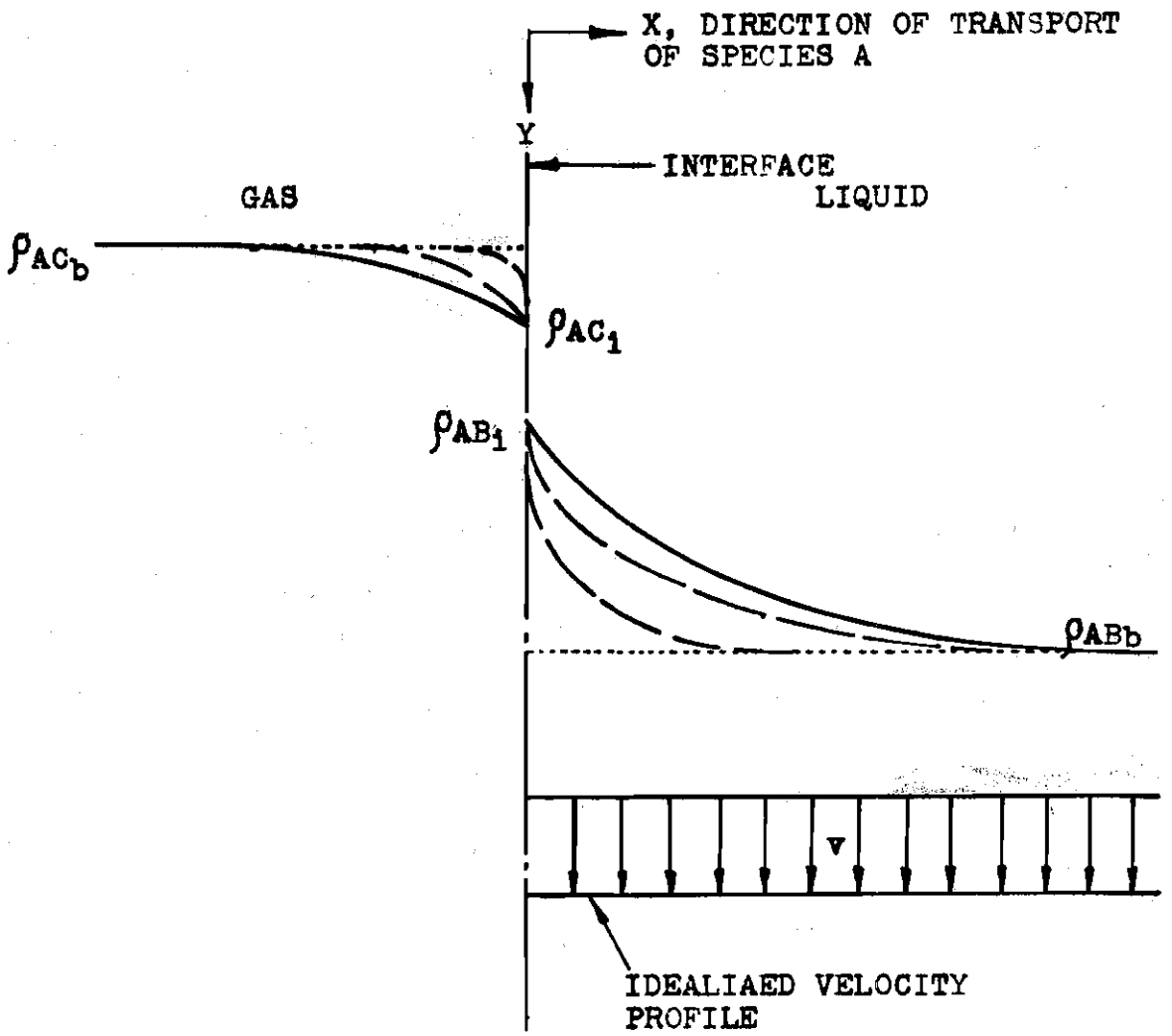


..... INITIAL CONCENTRATION PROFILE

— — — — TRANSIENT CONCENTRATION PROFILE

——————— STEADY STATE CONCENTRATION PROFILE

Figure 4. Penetration Model

rection while the liquid is flowing in the y direction only with a mass average velocity of v. A concentration gradient is assumed to exist only in the x direction, as shown in Fig. 4, so that no diffusion takes parallel to the interface. Assume further that the liquid solution is an isothermal one with constant diffusivity and is of such dilution that the density of the solution is essentially constant. Under the various assumptions made eq. (2.42) then reduces to

$$\frac{\partial \rho_A}{\partial t} = D \frac{\partial^2 \rho_A}{\partial x^2} \tag{2.87}$$

where the notation is as defined earlier. The boundary conditions for eq. (2.87) are the following:

$$\text{B.C.1: For } t \leq 0, \ \rho_A = \rho_{AB_b} \text{ for all } x, \tag{2.88}$$

$$\text{B.C.2: For } x = 0, \ \rho_A = \rho_{AB_i} \text{ for all } t > 0, \tag{2.89}$$

$$\text{B.C.3: For } x = \infty, \ \rho_A = \rho_{AB_b} \text{ for all } t > 0, \tag{2.90}$$

where t = 0 at the instant the two phases come into contact. With these boundary conditions the solution to eq. (2.87) becomes similar to that for viscous flow near a plane boundary impulsively set in motion. The solution, as shown by Lamb (142), is, with proper change of variables,

$$\rho_A = \rho_{AB_b} + (\rho_{AB_i} - \rho_{AB_b})\left[1 - \frac{2}{\sqrt{\pi}} \int_o^{\theta} e^{-\theta^2} d\theta\right] \qquad (2.91)$$

where

$$\theta = x/\sqrt{4Dt_{ct}} \qquad (2.92)$$

and e is the base of the natural logarithm. Eq. (2.91) can be written as

$$(\rho_A - \rho_{AB_b})/(\rho_{AB_i} - \rho_{AB_b}) = \text{erfc}(x/\sqrt{4Dt_{ct}}) \qquad (2.93)$$

where $t_{ct}$ is the contact time between the two phases and erfc is the complementary error function. Eq. (2.93) is similar to that in (8).

The mass flux of A being transported through the interface is $N_{A_x}$ evaluated at x = 0. From eq. (2.84)

$$N_{A_x}\Big|_{x=0} = [(\rho_A/\rho)(N_{A_x} + N_{B_x}) + J_{A_x}]_{x=0} \qquad (2.94)$$

If the net transfer of B is negligible, eq. (2.95) becomes, using eq. (2.1),

$$N_{A_x}\Big|_{x=0} = \left[-\frac{D}{1-(\rho_A/\rho)} \frac{\partial \rho_A}{\partial x}\right]_{x=0} \qquad (2.95)$$

Using eq. (2.91) evaluated at x equals zero,

$$N_{A_x}\Big|_{x=0} = \frac{\rho_{AB_i} - \rho_{AB_b}}{1-(\rho_A/\rho)_{x=0}} \sqrt{\frac{D}{\pi t}} \qquad (2.96)$$

Denoting the total amount of gas absorbed per unit area in a time t by $F_A(t)$, the total amount of gas absorbed per unit area of interface in a time, $t_{ct}$, equal to the contact time is, from eq. (2.96),

$$F_A(t_{ct}) = \int_0^{t_{ct}} (N_{G_x})_{x=0} dt = \int_0^{t_{ct}} \frac{\rho_{AB_i} - \rho_{AB_b}}{1-(\rho_A/\rho)_{x=0}} \sqrt{\frac{D}{\pi t}}\, dt \qquad (2.97)$$

Eq. (2.97) reduces to

$$F_A(t_{ct}) = \frac{2(\rho_{AB_i} - \rho_{AB_b})}{1-(\rho_A/\rho)_{x=0}} \sqrt{\frac{Dt_{ct}}{\pi}} \qquad (2.98)$$

For solutions of low concentration $\rho_A/\rho$ approximates zero, in which case eq. (2.98) becomes

$$F_A(ct) = 2(\rho_{AB_i} - \rho_{AB_b}) \sqrt{Dt_{ct}/\pi} \qquad (2.99)$$

which is similar to that given by Higbie in 1935 (103).

The instantaneous mass transfer coefficient for the system, which in this case is equivalent to a liquid film coefficient, is given by eq. (2.86) which reduces, under the assumptions made leading to eq. (2.95), to

$$k_L = [\sqrt{D/(\pi t_{ct})}]/[1-(\rho_A/\rho)] \qquad (2.100)$$

For the assumption of eq. (2.99), eq. (2.100) becomes

$$k_L = \sqrt{D/(\pi t_{ct})} \qquad (2.101)$$

the form given by Higbie. As defined by eq. (2.101), $k_L$ is also of the same nature as the transfer coefficient defined by eq. (2.83). Significantly, it is seen the penetration theory predicts the film coefficient to vary as the square root of the diffusivity. The two film theory, it will be noted from eq. (2.56), predicts the film coefficient to vary as the first power of the diffusivity.

Though Higbie's theoretical predictions seemed to overestimate the actual amount of gas absorbed when Higbie compared them with experimental values, Higbie's penetration theory has proven to be of extreme value in those situations involving short contact times. It continues to be found in current studies (15, 218).

Boundary Layer Theory

Extensive investigations of mass transfer have been conducted using the concepts of Prandtl's well known boundary layer theory. Near a boundary the velocity of a flowing fluid decreases from that of the main stream to that of the boundary itself if non-slip conditions exist. As Prandtl envisioned it, this decrease in velocity could be effectively concentrated in a thin layer which Prandtl termed the boundary layer (70). As the boundary layer concept has developed and has been enlarged upon, two types of boundary layers have come to be recognized: the laminar boundary layer and the turbulent boundary layer. In the laminar boundary layer all fluid motion is viscous while in the turbulent boundary layer the outer portions of the boundary layer are turbulent while the inner portions, composing what is termed the laminar sublayer, remain viscous. The transition from the turbulent zones is, of course, not a sharp transition but a gradual one occurring in what has been termed by some as a buffer zone.

Using an order of magnitude analysis, Prandtl was able to reduce the Navier-Stokes equations sufficiently to make them more amenable to solution. For incompressible two dimensional flow in the x direction parallel to a boundary Prandtl's boundary layer equations for laminar boundary layers, as his simplification has come to be known, are (194)

$$\frac{\partial u}{\partial t}+u\frac{\partial u}{\partial x}+v\frac{\partial u}{\partial y} = -\frac{1}{\rho}\frac{\partial p}{\partial x}+\nu\frac{\partial^2 u}{\partial y^2} \qquad (2.102)$$

and

$$\rho\mathbb{K}_c u^2 = \partial p/\partial y \qquad (2.103)$$

where u = velocity in x direction, v = velocity in the y direction, t = time, $\rho$ = fluid density, p = pressure, $\nu$ = kinematic viscosity, and $\mathbb{K}_c$ = boundary curvature. Even Prandtl's boundary layer equations become rather untractable in many situations, however, and resort is often made to more approximate but simpler equations. Foremost among these simpler forms is von Karman's integral momentum equation. Von Karman's equation obtains its relative simplicity from the fact that no attempt is made to describe the motion of every fluid particle in the boundary layer exactly at each point; rather, only the overall motion of the fluid is described and boundary conditions are satisfied only at certain points (194). For the same conditions under which eqs. (2.102) and (2.103) are valid, the momentum integral equation is (72)

$$\int_0^\delta \rho\frac{\partial u}{\partial t}dy+\frac{\partial}{\partial x}\int_0^\delta \rho u^2\,dy-U\frac{\partial}{\partial x}\int_0^\delta \rho u\,dy = -\delta\frac{\partial p}{\partial x}-\tau_o \qquad (2.104)$$

where U = free stream velocity, $\delta$ = boundary layer thickness, $\tau_o$ = shearing stress at boundary, and the other symbols are as

previously defined. Use of von Karman's momentum integral equation requires assumption of the shape of the velocity profile, the more accurate the assumption the more nearly exact the solution to eq. (2.104). Numerous solutions to eqs. (2.102), (2.103), and (2.104) for a variety of boundary conditions are given in (3, 42, 69, 140, 186).

Introduction of turbulence in the boundary layer results in the appearance of additional terms in the general equations of motion, these terms being the well known Reynold's stresses. These Reynold's stresses can be taken into consideration in eqs. (2.104) and (2.104) by the introduction of a kinematic eddy viscosity and a turbulent shear stress respectively. Except for the determination of the form of these new terms, solution of problems involving turbulent boundary layers then proceed in a somewhat analogous manner to those of laminar boundary layers. Thus for the purposes in the present discussion it becomes sufficient to restrict consideration to laminar boundary layers. The effects of turbulence on mass transport, similar to the effects of turbulence on momentum transport, will be examined more closely in the following section where it becomes valuable to view turbulence in a boundary layer and its treatment in a boundary layer in relation to other methods proposed to describe mass transport in turbulent fluids.

Boundary layer theory as applied to mass transport has developed along several lines. The most obvious of these is

that of the creation of a concentration boundary layer analogous to Prandtl's hydrodynamic boundary layer as shown in Fig. 5. Although the concentration boundary layer, when described and treated as such, seemly arises from Prandtl's concepts, review of previous discussions in this chapter will show that other mass transfer theories have essentially dealt with a concentration boundary layer, in the sense that concentration variations occur over some small finite distance. However, in the context of boundary layers, concentration variations assume two dimensional characteristics. As a fluid flows past some interface the development of the concentration profile occurs in a direction both normal and parallel to the interface in a manner similar to the hydrodynamic boundary layer. Furthermore the velocity in the boundary layer also becomes two dimensional. Reference to the film theory and the penetration theory will show that these theories treated the transfer as essentially a one dimensional phenomenon. Even in Higbie's analysis the assumption was made that the velocity was one dimensional even though it was in a direction perpendicular to the direction of dissolution of the solute. Thus in many instances the boundary layer approach becomes a distinct improvement.

The analysis of mass transfer in boundary layers has proceeded basically along the line of satisfying momentum, energy, and continuity requirements, the more stringent the requirements the greater the complexity that arises. For low

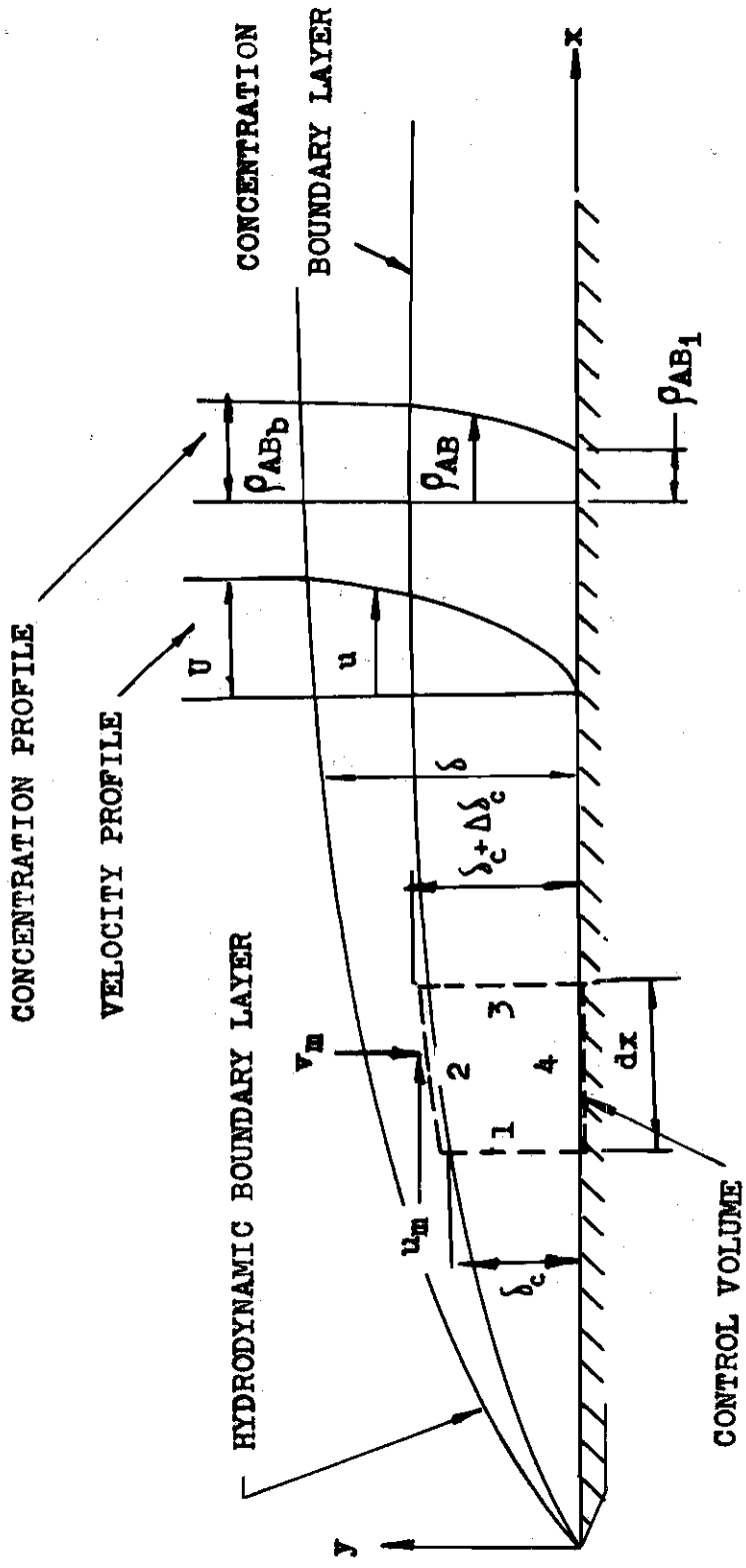


Figure 5. Hydrodynamic and Concentration Boundary Layers in Laminar Flow

mass transfer rates inter-effects of momentum, heat, and mass are generally minor and can safely be neglected. Thus the prediction of mass transfer becomes a problem of satisfying the appropriate equations of continuity. Boundary layer theory becomes of value here, however, because more reasonable and more nearly exact descriptions of the velocity of the flow and its variation are provided from solutions of appropriate momentum equations, such as eqs. (2.102), (2.103), and (2.104). For high transfer rates momentum, energy, and continuity equations must be satisfied, in essence, simultaneously. Though difficult, boundary layer theory provides here a rather realistic model of the transport occurring.

A second avenue of analysis that boundary layer theory has provided is that of the development of useful and pertinent parameters which have been of extreme value in analysis. Though dimensionless parameters can be developed from purely dimensional analysis if one is able to determine the pertinent variables by some means, boundary layer theory has provided a more firm physical basis and understanding of these various parameters. Of course this basis and understanding can arise by development of parameters from theories outside of the context of boundary layer theory but boundary layer theory has been used extensively in the development of pertinent dimensionless parameters (45, 185, 193).

To illustrate the above remarks consider the relatively simple example of steady, laminar flow of a binary solution

past a stationary flat plate, which could be considered equally well as an interface, in two dimensions. This example will demonstrate the basic method of attack in solving mass transfer problems at low transfer rates as well as illustrating the usefulness of boundary layer theory in developing dimensionless parameters. In addition the parameters developed will be ones which have found wide usage in the field of mass transfer.

The plate will be assumed oriented parallel to the free stream as shown in Fig. 5. Two dimensional x and y coordinates are positioned such that the x direction is parallel to the plate while the y direction extends normally to the plate. Within the hydrodynamic boundary layer which develops as the solution flows past the plate the velocity varies from zero at y equals zero, the plate, to U, the free stream velocity, at y equals $\delta$, the thickness of the hydrodynamic boundary layer. Within the hydrodynamic boundary layer lies the concentration boundary layer as shown in Fig. 5. In general it can not be said that the concentration boundary layer will necessarily be within the hydrodynamic boundary layer. Analysis is simplified, however, with this assumption and this assumption will not prevent the accomplishment of the purposes intended here. The solute will be designated as A, while B will designate the solvent. As the solution passes over the plate it is assumed that A is being absorbed at a uniform rate from the plate over its entire length. Since the flow is laminar the absorption mechanism is necessarily a diffusive one. Component B of the

system, for simplicity, is assumed not to be absorbed by the plate. The concentration of A, using the notation introduced previously, varies from $\rho_{AB_i}$ at the plate to $\rho_{AB_b}$ at $y = \delta_c$, the concentration boundary layer thickness. The solution will be considered sufficiently dilute such that the density of the solution is essentially constant.

Consider first the hydrodynamic boundary layer and the fluid motion within it. The pressure at the outer edge of the hydrodynamic boundary layer is essentially constant since the flow outside the boundary layer is approximately ideal and uniform. From eq. (2.103) the pressure variation normal to the plate is zero. The pressure gradient in the x direction can therefore be considered to be zero throughout the hydrodynamic boundary layer. Furthermore the boundary shear stress, since the flow is laminar, is given by Newton's law of viscosity. Eq. (2.104) thus reduces to

$$\rho \frac{\partial}{\partial x} \int_0^{\delta} u(U-u)dy = \mu \left.\frac{\partial u}{\partial y}\right|_{y=0} \qquad (2.105)$$

where $\mu \left.\frac{\partial u}{\partial y}\right|_{y=0}$ = shear stress at $y = 0$, $\mu$ = viscosity of the solution, $\rho$ = mass density of the solution, and the other notation is as defined previously. The following dimensionless ratios are defined:

$$u^* = u/U \tag{2.107}$$

$$y^* = y/x \tag{2.108}$$

$$\partial y^* = \partial y/x \tag{2.109}$$

$$\partial x^* = \partial x/x \tag{2.110}$$

$$\delta^* = \delta/x \tag{2.111}$$

Introduction of these ratios into eq. (2.105) results in the dimensionless equation, similar to that given by Eckert (46),

$$\frac{\partial}{\partial x^*} \int_0^{\delta^*} (1-u^*)u^* dy^* = \frac{\mu}{\rho U x} \left(\frac{\partial u^*}{\partial y^*}\right)_{y^*} = 0 \tag{2.112}$$

The dimensionless term $\mu/(\rho Ux)$ on the R.H.S. of eq. (2.112) is recognized as the reciprocal of a Reynolds number. The solution to eq. (2.112) determines the profile of the dimensionless velocity $u^*$. It can be represented in a general form as

$$u^* = f_1 (y^*, Re) \tag{2.113}$$

where

$$Re = \rho Ux/\mu \tag{2.114}$$

and $f_1$ = function. Eq. (2.113) shows the pertinent parameters of which $u^*$ is a function. These parameters will be of use in the following paragraphs as the mass transfer in the boundary layer is analyzed.

Construct a two dimensional control volume in the concentration boundary layer whose faces are designated as surfaces 1, 2, 3, and 4 as shown in Fig. 5. Surfaces 1 and 3 are normal to the plate while the plate itself forms surface 2. The outer edge of the concentration boundary layer forms surface 4. Surface 1 is $\delta_c$ long while surface 3 is $\delta_c+d\delta_c$ long. Surface 2 is dx long.

Consider the mass transfer across surface 2 at the plate. The mass flux of A is, from eq. (2.37),

$$N_A\Big|_{y=0} = \rho_{AB_i} V_w + J_{Ay}\Big|_{y=0} \tag{2.115}$$

where $V_w$ = the mass average velocity of the solution through surface 2 at the plate boundary, and the other notation is as previously defined. For component B the mass flux expression for surface 2 is similar to eq. (2.115). However, since no absorption of B is occurring

$$N_B\Big|_{y=0} = 0 \tag{2.116}$$

Therefore

$$\rho_{BA_i} V_w = -J_{By}\Big|_{y=0} \tag{2.117}$$

where $\rho_{BA_i}$ = mass concentration of B at the interface. The mass average velocity normal to the plate at the plate boundary is therefore, using eq. (2.1),

$$V_w = \frac{D}{\rho_{BA_i}} \frac{\partial \rho_B}{\partial y}\Big|_{y=0} \tag{2.118}$$

where the notation is similar to that defined earlier.

The mass transfer of solution across surface 1 into the control volume is

$$\int_o^{\delta_c} \rho u dy \tag{2.119}$$

while that across surface 3 out of the control volume is

$$\int_o^{\delta_c} \rho u dy + (\frac{\partial}{\partial x} \int_o^{\delta_c} \rho u dy) dx \tag{2.120}$$

At surface 2 the mass transfer into the control volume is

$$V_w \rho dx \tag{2.121}$$

The velocity of the solution along surface 4 in general has two components whose average values in the x and y directions may be designated as $u_c$ and $v_c$ respectively. The total mass transfer across surface 4 into the control volume is therefore

$$\rho u_c d\delta + \rho v_c dx \tag{2.122}$$

if $u_c$ and $v_c$ are considered positive when directed inward into the control volume. By the conservation of mass, eq. (2.9), using eqs. (2.119) through (2.122),

$$-\left(\frac{\partial}{\partial x}\int_0^{\delta_c} \rho u dy\right)dx + V_w \rho dx + \rho u_c d\delta + \rho v_c dx = 0 \tag{2.123}$$

Since the density of the solution is approximately constant, eq. (2.123) becomes

$$-\left(\frac{\partial}{\partial x}\int_0^{\delta_c} u dy\right)dx + V_w dx + u_c d\delta + v_c dx = 0 \tag{2.124}$$

Into the control volume across surface 1 the mass transfer of A is

$$\int_0^{\delta_c} \rho_{AB} u dy \tag{2.125}$$

while across surface 3 the transfer of A is

$$\int_o^{\delta_c} \rho_{AB} u dy + \left(\frac{\partial}{\partial x} \int_o^{\delta_c} \rho_{AB} u dy\right) dx \qquad (2.126)$$

Across surface 4 the mass transfer of A is only

$$\rho_{AB_c} u_c d\delta + \rho_{AB_c} v_c dx \qquad (2.127)$$

since the concentration gradient is zero there. $\rho_{AB_c}$ is the concentration of A at y equals $\delta_c$. From eq. (2.126) the transfer of A across surface 2 is

$$\rho_{AB_i} V_w dx + J_{Ay}\Big|_{y=0} dx \qquad (2.128)$$

Therefore from eqs. (2.1), (2.9), and (2.125) through (2.128)

$$-\left(\frac{\partial}{\partial x} \int_o^{\delta_c} \rho_A u dy\right) dx + \rho_{AB} u_c d\delta + \rho_{AB_c} v_c dx$$

$$+\rho_{AB_i} V_w dx - D\left(\frac{\partial \rho_A}{\partial y}\right)_{y=0} dx = 0 \qquad (2.129)$$

Using eq. (2.124), eq. (2.129) can then be easily be reduced to

$$\frac{\partial}{\partial x}\int_0^{\delta_c}(\rho_{AB_c}-\rho_{AB})u\,dy+V_w(\rho_{AB_i}-\rho_{AB_c}) = D\frac{\partial \rho_A}{\partial y}\bigg|_{y=0} \qquad (2.130)$$

For dilute solutions $V_w$ will generally be small (45) and can be neglected without loss of generality for the purposes intended here. Eq. (2.130) thus reduces to the relatively simple form

$$\frac{\partial}{\partial x}\int_0^{\delta_c}(\rho_{AB_c}-\rho_A)u\,dy = D\frac{\partial \rho_A}{\partial y}\bigg|_{y=0} \qquad (2.131)$$

Comparison of this equation with eq. (2.105) illustrates the comments made earlier concerning the analogies between the hydrodynamic boundary layer and the concentration boundary layer.

Define a dimensionless mass concentration as

$$\rho^* = (\rho_A-\rho_{AB_i})/(\rho_{AB_c}-\rho_{AB_i}) \qquad (2.132)$$

and a dimensionless concentration boundary layer thickness as

$$\delta_c^* = \delta_c/x \qquad (2.133)$$

Using eqs. (2.107) through (2.110) as well as eqs. (2.132) and (2.133), eq. (2.131) can be rewritten as

$$\frac{1}{x}\frac{\partial}{\partial x^*}\int_0^{\delta_c}\left(1-\frac{\rho_A-\rho_{AB_i}}{\rho_{AB_c}-\rho_{AB_i}}\right)(\rho_{AB_c}-\rho_{AB_i})u^* U x dy^* =$$

$$\frac{D}{x}\frac{\partial \rho^*}{\partial y^*}\bigg|_{y^*=0}(\rho_{AB_c}-\rho_{AB_i})$$

which reduces to

$$\frac{\partial}{\partial x^*}\int_0^{\delta_c^*}(1-\rho^*)u^*\,dy^* = \frac{D}{xU}\frac{\partial \rho^*}{\partial y^*}\bigg|_{y^*=0} \qquad (2.134)$$

From the solution of eq. (2.132) would be obtained a function describing the dimensionless concentration profile. The solution can be seen to be symbolically represented as

$$\rho^* = f_2(u^*, \frac{xU}{D}, y^*) \qquad (2.135)$$

where $f_2$ is an unknown function. Since $u^*$ and $y^*$ are related by eq. (2.113), eq. (2.135) takes the more general form

$$\rho^* = f_3(y^*, Re, \frac{xU}{D}) \qquad (2.136)$$

where $f_3$ is an unknown function. $xU/D$ is analogous to the Peclet number in heat transfer and can be considered a Peclet number for mass transfer (12). The symbol Pe will be used for the mass transfer Peclet number.

A more commonly encountered form is obtained from eq. (2.135) by defining a new parameter which is the quotient of Pe and Re. Thus the dimensionless concentration profile can likewise be represented by

$$\rho^* = f_4(y^*, \text{Re}, \text{Sc}) \tag{2.137}$$

where $f_4$ is an unknown function, Sc is the Schmidt number, originally introduced in 1929 (199). Sc is defined as

$$\text{Sc} = \frac{\nu}{D} \tag{2.138}$$

where $\nu$ = kinematic viscosity, D = diffusivity.

The parameters developed here will be discussed in relation to mass transfer parameters in general in a following section.

If for the form of the velocity profile a cubic parabola

$$u = ay + cy^3 \tag{2.139}$$

is assumed as has been done by Eckert (43), then

$$\frac{u}{U} = \frac{3}{2}\frac{y}{\delta} - \frac{1}{2}\left(\frac{y}{\delta}\right)^3 \tag{2.140}$$

since at

$$y = 0,\ u = 0 \tag{2.141}$$

$$y = \delta,\ u = U \tag{2.142}$$

and

$$y = \delta,\ \partial u/\partial y = 0 \tag{2.143}$$

Introduction of eq. (2.140) into eq. (2.112) results in, using eqs. (2.108) and (2.111),

$$\frac{\partial}{\partial x^*} \int_0^{\delta^*} I dy = \frac{1}{Re}\left(\frac{u^*}{y^*}\right)_{y=0} \tag{2.144}$$

where Re is defined as in eq. (2.114) and

$$I = \frac{3}{2}\left(\frac{y^*}{\delta^*}\right) - \frac{9}{4}\left(\frac{y^*}{\delta^*}\right)^2 - \frac{1}{2}\left(\frac{y^*}{\delta^*}\right)^3 + \frac{3}{2}\left(\frac{y^*}{\delta^*}\right)^4 - \frac{1}{4}\left(\frac{y^*}{\delta^*}\right)^6 \tag{2.145}$$

From eq. (2.140),

$$\left(\frac{\partial u^*}{\partial y^*}\right)_{y=0} = \frac{3}{2}\,\frac{1}{\delta^*} \tag{2.146}$$

Integrating eq. (2.145) with respect to $y^*$, eq. (2.144) reduces to, using eq. (2.146),

$$d\delta^*/dx^* = \frac{140}{13} \cdot Re^{-1} \cdot (\delta^*)^{-1} \qquad (2.147)$$

Separating variables and integrating, using eqs. (2.109), (2.111), and (2.114), results in

$$(\delta^*)^2 = \frac{280}{13} \cdot Re^{-1} + \text{Constant} \qquad (2.148)$$

Assuming $\delta$ equals 0 at $x = 0$, the constant in eq. (2.148) is zero. Therefore eq. (2.148) can be rewritten as

$$\delta^* = 4.64 \quad (Re)^{-1/2} \qquad (2.149)$$

which is similar to that given by Eckert (44) and Rouse (184).

If the concentration profile is approximated with a cubic parabola similar to that of eq. (2.139), viz.,

$$\rho_A - \rho_{AB_i} = ay + cy^3 \qquad (2.150)$$

then

$$\rho^* = \frac{3}{2}\frac{y}{\delta_c} - \frac{1}{2}\left(\frac{y}{\delta_c}\right)^3 \qquad (2.151)$$

since at

$$y = 0,\ \rho_A - \rho_{AB_i} = 0 \tag{2.152}$$

$$y = \delta_c,\ \rho_A - \rho_{AB_i} = \rho_{AB_b} - \rho_{AB_i} \tag{2.153}$$

and

$$y = \delta_c,\ \partial\rho_A/\partial y = 0 \tag{2.154}$$

Then from eq. (2.134)

$$\frac{\partial}{\partial x^*} \int_0^{\delta_c^*} M dy = \frac{1}{Re} \left(\frac{\partial \rho^*}{\partial y^*}\right)_{y=0} \tag{2.155}$$

where M is given by

$$M = \frac{3}{2}\frac{y^*}{\delta^*} - \frac{1}{2}\left(\frac{y^*}{\delta^*}\right)^3 - \frac{9}{4}\left(\frac{y^*}{\delta^*}\right)^2 \frac{1}{\phi^*} + \frac{3}{4}\left(\frac{y^*}{\delta^*}\right)^4 \frac{1}{\phi^*} + \frac{3}{4}\left(\frac{y^*}{\delta^*}\right)\frac{1}{\phi^{*3}} - \frac{1}{4}\left(\frac{y^*}{\delta^*}\right)^6 \frac{1}{\phi^{*3}} \tag{2.156}$$

$\phi^*$ is defined as

$$\phi^* = \delta_c/\delta = \delta_c^*/\delta^* \tag{2.157}$$

where $\phi^*$ is a function of x. From eq. (2.151)

$$\left(\frac{\partial \rho^*}{\partial y^*}\right)_{y=0} = \frac{3}{2}\frac{1}{\delta_c^*} \tag{2.158}$$

Eq. (2.155) thus becomes, using eqs. (2.156) and (2.158) and evaluating the integral in eq. (2.155),

$$\frac{\partial}{\partial x^*}\left[\delta^*\left(\frac{3}{20}\phi^{*2} - \frac{3}{280}\phi^{*4}\right)\right] = \frac{3}{2}\frac{1}{\delta^*}\frac{1}{Pe} \qquad (2.159)$$

For $\phi^*$ less than 1, the second term of the L.H.S. of eq. (2.159) can be neglected, in which case eq. (2.159) becomes, after performing the indicated differentiation,

$$\delta^*\phi^{*3}\frac{d\delta^*}{dx^*} + (\delta^*)^2 2\phi^{*2}\frac{d\phi^*}{dx^*} = \frac{10}{Pe} \qquad (2.160)$$

But using eqs. (2.147) and (2.148), this reduces to

$$\phi^{*3}\ \frac{140}{13}\frac{1}{Re} + \frac{280.2}{13}\frac{1}{Re}\ \phi^{*2}\frac{d\phi^*}{dx^*} = \frac{10}{Pe}$$

or

$$\frac{14}{13}(\phi^{*3} + 4\phi^{*2}\, d\phi^*/dx\ ) = Re\ Pe^{-1} = Sc^{-1} \qquad (2.161)$$

If the substitution

$$\phi^{*3} = \Omega \qquad (2.162)$$

is made, eq. (2.161) becomes

$$\Omega + \frac{26}{21}\frac{d\Omega}{dx} = \frac{1}{Sc} \tag{2.163}$$

The solution to eq. (2.163) is, as can be checked by substitution in eq. (2.163),

$$\Omega = \text{constant} \cdot e^{(-21/26)x} + Sc^{-1} \tag{2.164}$$

Assuming the boundary condition

$$\delta_c/\delta = \phi^* = \Omega^{1/3} = 0 \text{ at } x = 0 \tag{2.165}$$

the constant in eq. (2.164) becomes $-Sc^{-1}$. Thus

$$\delta_c/\delta = (Sc^{-1/3})(1-e^{-21x/26})^{1/3}$$

or

$$\delta_c^*/\delta^* = (Sc^{-1/3})(1-e^{-21x/26})^{1/3} \tag{2.166}$$

From eq. (2.149), eq. (2.166) can also be put in the form

$$\delta_c^* = \left(\frac{4.64}{\sqrt{Re}\sqrt[3]{Sc}}\right)(1-e^{-21x/26})^{1/3} \tag{2.167}$$

Thus it is seen that the concentration boundary layer thickness, for a given set of flow conditions, that is, a given Reynolds number, is a function of a Schmidt number, just as the hydrodynamic boundary layer thickness is a function of a Reynolds number.

Turbulence Theories

Most attempts to determine the effects of turbulence on mass transfer have proceeded from analogies with momentum and heat transfer in turbulent flow. While these analogies have been numerous and have proved to be quite valuable, investigation of mass transfer in turbulent flow seems to have lagged somewhat behind that of heat and momentum transfer. Early emphasis in this field was primarily that of attempting to apply the results of heat and momentum directly to mass transfer (28, 29, 176, 199, 207). More recently however, emphasis has been placed on the examination of turbulent mass transfer viewed more from its own sphere (23, 89).

With all turbulent phenomenon great difficulty is encountered in analysis and experimentation. Many investigators have necessarily been forced to rely on semi-empirical hypotheses. As has been noted by Schlichting (196), the complex nature of turbulence appears to defy ultimate understanding. Thus considerable reliance has been placed on the development of pertinent parameters. The development of these parameters will be examined in following sections. To be briefly examined presently are those concepts which have

been used to provide a rational basis for analysis of turbulent mass transport.

Turbulent transport has been approached from two viewpoints (94): (1) a quasi-steady state approach in which the mean conditions are of prime concern and (2) an unsteady state approach in which the time dependence of mass transfer on turbulence is of prime interest.

Quasi-Steady State Transfer. The existence of turbulence in a solution will result in movement of small balls or lumps, as Schlicting has described it (195), of fluid from one locale to another. Since the concentration of a species, say A, varies from point to point within the solution, the concentration at any particular point will be subject to fluctuations. Thus to describe the concentration variation in a turbulent solution, it becomes convenient, as with the division of the total velocity in turbulent flow into a mean and a fluctuating component, to subdivide the total concentration at a point into two parts:

$$\rho_A = \overline{\rho_A} + \rho_A' \qquad (2.168)$$

where $\rho_A$ = total concentration of A, $\overline{\rho_A}$ = mean concentration of A, and $\rho_A'$ = fluctuating component of the total concentration of A. Considering solutions of only constant diffusivity and approximately constant density the equation of continuity

for the solute A is given by eq. (2.42). Introduction of eq. (2.168) into eq. (2.42) will result, after time averaging, in the equation of continuity of A in turbulent flow. The time average process is considerably simplified by the rules for time averaging given by Schlichting (197). Thus, similar to that given by Goldstein (73),

$$\frac{\partial \overline{\rho_A}}{\partial t} + U\frac{\partial \overline{\rho_A}}{\partial x} + V\frac{\partial \overline{\rho_A}}{\partial y} + W\frac{\partial \overline{\rho_A}}{\partial z} =$$

$$D\nabla^2(\overline{\rho_A}) - [\frac{\partial}{\partial x}(\overline{u'\rho_A'}) + \frac{\partial}{\partial y}(\overline{v'\rho_A'}) + \frac{\partial}{\partial z}(\overline{w'\rho_A'})] \qquad (2.169)$$

where the fluid velocity in the x, y, and z directions is given by

$$u = U + u' \qquad (2.170\text{-a})$$

$$v = V + v' \qquad (2.170\text{-b})$$

$$w = W + w' \qquad (2.170\text{-c})$$

respectively. Here the total velocities are given as the sum of a mean and a fluctuating component, the primes denoting the fluctuating components. The L.H.S. and first term of the R.H.S. of eq. (2.169) is seen to be the equation of continuity of A in terms of the average concentration. The remaining

terms on the R.H.S. of eq. (2.108) arise because of the turbulent fluctuations of the velocity and concentration and are the net effect of turbulence on the concentration of the solution. The bars above the terms are used to denote time averages of the products shown. These additional terms are directly analogous to the Reynolds stresses in the equations of motion for turbulent fluids. Here these terms represent the mass flux of A due to turbulence. Except in those regions where the turbulent fluctuations become damped, as near a boundary, the turbulent mass flux is generally much larger than the diffusive flux.

For simplicity consider only one dimensional transfer, in which case eq. (2.169) may be rewritten as

$$\frac{\partial \rho_A}{\partial t} + U\frac{\partial \overline{\rho_A}}{\partial x} = D\frac{\partial^2 \overline{\rho_A}}{\partial x^2} - \frac{\partial}{\partial x}(\overline{u' \rho_A'}) \qquad (2.171)$$

Were it not for the last term in eq. (2.171), solutions to eq. (2.171) would be identical to laminar flow solutions of the equation of continuity. Thus the emphasis in turbulent mass transfer has been that of attempting to find a suitable expression for this last term which could be readily evaluated.

The most common method used to evaluate the turbulent mass flux has been that of making an analog to molecular diffusion. Thus defining, from eq. (2.171),

$$\overline{u' \rho_A'} = J_x(t) \qquad (2.172)$$

where $J_x(t)$ is the turbulent mass flux in the x direction, the general approach has been to say

$$J_x(t) = -E_D \frac{\partial \overline{\rho_A}}{\partial x} \qquad (2.173)$$

where $E_D$ is an eddy diffusivity. One of the more recent studies using this basic form was that of Harleman's (89). The difficulty in using this form is, of course, as with the eddy viscosity or mixing coefficient of Boussinesq (195), that the eddy diffusivity is a flow property and not a fluid property.

Sherwood (206) points out that one common method used in an attempt to determine the eddy diffusivity has been to assume that it is directly proportional to Boussinesq's eddy viscosity, such reasoning arising from the similarity of eq. (2.173) to Boussinesq's expression for the Reynolds' shear stress, viz., (198).

$$\tau_t = \varepsilon \frac{dU}{dy} \qquad (2.174)$$

where $\tau_t$ = Reynolds' shear stress and $\varepsilon$ = eddy viscosity. As Lin, Moulton, and Putnam (155) noted however, for flow with the same turbulence conditions the eddy viscosity is exactly equal to the eddy diffusivity (158). Using this relation in the investigation of mass transfer close to pipe walls they found the eddy diffusivity to be proportional to the cube of the

distance from the pipe wall. It is to be noted that their analysis assumed the existence of small scale turbulence, micro-turbulence, occurring even very near the pipe wall in the laminar sublayer. Using expressions for the velocity distributions in turbulent flow to determine expressions for eddy distribution, they found the total mass flux to vary as the two-thirds power of the molecular diffusivity near the pipe walls.

For transport in pipes, Deissler (9) has formulated a complex exponential function to predict the turbulent mass flux near a pipe wall assuming the mechanisms of momentum and mass transport are identical. For large values of the kinematic viscosity of the fluid, Deissler's equations predict the eddy diffusivity to vary as the square of the distance from the pipe wall while the mass transfer coefficient varies as three-fourths power of the molecular diffusivity (95).

As has been pointed out by Harriott (95) both Lin, Moulton, and Putnam's and Deissler's equations fit experimental data equally well since the equations contain constants which require experimental determination.

Unsteady State Transfer. Doubtful that a stagnant or even laminar liquid film existed at the free surface of an agitated liquid into which a gas was being absorbed, Danckwerts proposed his surface renewal theory in 1951 (23). Danckwerts' basic concept was that the turbulence in the liquid continually caused the transport of fresh fluid from

within the bulk of the liquid to the free surface. The fresh fluid would remain exposed at the free surface for a short period and then be swept back into the interior of the liquid. Thus, though he denied the existence of a laminar film, Danckwerts' hypothesis was similar to that of Higbie's penetration theory (103) in that contact time between phases was limited and absorption of a solute would be time dependent. Furthermore, the transfer through the interfacial region of each eddy swept to the surface was supposedly by molecular diffusion. Turbulence was then responsible for the transfer of solute to depths below the interfacial region. Thus in the interfacial region the transfer was unsteady as in Higbie's penetration theory.

To describe this surface renewal process, as Danckwerts termed it, he introduced a factor s, the rate of production of fresh surface. From a purely statistical standpoint, Danckwerts related the rate of fresh surface production to the area occupied by this fresh surface. Based on this formulation he found that the mass flux of a diffusing gas, say A, could be put in a form very similar to that introduced in connection with the two film theory. Thus for a gas A dissolving into a liquid B in the x direction, Danckwerts showed that

$$N_{A_x} = (\rho_{AB_i} - \rho_{AB_b})\sqrt{Ds} \qquad (2.175)$$

where s is the surface renewal rate and the other notation is as previously defined.

The difficulty with the surface renewal concept lies in the determination of s. As Danckwerts himself pointed out, the rate of surface renewal is some complex function of the hydrodynamics of the surface. In general it could not be predicted analytically but would have to be determined experimentally.

To be noted from eq. (2.175) is that, as in Higbie's penetration theory (103), the surface renewal theory predicts that the rate of absorption is proportional to the square root of the diffusivity.

Comparison of eq. (2.60) with eq. (2.175) shows that

$$k_L = \sqrt{Ds} \tag{2.176}$$

In a manner similar to that which leads to the definition in eq. (2.71) it can be shown that if there exists a gas resistance in addition to the liquid resistance predicted by the surface renewal theory then the total resistance is, in a dilute solution,

$$\frac{1}{K_L} = \frac{1}{k_L} + \frac{H}{k_G} = \frac{1}{\sqrt{Ds}} + \frac{H}{k_G} \tag{2.177}$$

where H, Henry's constant, takes the place of m in eq. (2.72) for dilute solutions. Indeed, as shown by Danckwerts, if one were to consider the situation in which there existed close to the free surface, say at a level a, a concentration $\rho_{AB_a}$, less than the interfacial concentration $\rho_{AB_i}$, but greater than the bulk concentration $\rho_{AB_b}$ at level b, then the total film resistance is

$$\frac{1}{k_L} = \frac{1}{k_e} + \frac{1}{\sqrt{Ds}} \qquad (2.178)$$

where $(1/k_e)$ is the resistance encountered in the transfer from levels a to b due to turbulence. Examination of eqs. (2.177) and (2.178) demonstrates the utility of Whitman's basic concept of additive resistances to transfer.

In 1935 Fage and Townend (57) had observed with an ultramicroscope that within the laminar sublayer at a solid surface, at approximately 1/40,000 of an in. from the flow boundary, the flow was not at all rectilinear but rather underwent apparently viscous motion in which fluid particles followed sinuous paths. Spurred by this observation, Hanratty in 1956 (86) proposed a modification of Higbie's penetration theory using Danckwerts' surface renewal concept. Rather than only one contact time as Higbie's original penetration theory assumed, Hanratty considered a distribution of contact times based on the probability that any eddy would be swept to the

interface and expose new surface for a limited time period. As opposed to Danckwerts' rate of surface production factor s, Hanratty introduced a general function $f(t_{ct})$ describing the distribution of contact times. Though Hanratty used an exponential function for $f(t_{ct})$, the form chosen was arbitrary.

With the introduction of the contact time distribution function into Higbie's analysis the rate of mass transport in the x direction, of a component A, became

$$\bar{N}_{A_x} = \frac{2(\rho_{AB_i} - \rho_{AB_b})}{\sqrt{\pi}} \int_0^\infty f(t_{ct}) \sqrt{\frac{D}{t_{ct}}}\, dt \qquad (2.179)$$

where t = time, $t_{ct}$ = contact time, $f(t_{ct})$ = contact time distribution function, $\bar{N}_{A_x}$ = time average value of $N_{A_x}$, and the other notation is as previously defined. In the special case in which the contact time is constant for all eddies, $f(t_{ct})$ equals $1/t_{tc}$ and, as shown by Hanratty, eq. (2.179) becomes

$$\bar{N}_{A_x} = 2(\rho_{AB_i} - \rho_{AB_b}) \sqrt{\frac{D}{\pi t_{ct}}} \qquad (2.180)$$

Comparison with eq. (2.97) will show the similarity of the two equations predicting the mass flux if the solution into which A is dissolving be considered dilute.

Defining the average mass transfer coefficient as

$$\overline{k_L} = \frac{\bar{N}_{A_x}}{\rho_{AB_i} - \rho_{AB_b}} \qquad (2.181)$$

in a form analogous to eq. (2.83), then for dilute solutions, from eq. (2.79),

$$\overline{K_L} = \frac{2}{\sqrt{\pi}} \int_0^{\infty} f(t_{ct}) \sqrt{\frac{D}{t_{ct}}}\, dt \qquad (2.182)$$

where $\overline{K_L}$ is the average value of $K_L$. This reduces to, as shown by Hanratty,

$$\overline{K_L} = 2\sqrt{\frac{D}{t_{ct}\pi}} \qquad (2.183)$$

for constant contact times for all fluid eddies.

To be noted, as with the penetration theory, the mass transfer coefficient varies as the square root of the diffusivity.

A turbulent mass transport model was proposed by Toor and Marchello (220) which combined the concepts of the film, penetration, and surface renewal models. Toor and Marchello considered the fact that eddies brought to an interface would remain at the surface different lengths of time. Though this was the idea that Hanratty proposed, Toor and Marchello approached it differently. Those eddies which remained only a short time near the surface would be subject to only a small degree of penetration by the solute. As the time which an eddy resided at the surface increased, penetration would in-

crease. As opposed to Higbie's model, however, this penetration would not go on indefinitely. If the average thickness of these eddies was L where at a depth L below the surface the concentration became that of the bulk of solution, then at some finite time after an eddy reached the surface, its concentration at depth L would reach the bulk concentration. When the concentration reached this level penetration ceased because a steady state concentration profile had been achieved. Now transfer became described by the film theory and proceeded at a rate given by the film theories discussed earlier. Some eddies, however, would begin to near the steady state condition but be swept away prior to its achievement. Thus it could be expected there would be eddies near the interface which had characteristics of both penetration and film models as well as those eddies which were closely described by the film theory or the penetration theory.

Within an eddy the transfer could be idealized as occurring by diffusion. Considering all the eddies, then, they could be idealized as a laminar film of thickness L which was subjected to periodic disruption or disturbance. During the periods of quiesence, then, the initial process became similar to that described in conjunction with Higbie's penetration theory. Thus the differential equation describing the transfer mechanism became the same as that which described Higbie's penetration theory, eq. (2.87). A change in boundary conditions, however, resulted in the model proposed by Toor

and Marchello. In place of eqs. (2.88), (2.89), and (2.90) Toor and Marchello had

$$\text{B.C.1: For } t \leq 0,\ \rho_A = \rho_{AB_b} \text{ for all } x \tag{2.184}$$

$$\text{B.C.2: For } x = 0,\ \rho_A = \rho_{AB_i} \text{ for all } t > 0 \tag{2.185}$$

$$\text{B.C.3: For } x = L,\ \rho_A = \rho_{AB_b} \text{ for all } t > 0 \tag{2.186}$$

To be noted is the change in B.C.3. The two equivalent solutions given by Toor and Marchello were

$$N_{A_x} = (\rho_{AB_i} - \rho_{AB_b}) \sqrt{\frac{D}{\pi t}} \cdot \phi_s \tag{2.187}$$

and

$$N_{A_x} = (\rho_{AB_i} - \rho_{AB_b}) \frac{D}{L} \cdot \phi_L \tag{2.188}$$

where eq. (2.187) describes the transfer for eddies of short life and eq. (2.188) describes the transfer for eddies which had been in existence at the interface for a relatively long time. $\phi_s$ and $\phi_L$ are defined by

$$\phi_s = 1 + 2 \sum_{n=1}^{\infty} \exp\left(- \frac{n^2 L^2}{Dt}\right) \tag{2.189}$$

and

$$\phi_L = 1 + 2 \sum_{n=1}^{\infty} \exp(-n^2 \pi^2 \frac{Dt}{L^2}) \qquad (2.190)$$

It is seen that $\phi_s$ and $\phi_L$ introduced the effects of the limiting steady state concentration profile. If eddy life is very short, eq. (2.187) merely reduces to the form predicted by Higbie's penetration theory while if eddy life is long eq. (2.188) approaches that of the simple film theory applied to transfer in one phase.

Though Toor and Marchello's concept of mass transfer near any interface bounding a turbulent fluid seems to be one of the more realistic, Harriott (91) has noted that, for pipe flow, use of Toor's and Marchello's equations predict transfer coefficients which are too large.

## Summary of Dimensionless Parameters

Most of the dimensionless parameters which have been developed in preceding pages and used to characterize mass transport have an analogous form in the fields of momentum and heat transfer. The basic similarity of momentum, heat, and mass transfer has long been recognized and has been one of the most frequently used methods in applying the analyses of relatively well understood phenomena to little understood phenomena. Many of the relationships developed in preceding paragraphs had their origin in the fields of momentum and

heat transfer. Indeed, Fick (59, 60) used as primary justification of his first law the apparent similarity between heat and mass transfer. Likewise, the extensions of Prandtl's boundary layer theory to heat and mass transport had their origin in the basic similarity of all transport phenomena. Thus many of the mass transfer parameters which shall be summarized here and which were introduced in previous sections of this chapter have completely analogous heat and momentum forms. However, in order that the relation to mass transfer be apparent they will be discussed on the basis of mass transfer considerations.

In any dynamical fluid system the ratio of the inertial forces to the viscous drag forces becomes of primary importance because of its distinctive characterization of the motion of the system. Thus it is that in mass transfer, as in all transport phenomena, the Reynolds number finds frequent usage, as, for instance, it did in the example of mass transfer in a laminar boundary layer over a flat plate given earlier.

Also developed earlier was the Peclet number for mass transfer, which in a general form is

$$Pe = \frac{LV}{D} \tag{2.191}$$

where L = characteristic length, V = characteristic velocity, and D = diffusivity. The basic significance of Pe can be understood if the development which led to eq. (2.136) be consid-

ered. The convective flux in a system can be represented by $\rho V$, where $\rho$ is a characteristic mass density, while the diffusive flux is represented by $D(d\rho/dx)$, where the notation is the same as used previously. The ratio of the convective flux to the diffusive flux thus becomes

$$\frac{\rho V}{D d\rho/dx} \tag{2.192}$$

Representing this ratio in terms of its basic dimensions, it reduces directly to Pe. Thus the Pe can be considered to provide a measure of the relative magnitude of the convective flux and diffusive flux in a system.

Examining eq. (2.166) it is seen the Schmidt number characterizes the concentration boundary layer and its thickness relative to the hydrodynamic boundary layer (132). It occupies the same role as the Prandtl number in heat transfer phenomena.

From eq. (2.83) the total mass flux of A is represented approximately by

$$N_A = K \Delta \rho_A$$

The diffusive flux, on the other hand, is given by eq. (2.1). In a finite difference form the diffusive flux becomes

$$J_A = D \frac{\Delta \rho_A}{\Delta x}$$

Thus the ratio of the total mass flux to the diffusive flux becomes

$$\frac{N_{A_x}}{J_{A_x}} = \frac{K\Delta\rho_A}{D\Delta\rho_A/\Delta x} = \frac{K\Delta x}{D} \qquad (2.193)$$

or, in general,

$$N_A/J_A = KL/D = Sh \qquad (2.194)$$

where K = mass transfer coefficient, L = characteristic length, D = diffusivity, and Sh is the Sherwood number (96, 98). Thus the Sherwood number is indicative of the relative amount of the total mass transfer which is occurring by diffusion. It can also be treated equally well as representing a dimensionless mass transfer coefficient (132).

To relate the Sherwood number to the Schmidt and Reynolds numbers consider eq. (2.137). Symbolically differentiating eq. (2.137) the general expression

$$\frac{\partial \rho^*}{\partial y^*} = f_5(Re,Sc) \qquad (2.195)$$

results, where $f_5$ is some function. From eq. (2.83)

$$N_A = K\Delta\rho_A = K(\rho_{AB_i} - \rho_{AB_b}) \qquad (2.196)$$

where the notation is similar to that used earlier. But for systems of low concentration, from eq. (2.84), with transfer in the y direction

$$N_A \simeq J_A = D\frac{\partial \rho_{AB}}{\partial y} \tag{2.197}$$

Therefore

$$D\frac{\partial \rho_{AB}}{\partial y} \simeq K(\rho_{AB_i} - \rho_{AB_b}) \tag{2.198}$$

or, from the definition of eq. (2.132),

$$D\frac{\partial \rho^*}{\partial y} \simeq K \tag{2.199}$$

This can be put in the equivalent form, from eq. (2.109),

$$\frac{\partial \rho^*}{\partial y^*} \simeq xK/D \tag{2.200}$$

which, replacing x with the general length term L, becomes

$$\frac{\partial \rho^*}{\partial y^*} \simeq LK/D = Sh \tag{2.201}$$

But from eq. (2.194) this is equivalent to, as given by Eckert (48),

$$Sh = f_s(Re,Sc) \qquad (2.202)$$

Thus it could be expected that the Sherwood number is a function of the Reynolds and Schmidt numbers in a mass transfer system. This expression finds wide usage in mass transfer studies.

Since interphase mass transfer involves transfer through an interface it would be expected that the forces existing at the interface would be useful in describing certain interfacial phenomena. Thus it is that the well known Weber number, the ratio of inertial forces to surface tension forces, also finds frequent usage in mass transfer literature. Thus the Weber number is defined as

$$We = \frac{\rho V^2 L}{\sigma} \qquad (2.203)$$

where $\sigma$ is the surface tension and the other notation is as defined previously.

In many instances free, or natural, convection of a solution becomes of considerable importance and it is desirable to have a parameter descriptive of the buoyant forces which give rise to the free convection. The buoyant force on a fluid particle or immersed body can be represented generally by

$$\text{Buoyant Force} = L^3 g \Delta\rho$$

where L = characteristic length, g = acceleration due to gravity, and $\Delta\rho$ = difference in densities of the fluid particle or immersed body and the surrounding fluid. In applications of boundary layer theory the difference in the densities is usually that between the free stream solution density and the interfacial density.

The relative magnitude of this buoyant force to the inertial force on the particle or immersed body is expressed by their ratio:

$$\frac{\text{buoyant force}}{\text{inertial force}} = \frac{L^3 g \Delta\rho}{\rho L^3 \cdot L/t} \qquad (2.204)$$

where $\rho$ = the surrounding fluid density and t = time. To express this in a more usable form this ratio is multiplied by the square of the Reynolds number in which case the above ratio reduces to, in general terms,

$$GR = \frac{L^3 g \rho}{\rho \nu^2} \qquad (2.205)$$

where GR = Grashof number (226) and $\nu$ = kinematic viscosity.

As eq. (2.202) is used to describe mass transfer in forced convection systems, a similar form can be used to describe free convection systems (49), viz.,

$$Sh = f_6(Gr, Sc) \qquad (2.206)$$

where $f_6$ = some function.

Other parameters, of course, can be, and have been developed in connection with mass transfer, but those presented here, or slight modifications of them, are those most commonly used. For this study the dimensionless quantities summarized here will be sufficient for the objectives of this study.

# CHAPTER III

## THEORY OF MASS TRANSFER IN LIQUID DROPLETS

Mass transfer in bubble and droplet systems has received enormous attention over the years. This topic has significant practical applications in such varied fields, for instance, as fractionation, liquid-liquid extraction, drying, combustion, gas scrubbing, and meteorology (51, 104, 127, 129). Furthermore it holds promise of useful and valuable applications in yet undeveloped areas.

While the discussion presented in this chapter can, in general, be applied equally well to bubbles of gas or droplets of liquid, attention will be focused on liquid droplets because the interests of this study lie in this area. Indeed, it should be realized that though the term droplet may be used, some of the information presented here has had its origin in studies dealing with gas bubbles rather than liquid droplets.

Many of the applications of droplet systems employ a spray operation in which numerous individual droplets are produced. A rigorous treatment of the mass transfer in such a system would include an analysis of each of the various sizes of droplets, such analysis, in all likelihood, being based on a consideration of the droplet size distribution. Comparatively few studies have been made that are of this rigor, although

Gal-Or and Hoelscher (63) presented a mathematical treatment of the effects of particle size distribution on mass transfer. Such a treatment, however, does necessitate a rather accurate knowledge of the particle distribution if it is to be of value.

Many experimental studies have dealt with droplets of a single, known size. This, of course, results in a considerable reduction in complexity. While the results of these studies can be amplified to take into consideration the effects of the dispersed phase (i.e., the droplet phase) distribution, often the results have been applied directly to multi-sized droplet systems by considering a particular size droplet to typify the system. Indeed, it has been noted (75) that consideration of an isolated droplet occasionally approximates the multi-droplet system quite well. In any case, the examination of a single droplet provides a starting point for study. Understanding of the single droplet is necessary if one is to obtain a clear understanding of the multi-droplet system. For these reasons, this discussion will consider transfer in a single droplet only.

Four zones of interest are often recognized in mass transfer in droplets: drop formation, drop deacceleration or acceleration to a steady velocity, drop rise or fall at a steady velocity, and drop coalescence (119, 122, 181). While some studies have analyzed end effects to a considerable degree (121, 208), many investigators have concentrated their efforts on the steady state period. Indeed, most theoretical

models proposed for mass transfer assume the droplet is translating at a constant velocity. Periods of acceleration or deacceleration can be treated, at least approximately, by assuming them to be composed of a finite number of periods of steady droplet velocity, each period having an increase or decrease in the velocity. In this present discussion it will be assumed that the droplet is translating at a constant velocity.

As with the discussion in the preceding chapter it will be assumed that transfer rates are sufficiently low that momentum and mass transfer are essentially independent of each other. Much work has proceeded on this basis (133). Consideration will also be limited to isothermal systems.

Considering the various fluid, flow, and transfer properties which might influence mass transfer in and around a single droplet, it would be expected that, in general, properties of the droplet (discontinuous phase) itself, as well as the surrounding fluid (continuous phase), would be of importance. Thus if the droplet were translating at a constant velocity relative to the surrounding fluid, the pertinent variables would appear to be, in addition to the relative velocity and size of the droplet, the viscosities, densities, and diffusivities of both phases, the overall transfer coefficient, the surface tension (209), and the difference in specific weight of the two phases. These variables can be arranged in the dimensionless equation

$$Sh = f(Re_c, Sc_c, We_c, Gr_c, \rho_d/\rho_c, \mu_d/\mu_c, D_d/D_c) \qquad (3.1)$$

where

$$Sh = \frac{Kd_d}{D_c} \qquad (3.2)$$

$$Re_c = \frac{Ud_d}{\mu_c} = \frac{Ud_d}{\nu_c} \qquad (3.3)$$

$$Sc_c = \frac{\mu_c}{\rho_c D_c} = \frac{\nu_c}{D_c} \qquad (3.4)$$

$$Gr_c = \frac{gd_d^3 \Delta\rho}{\rho_c \nu_c^2} \qquad (3.5)$$

$$We = \rho_c \frac{U^2 d_d}{\sigma} \qquad (3.6)$$

K = overall transfer coefficient, U = droplet velocity relative to surrounding fluid, $d_d$ = droplet diameter, $\rho$ = density, $\mu$ = viscosity, D = diffusivity, $\sigma$ = surface tension, $\nu$ = kinematic viscosity, g = acceleration of gravity, f = function, $\Delta\rho = \rho_d - \rho_c$, and the subscripts c and d refer to the continuous and the discontinuous phases, respectively. (In Chapter II, the subscript "C" was used to denote merely phase C. In this chapter the subscript "c" implies the continuous phase. Since the continuous phase can be treated merely as phase C, the subscripts "c" or "C" can be used interchangeably in this and remaining chapters.)

The difficulty in determining the functional form of eq. (3.1) is considerable, to say the least. Some progress has been made towards this end in the area of the continuous phase by the application of boundary layer theory, in which case the Sherwood number is based on the continuous phase transfer coefficient. However, in the forms thus far proposed, all parameters have not yet been successfully incorporated and little is known about the interrelations of the various parameters. For transfer within droplets mathematical models have generally been formulated and compared with experimental results rather than attempting to determine the form of eq. (3.1) (118). Thus the emphasis in mass transfer in the continuous phase has been the development of dimensionless correlations while within the dispersed phase, the droplet, emphasis has been upon mathematical models (181).

With the assumption of interfacial equilibrium, generally a reasonable assumption (230, 246), especially in systems with small mass transfer rates (229), mass transfer in droplet systems has therefore quite often been approached from one of two viewpoints: transfer within a droplet and transfer in the continuous phase surrounding the droplet (181). Both will be considered in the following paragraphs. Though they will be treated essentially separately, it should be apparent from previous discussions they are not at all independent. Indeed, this dependence will be quite evident when transfer inside a droplet is examined.

Even if transfer in only one phase is considered, the viscosity ratio in eq. (3.1) must still be included because of the possible existence of droplet circulation, that is, internal motion of the droplet. Such motion can be seen to affect the mass transfer within a droplet because of its obvious mixing effect. Perhaps not as apparent is its influence on transfer in the continuous phase surrounding the droplet. Movement of the droplet surface, because of internal motion, however, can greatly influence the boundary layers and concentration gradients in the surrounding fluid in near proximity of the droplet surface. Thus droplet circulation is an important consideration. For this reason, it will be worthwhile to briefly examine droplet circulation prior to considering mass transfer in the continuous and discontinuous phases of a droplet system. Surface tension, furthermore, has a considerable influence on the magnitude of droplet circulation (92, 187), thus explaining the need for the inclusion of the Weber number in eq. (3.1). Because of this influence, surface tension will also be briefly examined in relation to its effects on droplet circulation.

## Droplet Circulation

The movement of a liquid droplet through a fluid can be significantly different from that of a solid sphere because of the mobile interface which a liquid possesses. The viscous shear acting on the surface of a droplet translating through a

fluid will tend to set the surface layers of the droplet fluid in motion. This motion will be transmitted into the interior portions of the droplet creating an internal circulation within the droplet. The surrounding fluid literally drags the fluid inside the droplet from the region of the upstream stagnation point to that of the downstream stagnation point.

Assuming inertial terms to be of negligible magnitude, Hadamard (81) and Rybcznski (143) independently solved the Navier-Stokes equations for the internal motion of a liquid droplet of constant radius in 1911, although most writers attribute the solution to Hadamard. The flow pattern predicted by their solution for a droplet falling in the negative x direction is shown in Fig. 6. The internal motion is given by the stream function

$$\Psi_d = \frac{1}{2} B\left(1 - \frac{r^2}{a^2}\right) r^2 \sin^2\theta \qquad (3.7)$$

where

$$B = \frac{1}{2} \left(\frac{\mu_c}{\mu_d+\mu_c}\right) U \qquad (3.8)$$

$$U = \frac{2}{3} g(\rho_d-\rho_c) \frac{a^2}{\mu_c} \frac{\mu_c+\mu_d}{2\mu_c+3\mu_d} \qquad (3.9)$$

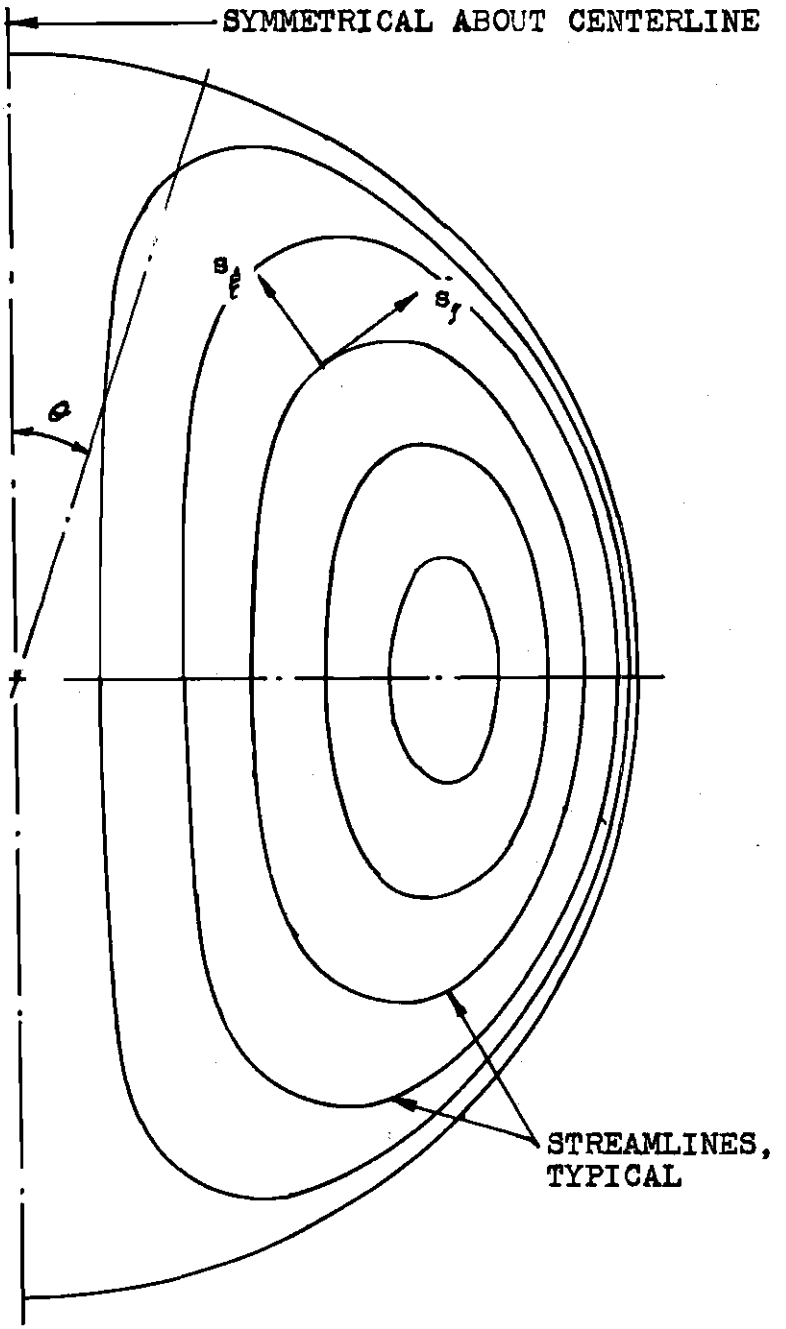


Figure 6. Droplet Circulation as Predicted by Hadamard

$\Psi_d$ = stream function for internal motion, r = radial distance, a = droplet radius, $\theta$ = polar angle as shown in Fig. 6, U = relative velocity of droplet, and the other notation is as used earlier. The radial velocity of the droplet fluid is therefore

$$V_r = -B(1 - r^2/a^2)\cos\theta \qquad (3.10)$$

while the tangential velocity is

$$V_\theta = B(1 - 2r^2/a^2)\sin\theta \qquad (3.11)$$

Because of axial symmetry, $V_\phi$, the velocity in the direction of the meridional angle, is zero.

Droplet circulation is a physical reality, not merely mathematical conjecture. It has been observed by numerous investigators (107, 119, 134, 150) and quite often has shown a striking similarity to that predicted by eq. (3.7). It has been observed for continuous phase Reynolds numbers, $Re_c$, less than 0.003 (232) and, though the circulation described by eq. (3.7) is theoretically applicable to droplets only in Stokian flow, that is, droplets for which $Re_c$ is less than approximately one, circulation similar to that predicted by eq. (3.7) has been observed for droplets considerably outside the Stokian range (108). Garner found this circulation to exist in droplets with $Re_c$ on the order of ten (119). Horton, Fritsch, and

Kintner (107) photographed droplets with circulation patterns very similar to the theoretical for a range of Reynolds numbers of four to 19. They also found the velocities predicted by eqs. (3.10) and (3.11) to agree moderately well with experimentally measured circulation velocities. Calderbank and Korchinski (19) indicate the existence of some type of internal motion at Reynolds numbers as high as approximately 120.

The droplet circulation which has been observed, however, has been in droplets moving in liquid media. Circulation of droplets in gaseous media has not been verified and it is questioned whether or not it exists (150). As seen from eqs. (3.5) and (3.6) the circulation velocity is dependent on the ratio of the continuous phase and dispersed phase viscosities and the droplet velocity. Since the viscosity ratio would be small for liquid droplets in gaseous media, circulation of appreciable magnitude would most likely not exist for small droplet velocities. In those velocity ranges which would supposedly give rise to noticeable circulation in drops moving in gaseous media, not only do Reynolds numbers become large but also experimental methods for circulation observation become more difficult. Thus the doubt surrounding circulation in liquid droplets moving through gaseous media exists.

Surface tension has a significant influence on droplet circulation. If a simplified droplet interface is visualized as in Fig. 7, where $u_c$ and $u_d$ are the fluid velocities in the

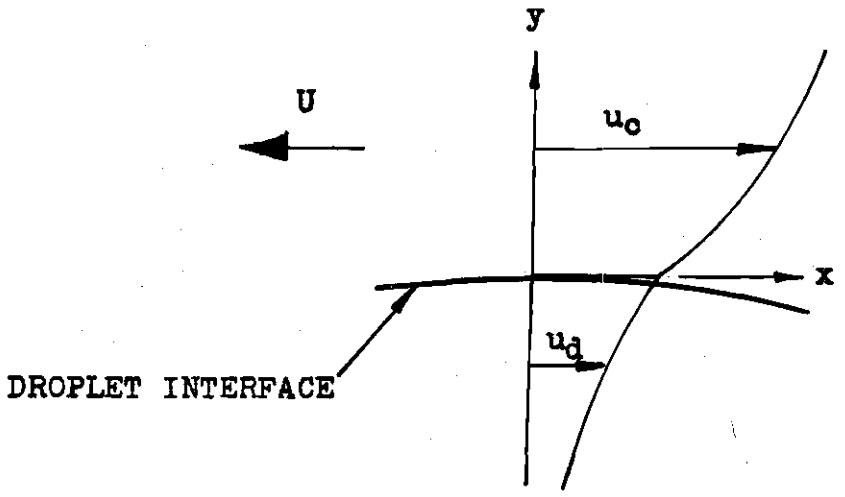


Velocities at Interface

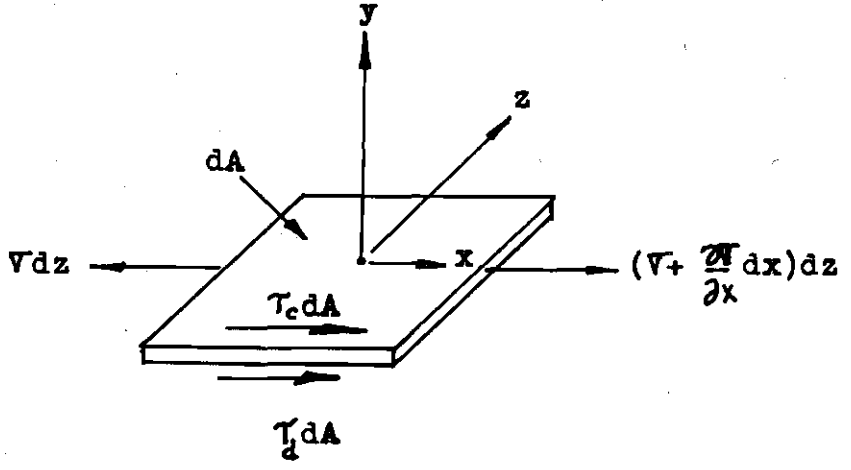


Force Balance

Figure 7. Forces at Droplet Interface

continuous and the droplet phases, respectively, it can be seen why. The shear stresses acting on each side of the interface are balanced by the surface tension gradient (90, 189). Considering a differential area of droplet interface, dA equal to dxdz as shown in Fig. 7, it is seen that a summation of forces acting on dA yields

$$\tau_d - \tau_c = \frac{\partial \sigma}{\partial x} \tag{3.12}$$

where $\tau_c$, $\tau_d$ = shear stress in continuous and discontinuous phases, respectively, and x = distance in direction of the tangential velocity of droplet interface. Assuming viscous flow at the interface and using Newton's law of viscosity, eq. (3.12) becomes

$$\mu_d \frac{\partial u_d}{\partial y}\bigg|_{y=o} - \mu_c \frac{\partial u_c}{\partial y}\bigg|_{y=o} = \frac{\partial \sigma}{\partial x} \tag{3.13}$$

For a given velocity in the continuous phase, an increasing surface tension gradient will result in a decreasing magnitude of the circulation velocity in the droplet. Indeed, if the surface tension gradient became sufficiently large, the circulation could cease altogether (76, 189).

Surface tension gradients can be produced by variations in the concentration of a surfactant at the droplet

surface since the interfacial tension is dependent on surfactant concentration (188). A surface active agent, if present in the droplet fluid, will tend to accumulate at the droplet surface (76, 109). The droplet circulation will sweep the surfactant to the rear of the droplet (96, 231) where it will tend to remain at the droplet surface because of the same molecular forces which originally brought the surfactant to the interface. The accumulation at the rear of the drop will create a variation in concentration of the surfactant over the drop surface resulting in a surface tension gradient (190).

Treybal (231) has noted that surface tension gradients could possibly occur even without surfactants because of nonuniformity of absorption rates over a droplet surface resulting in concentration gradients paralleling the droplet surface.

Bond and Newton (14) were the first (111) to examine the effects of surface tension on droplet circulation. Experimenting with water droplets in oil they observed that small droplets tended to approach the terminal velocity predicted by Stokes law for solid spheres, really a special case of eq. (3.9) (191). Using dimensional analysis they determined a critical droplet diameter at which the transition from rigid droplet to circulating droplet behavior supposedly occured. They proposed (101)

$$d_{dc} = 2\sqrt{\sigma/(\rho_d-\rho_c)g} \qquad (3.14)$$

where $d_{dc}$ is the critical droplet diameter and the other notation is as before. Bond and Newton's work has been criticized, however, since in all likelihood, surface contamination was present in their experiments and they failed to include the effects of a surface tension gradient in their analysis (191).

Savic (191) observed the formation of stagnant caps over the rear portion of droplets with surfactant contamination. Attempting to analyze this observed phenomenon and its effect on droplet drag and circulation, Savic concluded that droplet distortion must be considered in precise analysis of droplet motion. Schechter and Farley (187) proposed a surface tension distribution for a spherical droplet. Concluding this to be the only possible distribution compatible with sphericity, they incorporated this distribution into the boundary conditions for a droplet in creeping motion and derived a more general form of eq. (3.7) which included an interfacial tension parameter. Nonagreement of their theoretical model with the experimental results of Bond and Newton led them also to conclude that droplet distortion must be considered in analysis of droplet motion.

Inclusion of droplet distortion in analysis of droplet behavior, however, is quite difficult and many current investi-

gations continue to consider the idealized spherical droplet (117, 218). Retardation of circulation by surfactant accumulation, furthermore, may not be of consequence in many instances since surfactant accumulation at the droplet surface does not take place instantaneously. Horton, Fritsch, and Kintner found in their experimental studies that circulation seemed to decay exponentially with droplet age. They found that the circulation velocity reached approximately fifty per cent of its original value after only four minutes after droplet formation (109). Griffith has also pointed out that high droplet velocities, low interfacial tension, and short droplet lives all tend to decrease the importance of surface active agent effects (79). These factors, however, must be balanced against the consideration that surfactant effects are quite pronounced even for small concentrations of surfactant if surface tension is large (92).

## Transfer To and From Droplets

Investigations of mass transfer to and from drops have generally fallen in one of two realms (37): (1) mass transfer to stationary drops in a stagnant fluid and (2) transfer to drops in motion. While transfer to stationary drops does not have direct application to the interests of this study it is of value to briefly examine it since it furnishes a useful, theoretical lower limit on transfer rates in moving droplets.

Noncirculating Stationary Droplet in Stagnant Fluid

Consider a stationary, noncirculating droplet, that is a rigid sphere, in an infinite, stagnant medium. Assume a solute A is diffusing from, or to, the surface of the droplet which will be considered so well mixed that no concentration gradients exist in its interior. This being so, all resistance to the transfer of the solute will occur in the continuous phase. If the concentration at the surface, $\rho_{AC_i}$, and the concentration at infinity, $\rho_{AC_\infty}$, are maintained at a constant value, the rate of transfer will be constant. The equation of continuity for the dissolution of A in C, the solvent surrounding the droplet, since the transport mechanism is a diffusive one only, is given by eq. (2.19), which in spherical coordinates becomes (36)

$$\frac{\partial \rho_{AC}}{\partial t} = \frac{D}{r^2}\left[\frac{\partial}{\partial r}\left(r^2 \frac{\partial \rho_{AC}}{\partial r}\right) + \frac{1}{\sin\theta}\frac{\partial}{\partial \theta}\left(\sin\theta \frac{\partial \rho_{AC}}{\partial \theta}\right) + \frac{1}{\sin^2\theta}\frac{\partial^2 \rho_{AC}}{\partial \phi^2}\right] \tag{3.15}$$

Assuming complete symmetry with respect to $\theta$ and $\phi$, eq. (3.15) reduces to, since the diffusion is steady,

$$\frac{d}{dr}\left(r^2 \frac{d\rho_{AC}}{dr}\right) = 0 \tag{3.16}$$

where the notation is the same as that used previously. The boundary conditions are

$$\text{B.C.1:} \quad \rho_{AC} = \rho_{AC_i} \text{ at } r = a \tag{3.17}$$

$$\text{B.C.2:} \quad \rho_{AC} = \rho_{AC_\infty} \text{ at } r = \infty \tag{3.18}$$

where a is the radius of the sphere. The solution takes the general form (37)

$$\rho_{AC} = b/r + c \tag{3.19}$$

where b and c are arbitrary constants. Evaluation of b and c results in the solution

$$\rho_{AC} - \rho_{AC_\infty} = a(\rho_{AC_i} - \rho_{AC_\infty})/r \tag{3.20}$$

The mass flux is given by, from eq. (2.8) expressed in radial co-ordinates,

$$N_{Ar} = N_{Ar}\big|_{r=a} = J_{Ar}\big|_{r=a} = \left(-D_c \frac{d\rho_{AC}}{dr}\right)_{r=a} \tag{3.21}$$

where $N_{Ar}$ = total mass flux in radial direction, $J_{Ar}$ = diffusive flux in radial direction, and the other notation is as before. Evaluating eq. (3.21),

$$N_{Ar} = (D_c/a)(\rho_{AC_i} - \rho_{AC_\infty}) \tag{3.22}$$

From eq. (2.83) the term $D_c/a$ is recognized as a mass transfer coefficient. Therefore the Sherwood number, eq. (2.194), for the stagnant droplet, which shall be denoted by $Sh_s$, becomes

$$Sh_s = \frac{(D_c/a)2a}{D_c} = 2 \qquad (3.23)$$

where the droplet diameter has been used as the characteristic length. The appearance of this particular value of the Sherwood number occurs regularly in correlations for moving droplets as will be seen below. Since the rate at which the dissolution of a solute to or from the surface of a droplet of uniform concentration is minimal when both the surrounding fluid and the droplet itself are stationary, eq. (3.23) places a theoretical lower limit on the value of the Sherwood number for transfer in the continuous phase in moving droplet systems (4, 91, 101, 213).

It is to be noted from eq. (3.22) the transfer is directly proportional to the diffusivity. Only for the stagnant system is this predicted analytically (90). Significantly, it will be remembered that the two film theory of Whitman also predicts transfer proportional to the first power of the diffusivity. Their system was likewise assumed to be essentially stagnant.

Moving Droplets

Analysis of mass transfer to and from moving droplets has tended to fall in one of two areas: rigid drops and cir-

culating drops (212, 234), the rigid drops perhaps more properly being considered as spheres.

As might be expected, boundary layer theory has occupied a major position in the analysis of mass transfer to and from moving droplets and spheres. As discussed in the preceding chapter, the general, and rigorous, approach is that of solving appropriate momentum and continuity equations. Solution of boundary layer equations, especially when applied to spheres, is exceedingly difficult and recourse is almost always made to the various approximate methods. Analysis still remains difficult however and, as discussed previously, reliance on dimensionless parameters and correlations becomes the common mode of analysis, boundary layer theory having been used to indicate the pertinent parameters to be considered (53, 105).

Spheres. The most commonly found correlation, predominately so, for transfer to and from spheres and rigid droplets takes the general form (101, 212, 235)

$$Sh_c = Sh_s + gRe_c^{p}Sc_c^{r} \qquad (3.24)$$

where $Sh_c = k_c d_d/D_c$, $k_c$ = continuous phase transfer coefficient, g = coefficient, p,r = exponents, and the other notation is as defined earlier. For forced convection systems, $Sh_s$ is the Sherwood number for stationary drops in a stagnant medium previously calculated to be exactly 2 (see eq. 3.23). This

basic form was originally (5) proposed by Frossling in 1938 (62) in his study of evaporation from falling drops after obtaining an approximate solution to the Navier-Stokes equations. It will be recalled that in the discussion of dimensionless parameters in Chapter II a parametric form similar to eq. (3.24) was predicted (see eq. 2.202).

Ranz and Marshall extended Frossling's basic form to free convection systems. They proposed the similar form (40, 106)

$$Sh_c = Sh_s + hGr_c^{\ s}Sc_c^{\ t} \qquad (3.26)$$

where h = coefficient, s,t = exponents, and $Gr_c$ is the continuous phase Grashof number defined earlier. Eqs. (3.24) and (3.26) can be combined in the more general form (235)

$$Sh_c = 2 + gRe_c^{\ p}Sc_c^{\ r} + hGr_c^{\ s}Sc_c^{\ t} \qquad (3.27)$$

where $Sh_s$ has been replaced by its theoretically calculated value, and the second and third terms on the R.H.S. represent the effects of forced and free convection, respectively.

It should be pointed out that quite often the "2" in eqs. (3.24), (3.26), or (3.27) is omitted because it is of negligible magnitude in comparison to the other terms in many systems that are analyzed.

The flow conditions will, of course, influence to a considerable degree the values of these exponents and coefficients. The location of the separation point of the boundary layer will vary and thus the degree of transfer which occurs in the wake will likewise vary with flow conditions. Whether or not the boundary layer becomes turbulent or remains laminar can be expected to influence also the amount of transfer which occurs. As pointed out by Keey and Glen (131), the sometimes wide divergence in the various values reported for the coefficient and exponents in eq. (3.24) may be due to inadequate consideration of these factors. Indeed, they considered the general expression of eq. (3.24) to be not entirely adequate because of wake effects and turbulence in the boundary layer.

For Reynolds numbers of 2 - 800 (62) Frossling determined semi-empirically the coefficient h to be 0.552 and the exponents p and r to be 1/2 and 1/3, respectively (101, 106). Ranz and Marshall (101, 106) found p and r to be the same but h to be 0.600. For h, s, and t, Ranz and Marshall determined the similar values of 0.600, 1/4, and 1/3, respectively (40, 106). Numerous other determinations have been made of the values of the various exponents and coefficients in the above equations, although those determined for eq. (3.24) are more commonly encountered. Resort has often been made to the use of assumed polynominal expressions for the concentrations and velocities in the hydrodynamic and concentration boundary layers (106, 126, 128), such as was done in the example of laminar flow over a

flat plate considered in Chapter II. Some analyses, on the other hand, are concerned with flow in the Stokian range, in which case the Navier-Stokes equations can often be solved (61, 126).

Steinberger and Treybal (235) made an extensive review of the literature and proposed the following: for Grashof and Schmidt numbers less than $10^8$

$$Sh_c=2+0.569(Gr_c\ Sc_c)^{0.250}+0.347(Re_c\ Sc_c{}^{0.5})^{0.62} \qquad (3.28)$$

while for Grashof and Schmidt numbers greater than $10^8$

$$Sh_c=2+0.0254(Gr_c\ Sc_c)^{1/3}Sc_c{}^{0.244}+0.347(Re_c\ Sc_c{}^{0.5})^{0.62} \qquad (3.29)$$

For summaries and tabulations of various exponents and coefficients determined by many investigators the reader is referred to (74, 131, and 208). It is to be noted that most of these correlations predict the transfer rate to vary as the 1/2 to 2/3 power of the diffusivity (209).

Circulating Droplets. Internal circulation has a considerable influence on transfer in the continuous phase surrounding a droplet (126, 128, 192, 213) as well as in the droplet itself because of several reasons. The circulatory mixing inside the droplet tends to speed transfer there, thus reducing the internal transfer resistance and allowing higher

transfer rates in the exterior phase (212). Circulation, furthermore, considerably influences the external flow pattern, resulting in a decreased thickness of the surrounding hydrodynamic boundary layer (52) and concentration boundary layer (126, 129, 213). In addition, since circulation speeds the rate at which fluid flows over the droplet surface, the contact time between particular particles of the surrounding fluid and the droplet surface is shortened. Transfer, therefore, occurs at the higher initial rates of early contact times rather than at the slower rates reached after long contact times. Thus the overall transfer rate is increased (192). Though these effects have been experimentally verified (74, 128, 192), external effects of circulation have received less attention than the internal effects of circulation (93).

Correlations for circulating droplets have quite often taken forms similar to those for rigid spheres, the effects of circulation being introduced by the incorporation of additional factors or absorbed in exponents and coefficients (77, 210).

Boussinesq (93), and later Ruckenstein (213), used potential theory to calculate an average, steady state Sherwood number assuming negligible hydrodynamic boundary layer thickness. They obtained

$$Sh = 1.13\ Pe^{1/2} \qquad (3.30)$$

It is interesting to note that this same equation can be obtained directly from Higbie's penetration theory (96, 101) if the time of contact between the two phases is approximated as the velocity of the sphere divided by its diameter. For dilute solutions, from eq. (2.101), the instantaneous transfer coefficient for the continuous phase is

$$k_c = \sqrt{D_c/\pi t} \tag{3.31}$$

The average transfer coefficient therefore becomes

$$\bar{k}_c = \frac{1}{t_{ct}} \int_0^{t_{ct}} k_c dt = 2k_c \tag{3.32}$$

where $\bar{k}_c$ = the average value of $k_c$ and $t_{ct}$ = the contact time. Introducting the simplification for the contact time, eq. (3.32) becomes

$$\bar{k}_c = (2D_c U/\pi d_d)^{1/2} \tag{3.33}$$

where the notation is as used previously. Upon rearrangement, eq. (3.33) becomes eq. (3.30). Sideman and Shabtai (213) note this is not unexpected since both Boussinesq's and Higbie's derivations are essentially based on a diffusion model. Harriott (93) takes exception to this, considering the agreement to be pure coincidence since Boussinesq's development

takes into consideration acceleration at the droplet surface while Higbie's does not. Though they used it in the analysis of their own experimental data, Garner and Skelland have also questioned the validity of applying Higbie's analysis directly to spherical droplets (27).

Conic and Savic (78), considering the energy dissipation by viscous forces and the energy imparted to the continuous phase by droplet circulation, introduced a factor $k_v$, the ratio of the actual interfacial velocity to the interfacial velocity predicted by potential theory, to account for the reduction in the hydrodynamic boundary layer thickness with increasing circulation (93). They found the hydrodynamic boundary layer thickness to vary as $(1 - k_v)^{0.5}$, $k_v$ tending to zero at low $Re_c$ and one at high $Re_c$ (213). Griffith (74) extended Conic and Savic's concepts by employing their factor in eq. (3.30) and experimentally verifying this new form, viz.,

$$Sh_c = 2 + 1.13\ Pe^{1/2} k_v^{1/2} \qquad (3.34)$$

where the term "2" is introduced for the same reason it was employed in eq. (3.27).

The effects of circulation have also been considered by introducing terms involving the ratio of the continuous and the discontinuous phase viscosities. Elzinga and Banchero (50) found the Sherwood number to vary as

$$\left(\frac{\mu_c+\mu_d}{2\mu_c+3\mu_d}\right)^{3.47}$$

while Heertzes, Holve, and Talsma (98) correlated their experimental results with the term

$$2\left[\frac{\mu_c}{(\mu_c+\mu_d)}\right]$$

Wakesima (209), on the other hand, merely used a ratio of the discontinuous and the continuous phase viscosities. In general, however, these forms can be represented as (77, 209)

$$Sh = g' Re_c^{p'} Sc_c^{r'} f(\mu_d/\mu_c) \qquad (3.35)$$

where $f(\mu_d/\mu_c)$ is some function of the discontinuous and the continuous phase viscosities, varying with the investigator, and $g'$, $p'$, and $r'$ have similar roles to g, p, and r in eq. (3.25). For tabulations of some of the various forms proposed and used by different investigators, the reader is referred to (74, 125, 127, 131 and 208).

## Transfer in Droplets

As opposed to mass transfer in the continuous phase surrounding a droplet, analysis of mass transfer inside of a droplet has usually been based upon some assumed mathematical

model (118). Furthermore, since droplets are of finite extent, as opposed to the, comparatively speaking, unlimited extent of the surrounding continuous phase, most models have necessarily been unsteady ones.

Internal droplet motion has received considerable attention in connection with transfer inside a droplet. Internal circulation has already been discussed. The effects of this motion on mass transfer has stimulated many investigations, a great many of whom have used the circulatory motion of a droplet in creeping flow, eq. (3.1). It has been pointed out that many of the investigations using Hadamard's stream function have been of systems with Reynolds numbers, $Re_c$, approaching 2000, the implication being that models based on this stream function may have wider applicability than might be anticipated (20, 213). Indeed, Hamielec and Johnson (125), using polynominal expansions for stream functions, have shown that the streamline pattern in spherical droplets in viscous flow having Reynolds numbers as high as approximately 80 is very similar to that predicted by eq. (3.1) for a droplet in the Stokian regime.

The effect of surfactants on droplet circulation has been discussed briefly earlier in this chapter. Since internal circulatory motion can considerably enhance mass transfer, any effect which tends to reduce this circulation will likewise reduce the mass transfer. Since there is some point at which accumulations of a surfactant become great enough to effectively stop circulation, a point which is peculiar to the drop-

let, (126) droplets without surfactants and similar droplets with surfactants can be expected to exhibit different transfer characteristics, those with sufficient concentrations of surfactant having transfer rates similar to rigid spheres (216). It has been noted, however, that droplets on the order of less than two mm, "small" droplets as they are termed, are not greatly affected by surfactants since they tend not to exhibit circulation anyway (216).

While droplet oscillation and distortion have frequently been observed (19, 50, 135, 144, 150, 180, 188), relatively little work has been done on the effects of oscillation and distortion on mass transfer in the dispersed phase, although it is known that they generally produce higher transfer rates (21, 236). Kinter and Rose (180), however, proposed a model for large oscillating drops. Droplet oscillation and distortion is not pronounced in small droplets, (232) that is, droplets which are on the order of less than one or two mm in diameter. Such size droplets tend to act more as rigid spheres (215). As droplet size increases, however, the dynamic pressure force acting in the region of the upstream stagnation point becomes sufficiently large to cause distortion and instability leading to oscillation (232). Furthermore, experimenting with droplets of 0.2 to 0.5 cm diameter, Calderbank and Korchinski (19), did not observe oscillation until $Re_c$ reached approximately 200. Droplet distortion and oscillation may, therefore, be of little consequence in small diameter droplet systems. For detailed

reviews of various aspects of drop and sphere mechanics, reference should be made to (64, 65, 66, 67, 68, 110, 141, and 233).

Since a droplet can exhibit such a wide range of characteristics which, in general, would be expected to reflect considerable influence on mass transfer in the droplet, it is of value to examine droplet models both which are stagnant and which exhibit some type of circulatory or oscillatory motion.

Rather than express transfer coefficients, essentially explicitly, in the form of a Sherwood number as is usually done for mass transfer in the continuous phase, transfer coefficients for the droplet phase are generally expressed implicitly in the form of a transfer efficiency (122, 209). For dissolution of solute A into a droplet, it can be defined as

$$E = \frac{\bar{\rho}_{AD} - \rho_{AD_o}}{\rho_{AD_i} - \rho_{AD_o}} \qquad (3.36)$$

where E = transfer efficiency for a time period equal to t, t being zero at beginning of the time period, $\bar{\rho}_{AD}$ = average solute concentration in droplet at time t, $\rho_{AD_o}$ = initial, uniform solute concentration in droplet, $\rho_{AD_i}$ = solute concentration at droplet interface. It is seen that E merely represents that fraction of solute of the maximum possible which is actually absorbed in time period t if no supersaturation is assumed to occur.

Also to express the efficiency of an absorption mechanism, the expression (50)

$$E' = \frac{\rho_{AD_i} - \bar{\rho}_{AD}}{\rho_{AD_i} - \rho_{AD_o}} \tag{3.37}$$

can be used, which represents, for absorption of solute A into a droplet, the fraction of mass not yet absorbed at time t. Thus higher transfer efficiencies result in small values of E'. The relationship between E and E' is given by

$$E = 1 - E' \tag{3.38}$$

as can be easily shown.

If a mass parameter is defined as the amount of solute at time t in a droplet above its initial uniform value, that is,

$$M(t) = (\bar{\rho}_{AD} - \rho_{AD_o})\forall_d \tag{3.39}$$

where M(t) is the mass parameter and $\forall_d$ is the drop volume, and M(0) is defined as

$$M(0) = (\rho_{AD_i} - \rho_{AD_o})\forall_d$$

then, from eq. (3.36),

$$\frac{M(t)}{M(0)} = E \tag{3.40}$$

Likewise, a mass deficiency parameter can be defined as the amount of solute by which the droplet concentration is less than the interfacial concentration, that is,

$$M'(t) = (\rho_{AD_i} - \bar{\rho}_{AD})\Psi_d \tag{3.41}$$

where $M'(t)$ is the mass deficiency parameter. From eq. (3.37) then

$$\frac{M'(t)}{M(0)} = \frac{M(t)}{M'(0)} = E' \tag{3.42}$$

where $M(0) = M'(0)$.

In the special case where the initial concentration of the droplet is zero, the mass parameter represents the total mass of solute in the droplet.

Using the difference in concentration between the interfacial value and average value in the droplet as the characteristic driving potential, then from eq. (2.83) the mass flux of A being absorbed into the droplet from the surrounding fluid is given by

$$N_A = k_d(\rho_{AD_i} - \bar{\rho}_{AD}) \tag{3.43}$$

where $k_d$ is an instantaneous, internal, droplet (i.e., discontinuous phase) transfer coefficient. Since the mass flux is the rate of mass transfer per unit area, eq. (3.43) can be rewritten as

$$\frac{d\bar{\rho}_{AD}}{dt} = \frac{6\pi d_d^2}{\pi d_d^3} k_d(\rho_{AD_i} - \bar{\rho}_{AD}) = \frac{6k_d}{d_d}(\rho_{AD_i} - \bar{\rho}_{AD}) \tag{3.44}$$

A time average transfer coefficient can be defined as

$$\overline{k_d} = \frac{1}{t} \int_0^t k_d dt \tag{3.45}$$

Therefore, using eq. (3.44)

$$\overline{k_d} = \frac{1}{t} \int_0^t \frac{d_d}{6} \frac{1}{\rho_{AD_i} - \bar{\rho}_{AD}} \frac{d\bar{\rho}_{AD}}{dt} dt \tag{3.46}$$

Thus, similar to that given by Johns and Beckman (120), and Garner and Skelland (25),

$$\bar{k}_d = \frac{-d_d}{6t} \ln \frac{\rho_{AD_i} - \bar{\rho}_{AD}}{\rho_{AD_i} - \rho_{AD_o}} = \frac{-a}{3t} \ln E' \tag{3.47}$$

since $\bar{\rho}_{AD} = \rho_{AD_o}$ at t equals zero. Therefore, using eq. (3.41),

$$\frac{M'(t)}{M'(0)} = \exp\left(-\frac{3\bar{k}_d}{a} t\right) \tag{3.48}$$

Also used at times to describe transfer characteristics in droplets is an effective diffusivity ratio, $R^*$, proposed by Calderbank and Korchinski (19), which is the ratio of the effective diffusivity which would result in the transfer actually measured in a system, if it be assumed the transfer mechanism is that which would occur in a noncirculating droplet, to the actual molecular diffusivity (123). Since the definition of $R^*$ does depend on an understanding of the stagnant drop model, as well as that model's relation to other transfer models, more detailed discussion of $R^*$ will be deferred until later paragraphs.

Noncirculating Droplet

As has been discussed above, in many instances a droplet may behave as if it were noncirculating. In such instances the transfer mechanism is necessarily one of diffusion. The equation of continuity for a spherical drop with constant diffusivity is therefore given by eq. (3.15). Assuming symmetry with respect to $\theta$ and $\phi$, it reduces to, for the dissolution of solute A in the droplet,

$$\frac{\partial \rho_{AD}}{\partial t} = D_D\left(\frac{\partial^2 \rho_{AD}}{\partial r^2} + \frac{2}{r}\frac{\partial \rho_{AD}}{\partial r}\right) \tag{3.49}$$

Newman (174) solved eq. (3.49) for the case of no continuous phase resistance, that is, uniform concentration in the continuous phase. His solution, for absorption into a droplet, is

$$E = 1 - \frac{6}{\pi^2} \sum_{n=1}^{\infty} \frac{1}{n^2} \exp\left[- \frac{n^2 \pi^2 D_d t}{a^2}\right] \qquad (3.50)$$

where the notation is that as used previously. An empirically determined (123) approximation to eq. (3.50) is (20, 211)

$$E \simeq \left[1 - \exp \frac{-D_d \pi^2 t}{a^2}\right]^{1/2} \qquad (3.51)$$

If only the first term in eq. (3.50) be considered, then, from eq. (3.48),

$$\bar{k}_d = - \frac{a}{3t} \ln \frac{6}{\pi^2} + \frac{\pi^2}{3a} D_d \qquad (3.52)$$

Neglecting the first term, which becomes small as time proceeds,

$$\bar{k}_d \simeq \frac{2\pi^2 D_d}{3d_d} \qquad (3.53)$$

which is similar to that given by Treybal (234).

In the more general case, resistance to transfer will occur in the continuous phase. Grober (122) determined the solution for the noncirculating drop for various values of the parameter $Sh^*$, defined as

$$Sh^* = \frac{k_c d_d}{D_d} \tag{3.54}$$

His solution, for absorption into the droplet, is (212)

$$E = 1 - 6 \sum_{n=1}^{\infty} A_n \exp\left(- \frac{\lambda_n^2 D_d t}{a^2}\right) \tag{3.55}$$

where $A_n$ is a constant and $\lambda_n$ is the eigenvalue (n=1, 2, ...$\infty$). Values of $A_n$ and $\lambda_n$ for various values of $Sh^*$ are given in (214). For the limiting case of $Sh^*$ approaching infinity, corresponding to no continuous phase resistance, $A_1$ and $\lambda_1$ are listed in Table 2.

Approximating the droplet transfer coefficient as done in obtaining eq. (3.53), it is seen that for the noncirculating droplet with continuous phase resistance

$$\bar{k}_d \simeq \frac{\lambda_1}{3} \frac{D_d}{a} \tag{3.56}$$

Circulating Droplet

Kronig and Brink (137) were apparently the first to theoretically consider transfer in a droplet with internal

circulation. In 1950 they presented a paper which considered mass transfer in a droplet in Stokian flow with the circulation being that predicted by eq. (3.7), Hadamard's stream function. In the model proposed by Kronig and Brink, resistance to transport in the external phase was considered to be negligible. This restriction of no continuous phase resistance was removed in 1959 by Elzinga and Banchero (50) who analyzed exactly the same model as that proposed by Kronig and Brink except that a range of continuous phase resistances were considered. Elzinga and Banchero's mathematical formulations were likewise very similar to those of Kronig and Brink. In the model proposed, transfer across streamlines was, since the circulatory motion was viscous, by diffusion. Convective transport along streamlines was considered to be so rapid, when compared to diffusive transport, that the concentration of solute around a complete circuit of any particular streamline was constant. Establishing a system of orthogonal curvilinear co-ordinates, designated as $s_\xi$, $s_f$, and $s_\phi$, where $s_f$ is parallel to the streamlines, $s_\xi$ is parallel to the equipotential lines, and $s_\phi$ forms the remaining orthogonal trajectory, as shown in Fig. 6, and defining

$$\xi = \Psi_d \frac{24(3\mu_d+2\mu_c)}{g(\rho_c-\rho_c)a^2} = 4R^2(1-R^2)\sin^2\theta \qquad (3.57)$$

$$f = \frac{R^4\cos^4\theta}{2R^4-1} \qquad (3.58)$$

$$\phi = \phi \tag{3.59}$$

and

$$R = r/a \tag{3.60}$$

where $\psi$ can be shown to represent the orthogonal trajectories of the streamlines, the concentration therefore became independent of $\psi$ and $s_\psi$. Since symmetry was assumed to exist in the $s_\phi$ direction, the concentration became a function of and time only. It is to be noted that $\xi$ and $\gamma$ are merely dimensionless streamlines and equipotential lines, $\xi$ ranging from 0 at the droplet surface to one at the point of no circulation on the droplet equator (see Fig. 6).

Considering a differential control volume with dimensions $ds_\xi$, $ds_\psi$, $ds_\phi$, and summing the mass flux entering and leaving this control volume, the equation of continuity became, for dissolution of solute A,

$$\frac{\partial}{\partial s_\xi}\left(D_d \frac{\partial \rho_{AD}}{\partial s_\xi} ds_\psi\, ds_\phi\right) ds_\xi = \frac{\partial \rho_{AD}}{\partial t} ds_\xi\, ds_\psi\, ds_\phi \tag{3.61}$$

since the transport in the $s_\xi$ direction is by diffusion only and no net transport occurs in the $s_\psi$ or $s_\phi$ directions. Integrating in the $s_\psi$ and $s_\phi$ directions, eq. (3.61) became

$$\int_{s_\gamma}\int_{s_\phi} D_d \frac{\partial^2 \rho_{AD}}{\partial s_\xi} ds_\xi\, ds_\gamma\, ds_\phi = \frac{\partial}{\partial t}\int_{s_\gamma}\int_{s_\phi} \rho_{AD} ds_\xi\, ds_\gamma\, ds_\phi \qquad (3.62)$$

Using the definitions of $ds_\gamma$, $ds_\xi$, $ds_\phi$ in terms of $\xi$, $\gamma$, and $\phi$, which they had calculated to be

$$ds_\xi = \frac{a\,d\xi}{8R\sin\theta\, J} \qquad (3.63)$$

$$ds_\gamma = \frac{a(2R^2-1)\,d\gamma}{4R^3\cos^3\theta\, J} \qquad (3.64)$$

$$ds_\phi = aR\sin\theta\, d\phi \qquad (3.65)$$

where

$$J^2 = (1-R^2)^2\cos^2\theta + (2R^2-1)^2\sin^2\theta \qquad (3.66)$$

and performing the indicated integration, Kronig and Brink obtained the partial differential equation

$$\frac{\partial}{\partial\xi}\left[p(\xi)\frac{\partial\rho_{AD}}{\partial\xi}\right] = \frac{a^2}{16D_d}q(\xi)\frac{\partial\rho_{AD}}{\partial t} \qquad (3.67)$$

where $p(\xi)$ and $q(\xi)$ are elliptic integrals. Separating variables, eq. (3.67) resulted in two ordinary differential equations, one of which was of the Sturm-Liouville type. The

general solution assumed the form, for absorption into a droplet,

$$M(t)/M(0) = 1 - \frac{3}{8}\sum_{n=1}^{\infty} A_n^2 \exp\left(\frac{-\lambda_n 16 D_d t}{a^2}\right) \qquad (3.68)$$

In Kronig and Brink's solution of eq. (3.67), the boundary conditions on eq. (3.67) resulting in eq. (3.68) were

$$\text{B.C.1:} \quad \rho_{AD} = \rho_{AD_i} \text{ at } \xi = 0 \ (r = a) \text{ for all } t \qquad (3.69)$$

$$\text{B.C.2:} \quad \rho_{AD} \text{ is finite and constant at } \xi = 1 \ (r = \sqrt{2}/2) \text{ for all } t \qquad (3.70)$$

$$\text{B.C.3:} \quad \rho_{AD} = \rho_{AD_o} \text{ at } t = 0 \text{ for all } \xi \qquad (3.71)$$

The effects of continuous phase resistance were included by Elzinga and Banchero by imposing an additional boundary condition. The rate of mass transfer into the droplet across streamlines is, from Fick's First Law,

$$N_{A_\xi} = J_{A_\xi} = D_d \frac{\partial \rho_{AD}}{\partial s_\xi} \qquad (3.72)$$

where $J_{A_\xi}$ is the diffusive flux into the droplet normal to the streamlines and the negative sign is dropped from the term on

the right since, for absorption, the transfer is in the negative $s_\xi$ direction. For transfer in the external phase to the droplet surface, from eq. (2.83)

$$N_a = k_c(\rho_{AC_b} - \rho_{AC_i}) \tag{3.73}$$

At the droplet surface, r = a and $\xi$ = 0, the total rate of transfer over the droplet surface is the same in both phases. Therefore

$$\left( \int_{A_d} \int D_d \frac{\partial \rho_{AD}}{\partial s_\xi} ds_\zeta \, ds_\phi \right)_{\xi=0} = A_d k_c (\rho_{AC_b} - \rho_{AC_i})_{\xi=0} \tag{3.74}$$

where $A_d$ is the surface area of the droplet. Carrying out the integration in eq. (3.74), the additional boundary condition became

$$\left. \frac{\partial (\rho_{AC_b} - \rho_{AC_i})}{\partial \xi} \right|_{\substack{\xi=0 \\ r=a}} = \left. \frac{3ak_c}{16D_d} \right|_{\substack{\xi=0 \\ r=a}} \tag{3.75}$$

The case of an infinite continuous phase transfer coefficient corresponded to Kronig and Brink's solution.

The constants and eigenvalues in eq. (3.68) were determined by the method of Ritz (219). In their solution, Kronig and Brink determined the first two values for $A_n$ and $\lambda_n$. In

1954, Heertjes, Holve, and Talsma (100) calculated five additional values of $A_n$ and $\lambda_n$, as well as presenting somewhat different values for the first two values calculated by Kronig and Brink. These values are tabulated in Table 2 for the infinite value of the parameter $Sh^*$.

Elzinga and Banchero, using an electronic differential analyzer, calculated the first three values of $A_n$ and $\lambda_n$, as shown in Table 2, for several values of $Sh^*$. Comparison of $A_n$ and $\lambda_n$ for an infinite $k_c$ shows their values to be somewhat different from not only those determined by Kronig and Brink but also Heertjes, Holve, and Talsma.

Calderbank and Korchinski (20) determined an approximation to eq. (3.68) to be

$$M(t)/M(0) \simeq [1 - \exp(\frac{-2.25 D_d \pi^2 t}{a^2})]^{0.5} \qquad (3.76)$$

Examination of eqs. (3.64) and (3.48) shows the internal transfer coefficient to be approximately

$$\overline{k_d} \simeq \frac{32}{3} \lambda_1 \frac{D_d}{d_d} \qquad (3.77)$$

if $\overline{k_d}$ be determined as in eq. (3.53). From eq. (3.76), $\overline{k_d}$ is also approximated by (234)

$$\overline{k_d} \simeq \frac{17.9}{d_d} D_d \qquad (3.78)$$

Johns and Beckman (117) extended Kronig and Brink's analysis and proposed a more general droplet model which has Kronig and Brink's solution as a limiting case. The model proposed by Johns and Beckman is limited, at least in theory, to dilute solutions and no continuous phase resistance. The model examined by Kronig and Brink assumed, as did the model of Elzinga and Banchero, that solute transport along streamlines due to diffusion was negligible in comparison to the convective transport. Johns and Beckman, however, examined the situation in which the convective velocity may assume a wide range of values, from zero, corresponding to the non-circulating droplet, to, mathematically speaking, infinity, corresponding to Kronig and Brink's model. Thus in one model is encompassed a moderately wide range of physical conditions.

For dilute solutions the general equation of continuity is given by eq. (2.42). The inclusion of the convective flux is the distinguishing mathematical characteristic of Johns and Beckman's model from that of Kronig and Brink's. If the solution be sufficiently dilute, then the velocity in the droplet is given closely by

$$\vec{v} \simeq \vec{v}_{dr} \qquad (3.79)$$

where $\vec{v}$ is defined in eq. (2.32) and $\vec{v}_{dr}$ is the vector velocity of the solvent fluid. The components of $\vec{v}_{dr}$, in spherical co-ordinates, are given by eqs. (3.10) and (3.11) as derived

from Hadamard's stream function. Using eqs. (3.10), (3.11), (3.79) in eq. (2.42), expressed in spherical co-ordinates, assuming the transfer to be independent of the meridional angle because of axial symmetry, the equation of continuity becomes, in spherical co-ordinates,

$$\frac{\partial \rho_{AD}}{\partial t} = \frac{D_d}{r^2}\left[\frac{\partial}{\partial r^2}\left(r^2 \frac{\partial \rho_{AD}}{\partial r}\right) + \frac{1}{\sin\theta} \frac{\partial}{\partial \theta}\left(\sin\theta \frac{\partial \rho_{AD}}{\partial \theta}\right.\right.$$

$$\left.\left. + \frac{1}{2}\left(\frac{\mu_c}{\mu_d + \mu_c}\right) U\left[\left(1 - \frac{r^2}{a^2}\right)\cos\theta \frac{\partial \rho_{AD}}{\partial r} - \left(1 - \frac{2r^2}{a^2}\right)\sin\theta \frac{\partial \rho_{AD}}{\partial \theta}\right]\right. \quad (3.80)$$

If $C^*$ is defined as

$$C^* = \frac{\rho_{AD_i} - \rho_{AD}}{\rho_{AD_i} - \rho_{AD_o}} \quad (3.81)$$

then eq. (3.80) becomes

$$\frac{\partial C^*}{\partial T^*} = \frac{1}{R^2} \frac{\partial}{\partial R}\left(R^2 \frac{\partial C^*}{\partial R}\right) + \frac{1}{R^2 \sin\theta} \frac{\partial}{\partial \theta}\left(\sin\theta \frac{\partial C^*}{\partial \theta}\right)$$

$$+ \frac{Pe'_d}{4}\left[\left(1 - R^2\right)\cos\theta \frac{\partial C^*}{\partial R} + \frac{2R^2 - 1}{R}\sin\theta \frac{\partial C^*}{\partial \theta}\right. \quad (3.82)$$

where

$$T^* = \frac{D_d t}{a^2} \tag{3.83}$$

$$Pe_d' = \frac{Pe_d}{1+\mu_d/\mu_c}' = \frac{d_d U}{D_d(1+\mu_d/\mu_c)} \tag{3.84}$$

and R is defined as in eq. (3.59).

Eq. (3.82) was solved for various values of $Pe_d'$ by Johns and Beckman using finite difference methods after transformation to rectangular co-ordinates. Solutions for the discontinuous phase Sherwood number, average mass flux over the droplet surface, and the volumetric average concentration are given graphically as functions of the dimensionless time parameter, $T^*$, for five different values of $Pe_d'$ as follows: 0, corresponding to the non-circulating droplet and 40, 80, 160, and 320, corresponding to, essentially, increasing magnitudes of the convective velocity in the droplet.

Since the instantaneous droplet Sherwood number is defined as

$$Sh_d = \frac{k_d d_d}{D_d} \tag{3.85}$$

a time average droplet Sherwood number can be defined as

$$\overline{Sh}_d = \frac{\overline{k}_d d_d}{D_d} \tag{3.86}$$

which from eqs. (3.47) and (3.83) become

$$\overline{Sh}_d = -\frac{2}{3T^*} \ln E' \qquad (3.87)$$

As shown by Johns and Beckman, for dissolution into a droplet with initial average concentration of $\rho_{AD_o}$ both $Sh_d$ and $\overline{Sh}_d$ essentially reach their asymptote after a dimensionless time of $T^* = 0.15$. These asymptotic values of both $Sh_d$ and $\overline{Sh}_d$ vary from approximately 7 to 14 for $Pe'_d$ of 0 and 320 respectively. For $Pe'_d$ greater than 240, which are common, the asymptotic value of $Sh_d$ is within 95 per cent of the Kronig and Brink value of approximately 17.9 (see eq. 3.77). At initial early times less than the time required for the first complete circuit of a streamline, $Sh_d$, for large $Pe'_d$ (approximately greater than 240), fluctuates upward as much as 25 per cent of its asymptotic value because of the short time required for transport of solute around a streamline circuit as compared to the time of penetration of solute into the droplet. The average mass flux over the droplet surface also displays similar fluctuations for the same reason.

For an average initial concentration of $\rho_{AD_o}$, $E'$ drops off quite rapidly, reaching 50 per cent within a dimensionless time, $T^*$, of only 0.03 for all values of $Pe'_d$, the more rapid decrease, as would be expected, occurring at higher values of $Pe'_d$. Other values of the initial concentration, state Johns and Beckman, has a marked effect on $Sh_d$ at early contact times

while at greater times the effect becomes less apparent, the time to reach 95 per cent of the final equilibrium concentration distribution being relatively independent of the initial concentration level.

The concentration profiles at the equilibrium condition, that is, the concentration profile at time equal to infinity, for several values of $Pe'_d$ are given by Johns and Beckman. For the droplet of Kronig and Brink, the concentration contours are the same as the dimensionless streamlines, $\xi$.

Turbulent Droplet

In 1957 Handlos and Baron (83) proposed a model which attempted to consider the effects of turbulence on mass transfer inside of a liquid droplet. At high values of Reynolds numbers, $Re_c$, approximately greater than 1000, Handlos and Baron considered the motion inside of a droplet to be highly turbulent. Handlos and Baron attributed the extreme lack of correlation between predicted values and experimentally determined values of mass transfer coefficients in droplets at high Reynolds numbers to the existence of this turbulence.

To approximate the mean turbulent motion of the fluid solution within a droplet, supposedly arising because of both circulation within the droplet and oscillations and vibrations of the droplet as a whole, a system of tori of radius r', as shown in Fig. 8 was assumed. Fluid particles were assumed to be subject to turbulent fluctuations of a random nature

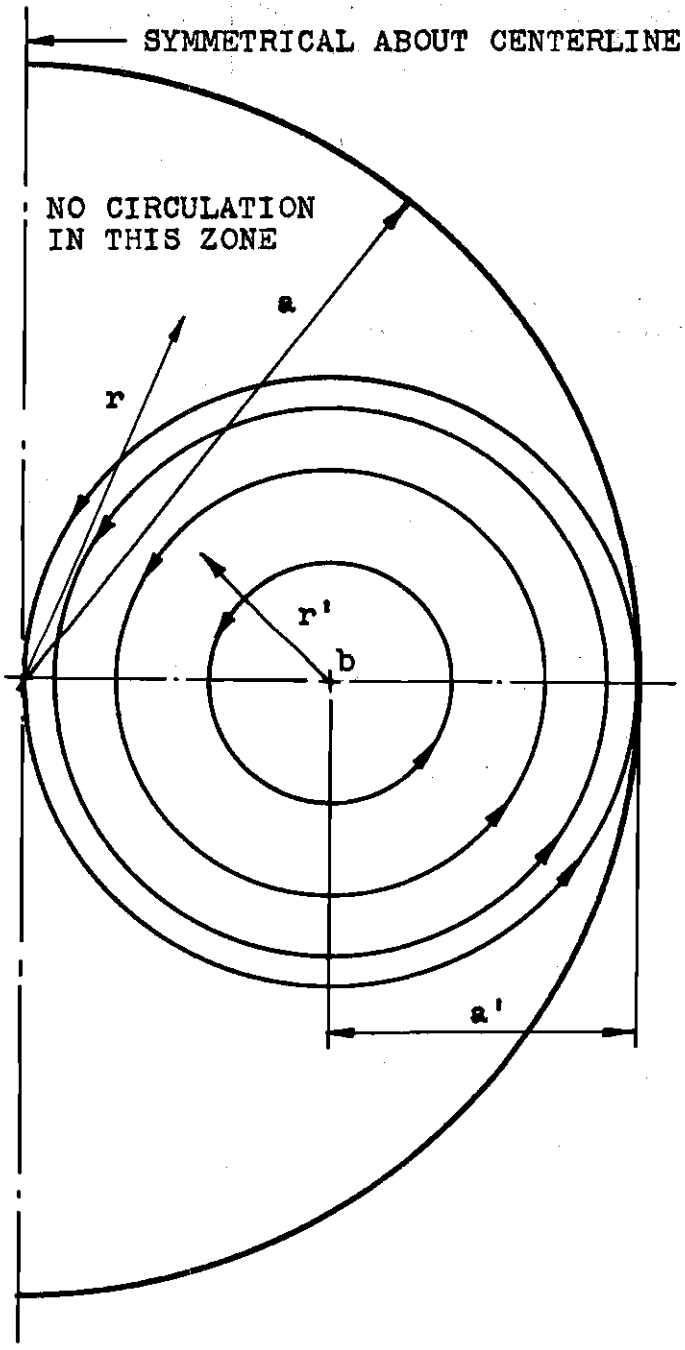


Firgure 8. Circulation in Turbulent Droplet

described probabilistically, each fluctuation occurring over a time interval equal to that for one complete circuit along a streamline. Under these assumptions, Einstein's equation (85) was then used to obtain an eddy diffusivity, $E_D$, which was calculated to be

$$E_D = \frac{d_d U(6r^2 - 8r + 3)}{2048(1+\mu_d/\mu_c)} \qquad (3.88)$$

where $r = 4r'/d_d$.

This eddy diffusivity was used to replace the molecular diffusivity in the equation of continuity assuming transport by eddy diffusion only. Boundary conditions and method of solution were similar to those employed by Kronig and Brink in their solution for a droplet with viscous circulation discussed previously. Handlos and Baron implicitly assumed no external transfer resistance. For dissolution of a solute into the droplet they found

$$E' = 2\sum_{n=1}^{\infty} A_n^2 \exp\left(\frac{-\lambda_n Dt}{512a^2} Pe_d'\right) \qquad (3.89)$$

where $Pe_d'$ is a modified Peclet number as defined by eq. (3.84) and the other notation is as before.

Handlos and Baron found that the second eigenvalue was sufficiently large that it could be neglected. For the first

eigenvalue they calculated a value of 2.88. The droplet transfer coefficient thus became approximately

$$\bar{k}_d \simeq \frac{16\lambda_1 D_d Pe}{(6)(2048)d_d} = \frac{0.00375\ U}{1+\mu_d/\mu_c} \qquad (3.90)$$

Comparing transfer coefficients predicted by eq. (3.87) to values determined experimentally in liquid-liquid systems by several investigators, as well as those values determined by their own experiments, they found their predicted values to agree within approximately 20 per cent (214).

Oscillating Droplet

Transfer in oscillating droplets generally shows a far greater rate of transfer than nonoscillating droplets (21, 236). This increased transfer rate results not only from increased mixing inside the droplet but also from reduction in effective film thicknesses and increase of surface area of the droplet, or interfacial area stretch as it has been termed (182).

Rose and Kintner (180) attempted to describe mass transfer in oscillating drops in liquid-liquid systems. The model which they proposed is based on a fully oscillating droplet, thus restricting it, theoretically at least, to larger droplets, greater than two or three mm as noted previously. Furthermore, the oscillations are restricted to those which are of either a random wobble type or which are axially symmetric, said by Rose and Kintner to occur only above Reynolds numbers,

$Re_c$, greater than 200. Internal circulation is assumed to be essentially nonexistent, being damped out by the droplet oscillations. Any internal motion which exists is assumed to be of a turbulent nature with perhaps only a slight tendency towards circulation.

Based on studies by Kintner and others in which photographs of droplet oscillation were made, the assumed oscillatory motion for the model was that from a nearly spherical shape to oblate ellipsoidal shape back to the spherical shape. Observations by Schroeder and Kintner (183) indicated that, at least for the droplets they examined, oscillations cause the droplet to vary in shape from a spherical shape to an oblate shape or from an initially oblate to a more oblate shape. It is to be noted this oscillatory mode is different from that observed by others. Garner and Skelland reported oblate to prolate oscillations in their experimentation (26).

The oscillation frequency was described by Rose and Kintner by the function

$$W^2 = W_f(a, d_{de}, \rho_D, \rho_c, n_i, T) \qquad (3.91)$$

where W = oscillation frequency, $d_{de}$ = equivalent spherical diameter, $\rho_c$,$\rho_D$ = average mass density of continuous and droplet phases, respectively, $n_i$ = oscillation index, and $W_f$ is the frequency function whose actual form is given by Rose and Kintner, and the other notation is as before.

The oscillation amplitude, $a_p$, was determined experimentally to be

$$a_p = \frac{A_{max}}{2} - a_o \tag{3.92}$$

where $A_{max}$ = maximum area of droplet surface and $a_o$ = initial spherical droplet radius, determined from examination of motion pictures of falling droplets.

The transfer resistance was assumed to lie in a thin zone or film at the droplet interface while the interior of the droplet was assumed to be well mixed. Within this film the transfer mechanism was assumed to be that of a stagnant film, so that, from eqs. (2.1) and (2.2), the absorption of solute A into the droplet was described by, for one dimensional transfer

$$\frac{\partial M_A}{\partial t} = D_d A_d \frac{\partial c}{\partial x} \tag{3.93}$$

which reduced to, assuming a constant droplet volume, $\forall_d$, and a linear driving force in an equivalent film thickness of f,

$$\forall_d \frac{\partial \rho_{AD_d}}{\partial t} = \frac{D_d A}{f} (\rho_{AD_i} - \rho_{AD_b}) \tag{3.94}$$

where $\rho_{AD_d}$ is the concentration in the well mixed interior of the droplet.

The film thickness, f, varies with the oscillations. From motion picture studies, Rose and Kintner found the minimum film thickness to occur in the region of the droplet stagnation points while the maximum thickness occurred in the equatorial zone. With the restriction that the film volume be constant, the film thickness at any time, t, could be expressed as a function of initial film thickness at the droplet equator, $f_o$, the major and minor radii of the droplet, $a_m$ and $b_m$, and $a_o$, the initial spherical radius. Thus

$$f = f_t(f_o, a_m, b_m, a_o) \qquad (3.95)$$

where the actual form of $f_t$ is given by Rose and Kintner.

Whitman's two film theory was used to account for transfer resistance in both phases assuming a binary system. The exterior film coefficient was determined from a correlation similar to eq. (3.24) in which g, p, and r were 0.60, 1/2, and 1/2, respectively, while $Sh_s$ was neglected. The interior film coefficient was based on Higbie's penetration theory with a contact time equal to the period of oscillation.

Using eqs. (3.91) through (3.95) and the various assumptions discussed above, Rose and Kintner determined the solution to eq. (3.94) to be

$$E' = \exp\left(-\frac{2\pi D_E}{\forall_d} \int_0^{t_{ct}} \frac{L'}{f_t}\, dt\right) \qquad (3.96)$$

where

$$D_E = \frac{K_D}{k_d} D_d + \frac{mK_D}{k_c} D_c \qquad (3.97)$$

$t_{ct}$ = time in which droplet is in contact with continuous phase, $f_t$ is defined by eq. (3.94),

$$\frac{1}{K_D} = \frac{m}{k_c} + \frac{1}{k_d}$$

similar to eq. (2.72), and $L'$ is given by

$$L' = \left(\frac{3\Psi_d}{4\pi s}\right)^2 \frac{1}{2b'} \ln\left(\frac{1+b'}{1-b'}\right) + S'^2 \qquad (3.98)$$

in which

$$S' = (a_o + a_p |\sin(2wt)|)^2 \qquad (3.99)$$

and

$$b'^2 = 1-(9\Psi_d^2)\,(16\pi^2 S^3) \qquad (3.100)$$

It is apparent that Rose and Kintner's solution is not readily amenable to solution. Furthermore, this solution necessitates knowledge of a great many more droplet characteristics than

models considered previously. This factor restricts its usefulness and wide applicability. Its complexity is indicative of the complications which exist in the mathematical analysis of mass transfer in oscillating droplets.

Solving eq. (3.96) on a digital computer, Rose and Kintner compared predicted values of $E'$ with the experimental results of five different investigators. The average deviation between experiment and theory was within 15 per cent, eq. (3.96) tending to predict higher values than actually measured at high transfer efficiencies while lower values than those measured were predicted at low transfer efficiencies.

Effective Diffusivity

Mention was made earlier of a means of describing transfer characteristics in the form of an effective diffusivity ratio, $R^*$, introduced originally by Calderbank and Korchinski (19). Review of the various models discussed in this section will show that several take the form

$$E' = \sum_{n=1}^{\infty} A_n^m \exp(-\text{Constant}\lambda_n^m T^*) \qquad (3.101)$$

where $T^*$ is defined as in eq. (3.83) and m may be either one or two. Examination of the general noncirculating droplet model, eq. (3.55), will show that the constant in eq. (3.101) is one while in other models the constant differs from one. This constant in these other models can thus be viewed as increasing the molecular diffusivity above that of the noncirculating

droplet, resulting in an effective diffusivity. The effective diffusivity ratio, $R^*$, can therefore be defined by the equation

$$E = 6\sum_{n=1}^{\infty} A_n^1 \exp(-R^*\lambda_n^2 T^*) \qquad (3.102)$$

where now, in eq. (3.101), $A_n$ and $\lambda_n$ are the constants and eigenvalues, respectively, corresponding to the non-circulating droplet given in Table 2.

Comparison of eq. (3.76), which approximates eq. (3.68), with the value of $\lambda_1$, 3.142, for the non-circulating droplet indicates that Kronig and Brink's model predicts an $R^*$ of approximately 2.25. Experimentally, Calderbank and Korchinski, for circulating droplets with $Re_c$ varying from 10 to 120, found $R^*$ to range from 1.8 to 3.3, agreeing moderately well with Kronig and Brink's predicted value of 2.25. For droplets with $Re_c$ of 315 to 620 in which oscillations were observed, they found $R^*$ to vary from 315 to 620 (21). Other values tabulated by Calderbank and Korchinski determined by other investigators indicate $R^*$ of 6 to 71 for oscillating droplets with $Re_c$ varying from 270 to 3000. For non-oscillating droplets they give values of $R^*$ varying from 1.6 to 2.4 for droplets having $Re_c$ greater than 700. Johnson and Hamieler (121) found experimentally $R^*$ to be approximately 3 for droplets with $Re_c$ less than 16 while for $Re_c$ ranging from

40 to 90, $R^*$ varied from approximately 8 to 35. For $Re_c$ on the order of 600, they found also that $R^*$ varied from approximately 30 to 50.

# CHAPTER IV

# EXPERIMENTATION

## Introduction

Experimental work was conducted in order to make a preliminary evaluation of the proposed process designed to obtain transfer of oxygen to liquid droplets produced by a spray in a high pressure oxygen atmosphere.

The apparatus and methods used are described in the following paragraphs. Considerable time was devoted to the calibration of the instruments used to measure dissolved oxygen concentrations since these instruments, galvanic cell oxygen analyzers (159, 162), were to be used under pressure ranges for which their characteristics had not previously been determined, as far as is known to this writer. The results of the experimentation involving the calibration of these instruments is emphasized since they may be significant beyond the scope of this study due to the expanding use of these instruments in a variety of applications.

The basic theory underlying the transfer process to be evaluated has been presented within the discussions in Chapters II and III. The pertinent theory directly applicable to this study will be presented and applied in the analysis of the experimental results. Because, however, the primary

purpose of this study is an evaluation of the proposed process, emphasis in analysis will be upon transfer efficiency and its variation, rather than determination of the exact nature of the various transfer mechanisms occurring in the apparatus.

Though the experimental work conducted was, of necessity, of a limited extent, the conclusions drawn from it provided the preliminary evaluation desired as well as elucidating areas which require more detailed consideration.

## Apparatus

The basic experimental apparatus is shown in Fig. 9. Essentially it consists of a 75 gallon, unlined steel tank (a reconditioned hot water tank), with an approximate height of 55 in. and an internal diameter of 19.6 in., into which water is injected at the top and from which water is drawn at the bottom. The tank interior was painted.

Plastic tubing of one-half inch diameter delivered ordinary city water from a laboratory faucet to a small positive displacement pump driven by a three-quarter horsepower motor. From the pump the plastic tubing led to a float type flow meter shown in Fig. 9. Maximum flow rates obtainable during times which the tank pressure was above atmospheric pressure did not exceed 1.7 gpm. Flow was regulated by a needle valve at the exit end of the flow meter. A three-quarter inch line by-passed the flow meter, but it was normally not used.

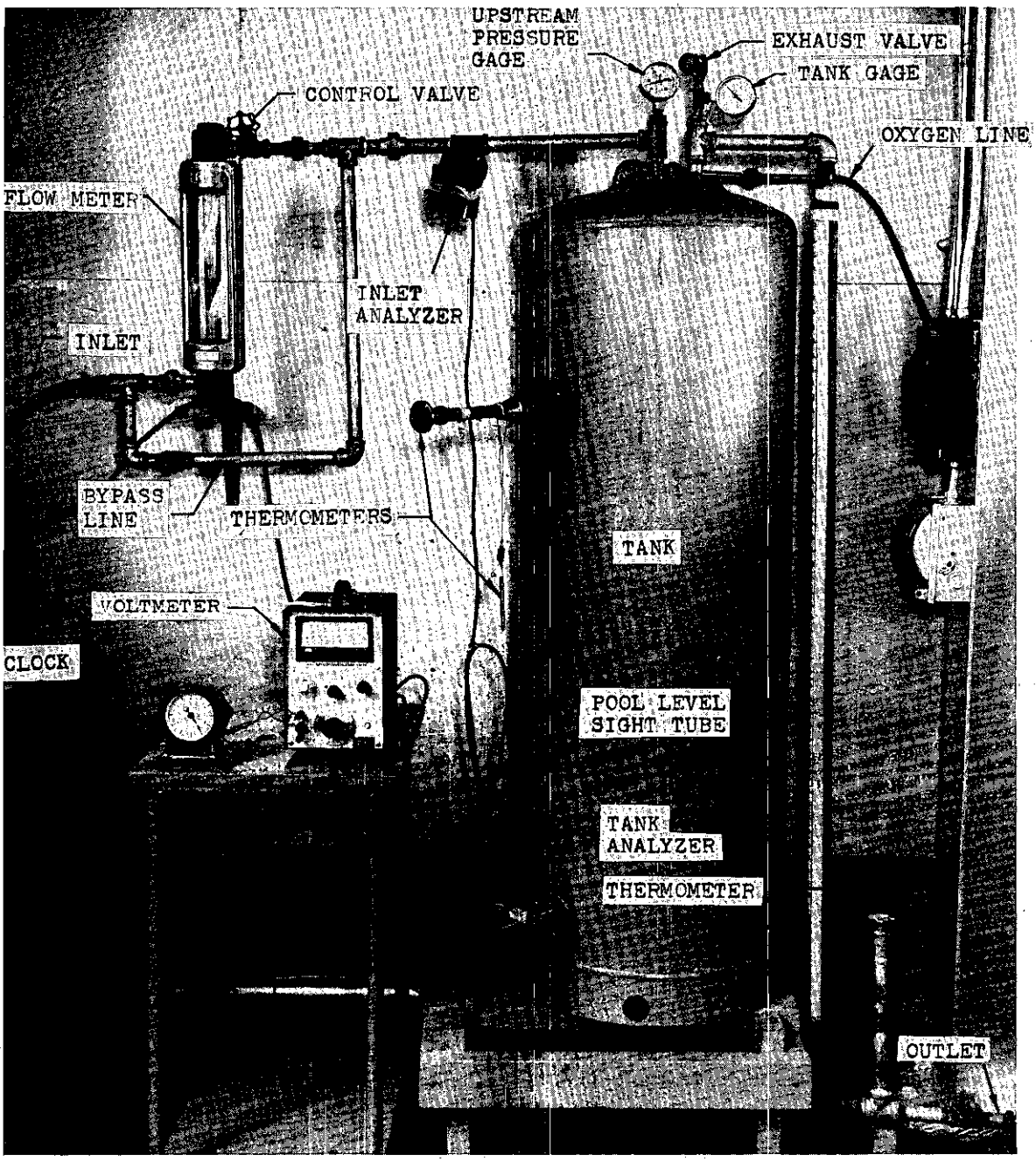


Figure 9. Experimental Apparatus

From the needle valve, three-quarter inch steel pipe led to the tank. A pressure gage, with five psi graduations, was inserted in a leg of a standard pipe tee near the end of the pipe at the top of the tank and was assumed to give closely the gage pressure of the water just prior to its passage through the spray nozzles described below.

At the top of the tank the three-quarter inch pipe passed through a flat plate to which it was welded to prevent gas leakage. Some leakage through the weld, however, was noticed during some runs of the apparatus. The flat plate was bolted down over a large hole in the top of the tank. The gasket used in early runs proved to be insufficient to stop gas leakage. Use of a gasket cut from heavy, flexible plastic sheet, however, seemed to effectively reduce gas leakage.

Inside the tank at the end of the three-quarter inch pipe, very nearly at the top of the tank, one of two nozzles was attached. Water was sprayed into the tank through these nozzles. Both nozzles were of whirl chamber type design and produced a cone shaped spray of essentially uniform spatial distribution over the base of the cone. One nozzle, nozzle MX-00, had an orifice diameter of 0.125 in. while the other nozzle, nozzle MX-0, had an orifice diameter of 0.082 in. More complete descriptions of the nozzles are given in the Appendix.

A photographic study was made of the droplets produced by the spray nozzles. A photographic technique was chosen because it seemed to offer a relatively simple and straightforward method of determining the mean drop size produced by the spray as a function of flow rate through the nozzle. Basically the technique was that of photographing the spray as it came from the nozzle and examining the photos under a microscope. By proper restriction of the spray with metal plates, photographs were obtained from which droplet counts and measurements could be made with use of the microscope. A full description of the technique and methods used in the evaluation of the spray is given in the Appendix. It was found that the mean drop size as a function of flow rate could be approximately represented by the equations, for the MX-0 nozzle,

$$d_d = 0.0081 - 0.0011Q \qquad (4.1)$$

and, for the MX-00 nozzle,

$$d_d = 0.0144 - 0.0044Q \qquad (4.2)$$

in which d = mean droplet diameter, in cm, and Q = flow rate, in gpm.

Droplets produced by the spray nozzle fell into a pool of water in the bottom of the tank. The pool elevation could be varied by regulation of a gate valve on the drain pipe of

the tank. The elevation of the pool could be determined by visual observation of the water level in a sight tube on the outside of the tank. A scale beside the sight tube was used to measure the pool elevation. The relation between pool elevation and volume of water in the tank was determined at the same time the tank volume was determined.

Water was discharged from the bottom of the tank through a three-quarter in. steel pipe line. To regulate the flow, a gate valve was placed on the line. A sampling valve was also inserted in the line as can be seen in Fig. 9. Water discharged from the end of this pipe. In those instances in which water was recirculated through the system, for the purpose of calibration to be described below, a hose was used to connect the end of this pipe to the intake side of the pump.

Industrial grade oxygen was delivered to the tank from cylinders through an inlet in the top of the tank. The pressure in the tank was regulated by a gage on the cylinder manifold with five-psi graduations. The maximum pressures produced in the tank were slightly less than 110 psig.

While the cylinder manifold gage was used to regulate pressures in the tank, actual pressures were measured by one of two gages. For tank pressures greater than 15 psig, a gage on the top of the tank, as seen in Fig. 9, was used. This gage was similar in construction to the cylinder manifold gage. For pressures less than 15 psig, a gage, with one-quarter psi graduations, was screwed into the exhaust

valve at the top of the tank. The same valve was also used to exhaust the high pressure gas in the tank at the end of a run. Atmospheric pressures were measured with a mercury barometer.

A thermometer projecting into the upper portion of the tank, as shown in Fig. 9, was used to measure temperatures inside the tank. During initial runs, a thermometer also projected into the discharge line as shown in Fig. 9. For later runs, this thermometer was placed in the position of the tank dissolved oxygen analyzer to be discussed below. Room temperatures were measured with the thermometer seen in Fig. 9. When samples were being withdrawn from the sampling valve or the laboratory faucet the temperature of the water was measured as it discharged from the valve or faucet.

Dissolved oxygen concentrations were measured with the galvanic cell oxygen analyzer which was originally developed by Mancy and his co-workers and is described in references (159) and (162). Basically the analyzer is a galvanic cell with a silver cathode surrounded by a lead anode both of which are embedded in a nonconductive plastic. Covering both electrodes is a one molar solution of KOH held on the electrodes by a small disc of lens paper. Covering the electrode and KOH electrolyte is a plastic membrane permeable to oxygen. The oxygen which passes through the membrane from the solution being tested initiates an electrochemical reaction which produces an electrical current which can be measured and related to the dissolved oxygen content of the solution being tested.

One oxygen analyzer, hereafter referred to as the inlet analyzer, was placed on the pipe leading into the top of the tank as shown in Fig. 9. A second analyzer, which will be called the tank analyzer, was placed in the side of the tank several inches above its bottom as shown in Fig. 9. Initial attempts at calibration of the tank analyzer gave such poor results that this tank analyzer was placed on the discharge line where the discharge line thermometer had originally been placed. In this new position, the analyzer will be referred to as the outlet analyzer.

To mount the tank analyzer, a piece of plastic tubing was slipped around the collar of the analyzer and the analyzer was placed in the end of a short piece of steel pipe projecting from the tank. Over the end of the analyzer a flat aluminum plate was positioned. Long bolts, projecting from a collar plate surrounding the steel pipe, passed through the aluminum plate, as did the analyzer leads. Wing nuts on the bolts were used to press the aluminum plate against the base of the analyzer and kept it tightly in its position in the end of the pipe. In its tightened position, the tank analyzer was several inches from the inside of the tank wall.

The inlet and the discharge analyzers were both mounted in a similar manner. Into the outstanding leg of a three-quarter in. pipe tee, a short pipe nipple was screwed. On the end of the nipple was placed a flange. The analyzer was placed into the end of the nipple through the flange orifice. On the

base of the analyzer, a flat aluminum plate was positioned and held tightly by bolts projecting from the flange. To protect the collar of the analyzer, a piece of plastic tubing was slipped over the end of the analyzer as was done with the tank analyzer. The leads of the analyzer passed through a hole in the aluminum plate. The tips of both analyzers were approximately one-half in. from the inside edge of the three-quarter in. pipe into which the analyzers were inserted. To insure that no air bubbles were trapped over the analyzer electrodes, the pipe tees were twisted downward at a 45 degree angle when in use.

Currents generated by the analyzers were measured on a Keithley, model 151, null detector-DC microvoltmeter. Rather than measure current directly, it was more convenient to measure the voltage drop across a resistor. Since a 100 ohm resistor was used, a one millivolt reading corresponded to a current of ten microamps. Whenever the meter was used, no readings were taken before a minimum warm-up time of one half hour, as recommended by the meter manufacturer.

Time measurements were made with the clock seen in Fig. 9.

## Procedure

To be described are the procedures associated with both regular test runs of the apparatus and runs made for the purpose of calibration of the oxygen analyzers. In many

respects, the procedures are similar and have common points. These will be discussed first.

Preparation of the oxygen analyzers was a delicate operation. The analyzer preparation technique which finally developed, and which was used for all runs upon which the conclusions of this study are based, is similar to that suggested by Mancy, et al. (159, 162). The analyzer electrodes were sanded clean with very fine sand paper and then washed in water. It was found that a very soft tooth brush was useful in removing particles from small pits in the plastic surrounding the electrodes. The electrodes were then washed in KOH and dried with tissue. The lens paper disc would be placed on the dry electrodes and one molar KOH would be dropped onto the lens paper. After smoothing of the lens paper, the plastic membrane would be pulled down and plastic tape would be used to seal the analyzer collar. Care was taken to obtain a smooth membrane surface and eliminate entrapped bubbles beneath the membrane. After a new membrane was placed on an analyzer, the analyzer head would be immersed in a saturated sodium sulfite solution for at least twelve hours to stabilize.

Before inserting an analyzer in the apparatus it would be tested to see if it seemed to be in proper condition. A careful visual inspection would first be made. Then voltage readings would be made with the electrode in air and with pure oxygen blowing on the electrode. Voltage readings with pure

oxygen would be four to five times as large as those with only air surrounding the analyzer. As suggested by Mancy, et al. (164), an ohmmeter was also used to check for holes in the membrane. One lead of the ohmmeter would be placed in tap water with the analyzer. The other lead would be connected to a wire from one of the electrodes of the analyzer. High resistances indicated a good membrane. Resistances varied, but for the membranes actually used, resistances were greater than 60,000 ohms.

During initial runs, analyzers would remain in the apparatus immersed in water when not in use. However, it was found soon after the outlet analyzer began to be used that rust dissolved in the water apparently settled out on the membrane. Therefore during almost all runs using the inlet and outlet analyzers, the analyzers were removed from the apparatus and immersed in sodium sulfite solution when not in use. As a further precaution against contamination of the analyzers, the tank was flushed and drained before each run.

When operating under normal atmospheric conditions, samples of water were often taken. Two sampling locations were used: a laboratory faucet on the same pipe supplying water to the apparatus and the outlet line sampling valve. The water from the faucet was assumed to have the same dissolved oxygen concentration as the water supplied to the apparatus. When samples were taken, tubing was slipped over the ends of the faucet and sampling valve so that water could be

injected directly into the 250 ml sampling bottles with little or no aeration.

Oxygen concentrations of the water samples taken were determined by the Alsterberg Modification of the Winkler Method (217). During initial runs, a time period of approximately fifteen minutes elapsed before the manganous sulfate reagent could be added. Refinement of procedures during runs with the inlet and outlet analyzers, however, enabled the manganous sulfate to be added within a very few minutes after the sample was obtained. Acidification also followed in a very short time.

When making voltage measurements with the apparatus in operation, a minimum time period equivalent to twice the theoretical detention time for the existing pool elevation was always allowed to pass after a change in the inflow rate or tank pressure before final readings were taken. Furthermore, even if this period had passed, final readings would not be taken until they apparently had reached a steady, constant value. During runs with no recirculation, which will be discussed below, very minor fluctuations always occurred even after a considerable length of time, so average readings were taken. With recirculation, readings usually approached a steady value with little fluctuation and remained very steady at their final value.

Inflow rates were adjusted with the needle valve shown in Fig. 9. To determine the outflow rate in non-recirculation runs, the gate valve on the discharge line was adjusted so as

to maintain a constant pool elevation, the outflow rate then equalling inflow rate. The outflow rate could be set and maintained within 0.1 gpm of the inflow rate. All readings were taken when inflow and outflow rates were essentially equal.

After a run had been made in which high pressures had existed in the tank, the pressure would be reduced to nearly atmospheric levels by exhausting the oxygen inside the tank.

During early runs using the tank analyzer, water would then be continued to be pumped through the system for a period of approximately 45 or 60 minutes until no bubbles were visible in the water as it passed through the sight glass of the flow meter. If it were anticipated the following run were to be conducted under atmospheric conditions, the exhaust valve would remain open until the next run, usually at least 12 hours later. After the first few runs it was decided that if the next run were to be conducted under high pressures, the exhaust valve would be closed and the tank kept under a pressure of approximately three psig.

During later runs, using the inlet and outlet analyzers, since it was found desirable to flush and drain the tank after each run, the exhaust valve would also remain open even if the next run were to be a high pressure run.

As mentioned above, the temperature of the water samples was determined from the water as it discharged from the faucet or the sampling valve. In runs with recirculation, an average

of the upper and the lower tank thermometer (the lower tank thermometer being on the outlet line in earlier runs) readings were used to determine the water temperature. Invariably, the temperatures were within one and a half degrees of each other. The room temperature was generally several degrees different from that of the water, being in a transient condition.

Galvanic Cell Oxygen Analyzer Calibration

In order to calibrate the oxygen analyzers, two different basic procedures were followed -- one being used to determine the relation between current generated by the analyzers and the dissolved oxygen content of the water in which the analyzer was immersed when the test solution was under atmospheric pressure and the other being used to examine the same relation when the test solution was under pressures considerably higher than normal atmospheric pressure.

Atmospheric Pressure Calibration. For calibration of the inlet and outlet analyzers under normal atmospheric pressure conditions, the best procedure found was that of pumping water through the system once only and discharging it without recirculating it. With this method, the water temperature remained fairly constant as it passed through the system. Temperature fluctuation was within one degree of its average value. A steady flow rate would be established and samples would be taken of both the inflow and outflow water. The meter readings taken immediately prior to obtaining samples were assumed to correspond to the dissolved oxygen levels in the

samples. By obtaining samples under a wide range of flow rates, the relation between the voltage drop measured and the dissolved oxygen concentration was determined for pipe Reynolds numbers ranging from approximately 1000 to 10,000.

No attempt was made to calibrate the tank analyzer under atmospheric conditions. It was hoped that the calibration curves for atmospheric conditions could be extrapolated from calibration curves obtained with the system operating under higher pressures.

High Pressure Calibration. To examine the characteristics of the analyzers under pressures up to approximately 110 psig, recirculation was used. When inlet and outlet analyzers were used, the system was drained and flushed between each run. The elevation of the tank pool would be set at the desired level and then the water in the tank would be recirculated by the pump.

During calibration runs using the tank analyzer, the first measurement would be made with tank pressure slightly above atmospheric. The water would be recirculated through the system until voltage readings became constant, this being assumed to indicate an attainment of saturation conditions. More oxygen would then be allowed to flow into the tank and increase the pressure and a new voltage reading would again be made after steady conditions were achieved. Repeating this process with pressure increments varying from 10 psi to 25 psi, readings were obtained for tank pressures to

slightly less than 110 psig. During such a run the pool level would remain fairly constant, varying only because of some leakage and expansion of the measuring sight tube. Within the limitations of the pump, the flow rate would be held at one value.

During calibration runs using the inlet and the outlet analyzers under high pressures, recirculation was also used as it was for the tank analyzer. The first voltage measurement, however, was made at atmospheric conditions in order that the initial concentration of the water being recirculated could be measured by titration of the samples. Once the initial reading and samples had been taken, the exhaust valve was closed and the procedure was the same as that used in the calibration runs with the tank analyzer. The flow rate would be maintained at a constant value for the entire run and, except for the initial loss of water due to removal of samples, the pool elevation remained essentially constant.

Gas leakage from the tank during runs using the inlet and outlet analyzers was reduced to minor proportions. During runs 22-41, to be described below, gas leakage was quite small, but during runs 42-50, leakage became considerable again.

Test Runs to Measure Oxygen Transfer Characteristics

For those runs which were made to study the transfer characteristics of the proposed system, the inlet and the outlet analyzers were used. The procedure followed was similar

in some respects to that used to calibrate the inlet and the outlet analyzers. After draining and flushing the tank, the pool level was raised to the desired level. Water was pumped straight through the system and discharged without recirculation. First measurements were made at atmospheric conditions in order that samples could be withdrawn. These samples were used to establish the initial concentration level of the water and provide a check on the constancy of the sensitivity, to be discussed below, of the analyzers obtained from the analyzer calibration discussed above. The exhaust valve was then closed and the pressure was increased incrementally, readings being made at each pressure level. At each pressure level, furthermore, flow rates were varied and readings were made for each of the flow rate levels. Final readings for each flow condition and pressure level were not made until at least a time period equal to twice the theoretical detention time had passed and readings appeared essentially constant.

## Results

The equipment and procedures described were used to conduct 49 basic experimental runs. For all these runs the inlet analyzer remained and was used in the same upstream position. For the first 21 runs the tank analyzer was used, while for remaining runs the outlet analyzer was used. The change was made because of the very poor results obtained with the tank analyzer. Since the analysis and conclusions of this study are not based on the runs using the tank analyzer, the

results in regard to analyzer calibration using the tank analyzer will be discussed only briefly in order that the deficiencies of the system using the tank analyzer can be pointed out.

Of the runs using the outlet analyzer, run numbers 22 through 50*, results fall within one of two categories: those directly relating to oxygen analyzer evaluation and calibration and those relating to the determination of the oxygen transfer characteristics of the experimental system. In some instances, a run was used to obtain data relating to both categories. In addition, any particular run, as discussed in the procedure, could be one in which the water was recirculated or was pumped straight through the system. The run may or may not have been conducted under higher than atmospheric pressures. Table 3 classifies each run: recirculation indicates the water in the system was recirculated, no recirculation being otherwise assumed; pressure indicates during some portion of the run the system was operated under greater than atmospheric pressure, otherwise normal atmospheric pressure prevailed at all times; calibration indicates at least one water sample was taken under normal atmospheric conditions and used in the development of calibration curves; and transfer indicates the oxygen trans-

*The discrepancy in the 49 runs having run numbers through 50 exists because of a misnumbering of one of the runs.

fer produced in the operating system was measured with the inlet and outlet analyzers. The series letters in Table 3 group those runs which were made during continuous operating of the apparatus, the run numbering thus being used to differentiate between either a change in basic operating conditions and/or a change in the basic purpose of a run, such as a change from a calibration run under normal atmospheric pressures to a transfer run under greater than atmospheric pressures.

Table 4 classifies runs 22-50 according to what spray nozzle was used. It is to be noticed that relatively few runs were made using the MX-0 nozzle, this because of the greater pressure loss across this smaller diameter nozzle. The reason for this restriction will be discussed below when the effects of high pressure on the analyzer operation are discussed. In Table 5 is a listing of various analyzer membranes used in the different runs, each code number representing a different membrane. The letters "I" and "O" merely indicate whether the membrane was used on the inlet or the outlet analyzer, respectively.

Tables 6 and 7 are a compilation of the basic experimental data obtained from runs 22-50. To distinguish between different operating conditions during a run, each run number is followed by a lower case letter and a capital "I" or "O", the letter being used merely to distinguish between different operating points while "I" and "O" indicate whether the data apply to the inlet or outlet analyzer, respectively. The

current generated by each analyzer as determined from voltage measurements is listed in Table 6. The temperature listed for each run is an average of the water temperature indicated by the upstream and downstream thermometers. Also tabulated is the flow rate through the system. If a water sample was titrated to determine its dissolved oxygen content, the concentration so determined is listed. In Table 7 atmospheric pressure, gage pressure just upstream of the nozzle, and the total gas pressure inside the tank are listed.

Saturation Concentration

Determination of the saturation dissolved oxygen concentration of the water in the experimental system for each operating point of the various runs was needed for two purposes: to aid in the evaluation of the analyzer calibration and the system transfer characteristics, both to be discussed below.

For dilute solutions of gases in liquids such as oxygen in water, the saturation concentration can be determined from the partial pressure of the gas above the liquid surface by using Henry's Law, which for the purposes here, takes the form

$$p = (H)(Mf) \qquad (4.3)$$

in which p = partial pressure of solute gas above liquid, H = Henry's constant, and Mf = mole fraction of gas in liquid.

H is a function of both temperature and partial pressure, though the variation of H with pressure for oxygen in water is small. The values of H at one atmosphere of partial pressure of oxygen at various temperatures which were used in calculations are those values determined by Fox (115). These values differ somewhat from those determined by Winkler (115), as can be seen from Fig. 10 where the variation of H with temperature is shown.

The change in H at a constant temperature with partial pressure is not well known, but some data are given by Perry (178) for 25.9°C. The ratio of these values of H to H at one atmosphere at the corresponding temperature, as given by Fox, was determined. Since H at one atmosphere as determined by Fox did not agree with that given by Perry (they differ by approximately ten per cent), the ratios were reduced proportionately such that the ratio at one atmosphere was exactly one. Then in calculating saturation concentrations the value of H at some particular temperature and one atmosphere was multiplied by this adjusted ratio to obtain H at the actual partial pressure of the oxygen. This adjusted ratio is plotted in Fig. 11 as a function of partial pressure of oxygen. It is seen that the pressure variation of H, for the pressure ranges of this study, is actually small. It was, however, included in calculations. The possible inaccuracy of this ratio, due to its adjustment and/or variation with temperature, which could not be determined, was assumed to

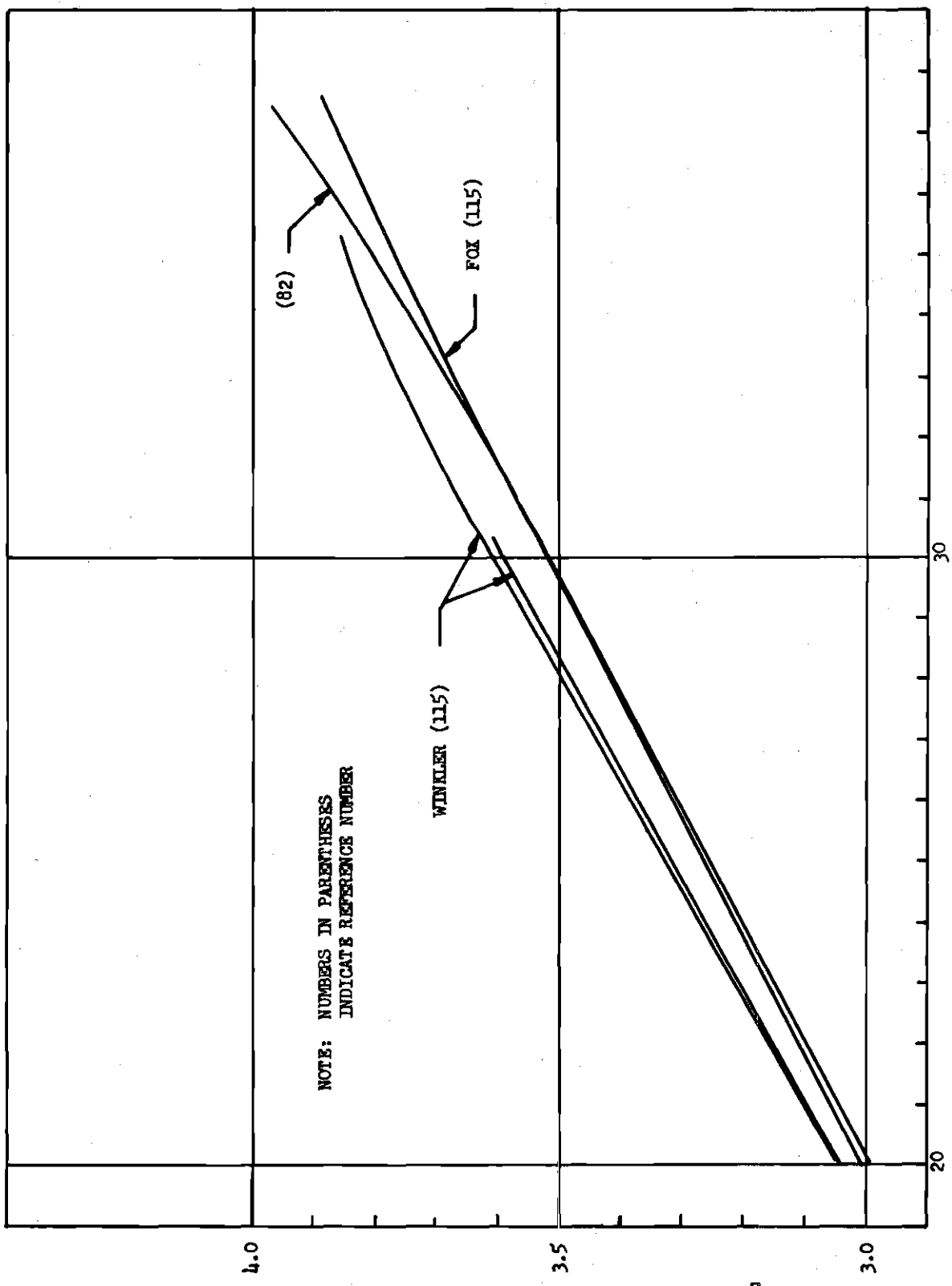


Figure 10. Henry's Constant at One Atmosphere

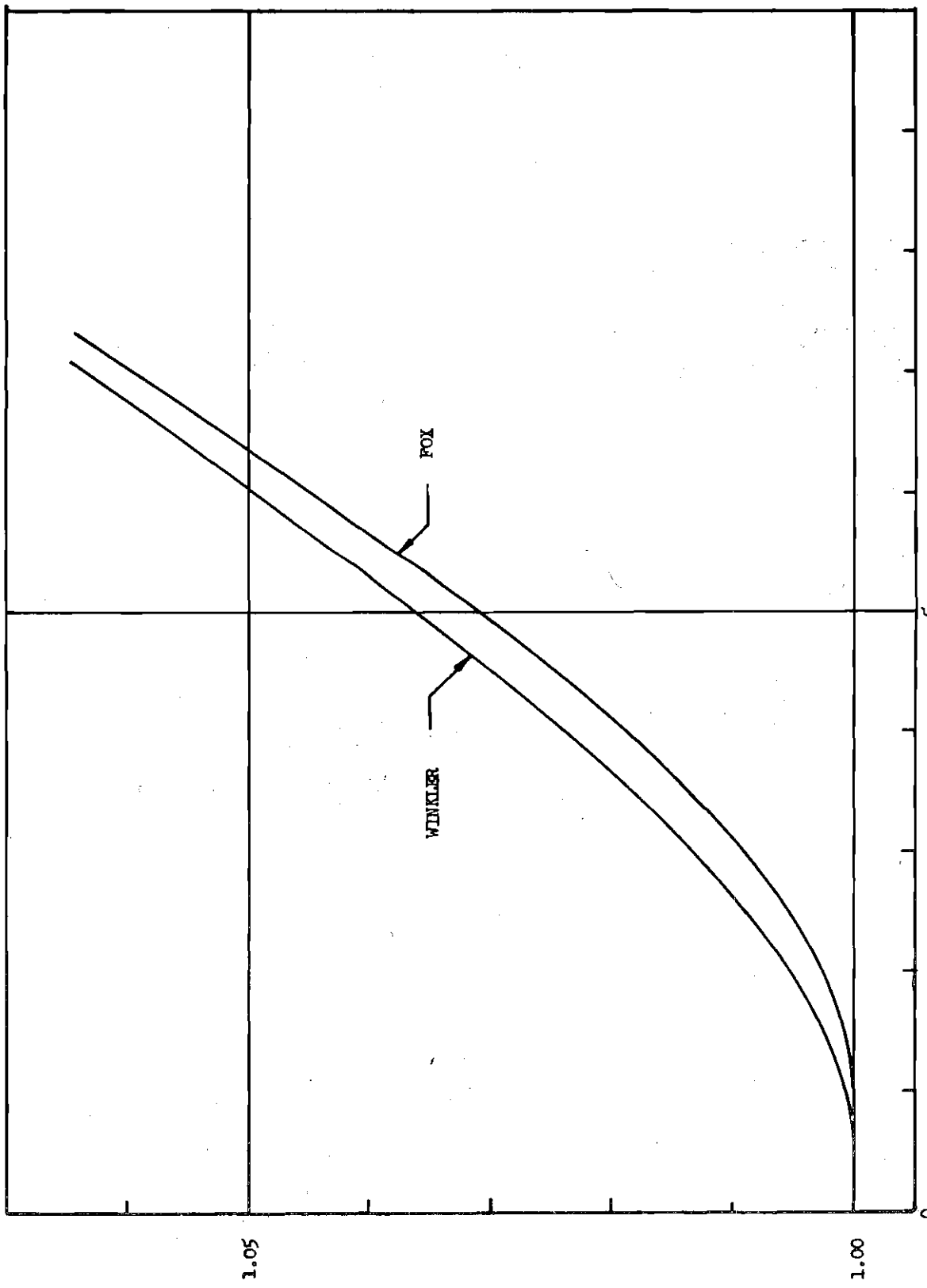


Figure 11. Variation of Henry's Constant with Partial Pressure

be negligibly small since the ratio itself is very nearly one.

The partial pressure of oxygen in the tank was determined from the readings of atmospheric pressure and gage pressure in the tank. Since the gas above the tank pool immediately prior to closure of the tank exhaust valve was air, it was necessary to subtract from the measured total pressure the partial pressures of the gases other than oxygen in the air. It was assumed that the only other significant constituents of the air were nitrogen and water vapor. The air above the pool was assumed to be saturated with water vapor. The total pressure inside the tank and the calculated partial pressure of oxygen for each of the various runs are tabulated in Table 7. The partial pressures of nitrogen gas and water vapor totaled approximately 600 mm of Hg for all runs.

Leakage in the system introduced some error in the calculated partial pressure of oxygen since the true amount of nitrogen gas in the tank was unknown because of the leakage and resultant continual influx of oxygen from the supply cylinder. Assuming an approximate value of the partial pressure of nitrogen as 570 mm of Hg and a range of partial pressures of oxygen of 600 to 2200 mm of Hg, the range over which the various transfer runs to be discussed below were conducted, a maximum error of approximately 50 per cent could conceivably have been introduced if all the nitrogen in the

system were lost to the atmosphere. This, in turn, would introduce roughly the same error in the calculated saturation concentration. However, it is not likely that all nitrogen would be lost. Also, the conditions at which the greatest possible error would be introduced, that is, the lower total pressures, usually existed shortly after the closure of the exhaust valve, thus reducing greatly the probability that large quantities of nitrogen had escaped. Leakage was not excessive in all runs, furthermore. It is to be noted, however, that any errors of this nature which existed would tend to overestimate the transfer efficiency of the system discussed below.

The saturation concentrations as determined in the above manner using the adjusted value of H in eq. (4.3) are tabulated in Table 8.

Galvanic Cell Oxygen Analyzer Calibration

The basic consideration in the calibration of the oxygen analyzer is that a transfer process is occurring between the fluid surrounding the exterior of the analyzer tip and the KOH solution beneath the analyzer membrane. Oxygen must be transported from the bulk of fluid phase across some concentration and hydrodynamic boundary layers to the membrane surface and then diffuse through the membrane to the KOH solution. Thus both the membrane and the fluid will offer a transfer resistance, as would be expected from the discussions in Chapter II. The steady-state resistance of the membrane will be essentially constant for a given temperature (160), but the thicknesses, and therefore resistance, of the

boundary layers on the exterior of the analyzer surface will vary with the flow characteristics. The total resistance to transfer, and therefore, the calibration of the analyzer, will thus be a function of the flow characteristics. As indicated in Chapter II, the parameter characterizing boundary layer development is a Reynolds number. Since, for a given fluid and temperature, the concentration boundary layer decreases in thickness with increasing Reynolds number (see eq. 2.167), it would be expected that the resistance of the boundary layer to the transport of oxygen across it would decrease with increasing Reynolds number. Stating it another way, as the Reynolds number of the flow grows, since the boundary layer becomes thinner, the transfer resistance and the associated analyzer calibration would become less and less dependent on the Reynolds number of the flow. For a properly chosen Reynolds number, this has been shown to be the case (159, 162). At sufficiently high Reynolds numbers, the analyzer sensitivity, that is, the current generation per unit concentration of oxygen, becomes essentially constant with Reynolds number variation. As has been shown, however, the analyzer sensitivity has a strong dependence on temperature (161, 163).

Atmospheric Pressure Calibration. Attempts at calibration of the tank analyzer proved to be almost futile. The basic cause of this was due to the fact that insufficient consideration was given to the factors discussed above. In some

of the first 21 runs a stagnant flow condition was maintained while the pressure was varied in order that effects of high pressure on the membranes could be ascertained. Such operation, however, produces a condition in which the concentration boundary layer outside the analyzer becomes the controlling transport factor. Since the transport would be diffusive in a still fluid, the establishment of steady conditions would require so long that all measurements made would be made in a transient state.

Even in the remaining of these runs in which the fluid was moving, however, severe deficiencies existed. The flow in the tank itself, if an analogy be made to a large conduit flow, was surely laminar. Thus boundary layers would be relatively large. In addition, the extreme recession of the analyzer from the main flow in its pipe receptacle on the side of the tank would reduce any flow around the nozzle tip greatly. Thus the desired constancy of the sensitivity with Reynolds number, even if the proper form could be found, would not be evident.

Finally, it was not until the completion of these first 21 runs that it was determined that the system required a complete flushing to remove the excess oxygen in the tank after a high pressure run. Merely opening of the exhaust valve and allowing the system to stand a long period of time did not remove all of the excess oxygen gas, due, in all likelihood, to the heavier molecular weight of oxygen than that

of air. Thus high concentrations of dissolved oxygen would be maintained in the water when it was not anticipated.

The expected dependence and variation of analyzer sensitivity with Reynolds number was realized with the inlet and outlet analyzers. A plot employing the pipe Reynolds number, $Re_p$, that is, a Reynolds number based on the pipe diameter and mean velocity in the pipe, indicated only moderate constancy of the experimentally determined analyzer sensitivities tabulated in Table 8. A large degree of this scatter was eliminated by consideration of the temperature variation for the various runs. It was found that if the experimentally determined sensitivity was multiplied by the ratio of the average temperature, in degrees centigrade, of all the measurements made using a particular membrane to the temperature, in degrees centigrade, of a particular measurement, a moderately good correlation of this adjusted sensitivity with Reynolds number resulted. Thus the following parameter was defined:

$$\phi' = \phi(T_M/T) \qquad (4.4)$$

in which $\phi'$ = the adjusted sensitivity, $\phi$ = actual sensitivity for a particular $Re_p$, $T_M$ = mean temperature, $^oC$, of all measurements used to determine $\phi'$, T = actual temperature, $^oC$ of measurement.

The experimentally determined values of $\phi'$ are listed in Table 8. The plots of $\phi'$ versus $Re_p$ for the various mem-

branes, that is, the analyzer calibration curves used for each membrane in all calculations of concentration, are presented in Figs. 12-17. It is seen that some Reynolds number dependence is apparent, but this was not completely unexpected since the lower Reynolds numbers encountered indicated the flow was still laminar in the pipe into which the analyzers projected. For the range of $Re_p$ of roughly 2000 to 4000, the pipe flow was in an unsteady transitory state. This could perhaps, account for some of the scatter remaining in $\phi'$, although no evidence exists to critically examine such a contention. It is to be noticed that each membrane had somewhat different characteristics, both in the exact manner of its dependence on $Re_p$ and, especially, in the magnitude of $\phi'$, although a rough value of $\phi'$ was one μa/mg/l for all the membranes. This value compares qualitatively with values given by Mancy et al. (159, 162) for similar fluid temperatures.

Only Fig. 15 for membrane 6.I displays any significant departure of the individual values of $\phi'$ from the average value. Here for runs 31-40 the approximate value of $\phi'$ was 1.3 μa/mg/l while for run 30 the approximate value was 0.8 μa/mg/l. To be noted is that run 30 was the first run using membrane 6.I. Thus it is possible that sufficient time had not been allowed for the stabilization of the membrane after its preparation. The use of the membrane during run 30 could have perhaps produced the final stabilization required. In any case, since this particular run was not used as a trans-

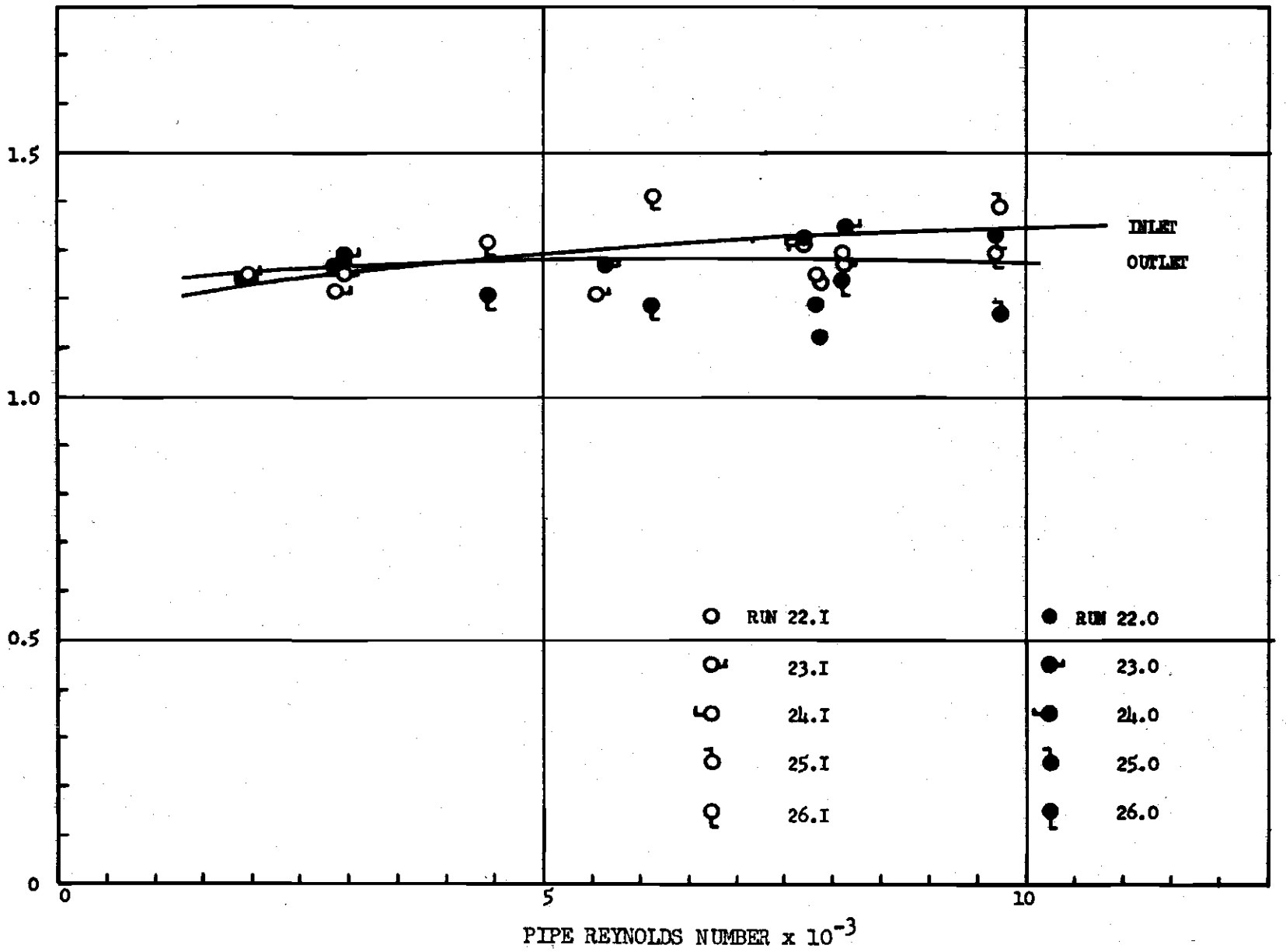


Figure 12. Sensitivity, Membranes 3

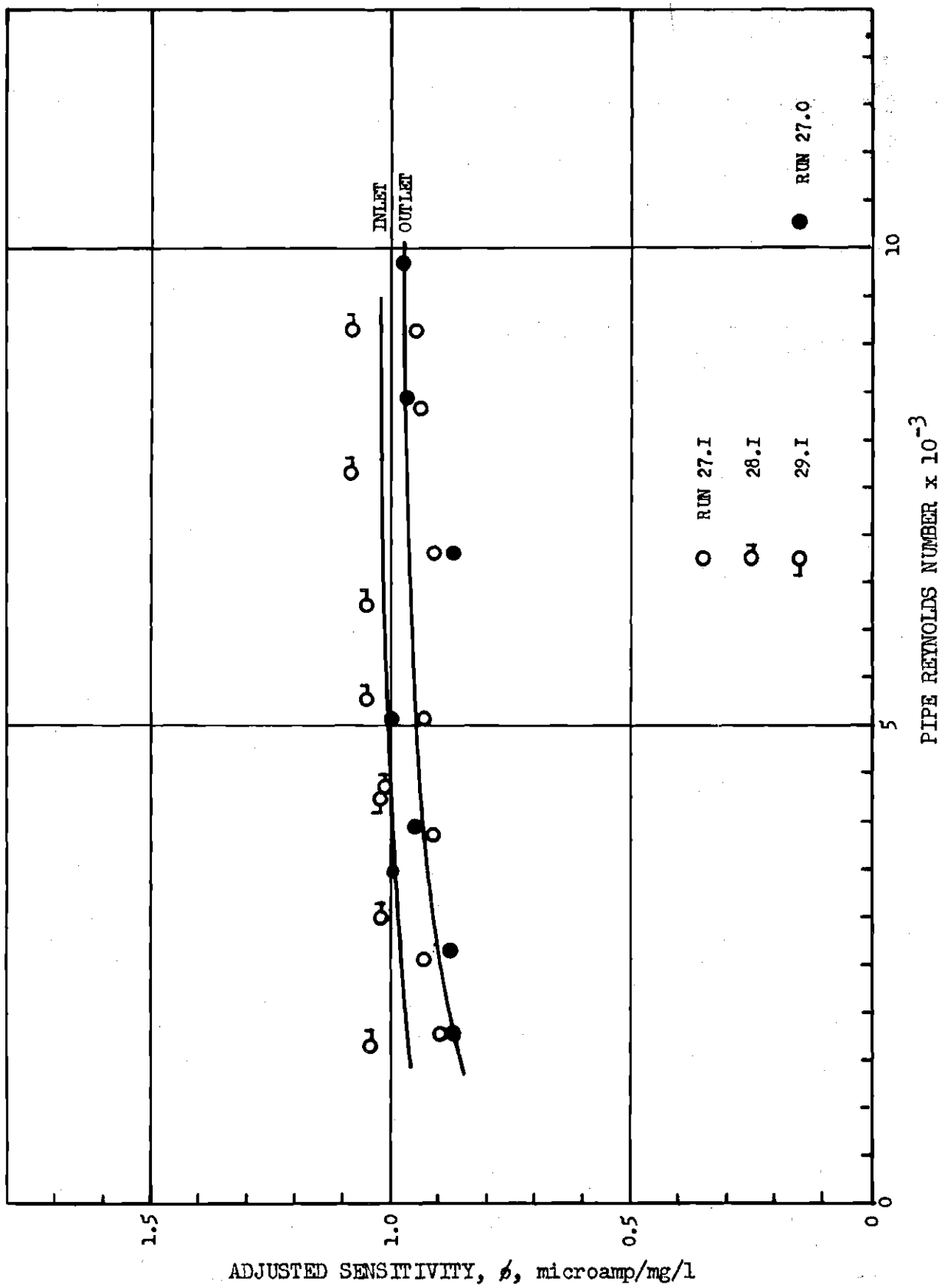


Figure 13. Sensitivity, Membranes 4

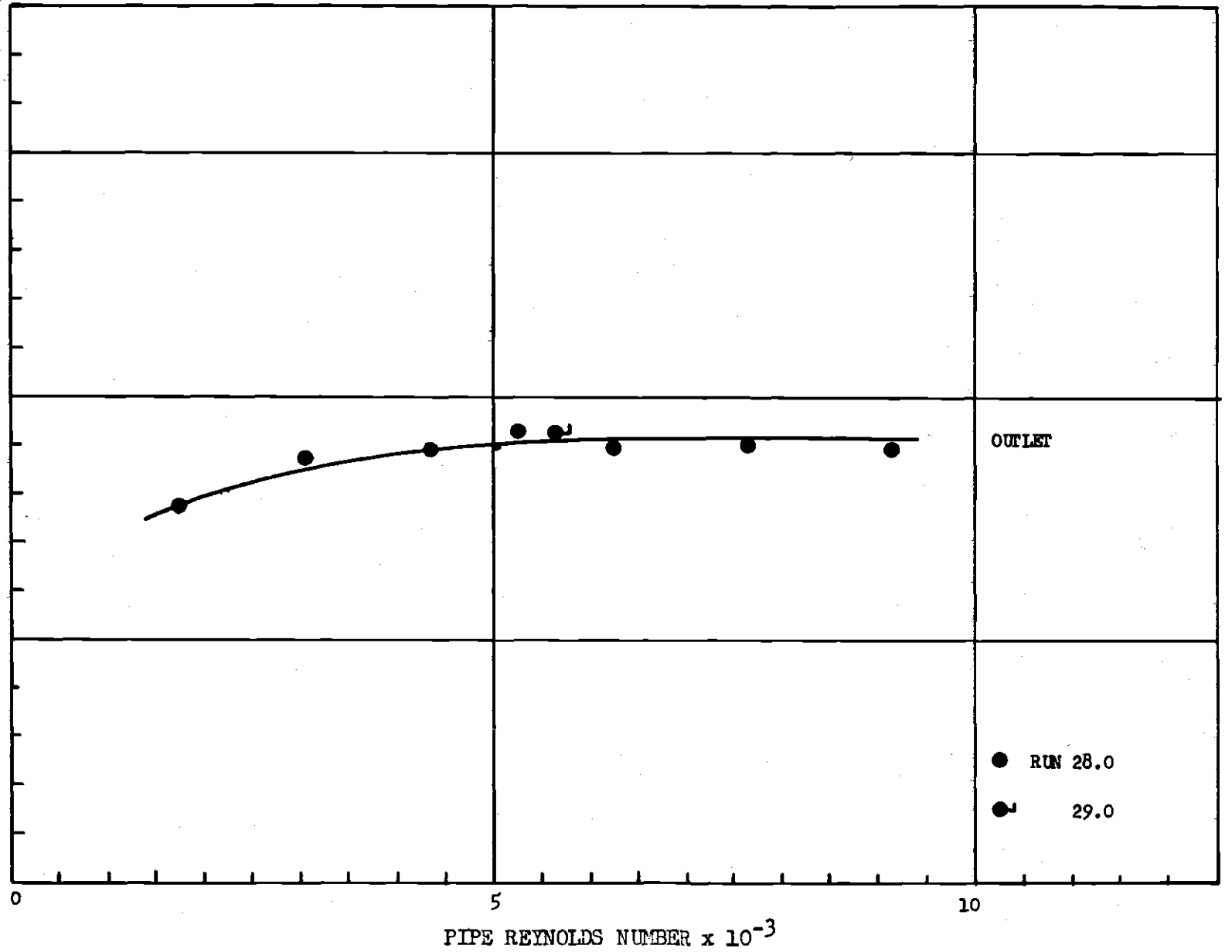


Figure 11. Sensitivity, Membranes 5

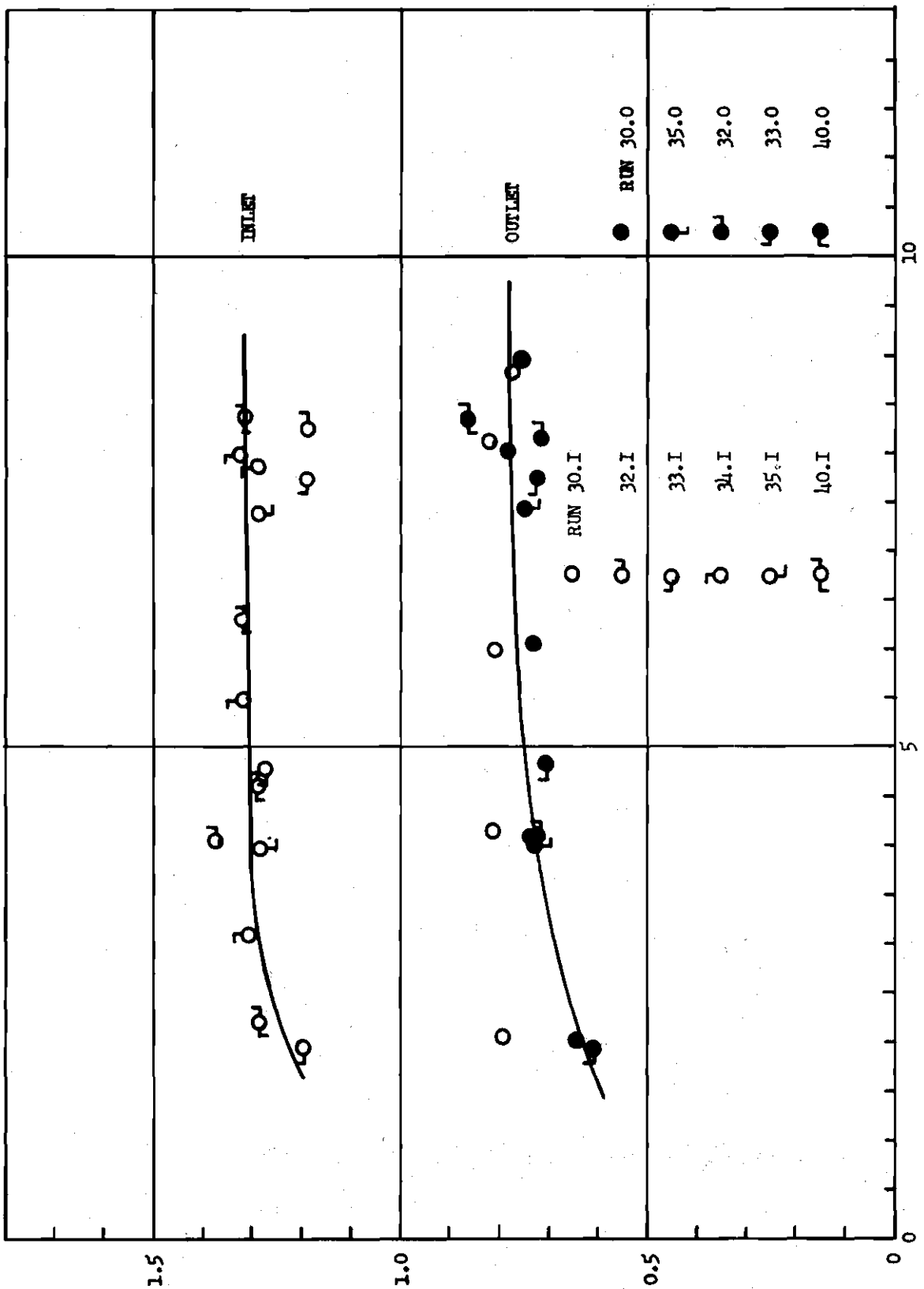


Figure 15. Sensitivity, Membrane 6

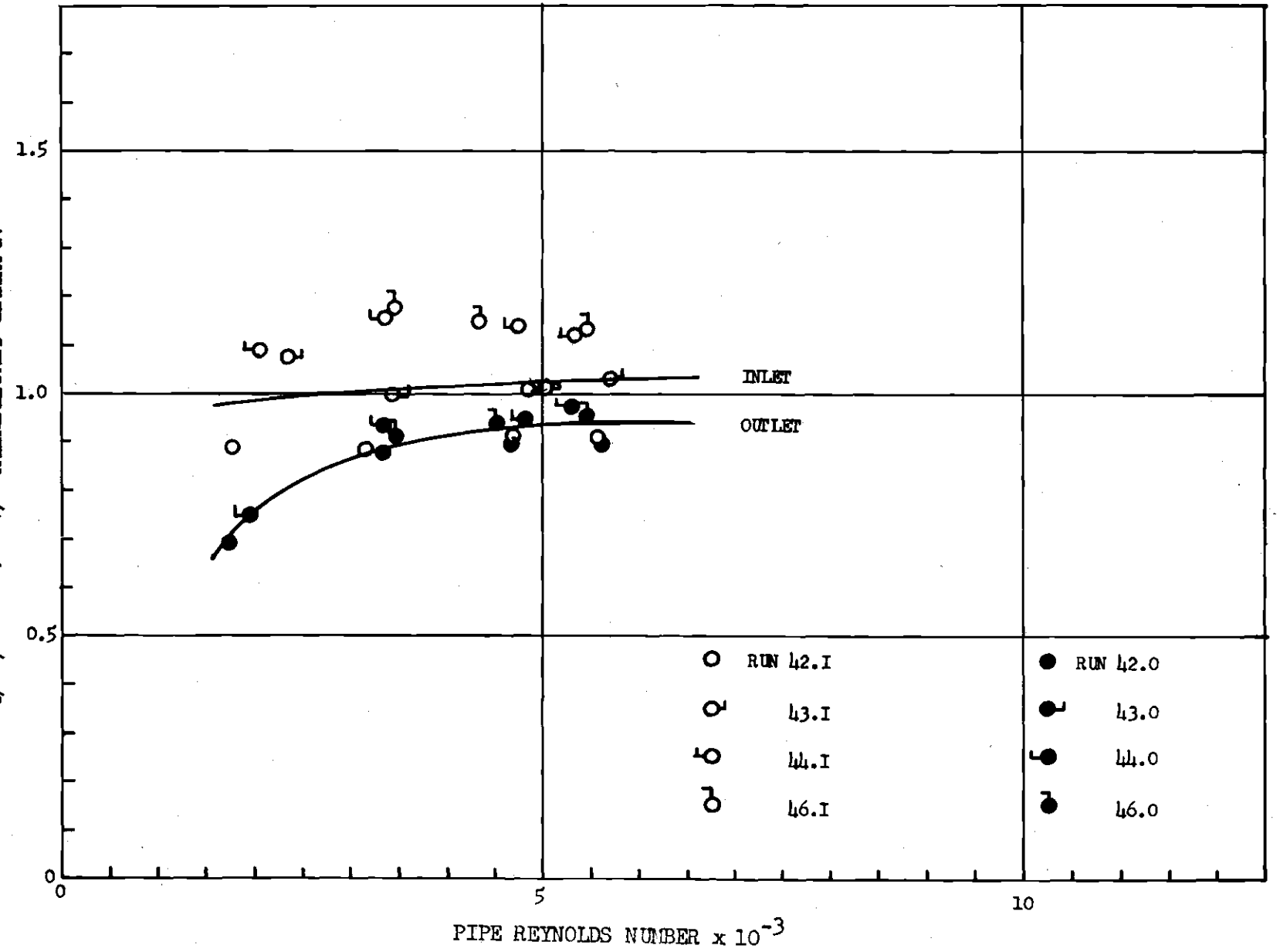


Figure 16. Sensitivity, Membrane 7

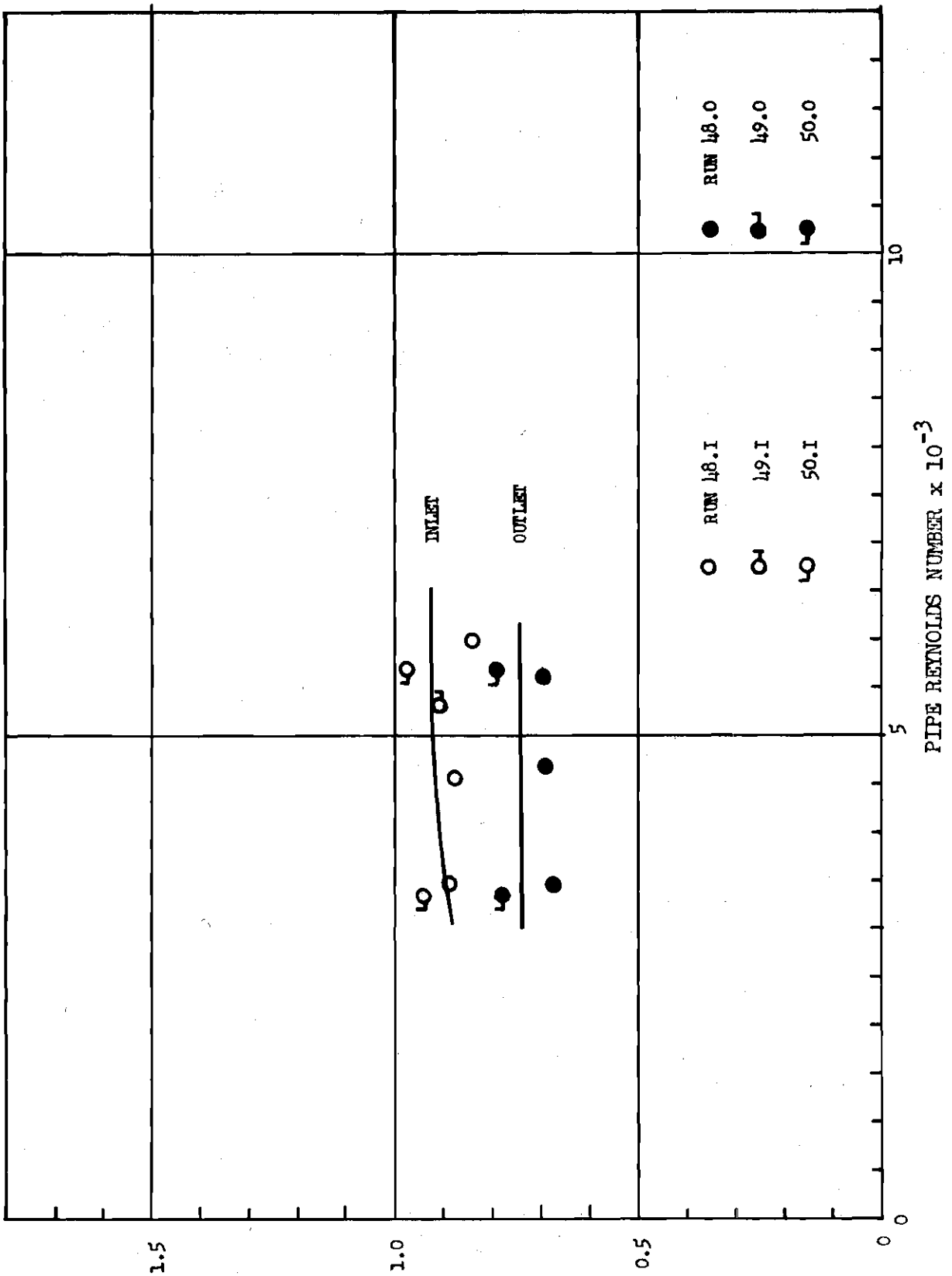


Figure 17. Sensitivity, Membrane 8

fer run and additional calibration runs followed run 30, this behavior did not influence the measurement of the transfer characteristics of the system.

The value of $\phi$ predicted from these calibration curves, adjusted for run temperature, are listed in Table 7. These values were used in calculating all concentrations used in examining the transfer characteristics of the system, even in those cases in which an experimentally determined $\phi$ was known.

High Pressure Calibration. To determine what effect, if any, high pressures had on analyzer operation and current generation, it was necessary to examine the current generation by the analyzer for known concentrations for essentially constant temperature and flow conditions under a range of pressure levels. The calculation of this saturation concentration, which was assumed to exist after sufficient recirculation of the water in the system as indicated by measured voltage drops remaining essentially constant, has been discussed above. With the inlet and outlet analyzers in the system, runs 24, 29, 47, and 50 were used to examine the effects of high pressure on the analyzers.

Fig. 18 shows a plot of saturation concentration of the recirculated water against the current generation by the analyzers. Some unexpected results are apparent. In this plot the solid portion of a curve connects points determined at saturation conditions while the dashed portion connects points measured during a transient, nonequilibrium condition. Runs

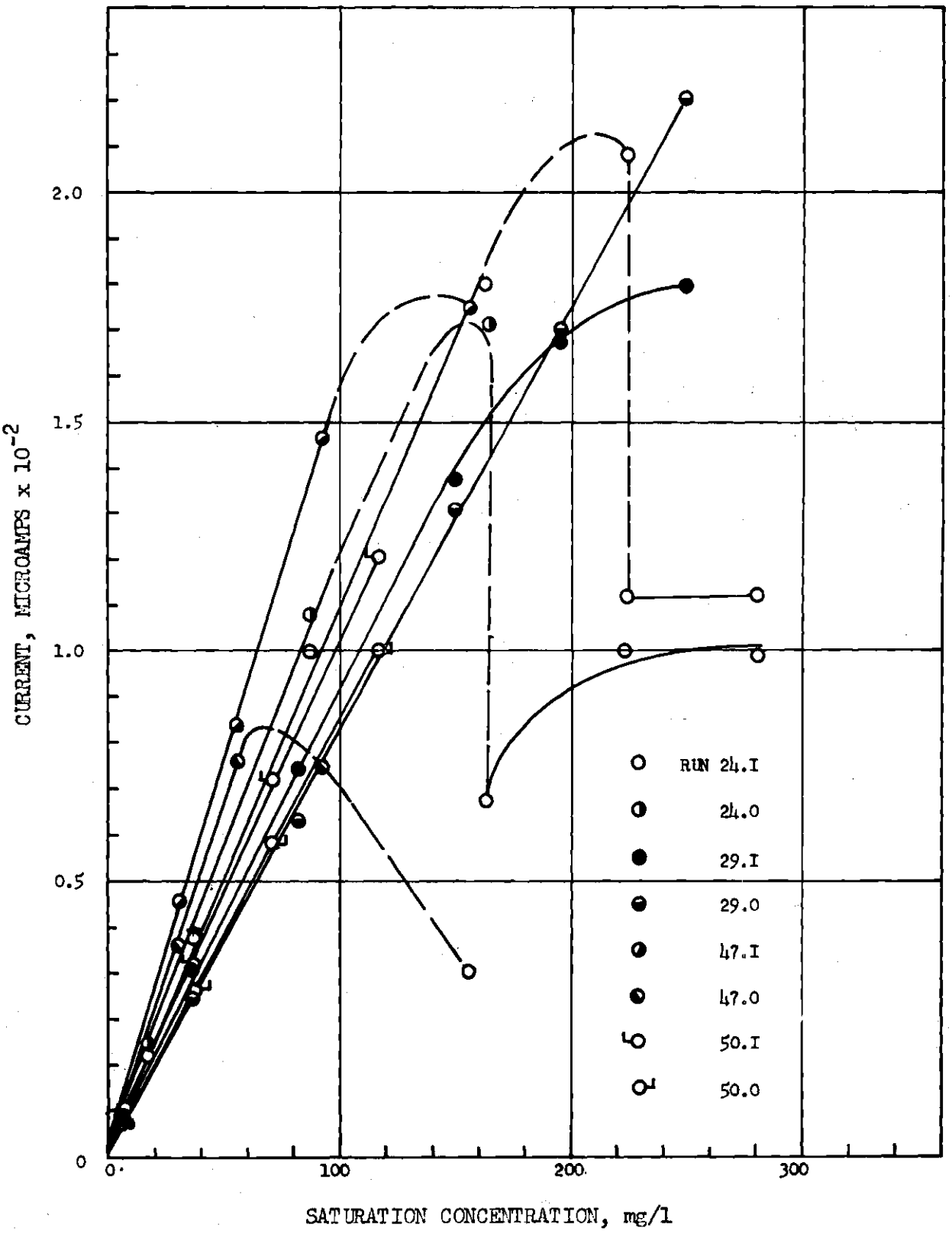


Figure 18. Analyzer Current at High Concentrations

29.0, 50.I, and 50.0 exhibit essentially a linear relationship between current and saturation concentration, indicating essentially a constant sensitivity. Run 29.I, on the other hand, exhibits this linear relationship to approximately only a concentration of 160 mg/l. Runs 24.I, 24.0, 47.I, and 47.0, however, are quite different in that they display a sudden drop in current generation with increasing concentration.

During the actual operation of the apparatus these drops were easily noticed, occurring over a period of roughly one half hour. This type of behavior has not been reported previously and was quite unexpected. Visual examination of the analyzer membranes after the runs failed to reveal any holes or punctures in the membrane. Furthermore, from Table 4, no distinguishable pattern of use particular to these runs is seen. Thus the cause of this behavior is unknown.

The variation of current with gage pressure, as determined by the gage upstream of the tank for the inlet analyzer and as determined by the tank gage for the outlet analyzer, is shown in Fig. 19. Variations are similar to those in Fig. 18.

From Fig. 18 and Fig. 19 it appears that unless a radical and relatively sudden change in current generation occurs, the sensitivity of an analyzer, for a given set of temperature and flow conditions, remains very nearly constant with increases in total pressures to roughly 70 psia. Based on the admittedly limited results of runs 24 and 29,

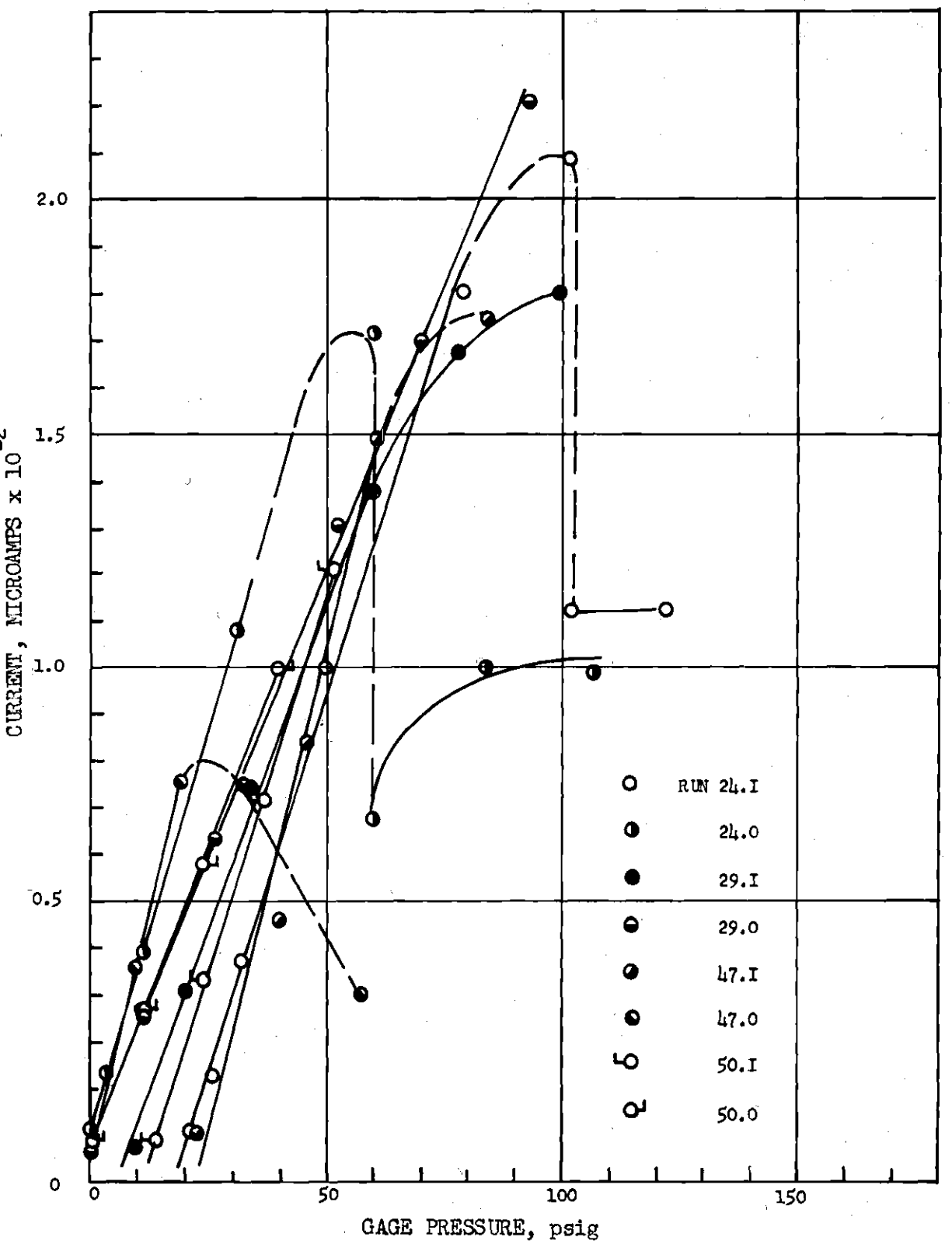


Figure 19. Analyzer Current at High Pressure

it was decided to limit the maximum total pressure to which an analyzer was subjected during transfer runs to approximately 40 psig. Operating under this limitation, it was anticipated that the nonlinear analyzer behavior would be avoided, thus enabling the use of analyzer sensitivities determined from operation of the apparatus at normal atmospheric pressure in the calculation of concentrations under conditions of high pressure. When this limit was chosen run 49 was not available. However, no sudden decreases were noted during the various transfer runs made and so it is believed for the restricted range of pressures used during transfer runs, the sensitivity of an analyzer remained constant for similar temperature and $Re_p$. It is to be noted that this restricted pressure range severely curtailed the use of the MX-0 nozzle because of the relatively large pressure drop which existed across the nozzle.

System Transfer Characteristics

From the predicted values of $\phi$ listed in Table 8, the inlet and outlet concentrations were calculated for the various operating points of the several transfer runs in which the tank pressure was greater than atmospheric. Using the calculated saturation concentration an overall transfer efficiency for the system, $E_o$, was calculated according to eq. (3.36) where the initial concentration is that at the inlet analyzer, the interfacial concentration is the saturation concentration, and the concentration at time t is assumed to be the concen-

tration at the outlet analyzer. These values are listed in Table 9.

For each of these runs, Table 10 lists the mean droplet diameter, $d_d$, as determined from eqs. (4.1) and (4.2). The average fall distance for this mean droplet, calculated as the distance between the tip of the nozzle and the pool surface, is also tabulated. The average velocity, U, of all droplets was assumed to be constant over the entire length of fall of the droplets and to be approximated by the volume rate of flow divided by the nozzle outlet area. From this fall distance and nozzle velocity, an approximate droplet contact time, $t_{ct}$, was determined. The molecular diffusivities of oxygen in water listed in Table 10 were determined from the formulations of Wilke (244) and have an approximate value of $2.5 \times 10^{-5}$ $cm^2/sec$. It is to be noted Wilke's formulations predict diffusivities which agree well with observed values (see ref. 245 and Table 11).

Listed in Table 11 are a drop Reynolds number, $Re_d$, continuous phase Reynolds number, $Re_c$, drop Schmidt number, $Sc_d$, and drop Weber number, $We_d$, as given by eqs. (3.3), (3.4), and (3.6) respectively, except that the fluid properties of the droplet are used for $Re_d$, $Sc_d$, and $We_d$. The surface tension used to calculate $We_d$ was that of water in contact with air rather than that of water in contact with oxygen since these latter values were unavailable. Also listed is the modified Peclet number, $Pe'_d$, as given by eq. (3.84), based on the vis-

cosities of water and oxygen gas. It is to be seen that the transfer runs had the following ranges for these dimensionless parameters: $Re_d$, 526 to 1695; $Re_c$, 29 to 97; $Sc_d$, 0.34 to 0.38; and $Pe'_d$, 4.1 to 13.5.

## Analysis

To be discussed and analyzed here are the oxygen transfer characteristics of the droplet system as exhibited by the system during transfer runs when operating under greater than atmospheric pressures. As previous discussions have indicated, the analysis of the droplet system produced by each nozzle is to be based on a simplified model which assumes a single spherical droplet with a diameter equal to the mean diameter of all droplets to adequately typify the system.

### External Phase Transfer

It has been pointed out in the discussion of the two film theory that for the diffusion of slightly soluble gases in liquids, such as oxygen in water, the gas film offers comparatively little transfer resistance. Also, in this droplet system the gas surrounding each droplet, for the transfer runs, had a volume concentration ranging from 20 to 80 per cent oxygen. Thus the effects of the external, continuous phase on the transfer characteristics of the droplet system would be expected to be negligible.

Furthermore, experimental results also support this assumption. Eqs. (3.24) and (3.35) are the two basic correlations for transfer in the external phase surrounding a

sphere and a circulating droplet, respectively. Examination of Table 13 will show that the ratio of the viscosity of oxygen, assumed to be essentially that of the gas actually surrounding the droplets, and the viscosity of water is very nearly constant for the transfer runs. The function of the ratio of these two viscosities in eq. (3.35) thus becomes essentially a constant. Replacing $Sh_c$ by $Sh_c - Sh_s$ in eq. (3.24), it is seen that these two forms are basically similar for the droplet system being considered here.

The diffusivity of oxygen in the continuous phase would be expected to be roughly proportional to that of oxygen in water for the small temperature range of the various transfer runs. A similar statement applies to the kinematic viscosities of the continuous and droplet phases. Furthermore, the overall transfer coefficient of the system, K (see eq. 3.2), could be at least approximated by that calculated from eq. (3.47) using the transfer efficiency based on the transfer characteristics of the entire system. Thus, from eqs. (3.2), (3.3), and (3.4), based on the above reasoning, the continuous phase Sherwood, Reynolds, and Schmidt numbers should, for the various transfer runs, be approximately proportional to their droplet phase counterparts. This, in turn, implies that, at least in an approximate sense, from eqs. (3.24) and (3.35),

$$Sh_o = (\text{constant})\ Re_d^p\ Sc_d^r \qquad (4.5)$$

in which $Sh_o$ is an overall Sherwood number based on the diffusivity of oxygen in water, listed in Table 10, and on the calculated overall transfer efficiency of the system tabulated in Table 9.

If the transfer in the droplet system is essentially independent of the external phase, then $Sh_o$ should be independent of the R.H.S. of eq. (4.5) since it is this parametric form which, from the above discussion and discussions in Chapter III, should characterize the transfer in the external phase for the transfer runs.

In Table 13 is listed $Sh_o$ for the various transfer runs in which the overall transfer efficiency, $E_o$, did not exceed unity. Since $Sh_o$ was calculated using eq. (3.47) it was not possible to determine $Sh_o$ for values of $E_o$ greater than unity. From the discussion of transfer to and from droplets in Chapter III, approximate values of p and r are 0.5. In Table 13 are listed the computed values of $(Re_d Sc_d)^{1/2}$. Fig. 20 presents a plot of $Sh_o$ versus $(Re_d Sc_d)^{1/2}$. From this plot it appears that $Sh_o$ is quite independent of $(Re_d Sc_d)^{1/2}$.

The above discussion and experimental results indicate that any oxygen transfer in the continuous phase has negligible influence on the transfer characteristics of the total droplet system. Oxygen transfer in the system is essentially dependent only on the transfer in the droplets themselves. Thus, transfer in the droplets need be considered only in the remainder of the analysis.

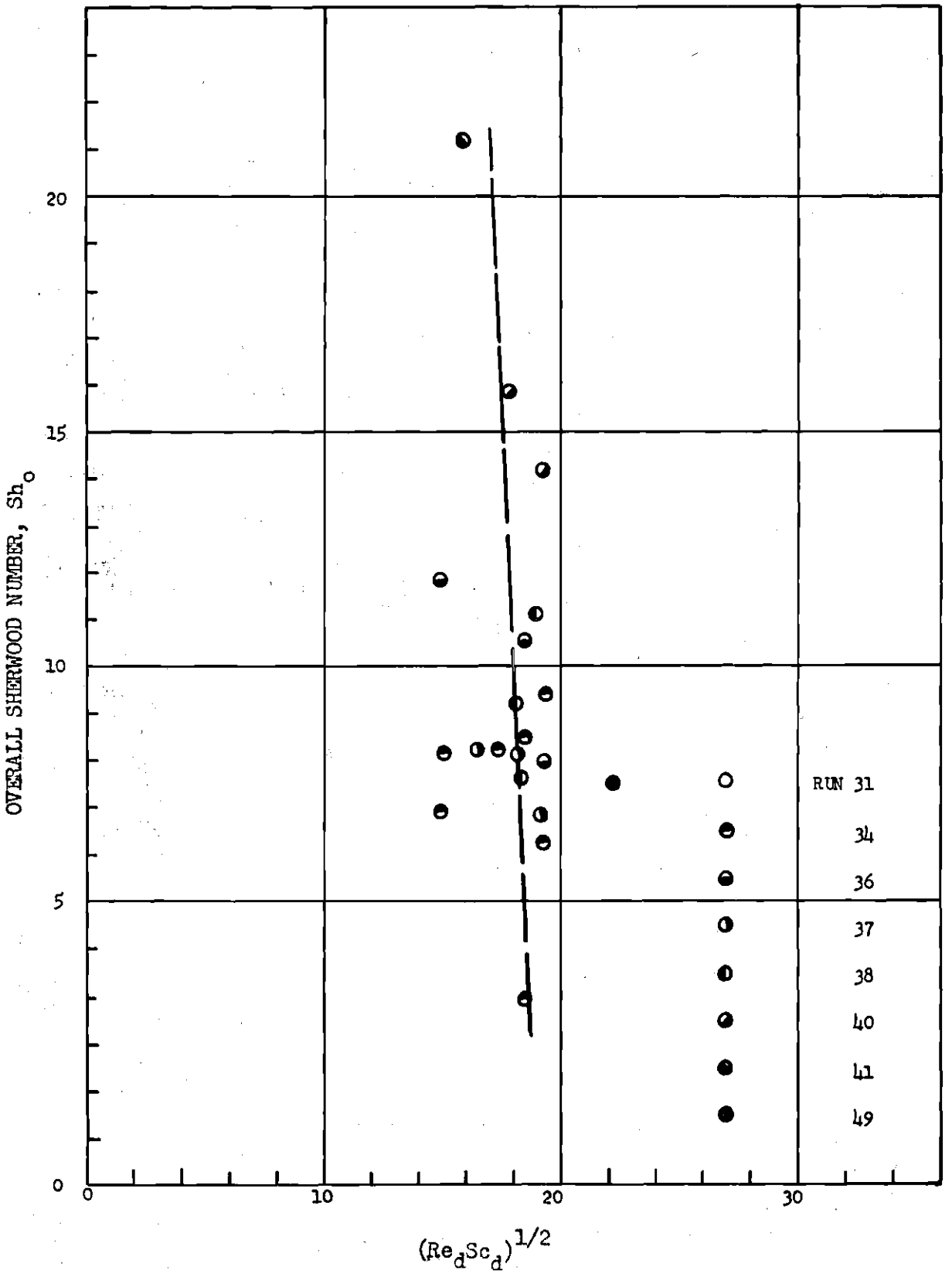


Figure 20. Overall Sherwood Number

Transfer in Droplets

In Table 9 it is seen that some values of the overall transfer efficiency, $E_o$, are greater than unity, indicating that in some cases, the water passing the outlet analyzer was apparently significantly super-saturated with oxygen. In order to qualitatively compare the measured transfer efficiencies, the dimensionless time parameter $T^*$ (see eqs. 3.83 and 3.101), with t set equal to $t_{ct}$, was used. Since this is the physical parameter which is used in most of the droplet models discussed in Chapter III, it would be expected that, if these models are at all accurate, this parameter could be used to obtain a successful correlation of the experimental data. Table 13 tabulates $T^*$ for the various transfer runs. In Fig. 21 the variation of $E_o$ with $T^*$ is shown. It is immediately apparent the two nozzles display entirely different characteristics. Nozzle MX-00 shows a gradual increase in $E_o$ with increasing $T^*$, reaching values of $E_o$ of roughly unity. Nozzle MX-0, on the other hand, shows a gradual decrease in $E_o$ with increasing $T^*$, from an initial value of approximately 2 to a final value of approximately unity.

MX-0 Nozzle. An approximate linear equation describing the data in Fig. 21 for the MX-0 nozzle is

$$E_o = 2.3 - 6.6T^* \qquad (4.6)$$

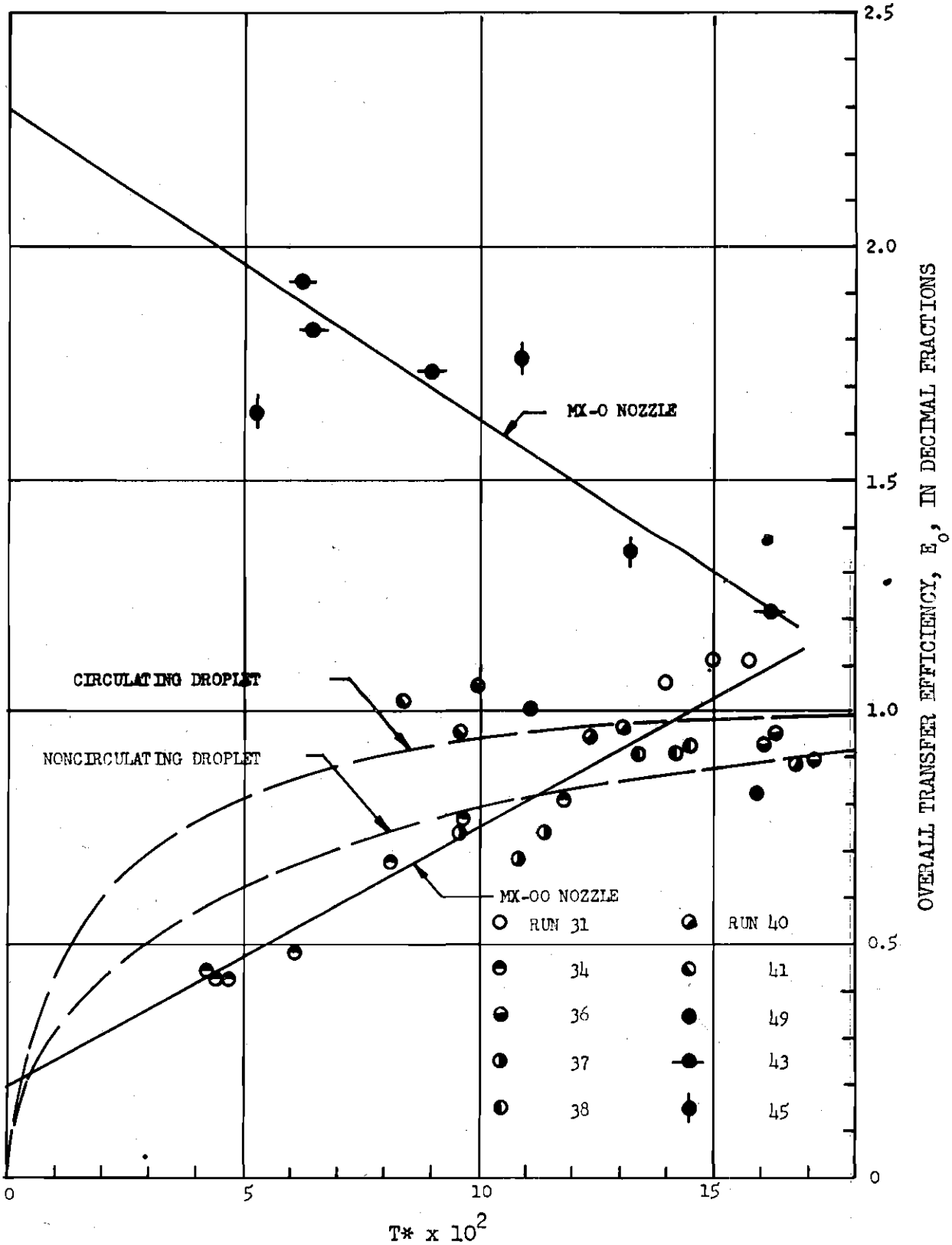


Figure 21. Overall Transfer Efficiency

Other nonlinear relationships were derived but none fit the data more adequately than eq. (4.6). The time decreasing transfer efficiency of this relationship is to be noted. The apparent transfer efficiency at zero time of 2.3 indicates an extremely high degree of contact and mixing of the incoming water and oxygen atmosphere in and very near the nozzle.

Though the initial super-saturated condition is unexpected, the decay of this super-saturated condition with time, as indicated by the decrease of $E_o$ with $T^*$, is not. The super-saturated state is an unstable one, and one which would approach a stable state by the dissolution of oxygen in essentially the same manner that absorption of oxygen would occur. In addition to the decay in $E_o$ itself, it is to be noted that the dimensionless time required to reach a unit value of $E_o$ is roughly the same time as that required by the droplets produced by the MX-00 nozzle. Furthermore, this dimensionless time, approximately 0.2 as predicted by eq. (4.6), is comparable to a dimensionless time of approximately 0.18 which is predicted by eq. (3.76) as the time for a circulating droplet to reach a transfer efficiency of 0.99.

The above remarks must be viewed with caution because of the following four factors: (1) The data for the MX-0 nozzle are extremely limited, of necessity because of the pressure limitations discussed earlier. (2) The scatter in the data is more than is completely acceptable. (3) In addition, as mentioned earlier in this chapter, gas leakage from

the tank was considerable during the runs using the MX-0 nozzle. Thus any errors which are present in calculations due to incorrect saturation concentrations would tend to over-estimate the actual value of $E_o$. In Table 14 values of $E_o$ for runs 43 and 45 are presented which assume a 50 per cent increase in the saturation concentration over that used to originally calculate $E_o$, the 50 per cent figure being the estimated maximum possible error in saturation concentration due to leakage as discussed previously. It is to be remembered that it was pointed out that this percentage was not likely to have occurred. This contention is also somewhat supported by the fact, as can be seen from Fig. 21, that the data for run 49, which likewise suffered from similar considerable gas leakage, show no extreme differences from that of the other data for the MX-00 nozzle which was collected from transfer runs in which the leakage was not excessive. Table 14 shows a considerable change in the values of $E_o$. A plot, not presented here, of these values against $T^*$, however, showed even more scatter and lack of systematic variation than did the original values. (4) A final factor which must be realized in comparing the value of $T^*$ at $E_o$ equal to unity with $T^*$ for an $E_o$ of 0.99 predicted by the circulating droplet model is that $E_o$ includes all end effects, while the transfer efficiencies predicted by the various models in Chapter III did not include any type of end effects.

Evaluation of end effects was made for the MX-00 nozzle, as will be seen below. However, examination of the calculations necessary to evaluate these end effects will show that they can be made only if $E_o$ is less than unity. This precluded the evaluation of end effects for the system with the MX-0 nozzle in operation.

MX-00 Nozzle. The variation of $E_o$ with $T^*$ for the MX-00 nozzle is shown in Fig. 21. Also shown, for qualitative comparison purposes, are the theoretical variation of transfer efficiency as predicted by the circulating and stagnant droplet models. The data can be approximately represented by

$$E_o = 0.2 + 5.5T^* \qquad (4.7)$$

In contrast to the MX-0 nozzle, only a moderate initial mixing and transfer apparently occurs in the MX-00 nozzle.

The overall transfer efficiency, of course, includes end effects. In order to properly compare the transfer efficiency of the droplet system, it is necessary to make a correction for end effects. A procedure presented by Johnson and Hamielec (124) will be following: Let $\rho_1$, $\rho_2$, $\rho_3$, and $\rho_4$ be the concentrations of oxygen at the following locations, respectively: 1, at the inlet analyzer; 2, at the nozzle tip where the droplet begins its free fall; 3, at the pool surface where the droplet strikes the water; and 4, at the outlet analyzer. Let $\rho_s$ be the saturation concentration as

before. Define the following transfer efficiencies:

$$E_1 = \frac{\rho_2-\rho_1}{\rho_s-\rho_1} \tag{4.8}$$

$$E_2 = \frac{\rho_4-\rho_3}{\rho_s-\rho_3} \tag{4.9}$$

$$E = \frac{\rho_3-\rho_2}{\rho_s-\rho_2} \tag{4.10}$$

It is seen that E corresponds to the same E predicted by the various models in Chapter III. The overall transfer efficiency is now explicitly defined, consistently with the definition used previously, as

$$E_o = \frac{\rho_4-\rho_1}{\rho_s-\rho_1} \tag{4.11}$$

Letting

$$E_F = E_1 + E_2 - (E_1)(E_2) \tag{4.12}$$

then

$$E = \frac{E_o-E_F}{1-E_F} \tag{4.13}$$

Eq. (3.102) gives the general form of E for the various droplet models. For values of E greater than approximately 0.5, eq. (3.102) is given closely by a first term approximation (123), that is,

$$E \simeq 1 - 6A_1 \exp(-\lambda_1^2 T^* R^*) \qquad (4.14)$$

Combining eqs. (4.13) and (4.14),

$$\ln(1-E_o) = -\lambda_1^2 R^* T^* + \ln 6A_1(1-E_F) \qquad (4.15)$$

The R.H.S. of eq. (4.15) indicates why only transfer efficiencies less than unity can be considered in evaluating end effects. Since, even for the MX-00 nozzle, a few values of $E_o$ were slightly greater unity, all values were necessarily not included in the determination of end effects. Fortunately, only a few values had to be disregarded, as can be seen from Table 9.

If $E_F$ and $R^*$ are constant for all operating conditions, that is, a similar overall transfer mechanisms exists for all operating conditions, then a plot of $\ln(1-E_o)$ against $T^*$ should yield a straight line whose slope is $\lambda_1^2 R$ and whose intercept is $\ln 6A_1(1-E_F)$. Using an eigenvalue of 3.142, from Table 2, the values of $-\ln(1-E_o)$ are plotted against T in Fig. 22. The scatter is considerable. It is to be realized, however, that because the values of $1-E_o$ were small for

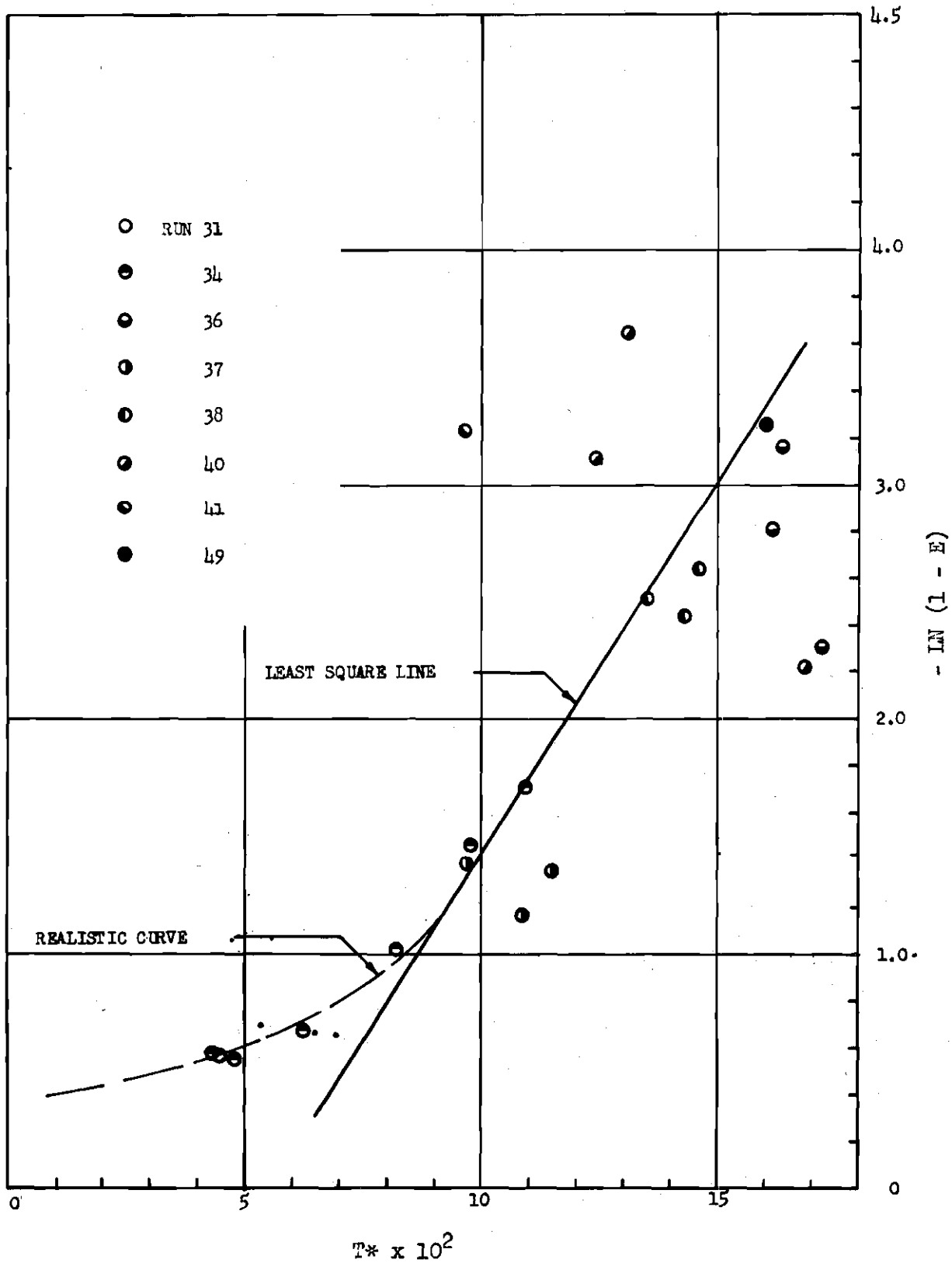


Figure 22. Evaluation of End Effects

most runs, the logarithm plot tended to exaggerate differences between experimental values. A least squares line was passed through the data and is given by

$$-\ln(1-E_o) = -1.78 + 32.3T^* \qquad (4.16)$$

Evaluating eqs. (4.15) and (4.16) for $T^*$ equal to zero, the value of $E_F$ is -8.79. Using an approximate value of $E_1$ equal to 0.2 from eq. (4.7), $E_2$ becomes approximately -11.2. Such a value indicates an extremely high degree of dissolution of oxygen after the droplet strikes the pool of water. While dissolution could perhaps occur at this point, it seems unlikely that dissolution of such magnitude could occur. These points, however, should be borne in mind. As mentioned previously there may be some error in the value of saturation concentration due to gas leakage from the system. This, of course, will affect the value of $E_o$. Furthermore, since $\rho_3$ will be approaching $\rho_s$, small errors in $\rho_s$ could, effectively, produce significant errors in $E_2$, as seen from its definition in eq. (4.9). Most importantly, the assumption of constant end effects and constant $R^*$ is not necessarily a valid assumption for the droplet system under consideration, especially in light of the fact that $Re_c$ ranged from 29 to 97. In this regard, it is enlightening to review the discussion associated with eq. (3.102). Indeed, a somewhat more reasonable relation between $\ln(1-E_o)$ and $T^*$ is shown in

Fig. 22 by the nonlinear dashed curve. While open to question, the least squares line of Fig. 22, for lack of anything better, was used to determine $R^*$.

From the slope of eq. (4.16), $R^*$ was calculated to be approximately 3.3. Using this value, the theoretical solution, as obtained from a first term approximation, to eq. (3.102) was plotted in Fig. 23. From eq. (4.13), with $E_F$ equal to -8.79 as determined above, values of E were determined. These are given in Table 15 and are compared with the theoretical solution in Fig. 23. For comparison purposes, the theoretical solutions for the noncirculating droplet ($R^*$ equal to 2.25) were also shown. A curve could not be presented for the turbulent model because no eigenvalue has been determined for this model. The oscillating droplet model could not be considered since, as was brought out in the discussion of it, considerable droplet information is necessary, much more than was available from this study.

Examination of Fig. 23 shows a good correlation between the theoretical solution for $R^* = 3.3$ and the experimental results. However, care must be taken in evaluating this close correlation because of the actual numbers involved in calculating E. With the previously mentioned value of $E_F$ equal to -8.79, E, from eq. (4.13), becomes

$$E = \frac{E_o+8.79}{1+8.79} = \frac{E_o}{9.79} + 0.898 \qquad (4.17)$$

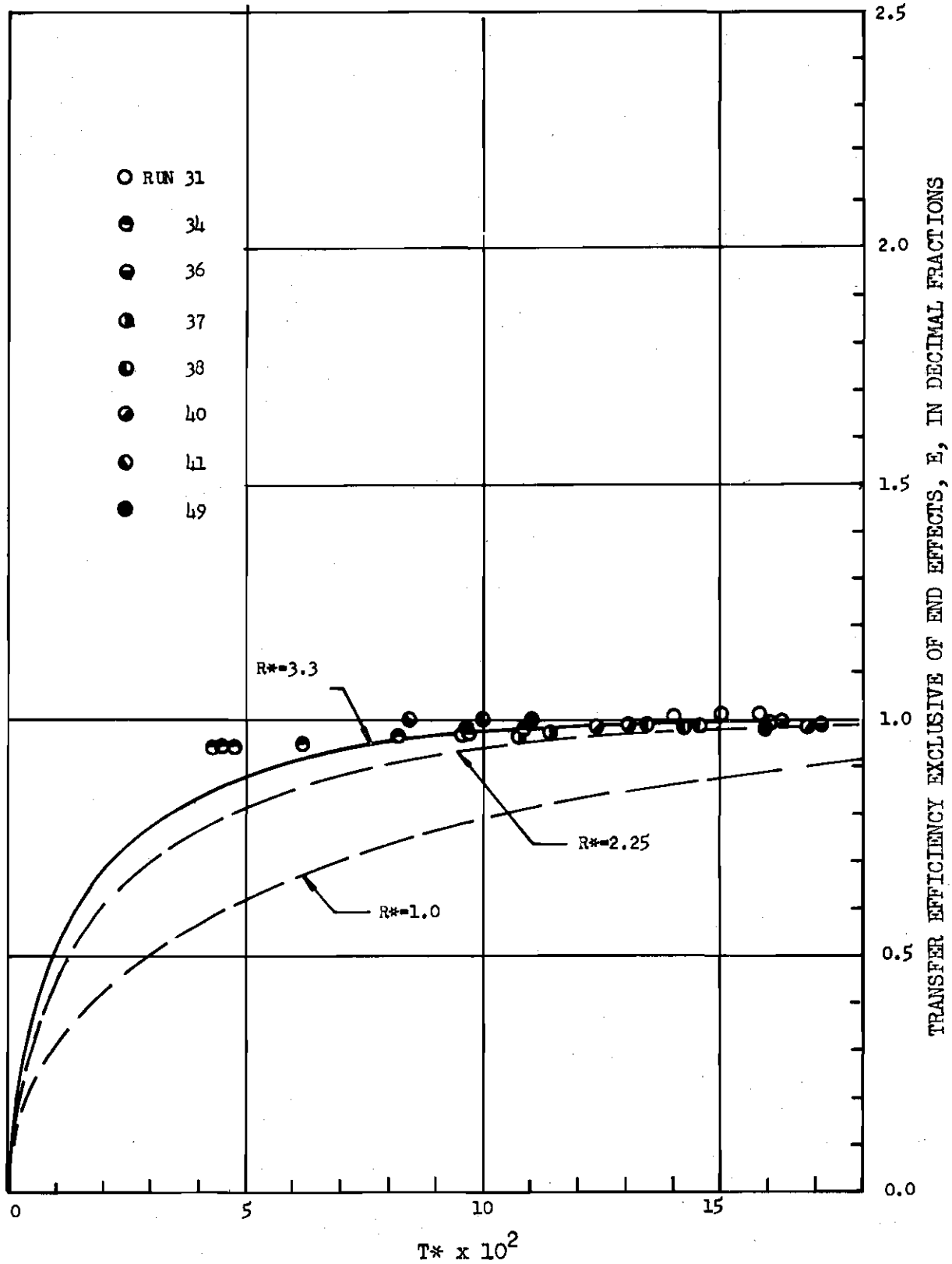


Figure 23. Droplet Transfer Efficiency

Thus the experimentally determined values of $E_o$ are divided by a relatively large number. This tends to mask possible errors in $E_o$.

An effective diffusivity ratio of 3.3 indicates a considerable amount of internal mixing within the droplet. It is to be remembered that the circulating droplet model predicts a value of only approximately 2.25. The type of internal droplet motion which actually exists is, of course, unknown. However, the following points should be noted: Bond and Newton's equation for the critical droplet diameter, eq. (3.14), indicates an approximately critical diameter, assuming a temperature of 30°C, of 0.3 cm, which is larger than the droplets actually produced by the two spray nozzles. Thus, Bond and Newton's criterion indicates the droplets would act as rigid spheres and exhibit no circulation due to drag forces on the droplet surface. However, considering the violent break-up which must occur inside the nozzles as the droplets are formed, it would seem likely that some type, not necessarily a well defined type, of motion would exist inside the droplets. This internal motion, developed during droplet formulation rather than during droplet fall, would be in qualitative agreement with the relatively large value of $R^*$ equal to 3.3. Review of the discussion following eq. (3.102) will show, furthermore, that 3.3, for the range of $Re_c$ in this study, agrees quite well with values presented there. In particular it is to be noted that Calderbank and Korchinski

(19) found $R^*$ to vary from 1.8 to 3.3 for circulating droplets with $Re_c$ from 10 to 120 while Johnson and Hamielec (121) found $R^*$ to range from 3 to 35 for $Re_c$ less than 90.

To further compare the transfer in the droplets from the MX-00 nozzle with theoretical models, the average film coefficients, $\bar{k}_d$, for the various runs were computed from E using eq. (3.47) and are tabulated in Table 15. The values of $\bar{k}_d$ are of comparable magnitude, though tending to be somewhat smaller, to those values tabulated in Table 1 for various types of non-spray systems. From the values of $\bar{k}_d$, the Sherwood numbers, $\overline{Sh}_d$, (see eq. 3.86), were calculated and are presented in Table 15. A plot of $\overline{Sh}_d$ against $T^*$ is shown in Fig. 24 along with that predicted by the analysis of Johns and Beckman which was discussed in Chapter III. It is to be noted that though the experimental results indicate greater values of $\overline{Sh}_d$ than Johns and Beckman's results, the decay behavior is similar and agrees qualitatively.

In Fig. 25 the ratio of the experimentally determined $\bar{k}_d$ and the theoretically predicted asymptotic value $\bar{k}_d$, as predicted by the circulating and turbulent droplet models, is plotted against $T^*$. The data for this plot is given in Table 16 as calculated from eqs. (3.52) and (3.90). For increasing $T^*$, a ratio of unity should be approached if a model properly describes the transfer phenomenon. Though scatter is appreciable, the general data trend is that of approaching approximately unity. As would be expected from $R^*$ being equal to 3.3,

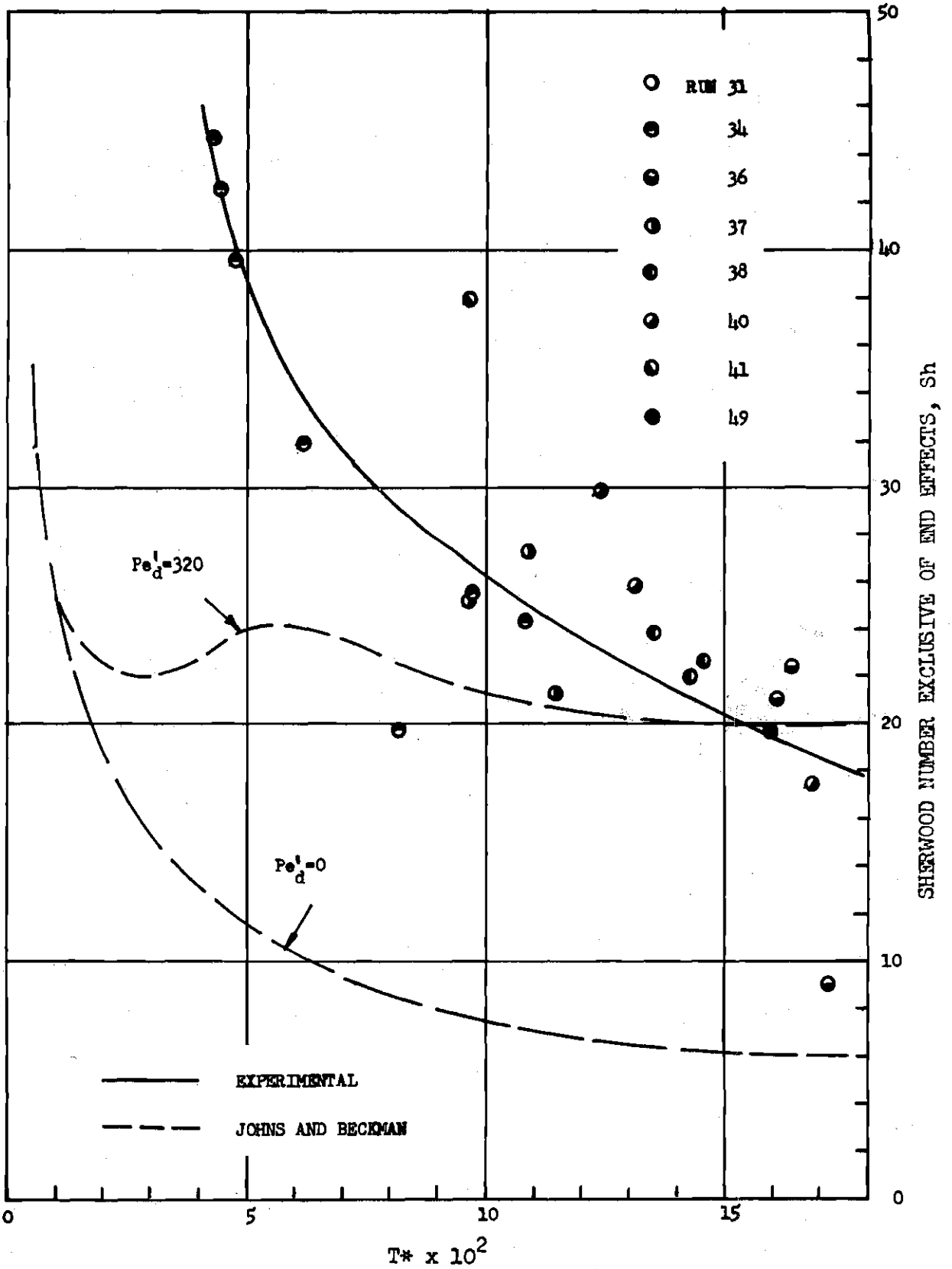


Figure 24. Time Average Sherwood Number

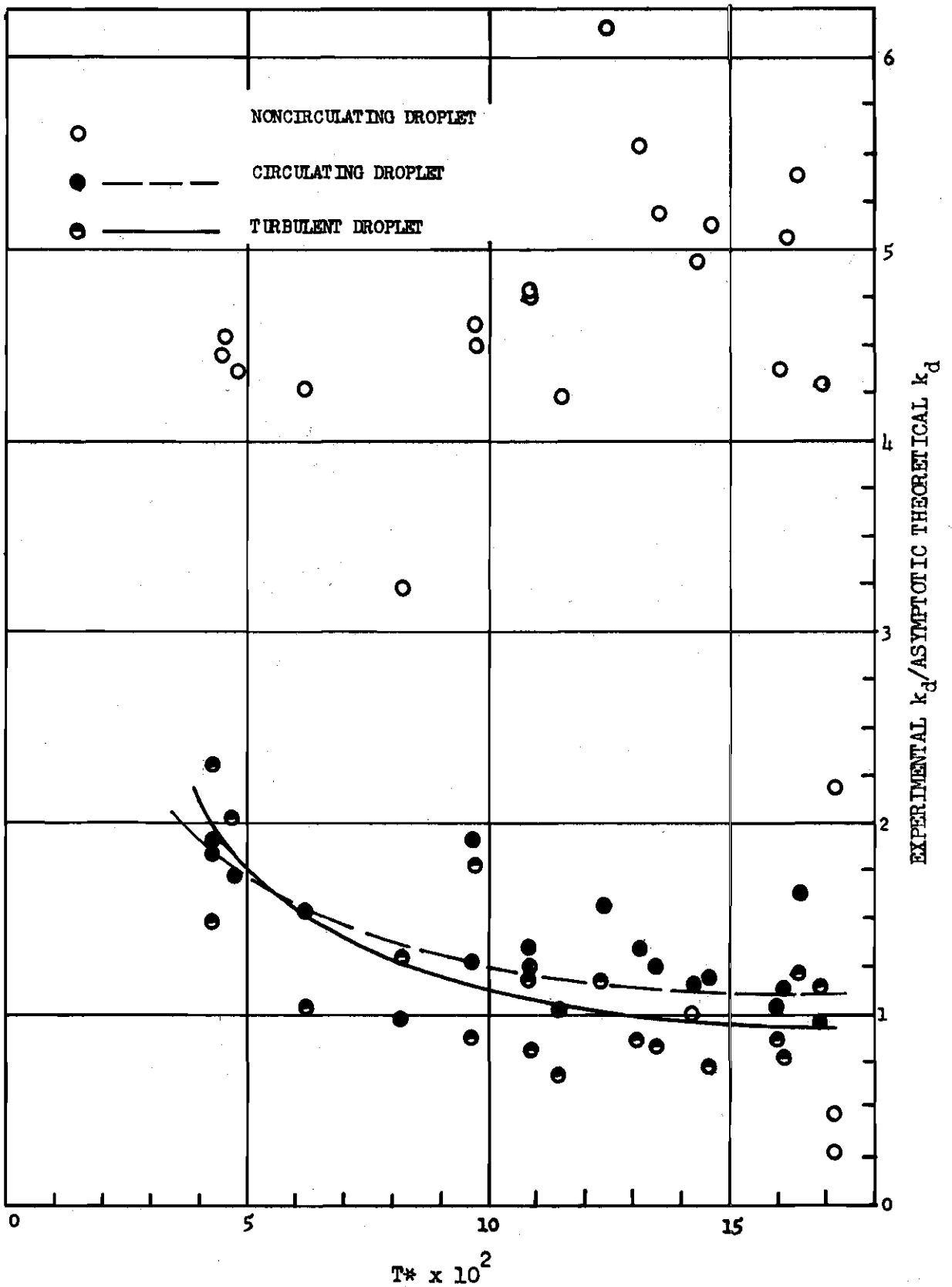


Figure 25. Asymptotic Time Average Film Coefficient Ratio

the faired curve for the circulating droplet data appears to approach a value somewhat greater than unity. The turbulent droplet data, however, seems to approach unity rather closely, indicating that the turbulent model more closely describes the transfer phenomenon than the circulating droplet model. An extreme degree of confidence cannot be placed in this conclusion because of the scatter in the data.

Comparison cannot be made between the experimental results and the oscillating droplet model because of the many factors necessary to utilize this model which could not be determined in this study. It has been pointed out in Chapter III, however, droplet oscillation is not pronounced in droplets less than one or two mm in diameter. Thus, it is likely for the droplets of this study that droplet oscillation was of little significance.

Summary of Transfer Results. The following is a brief summary of the significant results discussed above:

1. Water with high concentrations of oxygen was obtained from water with relatively low concentrations of oxygen for certain operating conditions. Higher concentrations were obtained with the MX-0 nozzle for similar pressure, entrance, and flow conditions. With inlet concentrations of approximately 6-10 mg/l, outlet concentrations could be obtained, using partial pressures of oxygen of approximately 2200 mm of Hg, which were greater than 120 mg/l.

2. When the MX-O spray nozzle was used, the outlet water was supersaturated, the degree of supersaturation decreasing with increasing $T^*$. Extrapolation of experimental data indicate that the saturation concentration would be reached at approximately $T^*$ equal to 0.2.

3. With the MX-OO spray nozzle in use, the outlet oxygen concentration generally did not exceed saturation although in those cases in which it did, the degree of supersaturation was small. As opposed to the MX-O nozzle, the degree of saturation increased with increasing $T^*$.

4. The overall transfer efficiency of the system with the MX-O nozzle decreased with time, the decrease being qualitatively similar to that which might be anticipated from a consideration of the absorption of oxygen by undersaturated droplets. The dimensionless time of 0.2 required to reach a saturation concentration is closely similar to that time required for an undersaturated droplet to approach a saturation condition as predicted by the circulating droplet model.

5. Evaluation of end effect oxygen transfer in the droplets produced by the MX-OO nozzle, assuming a constant $R^*$ and constant end effects, indicate a moderate amount of absorption during droplet formation in the nozzle and an extreme degree of dissolution from the water after the droplet strikes the pool inside the tank. This extreme degree of dissolution, as well as the trend of the experimental data, indicate a strong possibility that end effects and $R^*$ are not constant for different operating conditions.

6. Assuming constant end effects, $R^*$ is calculated to be 3.3. For this high value of $R^*$, the data agrees well with the theoretical solution for the variation of E with $T^*$. This value agrees moderately well with values of $R^*$ determined by other investigators for droplets of similar $Re_c$.

7. The asymptotic value of $\bar{k}_d$ determined experimentally agrees well with that predicted by both the turbulent and circulating droplet models, though the turbulent model agrees slightly better.

8. The complexity of the oscillating droplet model precludes comparison of this model with experimental results. However, since the droplets are so small, it is doubtful that oscillation is of consequence.

# CHAPTER V

# CONCLUSIONS AND RECOMMENDATIONS

## Conclusions

The conclusions of this study lie within one of two areas: those relating to the oxygen transfer characteristics of the pressurized tank system and those relating to the operation of the galvanic cell oxygen analyzers.

### Oxygen Transfer Characteristics

The conclusions concerning the oxygen transfer characteristics of the experimental system are based upon the droplet systems produced by the two spray nozzle during transfer runs. These droplet systems had a mean droplet diameter ranging from approximately $6 \times 10^{-3}$ to $12 \times 10^{-3}$ cm and had the following ranges of droplet parameters (based on a mean droplet diameter): drop Reynolds number, 526 to 1695; continuous phase Reynolds number, 29 to 97; drop Schmidt number, 0.34 to 0.38; and modified drop Peclet number, 4.1 to 13.5. Total pressures and partial pressures of oxygen had ranges of approximately 1200 to 2800 and 600 to 2200 mm of Hg absolute, respectively. Gas leakage from the tank introduced the source of greatest possible error in calculations of transfer characteristics, but for all transfer runs, except run 49, using the MX-00 nozzle, gas leakage was of minor magnitude. For

all runs with the MX-0 nozzle, as well as run 49, however, considerable leakage did occur. The pressure ranges and nature of these runs as discussed previously, as well as the consistency of the calculated transfer efficiencies, indicate, however, that even in these runs, effects of gas leakage were not of extreme consequence.

Based on the experimental results and theoretical discussions of this study the following conclusions are reached:

1. Water with very high concentrations of dissolved oxygen can be successfully obtained from water with relatively low concentrations of dissolved oxygen using the experimental apparatus of this study, in some cases fifteen-fold increases from approximately eight to 120 mg/l being obtained with partial pressures of oxygen inside the tank of approximately 45 psia.

2. The overall transfer of oxygen to the water as it passes through the system is dependent essentially on transfer in the liquid phase and is influenced negligibly by oxygen transfer in the gaseous phase.

3. The MX-0 nozzle forms droplets which are initially supersaturated while the MX-00 nozzle forms droplets which are initially undersaturated.

4. The overall transfer efficiency of the system, $E_o$, is strongly dependent on the time of contact between droplets and surrounding gas phase, the molecular diffusivity of oxygen in water, and the square of the mean droplet radius. For the initially supersaturated droplets produced by the MX-0 nozzle,

the overall transfer efficiency decreases approximately linearly with contact time, diffusivity, and the inverse of the square of the droplet radius. For the initially undersaturated droplets produced by the MX-00 nozzle, the overall transfer efficiency increases approximately linearly with the same three parameters.

5. Assuming the end effect transfer and the effective diffusivity ratio are constant under all operating conditions, the effective diffusivity ratio for the droplets produced by MX-00 nozzle is approximately 3.3.

6. The assumption of constant end effect transfer and constant effective diffusivity ratio in the droplets produced by the MX-00 nozzle under various operating conditions leads to results which indicate a moderate amount of transfer of oxygen to droplets during droplet formation but a large degree of dissolution of oxygen from the water after a droplet strikes the tank pool. These results as well as data scatter and data trend place doubt upon the complete validity of this assumption.

7. The transfer of oxygen in droplets produced by the MX-00 nozzle exclusive of end effects behaves similarly to that predicted theoretically by various droplet models if the calculated value of 3.3 for the effective diffusivity ratio be accepted as approximately correct.

8. The asymptotic magnitude of the time average transfer coefficient, $\bar{k}_d$, exclusive of end effects, for the droplets produced by the MX-00 nozzle is approximately the

same as that predicted by the circulating droplet model of Kronig and Brink (137) and that predicted by the turbulent droplet model of Handlos and Baron (83), though the turbulent droplet model gives slightly better predictions.

Galvanic Cell Oxygen Analyzer Characteristics

Experimentation devoted to explicitly examining the characteristics of the galvanic cell oxygen analyzers has shown the following:

1. The analyzers can be used successfully in pipe line systems to measure dissolved oxygen concentrations when the pipe Reynolds number is even less than 2000.

2. The behavior of the oxygen analyzers when subjected to gage pressures greater than approximately 20 psig is sometimes erratic, in some instances having an unexplained sharp decrease in current generation for essentially constant flow conditions. In those instances when this unusual behavior was not observed, the increase in current generation by the analyzers was very nearly directly proportional to the dissolved oxygen concentration to at least a concentration of 150 mg/l. When the unexpected decrease in current generation occurred, it occurred over a time period of approximately one half hour, after which the sensitivity of the analyzer was radically different from that prior to the decrease. Visual inspection of the analyzer membranes which exhibited this unusual behavior failed to reveal any tears or punctures.

## Recommendations

The experimental experience of this exploratory investigation suggests certain recommendations. These recommendations will be made in regard to the spray apparatus used in this study, but it should be apparent that they can be viewed in light of any similar spray system which might be used for study.

1. Further experimental investigation should be undertaken to more precisely determine the transfer characteristics of the spray system. Emphasis must be placed upon more precise control and measurement of the experimental variables, particularly with regard to the determination of partial pressures of oxygen. Transfer characteristics under a much greater range of flow and pressure conditions should likewise be investigated.

2. The power requirements necessary to produce certain dissolved oxygen concentrations operating under various conditions should be examined. At the same time, investigation should be undertaken to qualify and quantify the dissolved oxygen requirements which a spray system operating under high pressure would be required to provide in order that the system capabilities can be optimized. Serious consideration should be given to specific practical applications in order that the ability of the spray system to meet the requirements of the application can be determined.

3. Additional investigation should be undertaken to gain an accurate knowledge of end effect transfer in order that both end effect transfer and transfer during droplet fall can be more precisely predicted.

4. A systematic investigation should be undertaken to determine the effects of different nozzle types and droplet size distributions on the oxygen transfer in the spray system.

5. Study should be undertaken to more precisely determine the mechanical behavior of droplets after their formation in order to be able to more accurately determine the transfer characteristics of the spray system.

6. Study should be conducted to examine the possibilities of multiple nozzle systems.

7. A much more detailed and complete investigation should be made of the operating characteristics of the galvanic cell oxygen analyzer under conditions of high pressure, particularly in regard to the erratic behavior observed in this study.

# APPENDIX

## SPRAY EVALUATION

### Objective

Investigation of the droplet characteristics of the two spray nozzles used in the experimental work of this study was required in order that the mean drop size as a function of flow rate could be determined.

### Apparatus and Methods

#### Nozzles

The two nozzles for which the mean drop sizes were to be examined are described as follows: Each nozzle was of whirl chamber type design as manufactured by Binks Manufacturing Company (Chicago, Illinois). Both were full cone, short body pattern, series MX, Spra-Rite nozzles with the following characteristics.

1. Nozzle MX-0: cone angle of 52 degrees, 0.082 in. orifice, and 0.44 gpm rated flow at eight psi.

2. Nozzle MX-00: cone angle of 69 degrees, 0.125 in. orifice, and 1.0 gpm rated flow at eight psi.

#### Photography

To accomplish the above objective a photographic technique was chosen as being relatively simple and straight-

forward and yet sufficient to determine the desired information. Some 30 photographs were taken of the spray from the two nozzles operating over a range of flow rates. Of these, eight, four of each nozzle, proved to be of sufficient quality to enable their effective evaluation. From microscopic examination of these photographs droplet size and distribution were determined as discussed in following paragraphs.

In order that the effectiveness of the various photographic techniques attempted could be evaluated as the photomaking progressed, ten second developing film was used. Each photograph could thus be used to indicate and suggest improvements in the camera position, exposure time, and lighting method for the following photographs to be taken. The film itself was only of moderately fine grain and because of this a certain amount of fuzziness was apparent when the photographs were viewed under a microscope. Proper choice of microscope, as described below, however, eliminated this problem to a certain degree.

Two different cameras were used, both ordinary bellows type. The second camera, which made the photos chosen for evaluation, was of higher quality than the first, having a finer quality lens and greater distance between lens and photo plate.

Various lighting methods and nozzle positions were tried. Initially the nozzle was placed on the end of a long pipe and allowed to spray horizontally into the open air with-

out restriction. For this nozzle position a strobotac operating at various frequencies was placed in different positions and photos were taken looking through the spray either directly towards or off to the side of the strobotac light. Microscopic examination of these photos revealed that they were deficient due primarily to multiple drop images, indistinct drop outlines, long droplet tails arising from exposures of too great a time period, and, most importantly, too many droplets both in and out of the focal plane of the camera.

The use of the better quality camera described above and restriction of the spray as it exited from the nozzle improved the photographs obtained sufficiently to enable evaluation of the spray. The method of restricting the spray will be discussed in the following paragraph. The camera was aimed directly through the restricted spray onto a lighted, at least for the eight photos evaluated, white background. The background was illuminated by a high speed, high intensity flash. The flash speed, 1/1200 of a second, controlled the exposure time, the camera speed being considerably greater than this. The lens setting for the eight evaluated photos was f45.

Spray Restriction

Mentioned above was the difficulty encountered due to the many drops both in and out of the focal plane, those drops being in or out of the focal plane not readily determined. To overcome this difficulty it was finally decided to restrict the spreading of the spray by the use of two flat metal plates pro-

jecting into the spray so as to prevent the spray from spreading outwards except in a direction parallel to the two plates. Thus the spray was very effectively narrowed and the spray depth through which the photographs were made became sufficiently small to produce photographs which had a relatively small number of droplets.

Water was drawn from the laboratory supply with a small positive displacement pump and pumped through a flow meter, hose, and steel pipe to the nozzle. The pump and flow meter were the same as those used in the experimentation described elsewhere in this paper. The pipe was connected to a ceiling I beam so as to project vertically downward with the nozzle some three feet above the floor.

On each side of the nozzle were clamped two steel plates in such a manner so as to permit their separate rotation some 45 degrees each way from the vertical. By using various size wood and metal spacing blocks, different widths between the two plates could be obtained which were very nearly constant the entire length of the plates. Each plate was essentially of the same size: 26 1/2 in. long by seven in. wide. Both plates had moderate rigidity, being 0.055 in. thick. Of the various plate spacings tried, the narrowest possible with this equipment gave the best photo results. This narrow spacing was used in the evaluated photographs. For the MX-0 nozzle this spacing was approximately 0.56 in. while for the MX-00 nozzle the spacing was approximately 0.69 in. This

narrow spacing was accomplished by clamping the plates directly to the nut head of the nozzle.

Preliminary experimentation with the plates while the spray was in operation showed that proper inclination of the plates with respect to the vertical would result in the spray issuing from between the plates relatively free of drops springing from the edges of the plates. The major portion of spray striking the inner faces of the plates flowed vertically downward and off the bottom edge of the plates. The net effective was that of obtaining a relatively narrow band of spray on each side of the plates. It was estimated that for several inches from the edge of each plate the spray did not widen more than approximately 3/4 in. Thus by making photos of the spray along the sides of the plates it was possible to photograph droplets which all were virtually within a few inches of the focal plane of the camera when it was focused on one of the plate edges.

Calibration

For purposes of calibrating the photos numerous small notches were filed in the edges of both plates and identified. Measurement under a microscope of the actual size of these notches and their apparent size on the various photos enabled the determination of the photo scale ratio, that is, the value by which photo measurements had to be multiplied to obtain their actual size. Examination of the actual notches and the notches on the photos showed that certain ones were not ame-

nable to accurate measurement. These, therefore, were not included in the calculations made to determine the various scale ratios. Only those measurements which were considered relatively reliable were used to determine a scale ratio for each notch. The various values obtained from each notch were then averaged for each photo to obtain the photo scale ratio actually used in calculations. The scale ratios determined for each of the eight photos evaluated are listed in Table 17 as are the maximum per cent error, rounded to the next highest whole per cent, of the individual notch ratios from the average scale ratio.

Measurement

Measurements were made under a 40 power Bausch and Lomb binocular microscope which had an eye piece with an internal scale with 0.002 in. divisions. It was found that this microscope, with its fairly wide field, struck a reasonable compromise between the need for photo enlargement necessary for accurate measurement and the limitation on enlargement placed by the photo grain.

The droplets on each photo were measured merely by moving the photo across the field of vision until the particular droplet to be measured lay within the divisions of the eye piece scale. To insure that no droplet was measured twice a minute indentation, invisible to the naked eye but clearly discernible under the microscope, was made on the photograph very close to the droplet effectively identifying measured

droplets. All droplets appearing on a photo were not measured but rather only those which appeared considerably brighter and sharper than the majority of the drops on the photograph. It was believed that by measuring these particular droplets, the drops measured were those only which were very nearly in the focal plane of the camera. Thus for a given measured size on the photo itself, multiplication of the measured size by the photo scale ratio would not introduce great error even though the drop might not be exactly in the focal plane.

The greatest difficulty, and the greatest source of error it is believed, lay in the measurement of each particular drop on a photo chosen as being essentially in the camera focal plane. Though these drops had greater clarity than the remaining, the edges of a drop were far from being distinct. Furthermore only one measurement could be made on each droplet since the droplets appeared not as spheres or ellipses but rather as bright white dots with long tails. The flash used to illuminate the spray had not been sufficiently fast to stop the motion of the droplets. The smaller dimension of the drop streak was thus assumed to be equivalent to the drop diameter. Measurement of this smaller dimension, however, still left considerable room for error since it was somewhat of an arbitrary choice as to where the droplet edge exactly lay. It is believed, however, this edge could be located to the nearest 0.001 in. on the photo.

## Analysis

Eight photos, as mentioned previously, were considered to be adequate for evaluation and analysis. Since droplets could be measured to approximately only the nearest .001 in., the droplet measurements actually fell into classes of size rather than approximating a continuous distribution. The class size of 0.001 in. was based on the size of the drops as they appeared in the photo rather than on the actual droplet size. The midpoint of each class was considered to be representative of the drop diameters in each class. These class midpoint values are listed in Table 17 along with the number of drops which were measured in each class from each photo. The total number of drops measured on each photo is also tabulated. In no case were less than 15 drops measured.

### Drop Diameter

From the size distributions in Table 18, after making photo scale ratio corrections, mean drop diameters were calculated. Mean drop diameters for each photo are listed in Table 19. A plot of mean drop diameter as a function of flow rate is given in Fig. 26 for each of the two nozzles investigated. It is seen that for the MX-0 nozzle the mean drop size varies almost linearly with flow rate. The variation of mean drop size with flow rate for the MX-00 nozzle, however, is not at all readily discernible. The wide scatter of data for the MX-00 nozzle is not completely unexpected since droplet sizes from this nozzle had greater variation thus subjecting them to

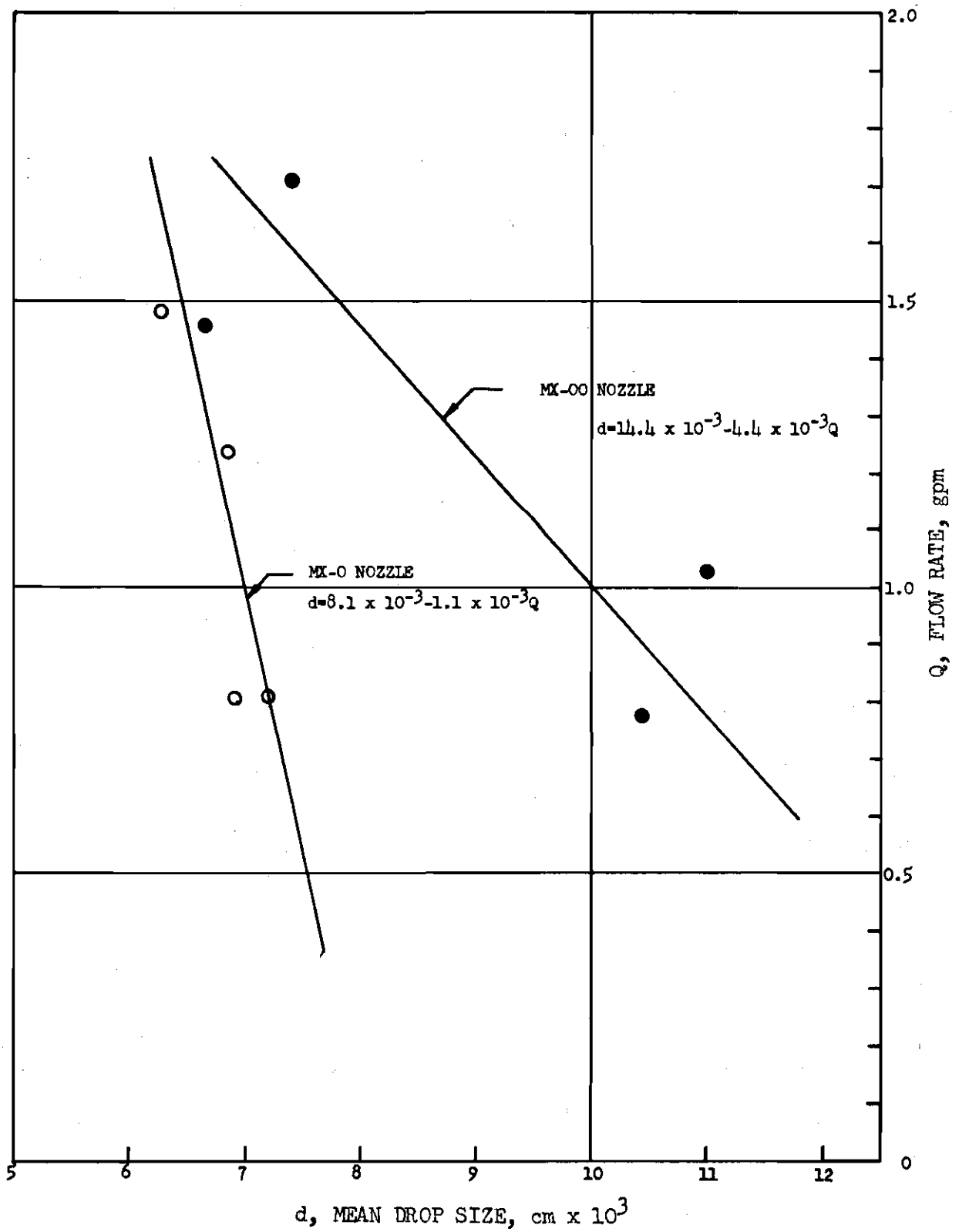


Figure 26. Mean Droplet Diameter

greater possible error in measurement. Also the plate separation width, discussed earlier, was necessarily larger for the MX-00 than it was for the MX-0 nozzle.

The data for the MX-0 nozzle could be fitted quite well by a straight line. Using the existence of this linear fit for the MX-0 nozzle as justification, the data for the MX-00 nozzle was also fitted with a straight line. Both linear curves shown in Fig. 26 were determined by the least squares method. The equations of these least squares lines are, for the MX-0 nozzle,

$$d_d = 0.0081 - 0.0011Q$$

and, for the MX-00 nozzle,

$$d_d = 0.0144 - 0.0044Q$$

where $d_d$ is mean diameter in centimeters and Q is flow rate in gpm.

# TABLES

Table 1. Liquid Film Coefficients

| Liquid Film Coefficient (cm/sec)x10³ | Description | Temperature °C | Source (See Literature Citations) |
|---|---|---|---|
| 0.92 | Absorption of $O_2$ through free surface of water stirred at 60 rpm | 20 | 242 |
| 3.7 | Same as above except stirred at 200 rpm | 25 | 39 |
| 2.2 | Same as above except stirred at 400 rpm | 25 | 39 |
| 11.4 | $O_2$ absorbed from large cylindrical bubble rising in column of water | 35 | 39 |
| 10 | Same as above | 25 | 39 |
| 8.5 | Same as above | 16 | 39 |
| 23 | Absorption of $O_2$ through free surface of water shaken 400 times/minute | 25 | 39 |
| 0.1 | Absorption of air by stagnant water | 15 | 154 |

Table 1. Continued

| Liquid Film Coefficient (cm/sec)x10³ | Description | Temperature °C | Source (See Literature Citations) |
|---|---|---|---|
| 1.4 | Absorption of air through free surface of water stirred at 150 rpm | 15 | 154 |
| 4.2 | Same as above except 1000 rpm | 15 | 154 |
| 8.9 | Air absorbed from large cylindrical bubble rising in column of water | 25 | 39 |
| 11.1 | $CO_2$ absorbed by water in wetted wall column; velocity range of carrier gas: 0.03 to 1.5 ft/sec | 20 | 97 |
| 2.1 | Absorption of $CO_2$ through free surface of water stirred at 250 rpm | 15 | 154 |
| 2.9 | Same as above except 400 rpm | 25 | 39 |
| 20 | Absorption of $CO_2$ from bubbles rising in water column | 25 | 39 |
| 36 | Absorption of $H_2$ through free surface of water shaken 400 times/minute | 25 | 39 |

Table 1. Continued

| Liquid Film Coefficient (cm/sec)x10$^3$ | Description | Temperature $^oC$ | Source (See Literature Citations) |
|---|---|---|---|
| 306 | Absorption of $CO_2$ from large gas bubbles rising through water column at rate of 100 bubbles/ minute | 25 | 17 |
| 780 | Same as above except bubble rate of 600 bubbles/ minute | 25 | 17 |
| 0.187 | Absorption of $SO_2$ by air in wetted wall tower; carrier gas velocity of 0.05 ft/sec | 20 | 97 |
| 2.67 | Same as above except 1.30 ft/sec | 20 | 97 |

Table 2. Eigenvalues and Coefficients for Droplet with No Continuous Phase Resistance

| Type of Droplet | $\lambda_1$ | $\lambda_2$ | $\lambda_3$ | $\lambda_4$ | $\lambda_5$ | $\lambda_6$ | $\lambda_7$ | Source (See Literature Citations) |
|---|---|---|---|---|---|---|---|---|
| Noncirculating | 3.142 | | | | | | | 55 |
| Circulating | 1.678 | 8.48 | 21.10 | 38.5 | 63.0 | 89.8 | 123.8 | 100 |
| Circulating | 1.656 | 9.08 | 22.2 | | | | | 54 |
| Circulating | 1.678 | 9.83 | | | | | | 138 |

| Type of Droplet | $A_1$ | $A_2$ | $A_3$ | $A_4$ | $A_5$ | $A_6$ | $A_7$ | Source |
|---|---|---|---|---|---|---|---|---|
| Noncirculating | 0.101 | | | | | | | 55 |
| Circulating | 1.33 | 0.60 | 0.36 | 0.35 | 0.28 | 0.22 | 0.16 | 100 |
| Circulating | 1.29 | 0.596 | 0.386 | | | | | 54 |
| Circulating | 1.32 | 0.73 | | | | | | 138 |

Table 3. Classification of Runs by Type

| Run | Series | Recirculation | Pressure | Calibration | Transfer |
|---|---|---|---|---|---|
| 22 | A | x | | x | |
| 23 | B | x | | x | |
| 24 | C | x | x | x | |
| 25 | D | x | | x | x |
| 26 | E | | | x | x |
| 27 | F | | | x | x |
| 28 | G | | | x | x |
| 29 | G | x | x | x | |
| 30 | H | | | x | x |
| 31 | H | | x | | x |
| 32 | H | | | x | x |
| 33 | I | | | x | x |
| 34 | I | | x | x | x |
| 35 | J | | | x | x |
| 36 | J | | x | | x |
| 37 | J | | x | | x |

Table 3. Continued

| Run | Series | Recirculation | Pressure | Calibration | Transfer |
|---|---|---|---|---|---|
| 38 | J | | x | | x |
| 39 | No run made | | | | |
| 40 | K | | x | x | x |
| 41 | K | | x | | x |
| 42 | L | | | x | x |
| 43 | L | | x | x | x |
| 44 | M | | | x | x |
| 45 | M | | x | | x |
| 46 | N | | | x | x |
| 47 | N | x | x | | |
| 48 | O | | | x | x |
| 49 | O | | x | x | x |
| 50 | P | x | x | x | |

Table 4. Classification of Runs by Nozzle Type

| Run | Nozzle |
|---|---|
| 22 | MX-00 |
| 23 | " |
| 24 | " |
| 25 | " |
| 26 | " |
| 27 | " |
| 28 | " |
| 29 | " |
| 30 | " |
| 31 | " |
| 32 | " |
| 33 | " |
| 34 | " |
| 35 | " |
| 36 | " |
| 37 | MX-00 |
| 38 | " |
| 39 | No run made |
| 40 | MX-00 |
| 41 | " |
| 42 | MX-0 |
| 43 | " |
| 44 | " |
| 45 | " |
| 46 | " |
| 47 | " |
| 48 | MX-00 |
| 49 | " |
| 50 | " |

Table 5. Classification of Runs by Membrane

| Run | Membrane Designation | |
|---|---|---|
| | Inlet | Outlet |
| 22 | 3.I | 3.0 |
| 23 | " | " |
| 24 | " | " |
| 25 | " | " |
| 26 | " | " |
| 27 | 4.I | 4.0 |
| 28 | " | 5.0 |
| 29 | " | " |
| 30 | 6.I | 6.0 |
| 31 | " | " |
| 32 | " | " |
| 33 | " | " |
| 34 | " | " |
| 35 | " | " |
| 36 | " | " |
| 37 | 6.I | 6.0 |
| 38 | " | " |
| 39 | No run made | |
| 40 | 7.I | 7.0 |
| 41 | " | " |
| 42 | " | " |
| 43 | " | " |
| 44 | " | " |
| 45 | " | " |
| 46 | " | " |
| 47 | " | " |
| 48 | 8.I | 8.0 |
| 49 | " | " |
| 50 | " | " |

Table 6. Experimental Data

| Run | Temp °C | Flowrate gpm | Measured Current μa | Titrated D.O. mg/l |
|---|---|---|---|---|
| 22.a.I | 27.7 | 1.58 | 11.0 | 8.54 |
| 22.a.O | " | " | 10.0 | " |
| 22.b.I | 28.5 | 1.55 | 11.1 | 8.28 |
| 22.b.O | " | " | 10.6 | " |
| 22.c.I | 28.8 | 1.55 | 11.2 | - |
| 22.c.O | " | " | 11.0 | - |
| 23.a.I | 26.6 | 1.13 | 10.3 | 8.44 |
| 23.a.O | " | 1.15 | 10.8 | " |
| 23.b.I | 26.9 | 0.82 | 10.3 | - |
| 23.b.O | " | " | 10.8 | - |
| 23.c.I | 27.4 | 0.58 | 10.4 | 8.23 |
| 23.c.O | " | " | 10.8 | " |
| 23.d.I | 28.0 | 0.59 | 10.6 | 8.05 |
| 23.d.O | " | " | 11.0 | " |
| 23.e.I | 28.0 | 0.39 | 10.6 | " |
| 23.e.O | " | " | " | " |
| 23.f.I | 29.1 | 1.58 | 11.2 | 8.03 |
| 23.f.O | " | " | 11.9 | " |
| 24.a.I | 27.4 | 1.55 | 11.07 | 8.12 |
| 24.a.O | " | " | 11.25 | " |
| 24.b.I | 28.0 | " | 22.7 | - |
| 24.b.O | " | " | 23.9 | - |
| 24.c.I | 28.5 | " | 47.2 | - |
| 24.c.O | " | " | 48.9 | - |
| 24.d.I | 29.1 | " | 110 | - |
| 24.d.O | " | " | 118 | - |
| 24.e.I | 28.8 | " | 190 | - |
| 24.e.O | " | " | 77.3 | - |

Table 6. Continued

| Run | Temp °C | Flowrate gpm | Measured Current µa | Titrated D.O. mg/l |
|---|---|---|---|---|
| 24.f.I | - | - | - | - |
| 24.f.0 | 29.1 | 1.55 | 182 | - |
| 24.g.I | 28.8 | " | 122 | - |
| 24.g.0 | " | " | 110 | - |
| 24.h.I | 28.8 | 1.55 | 219 | - |
| 24.h.0 | - | - | - | - |
| 24.i.I | 28.5 | 1.55 | 122.3 | - |
| 24.i.0 | " | " | 109 | - |
| 25.a.I | 24.4 | 2.11 | 10.3 | 8.05 |
| 25.a.0 | " | " | 9.0 | 8.35 |
| 26.a.I | 24.1 | 2.11 | 10.3 | 8.70 |
| 26.a.0 | " | " | 9.9 | 8.15 |
| 26.b.I | 24.1 | 1.76 | 10.25 | 8.70 |
| 26.b.0 | " | " | 9.15 | 8.13 |
| 26.c.I | 24.1 | 1.50 | 10.3 | - |
| 26.c.0 | " | " | 9.15 | - |
| 26.d.I | 24.1 | 1.33 | 10.25 | 7.98 |
| 26.d.0 | " | " | 9.1 | 8.41 |
| 26.e.I | 24.1 | 1.15 | 10.3 | - |
| 26.e.0 | " | " | 9.25 | - |
| 26.f.I | 24.7 | 0.95 | 10.3 | 8.44 |
| 26.f.0 | " | " | 9.15 | 8.10 |
| 26.g.I | 24.7 | 0.68 | 10.3 | - |
| 26.g.0 | " | " | 9.1 | - |
| 27.a.I | 23.8 | 1.98 | 8.0 | 8.80 |
| 27.a.0 | " | " | 8.05 | 8.35 |
| 27.b.I | 23.8 | 1.70 | 7.90 | 8.71 |
| 27.b.0 | " | " | 8.0 | 8.34 |
| 27.c.I | 24.0 | 1.37 | 8.0 | 8.93 |
| 27.c.0 | " | " | 7.97 | 8.37 |

Table 6. Continued

| Run | Temp °C | Flowrate gpm | Measured Current µa | Titrated D.O. mg/l |
|---|---|---|---|---|
| 27.d.I | 24.0 | 1.02 | 8.05 | 8.73 |
| 27.d.O | " | " | 8.02 | 8.12 |
| 27.e.I | 24.2 | 0.78 | 8.00 | 8.88 |
| 27.e.O | " | " | 8.10 | 8.45 |
| 27.f.I | 24.5 | 0.52 | 8.00 | 8.73 |
| 27.f.O | " | " | 7.4 | 8.25 |
| 27.g.I | 24.8 | 0.35 | 7.95 | 8.79 |
| 27.g.O | " | " | 7.15 | 7.96 |
| 28.a.I | 24.5 | 1.97 | 9.9 | 9.11 |
| 28.a.O | " | " | 7.1 | 8.35 |
| 28.b.I | 24.8 | 1.63 | 9.8 | 9.02 |
| 28.b.O | " | " | 7.1 | 8.12 |
| 28.c.I | 24.9 | 1.33 | 9.5 | 8.93 |
| 28.c.O | " | " | 7.05 | 8.10 |
| 28.d.I | 25.0 | 0.92 | 9.35 | 9.02 |
| 28.d.O | " | 0.93 | 7.1 | 8.15 |
| 28.e.I | 25.2 | 0.64 | 9.25 | 8.82 |
| 28.e.O | " | " | 7.1 | 8.25 |
| 28.f.I | 23.8 | 0.37 | 8.75 | 8.88 |
| 28.f.O | " | " | 6.1 | 8.25 |
| 28.g.I | 24.5 | 1.12 | 9.4 | 8.68 |
| 28.g.O | " | " | 7.25 | 8.15 |
| 29.a.I | 26.3 | 0.87 | 8.9 | 8.05 |
| 29.a.O | " | 1.16 | 7.6 | " |
| 29.b.I | 26.9 | 0.90 | 41.0 | - |
| 29.b.O | " | " | 34.5 | - |
| 29.c.I | 26.9 | " | 84.5 | - |
| 29.c.O | " | " | 73.5 | - |

Table 6. Continued

| Run | Temp °C | Flowrate gpm | Measured Current µa | Titrated D.O. mg/l |
|---|---|---|---|---|
| 29.d.I | 27.3 | 0.90 | 148.3 | - |
| 29.d.0 | " | " | 141.0 | - |
| 29.e.I | 27.0 | " | 178 | - |
| 29.e.0 | " | " | 180 | - |
| 29.f.I | 28.0 | " | 190 | - |
| 29.f.0 | " | " | 231 | - |
| 30.a.I | 24.2 | 1.93 | 6.6 | 8.68 |
| 30.a.0 | " | " | 14.2 | 18.81 |
| 30.b.I | 24.8 | 1.29 | 7.0 | 8.68 |
| 30.b.0 | " | " | 13.1 | 17.79 |
| 30.c.I | 24.9 | 0.88 | 7.1 | 8.63 |
| 30.c.0 | " | 0.87 | 12.5 | 16.69 |
| 30.d.I | 25.0 | 0.43 | 6.9 | 8.53 |
| 30.d.0 | " | " | 10.3 | 15.82 |
| 30.e.I | 24.5 | 1.75 | 7.3 | 8.87 |
| 30.e.0 | " | 1.73 | 12.5 | 16.05 |
| 31.a.I | 24.9 | 1.71 | 7.7 | - |
| 31.a.0 | " | " | 28.0 | - |
| 31.b.I | 25.2 | 1.12 | 8.0 | - |
| 31.b.0 | " | " | 26.2 | - |
| 31.c.I | 25.7 | 0.65 | 8.1 | - |
| 31.c.0 | " | " | 24.2 | - |
| 32.a.I | 25.8 | 1.72 | 11.0 | 8.67 |
| 32.a.0 | " | " | 6.0 | 8.05 |
| 32.b.I | 25.5 | 0.85 | 11.0 | 8.72 |
| 32.b.0 | " | " | 6.0 | 8.05 |
| 33.a.I | 24.0 | 1.68 | 10.3 | 8.82 |
| 33.a.0 | " | 1.69 | 5.8 | 8.24 |

Table 6. Continued

| Run | Temp °C | Flowrate gpm | Measured Current µa | Titrated D.O. mg/l |
|---|---|---|---|---|
| 33.b.I | 24.1 | 1.04 | 10.8 | 8.73 |
| 33.b.O | " | 1.05 | 5.65 | 8.15 |
| 33.c.I | 24.2 | 0.42 | 10.2 | 8.68 |
| 33.c.O | " | 0.43 | 4.9 | 8.10 |
| 34.a.I | 23.0 | 1.76 | 11.0 | 8.68 |
| 34.a.O | " | " | 24.9 | - |
| 34.b.I | 24.4 | 1.16 | 11.2 | - |
| 34.b.O | " | " | 23.0 | - |
| 34.c.I | 25.0 | 0.65 | 11.0 | - |
| 34.c.O | " | " | 20.1 | - |
| 34.d.I | 24.5 | 1.72 | 11.5 | 8.68 |
| 34.d.O | " | - | - | - |
| 34.e.I | 24.5 | 1.79 | 11.9 | - |
| 34.e.O | " | " | 35.0 | - |
| 34.f.I | 24.5 | 1.18 | 11.8 | 8.92 |
| 34.f.O | - | - | - | - |
| 34.g.I | 24.9 | 1.20 | 11.9 | - |
| 34.g.O | " | " | 27.0 | - |
| 34.h.I | 25.2 | 0.65 | 12.0 | 8.83 |
| 34.h.O | " | 0.64 | 23.0 | - |
| 34.i.I | 24.8 | 0.64 | 11.9 | - |
| 34.i.O | " | " | 23.5 | - |
| 35.a.I | 23.6 | 1.63 | 11.0 | 8.88 |
| 35.a.O | " | " | 6.1 | 8.43 |
| 35.b.I | 23.9 | 0.87 | 11.0 | 8.83 |
| 35.b.O | " | " | 5.9 | 8.34 |
| 36.a.I | 23.8 | 1.76 | 11.0 | - |
| 36.a.O | " | " | 22.2 | - |

Table 6. Continued

| Run | Temp °C | Flowrate gpm | Measured Current µa | Titrated D.O. mg/l |
|---|---|---|---|---|
| 36.b.I | 24.0 | 1.12 | 11.1 | - |
| 36.b.O | " | " | 21.2 | - |
| 36.c.I | 24.0 | 0.59 | 11.0 | - |
| 36.c.O | " | 0.57 | 19.1 | - |
| 37.a.I | 24.8 | 0.82 | 11.8 | - |
| 37.a.O | " | " | 45.5 | - |
| 37.b.I | 24.7 | 1.20 | 11.5 | - |
| 37.b.O | " | " | 50.0 | - |
| 37.c.I | 24.5 | 1.72 | 11.5 | - |
| 37.c.O | " | " | 51.0 | - |
| 38.a.I | 24.8 | 0.76 | 11.65 | - |
| 38.a.O | " | " | 67.7 | - |
| 38.b.I | 25.0 | 1.20 | 11.8 | - |
| 38.b.O | " | " | 72.0 | - |
| 38.c.I | 24.9 | 1.53 | 11.7 | - |
| 38.c.O | " | " | 72.0 | - |
| 39 | No run | | | |
| 40.a.I | 24.0 | 1.82 | 11.8 | 9.02 |
| 40.a.O | " | " | 7.5 | 8.92 |
| 40.b.I | 24.0 | 1.37 | 11.45 | 8.83 |
| 40.b.O | " | " | 88.5 | - |
| 40.c.I | 24.5 | 0.99 | 11.7 | 9.11 |
| 40.c.O | " | " | 86.0 | - |
| 40.d.I | 24.9 | 0.47 | 11.5 | 8.88 |
| 40.d.O | " | 0.49 | 71.5 | - |
| 41.a.I | 24.0 | 1.08 | 11.8 | - |
| 41.a.O | " | " | 91.0 | - |

Table 6. Continued

| Run | Temp °C | Flowrate gpm | Measured Current µa | Titrated D.O. mg/l |
|---|---|---|---|---|
| 41.b.I | 24.8 | 0.73 | 11.8 | - |
| 41.b.O | " | " | 82.5 | - |
| 41.c.I | 24.8 | 1.37 | 12.0 | - |
| 41.c.O | " | " | 97.0 | - |
| 42.a.I | 24.0 | 1.02 | 8.4 | 9.37 |
| 42.a.O | " | " | 7.3 | 8.35 |
| 42.b.I | 23.8 | 1.22 | 8.25 | 9.43 |
| 42.b.O | " | " | 7.35 | 8.44 |
| 42.c.I | 24.0 | 0.69 | 8.17 | 9.43 |
| 42.c.O | " | 0.73 | 7.1 | 8.35 |
| 42.d.I | 24.1 | 0.38 | 8.25 | 9.43 |
| 42.d.O | " | 0.37 | 5.6 | 8.30 |
| 43.a.I | 23.2 | 0.53 | 8.2 | 8.25 |
| 43.a.O | " | 0.57 | 26.0 | - |
| 43.b.I | 24.9 | 0.73 | 9.4 | 9.22 |
| 43.b.O | " | " | 40.0 | - |
| 43.c.I | 25.0 | 1.07 | 9.60 | 9.22 |
| 43.c.O | - | - | - | - |
| 43.d.I | 24.9 | 1.06 | 9.25 | 9.36 |
| 43.d.O | " | 1.03 | 52.0 | - |
| 43.e.I | 24.2 | 1.24 | 9.40 | 9.22 |
| 43.e.O | " | " | 53.0 | - |
| 44.a.I | 24.5 | 0.74 | 10.9 | 9.36 |
| 44.a.O | " | " | 7.8 | 8.41 |
| 44.b.I | 24.6 | 1.03 | 10.8 | 9.41 |
| 44.b.O | " | " | 7.95 | 8.35 |
| 44.c.I | 24.2 | 1.16 | 10.5 | 9.41 |
| 44.c.O | " | " | 7.95 | 8.35 |

Table 6. Continued

| Run | Temp °C | Flowrate gpm | Measured Current µa | Titrated D.O. mg/l |
|---|---|---|---|---|
| 44.d.I | 24.8 | 0.43 | 10.2 | 9.17 |
| 44.d.0 | " | " | 6.05 | 8.20 |
| 45.a.I | 24.9 | 0.95 | 10.5 | - |
| 45.a.0 | " | " | 28.9 | - |
| 45.b.I | 24.8 | 0.90 | 10.8 | - |
| 45.b.0 | " | " | 46.5 | - |
| 45.c.I | 24.8 | 0.93 | 10.6 | - |
| 45.c.0 | " | " | 60.0 | - |
| 46.a.I | 25.1 | 1.16 | 10.9 | 9.37 |
| 46.a.0 | " | " | 8.4 | 8.64 |
| 46.b.I | 25.0 | 0.93 | 10.9 | 9.37 |
| 46.b.0 | " | 0.95 | 8.35 | 8.59 |
| 46.c.I | 25.3 | 0.73 | 10.9 | 9.46 |
| 46.c.0 | " | " | 8.2 | 8.63 |
| 47.a.I | 24.8 | 0.87 | 11.0 | - |
| 47.a.0 | " | " | 8.7 | - |
| 47.b.I | 28.5 | 0.87 | 56.0 | - |
| 47.b.0 | " | " | 46.0 | - |
| 47.c.I | 29.6 | 0.86 | 94.0 | - |
| 47.c.0 | " | " | 86.0 | - |
| 47.d.I | 29.8 | 0.87 | 159 | - |
| 47.d.0 | " | " | 85 | - |
| 47.e.I | 29.8 | 0.85 | 185 | - |
| 47.e.0 | " | " | 40 | - |
| 48.a.I | 25.2 | 1.28 | 7.7 | 9.21 |
| 48.a.0 | " | " | 5.9 | 8.44 |
| 48.b.I | 24.7 | 0.99 | 7.8 | 9.21 |
| 48.b.0 | " | " | 5.75 | 8.44 |

Table 6. Continued

| Run | Temp °C | Flowrate gpm | Measured Current µa | Titrated D.O. mg/l |
|---|---|---|---|---|
| 48.c.I | 24.8 | 0.73 | 7.9 | 9.12 |
| 48.c.0 | " | " | 5.55 | 8.40 |
| 49.a.I | 25.5 | 0.82 | 8.20 | - |
| 49.a.0 | " | " | 58.0 | - |
| 49.b.I | 24.8 | 1.14 | 8.1 | - |
| 49.b.0 | " | " | 79 | - |
| 49.c.I | 24.4 | " | 8.15 | 9.12 |
| 49.c.0 | " | " | - | - |
| 50.a.I | 25.5 | 1.20 | 8.62 | 8.63 |
| 50.a.0 | " | " | 6.80 | " |
| 50.b.I | 26.3 | 0.69 | 8.40 | 8.49 |
| 50.b.0 | " | " | 6.80 | " |
| 50.c.I | 27.1 | 1.24 | 45.5 | - |
| 50.c.0 | " | " | 36.5 | - |
| 50.d.I | 27.7 | " | 82 | - |
| 50.d.0 | " | " | 68 | - |
| 50.e.I | 28.0 | " | 131 | - |
| 50.e.0 | " | " | 110 | - |

Table 7. Pressures

| Run | Atmos. Pressure mm of Hg | Upstream Pressure psig | Tank Pressure psig | Partial Pressure of $O_2$ mm of Hg |
|---|---|---|---|---|
| 22.a | 742 | 22 | 0 | 150 |
| 22.b | " | 20 | 0 | 151 |
| 22.c | " | 23 | 0 | 149 |
| 23.a | 743 | 12 | 0 | 153 |
| 23.b | " | 7 | 0 | 150 |
| 23.c | " | - | 0 | 151 |
| 23.d | 742 | - | 0 | 150 |
| 23.e | " | - | 0 | 151 |
| 23.f | 741 | 18 | 0 | 149 |
| 24.a | 744 | 21 | 0 | 153 |
| 24.b | " | 26 | 3.8 | 347 |
| 24.c | 743 | 32 | 11.2 | 768 |
| 24.d | " | 50 | 31 | 1749 |
| 24.e | " | 79 | 60 | 3252 |
| 24.f.0 | " | 79 | 60 | 3251 |
| 24.g | " | 102 | 84 | 4487 |
| 24.h.I | " | 102 | 85 | 4547 |
| 24.i | " | 123 | 107 | 5678 |
| 25.a | 742 | 22 | 0 | 152 |
| 26.a | 744 | 22 | 0 | 151 |
| 26.b | " | - | 0 | 152 |
| 26.c | 743 | - | 0 | 151 |
| 26.d | " | - | 0 | |
| 26.e | 742 | - | 0 | |
| 26.f | " | - | 0 | 152 |
| 26.g | " | - | 0 | |
| 27.a | 744 | - | 0 | 153 |
| 27.b | " | - | 0 | |
| 27.c | " | - | 0 | 152 |
| 27.d | 743 | - | 0 | |
| 27.e | 742 | - | 0 | |
| 27.f | " | - | 0 | 149 |
| 27.g | " | - | 0 | 151 |

Table 7. Continued

| Run | Atmos. Pressure mm of Hg | Upstream Pressure psig | Tank Pressure psig | Partial Pressure of $O_2$ mm of Hg |
|---|---|---|---|---|
| 28.a | 744 | - | 0 | 151 |
| 28.b | " | - | 0 | " |
| 28.c | 743 | - | 0 | " |
| 28.d | " | - | 0 | " |
| 28.e | " | - | 0 | 152 |
| 28.f | 742 | - | 0 | 151 |
| 28.g | " | - | 0 | 150 |
| 29.a | 742 | - | 0 | 150 |
| 29.b | " | 20 | 10.9 | 714 |
| 29.c | " | 34 | 26 | 1750 |
| 29.d | " | 60 | 53 | 2886 |
| 29.e | " | 78 | 70 | 3769 |
| 29.f | " | 100 | 93 | 4955 |
| 30.a | " | - | 0 | 151 |
| 30.b | " | - | 0 | 150 |
| 30.c | " | - | 0 | 151 |
| 30.d | " | - | 0 | " |
| 30.e | " | - | 0 | " |
| 31.a | 741 | 34 | 8.6 | 593 |
| 31.b | " | 20 | 8.7 | 596 |
| 31.c | 740 | 14 | 8.3 | 574 |
| 32.a | " | - | 0 | 151 |
| 32.b | " | - | 0 | 151 |
| 33.a | 742 | - | 0 | 152 |
| 33.b | " | - | 0 | 151 |
| 33.c | " | - | 0 | 152 |
| 34.a | 741 | 38 | 10.9 | 716 |
| 34.b | " | 25 | 11.3 | 734 |
| 34.c | " | 15 | 9.5 | 640 |
| 34.d | " | 55 | 30 | 1700 |
| 34.e | 742 | 52 | 26 | 1495 |
| 34.f | " | 34 | 23 | - |
| 34.g | " | 35 | 22 | 1287 |
| 34.h | " | 25 | 20 | 1183 |
| 34.i | " | 25 | 20 | 1184 |

Table 7. Continued

| Run | Atmos. Pressure mm of Hg | Upstream Pressure psig | Tank Pressure psig | Partial Pressure of $O_2$ mm of Hg |
|---|---|---|---|---|
| 35.a | 743 | 24 | 0 | 152 |
| 35.b | " | - | 0 | 151 |
| 36.a | " | 35 | 8 | 565 |
| 36.b | " | 20 | 7.5 | 539 |
| 36.c | " | 12 | 7.5 | " |
| 37.a | " | 34 | 28 | 1597 |
| 37.b | 742 | 40 | 27 | 1545 |
| 37.c | 744 | 51 | 27 | 1548 |
| 38.a | 744 | 40 | 34 | 1908 |
| 38.b | " | 44 | 33 | 1856 |
| 38.c | " | 52 | 32 | 1805 |
| 39 | No run | | | |
| 40.a | 746 | 29 | 0 | 153 |
| 40.b | 745 | 56 | 40 | 2217 |
| 40.c | 744 | 49 | 40 | 2214 |
| 40.d | " | 43 | 40 | 2211 |
| 41.a | " | 49 | 40 | 2216 |
| 41.b | " | 44 | 40 | 2212 |
| 41.c | " | 55 | 40 | 2213 |
| 42.a | " | 39 | 0 | 152 |
| 42.b | " | - | 0 | " |
| 42.c | " | - | 0 | " |
| 42.d | 743 | - | 0 | 151 |
| 43.a | 743 | 20 | 6.6 | 503 |
| 43.b | " | 30 | 7.6 | 541 |
| 43.c | " | 52 | 9.7 | - |
| 43.d | 744 | 52 | 9.2 | 627 |
| 43.e | " | 57 | 9.0 | 613 |
| 44.a | " | 22 | 0 | 152 |
| 44.b | " | 40 | 0 | 151 |
| 44.c | " | 50 | 0 | " |
| 44.d | 743 | 10 | 0 | 153 |

Table 7. Continued

| Run | Atmos. Pressure mm of Hg | Upstream Pressure psig | Tank Pressure psig | Partial Pressure of $O_2$ mm of Hg |
|---|---|---|---|---|
| 45.a | 743 | 40 | 6.1 | 469 |
| 45.b | " | 41 | 9.2 | 629 |
| 45.c | " | 45 | 11.5 | 747 |
| 46.a | " | 51 | 0 | 152 |
| 46.b | " | - | 0 | 150 |
| 46.c | 742 | 22 | 0 | " |
| 47.a | " | 22 | 0 | " |
| 47.b | 741 | 40 | 9.2 | 613 |
| 47.c | " | 46 | 19 | 1117 |
| 47.d | " | 61 | 33 | 1839 |
| 47.e | " | 85 | 58 | 3131 |
| 48.a | 741 | - | 0 | 150 |
| 48.b | " | - | 0 | 151 |
| 48.c | " | - | 0 | " |
| 49.a | " | 35 | 29 | 1649 |
| 49.b | 740 | 46 | 35 | 1961 |
| 49.c | " | 46 | 35 | 1913 |
| 50.a | " | 14 | 0 | 151 |
| 50.b | 741 | - | 0 | 150 |
| 50.c | " | 24 | 11.4 | 737 |
| 50.d | " | 37 | 24 | 1387 |
| 50.e | " | 52 | 40 | 2210 |

Table 8. Concentration and Sensitivity

| Run | Saturation Concentration mg/l | ø, as found by titration mg/l | $ø(T_m/T)$ mg/l | ø, from curves mg/l | $Re_p$ |
|---|---|---|---|---|---|
| 22.a.I | | 1.29 | 1.231 | 1.39 | 7900 |
| 22.a.0 | 7.84 | 1.17 | 1.120 | 1.22 | " |
| 22.b.I | | 1.34 | 1.242 | 1.43 | 7860 |
| 22.b.0 | 7.80 | 1.28 | 1.189 | 1.38 | " |
| 22.c.I | | - | - | 1.45 | 7900 |
| 22.c.0 | 7.67 | - | - | 1.39 | " |
| 23.a.I | | 1.22 | 1.212 | 1.31 | 5540 |
| 23.a.0 | 8.14 | 1.28 | 1.271 | 1.29 | 5640 |
| 23.b.I | | - | - | 1.30 | 4060 |
| 23.b.0 | 7.95 | - | - | 1.29 | " |
| 23.c.I | | 1.26 | 1.218 | 1.29 | 2895 |
| 23.c.0 | 7.92 | 1.31 | 1.265 | 1.30 | " |
| 23.d.I | | 1.32 | 1.250 | 1.32 | 2965 |
| 23.d.0 | 7.79 | 1.37 | 1.295 | 1.33 | " |
| 23.e.I | | 1.32 | 1.248 | 1.30 | 1960 |
| 23.e.0 | 7.68 | | | 1.32 | " |
| 23.f.I | | 1.40 | 1.271 | 1.46 | 8130 |
| 23.f.0 | 7.65 | 1.48 | 1.348 | 1.41 | " |
| 24.a.I | | 1.36 | 1.311 | 1.38 | 7740 |
| 24.a.0 | 8.02 | 1.38 | 1.308 | 1.33 | " |

Table 8. Continued

| Run | Saturation Concentration mg/l | ø, as found by titration mg/l | $ø(T_m/T)$ mg/l | ø, from curves mg/l | $Re_p$ |
|---|---|---|---|---|---|
| 24.b.I | | - | - | 1.41 | 7790 |
| 24.b.0 | 18.02 | - | - | 1.35 | " |
| 24.c.I | | - | - | 1.43 | 7860 |
| 24.c.0 | 39.6 | - | - | 1.38 | " |
| 24.d.I | | - | - | 1.46 | 7970 |
| 24.d.0 | 88.3 | - | - | 1.41 | " |
| 24.e.I | | - | - | 1.45 | 7900 |
| 24.e.0 | 165 | - | - | 1.35 | " |
| 24.f.I | | - | - | - | - |
| 24.f.0 | 166 | - | - | 1.41 | 7860 |
| 24.g.I | | - | - | 1.41 | 7900 |
| 24.g.0 | 225 | - | - | 1.35 | " |
| 24.h.I | | - | - | 1.41 | " |
| 24.h.0 | - | - | - | - | - |
| 24.i.I | | - | - | 1.43 | 7860 |
| 24.i.0 | 282 | - | - | 1.38 | " |
| 25.a.I | | 1.28 | 1.389 | 1.28 | 9750 |
| 25.b.0 | 8.40 | 1.08 | 1.170 | 1.18 | " |
| 26.a.I | | 1.18 | 1.298 | 1.22 | 9700 |
| 26.a.0 | 8.36 | 1.21 | 1.330 | 1.17 | " |

Table 8. Continued

| Run | Saturation Concentration mg/l | ø, as found by titration mg/l | $ø(T_m/T)$ mg/l | ø, from curves mg/l | $Re_p$ |
|---|---|---|---|---|---|
| 26.b.I | | 1.18 | 1.299 | 1.21 | 8100 |
| 26.b.0 | 8.40 | 1.13 | 1.240 | 1.17 | " |
| 26.c.I | | - | 1.405 | 1.19 | 6900 |
| 26.c.0 | 8.37 | - | 1.185 | 1.17 | " |
| 26.d.I | | 1.28 | 1.405 | 1.19 | 6120 |
| 26.d.0 | 8.37 | 1.08 | 1.185 | 1.17 | " |
| 26.e.I | | - | - | 1.18 | 5310 |
| 26.e.0 | | - | - | 1.17 | " |
| 26.f.I | | 1.22 | 1.309 | 1.19 | 4430 |
| 26.f.0 | 8.29 | 1.13 | 1.211 | 1.19 | " |
| 26.g.I | | - | - | 1.18 | 3170 |
| 26.g.0 | | - | - | 1.18 | " |
| 27.a.I | | 0.910 | 0.944 | 0.98 | 9710 |
| 27.a.0 | 8.50 | 0.963 | 0.976 | 0.97 | 9840 |
| 27.b.I | | 0.907 | 0.940 | 0.98 | 8350 |
| 27.b.0 | | 0.960 | 0.974 | 0.96 | 8450 |
| 27.c.I | | 0.896 | 0.909 | 1.08 | 6800 |
| 27.c.0 | 8.45 | 0.853 | 0.864 | .95 | " |
| 27.d.I | | 0.922 | 0.935 | 0.99 | 5070 |
| 27.d.0 | 8.45 | 0.988 | 1.000 | 0.93 | " |

Table 8. Continued

| Run | Saturation Concentration mg/l | ø, as found by titration mg/l | $ø(T_m/T)$ mg/l | ø, from curves mg/l | $Re_p$ |
|---|---|---|---|---|---|
| 27.e.I | | 0.901 | 0.914 | 0.98 | 3880 |
| 27.e.0 | 8.37 | 0.959 | 0.951 | 0.94 | 3925 |
| 27.f.I | | 0.917 | 0.930 | 0.97 | 2585 |
| 27.f.0 | 8.12 | 0.897 | 0.873 | 0.92 | 2645 |
| 27.g.I | | 0.905 | 0.899 | 0.97 | 1760 |
| 27.g.0 | 8.23 | 0.897 | 0.874 | 0.90 | 1780 |
| 28.a.I | | 1.088 | 1.080 | 1.03 | 9150 |
| 28.a.0 | 8.32 | 0.850 | 0.892 | 0.92 | " |
| 28.b.I | | 1.088 | 1.080 | 1.03 | 7660 |
| 28.b.0 | 8.23 | 0.874 | 0.900 | 0.94 | " |
| 28.c.I | | 1.062 | 1.042 | 1.03 | 6240 |
| 28.c.0 | | 0.870 | 0.895 | 0.89 | 6250 |
| 28.d.I | | 1.038 | 1.010 | 1.03 | 4325 |
| 28.d.0 | | 0.871 | 0.897 | 0.86 | 4370 |
| 28.e.I | | 1.05 | 1.021 | 1.01 | 3000 |
| 28.e.0 | 8.23 | 0.86 | 0.867 | 0.84 | 3040 |
| 28.f.I | | 0.985 | 1.041 | 0.91 | 1659 |
| 28.f.0 | 8.32 | 0.740 | 0.771 | 0.73 | 1720 |
| 28.g.I | | 1.082 | 1.058 | 1.08 | 5290 |
| 28.g.0 | 8.18 | 0.890 | 0.924 | 0.87 | 5250 |

Table 8. Continued

| Run | Saturation Concentration mg/l | ø, as found by titration mg/l | $ø(T_m/T)$ mg/l | ø, from curves mg/l | $Re_p$ |
|---|---|---|---|---|---|
| 29.a.I | | 1.105 | 1.021 | 1.10 | 4220 |
| 29.a.0 | 8.02 | 0.945 | 0.925 | 0.93 | 5640 |
| 29.b.I | | - | - | 1.10 | 4450 |
| 29.b.0 | 37.9 | - | - | 0.93 | " |
| 29.c.I | | - | - | 1.10 | " |
| 29.c.0 | 92.5 | - | - | 0.93 | " |
| 29.d.I | | - | - | 1.12 | 4480 |
| 29.d.0 | 151 | - | - | 0.94 | " |
| 29.e.I | | - | - | 1.11 | 4470 |
| 29.e.0 | 197 | - | - | 0.93 | " |
| 29.f.I | | - | - | 1.15 | 4520 |
| 29.f.0 | 251 | - | - | 0.97 | " |
| 30.a.I | | 0.760 | 0.774 | 0.78 | 8830 |
| 30.a.0 | 8.32 | 0.755 | 0.756 | | 8960 |
| 30.b.I | | 0.812 | 0.808 | 0.80 | 5990 |
| 30.b.0 | 8.27 | 0.738 | 0.725 | 0.77 | 6050 |
| 30.c.I | | 0.824 | 0.812 | 0.81 | 4120 |
| 30.c.0 | | 0.750 | 0.734 | 0.74 | 4090 |
| 30.d.I | | 0.809 | 0.791 | 0.82 | 2020 |
| 30.d.0 | | 0.651 | 0.640 | 0.64 | " |

Table 8. Continued

| Run | Saturation Concentration mg/l | ø, as found by titration mg/l | $ø(T_m/T)$ mg/l | ø, from curves mg/l | $Re_p$ |
|---|---|---|---|---|---|
| 30.e.I | | 0.823 | 0.821 | 0.80 | 8130 |
| 30.e.O | 8.33 | 0.779 | 0.780 | 0.78 | 8040 |
| 31.a.I | | - | - | 1.34 | 8010 |
| 31.a.O | 32.4 | - | - | 0.79 | " |
| 31.b.I | | - | - | 1.35 | 5280 |
| 31.b.O | 32.4 | - | - | 0.77 | " |
| 31.c.I | | - | - | 1.36 | 3080 |
| 31.c.O | 30.8 | - | - | 0.72 | " |
| 32.a.I | | 1.27 | 1.192 | 1.40 | 8250 |
| 32.a.O | 8.18 | .745 | 0.716 | 0.81 | 8150 |
| 32.b.I | | 1.425 | 1.368 | 1.36 | 4040 |
| 32.b.O | | 0.746 | 0.718 | 0.76 | " |
| 33.a.I | | 1.169 | 1.190 | 1.29 | 7730 |
| 33.a.O | 8.45 | .705 | 0.721 | 0.76 | 7770 |
| 33.b.I | | 1.24 | 1.265 | 1.28 | 4780 |
| 33.b.O | 8.37 | 0.693 | 0.702 | 0.73 | 4830 |
| 33.c.I | | 1.177 | 1.199 | 1.21 | 1930 |
| 33.c.O | | 0.605 | 0.605 | 0.63 | 1999 |
| 34.a.I | | 1.270 | 1.285 | 1.24 | 7890 |
| 34.a.O | 40.3 | - | - | 0.72 | " |

Table 8. Continued

| Run | Saturation Concentration mg/l | ø, as found by titration mg/l | $ø(T_m/T)$ mg/l | ø, from curves mg/l | $Re_p$ |
|---|---|---|---|---|---|
| 34.b.I | | - | - | 1.29 | 5340 |
| 34.b.0 | 40.2 | - | - | 0.76 | 5410 |
| 34.c.I | | - | - | 1.32 | 3050 |
| 34.c.0 | 35.0 | - | - | 0.70 | 3040 |
| 34.d.I | | 1.328 | 1.325 | 1.32 | 8000 |
| 34.d.0 | 93.3 | - | - | 0.78 | - |
| 34.e.I | | - | - | 1.32 | 8310 |
| 34.e.0 | 82.0 | - | - | 0.78 | " |
| 34.f.I | | 1.321 | 1.320 | 1.31 | 5490 |
| 34.f.0 | - | - | - | - | - |
| 34.g.I | | - | - | 1.34 | 5640 |
| 34.g.0 | 70.0 | - | - | 0.77 | 5630 |
| 34.h.I | | 1.36 | 1.302 | 1.34 | 3085 |
| 34.h.0 | 64.7 | - | - | 0.70 | 3050 |
| 34.i.I | | - | - | 1.32 | 3020 |
| 34.i.0 | 65.2 | - | - | 0.69 | 2975 |
| 35.a.I | | 1.240 | 1.291 | 1.27 | 7400 |
| 35.a.0 | 8.48 | 0.724 | 0.746 | 0.75 | 7450 |
| 35.b.I | | 1.248 | 1.280 | 1.27 | 3980 |
| 35.b.0 | 8.40 | 0.708 | 0.724 | 0.72 | 4000 |

Table 8. Continued

| Run | Saturation Concentration mg/l | ø, as found by titration mg/l | ø($T_m$/T) mg/l | ø, from curves mg/l | $Re_p$ |
|---|---|---|---|---|---|
| 36.a.I | | - | - | 1.28 | 8050 |
| 36.a.0 | 31.5 | - | - | 1.28 | 8050 |
| 36.b.I | | - | - | 1.28 | 5150 |
| 36.b.0 | 29.9 | - | - | 0.74 | " |
| 36.c.I | | - | - | 1.26 | 2715 |
| 36.c.0 | 29.9 | - | - | 0.66 | 2720 |
| 37.a.I | | - | - | 1.30 | 3805 |
| 37.a.0 | 86.7 | - | - | 0.73 | 3845 |
| 37.b.I | | - | - | 1.31 | 5580 |
| 37.b.0 | 84.3 | - | - | 0.77 | 5630 |
| 37.c.I | | - | - | 1.32 | 8000 |
| 37.c.0 | 85.2 | - | - | 0.78 | " |
| 38.a.I | | - | - | 1.32 | 3555 |
| 38.a.0 | 104.2 | - | - | 0.72 | " |
| 38.b.I | | - | - | 1.32 | 5640 |
| 38.b.0 | 101.1 | - | - | 0.77 | " |
| 38.c.I | | - | - | 1.32 | 7190 |
| 38.c.0 | 98.7 | - | - | 0.78 | 7160 |
| 39 | No run | | | | |

Table 8. Continued

| Run | Saturation Concentration mg/l | ø, as found by titration mg/l | $ø(T_m/T)$ mg/l | ø, from curves mg/l | $Re_p$ |
|---|---|---|---|---|---|
| 40.a.I | | 1.31 | 1.31 | 1.29 | 8360 |
| 40.a.0 | 8.50 | 0.841 | 0.86 | 0.76 | " |
| 40.b.I | | 1.299 | 1.32 | 1.29 | 6300 |
| 40.b.0 | 122.8 | - | - | 0.74 | " |
| 40.c.I | | 1.282 | 1.28 | 1.31 | 4600 |
| 40.c.0 | 121.2 | - | - | 0.74 | " |
| 40.d.I | | 1.298 | 1.28 | 1.27 | 2200 |
| 40.d.0 | 120.1 | - | - | 0.66 | 2300 |
| 41.a.I | | - | - | 1.28 | 4920 |
| 41.a.0 | 122.1 | - | - | 0.73 | " |
| 41.b.I | | - | - | 1.32 | 3420 |
| 41.b.0 | 120.9 | - | - | 0.71 | " |
| 41.c.I | | - | - | 1.34 | 6440 |
| 41.c.0 | 121.2 | - | - | 0.76 | 6360 |
| 42.a.I | | 0.897 | 0.907 | 1.01 | 4690 |
| 42.a.0 | 8.45 | 0.875 | 0.896 | 0.91 | " |
| 42.b.I | | 0.875 | 0.904 | 1.00 | 5540 |
| 42.b.0 | " | 0.871 | 0.894 | 0.92 | 5610 |
| 42.c.I | | 0.867 | 0.881 | 0.98 | 3160 |
| 42.c.0 | " | 0.850 | 0.872 | 0.86 | 3355 |

Table 8. Continued

| Run | Saturation Concentration mg/l | ø, as found by titration mg/l | $ø(T_m/T)$ mg/l | ø, from curves mg/l | $Re_p$ |
|---|---|---|---|---|---|
| 42.d.I | | 0.875 | 0.885 | 0.97 | 1748 |
| 42.d.O | 8.38 | 0.675 | 0.686 | 0.69 | 1710 |
| 43.a.I | | 0.995 | 1.072 | 0.92 | 2342 |
| 43.a.O | 27.9 | - | - | 0.81 | 2620 |
| 43.b.I | | 1.020 | 0.999 | 1.02 | 3415 |
| 43.b.O | 29.5 | - | - | 0.90 | 3465 |
| 43.c.I | | 1.041 | 1.011 | 1.05 | 5030 |
| 43.c.O | - | - | - | - | " |
| 43.d.I | | 0.99 | 1.001 | 1.01 | 4860 |
| 43.d.O | 34.4 | - | - | 0.94 | 4820 |
| 43.e.I | | 1.02 | 1.031 | 1.02 | 5700 |
| 43.e.O | 33.9 | - | - | 0.93 | 5740 |
| 44.a.I | | 1.165 | 1.155 | 1.01 | 3360 |
| 44.a.O | 8.38 | 0.927 | 0.931 | 0.88 | " |
| 44.b.I | | 1.149 | 1.140 | 1.03 | 4790 |
| 44.b.O | 8.31 | 0.952 | 0.943 | 0.94 | 4810 |
| 44.c.I | | 1.115 | 1.110 | 1.03 | 5360 |
| 44.c.O | 8.38 | 0.952 | 0.970 | 0.92 | 5340 |
| 44.d.I | | 1.112 | 1.081 | 1.01 | 2020 |
| 44.d.O | 8.43 | 0.739 | 0.741 | 0.75 | 1998 |

Table 8. Continued

| Run | Saturation Concentration mg/l | ø, as found by titration mg/l | $ø(T_m/T)$ mg/l | ø, from curves mg/l | $Re_p$ |
|---|---|---|---|---|---|
| 45.a.I | | - | - | 1.05 | 4460 |
| 45.a.0 | 25.7 | - | - | 0.93 | 4450 |
| 45.b.I | | - | - | 1.04 | 4210 |
| 45.b.0 | 34.4 | - | - | 0.93 | 4220 |
| 45.c.I | | - | - | 1.05 | 4360 |
| 45.c.0 | 41.2 | - | - | 0.92 | 4310 |
| 46.a.I | | 1.163 | 1.131 | 1.06 | 5450 |
| 46.a.0 | 8.27 | 0.973 | 0.950 | 0.96 | 5470 |
| 46.b.I | | 1.163 | 1.150 | 1.03 | 4330 |
| 46.b.0 | 8.30 | 0.973 | 0.939 | 0.95 | 4510 |
| 46.c.I | | 1.152 | 1.178 | 1.02 | 3420 |
| 46.c.0 | 8.07 | 0.951 | 0.907 | 0.93 | 3490 |
| 47.a.I | | - | - | 1.03 | 4070 |
| 47.a.0 | 8.23 | - | - | 0.92 | " |
| 47.b.I | | - | - | 1.20 | 4430 |
| 47.b.0 | 31.8 | - | - | 1.06 | 4450 |
| 47.c.I | | - | - | 1.25 | 4480 |
| 47.c.0 | 57.0 | - | - | 1.10 | 4450 |
| 47.d.I | | - | - | 1.25 | 4540 |
| 47.d.0 | 93.0 | - | - | 1.11 | " |

Table 8. Continued

| Run | Saturation Concentration mg/l | ø, as found by titration mg/l | $ø(T_m/T)$ mg/l | ø, from curves mg/l | $Re_p$ |
|---|---|---|---|---|---|
| 47.e.I | | - | - | 1.25 | 4430 |
| 47.e.0 | 157 | - | - | 1.11 | " |
| 48.a.I | | 0.836 | 0.840 | 0.92 | 5990 |
| 48.a.0 | 8.13 | 0.699 | 0.694 | 0.74 | 6100 |
| 48.b.I | | 0.847 | 0.876 | 0.89 | 4550 |
| 48.b.0 | 8.23 | 0.682 | 0.690 | 0.73 | 4690 |
| 48.c.I | | 0.866 | 0.881 | 0.88 | 3465 |
| 48.c.0 | " | 0.660 | 0.671 | 0.73 | 3445 |
| 49.a.I | | - | - | 0.91 | 3845 |
| 49.a.0 | 88.5 | - | - | 0.75 | 3940 |
| 49.b.I | | - | - | 0.90 | 5300 |
| 49.b.0 | 106.8 | - | - | 0.73 | 5370 |
| 49.c.I | | 0.894 | 0.911 | 0.90 | 5300 |
| 49.c.0 | 105.5 | - | - | 0.71 | " |
| 50.a.I | | 0.999 | 0.976 | 0.94 | 5700 |
| 50.a.0 | 8.20 | 0.788 | 0.791 | 0.74 | " |
| 50.b.I | | 0.990 | 0.937 | 0.94 | 3345 |
| 50.b.0 | 8.05 | 0.801 | 0.776 | 0.76 | " |
| 50.c.I | | - | - | 1.00 | 6160 |
| 50.c.0 | 39.0 | - | - | 0.78 | " |

Table 8. Continued

| Run | Saturation Concentration mg/l | ø, as found by titration mg/l | $ø(T_m/T)$ mg/l | ø, from curves mg/l | $Re_p$ |
|---|---|---|---|---|---|
| 50.d.I | | - | - | 1.02 | 6200 |
| 50.d.0 | 72.4 | - | - | 0.80 | " |
| 50.e.I | | - | - | 1.03 | 6230 |
| 50.e.0 | 118.0 | - | - | 0.81 | " |

Table 9. Transfer Data, I

| Run | Concentration at Inlet, mg/l | Concentration at Outlet, mg/l | $E_o$ |
|---|---|---|---|
| 31.a | 5.75 | 35.4 | 1.11 |
| 31.b | 5.93 | 34.0 | 1.06 |
| 31.c | 5.96 | 33.6 | 1.11 |
| 34.a | 8.87 | 34.6 | 0.82 |
| 34.b | 8.68 | 30.3 | 0.68 |
| 34.c | 8.34 | 28.7 | 0.77 |
| 34.d | 8.72 | - | - |
| 34.e | 9.01 | 44.8 | 0.49 |
| 34.g | 8.88 | 35.1 | 0.43 |
| 34.h | 8.95 | 32.8 | 0.43 |
| 34.i | 9.01 | 34.0 | 0.44 |
| 36.a | 8.60 | 29.2 | 0.90 |
| 36.b | 8.66 | 28.6 | 0.94 |
| 36.c | 8.73 | 29.0 | 0.96 |
| 37.a | 9.08 | 62.4 | 0.67 |
| 37.b | 8.78 | 65.0 | 0.74 |
| 37.c | 8.71 | 65.4 | 0.74 |
| 38.a | 8.83 | 94.1 | 0.91 |
| 38.b | 8.93 | 93.6 | 0.92 |
| 38.c | 8.86 | 92.3 | 0.93 |
| 40.b | 8.88 | 119.6 | 0.97 |
| 40.c | 8.93 | 116.2 | 0.96 |
| 40.d | 9.05 | 108.2 | 0.89 |
| 41.a | 9.22 | 124.8 | 1.02 |
| 41.b | 8.94 | 116.2 | 0.96 |
| 41.c | 8.96 | 127.8 | 1.06 |
| 43.a | 8.81 | 32.1 | 1.22 |
| 43.b | 9.23 | 44.5 | 1.74 |
| 43.d | 9.17 | 55.3 | 1.83 |
| 43.e | 9.23 | 57.0 | 1.94 |
| 45.a | 10.0 | 31.1 | 1.34 |
| 45.b | 10.4 | 50.0 | 1.65 |
| 45.c | 10.1 | 65.2 | 1.77 |
| 49.a | 9.01 | 74.8 | 0.83 |
| 49.b | 9.00 | 108.2 | 1.02 |

Table 10. Transfer Data, II

| Run | $d_d$ cm, x10³ | Fall Distance in | U ft/sec | $t_{ct}$ sec | $D_d$ cm²/sec x10⁶ |
|---|---|---|---|---|---|
| 31.a | 6.90 | 39.3 | 44.8 | .0730 | 2.59 |
| 31.b | 9.45 | 38.5 | 26.7 | .120 | 2.61 |
| 31.c | 11.55 | 38.7 | 17.0 | .190 | 2.64 |
| 34.a | 6.66 | 27.1 | 46.0 | .0491 | 2.47 |
| 34.b | 9.30 | 25.3 | 30.4 | .0694 | 2.56 |
| 34.c | 11.55 | 25.8 | 17.0 | .126 | 2.59 |
| 34.d | 6.85 | 12.5 | - | - | - |
| 34.e | 6.65 | 12.5 | 46.8 | .0267 | 2.56 |
| 34.g | 9.15 | 13.6 | 31.4 | .0362 | 2.59 |
| 34.h | 11.57 | 12.4 | 16.9 | .0609 | 2.61 |
| 34.i | 11.60 | 11.3 | 16.8 | .0560 | 2.58 |
| 36.a | 6.66 | 41.8 | 46.0 | .0757 | 2.52 |
| 36.b | 9.50 | 42.3 | 29.3 | .144 | 2.53 |
| 36.c | 11.85 | 41.7 | 15.2 | .228 | 2.53 |
| 37.a | 10.80 | 27.0 | 21.4 | .105 | 2.58 |
| 37.b | 9.10 | 29.1 | 31.4 | .0774 | 2.58 |
| 37.c | 6.85 | 28.3 | 45.0 | .0524 | 2.57 |
| 38.a | 11.05 | 40.5 | 19.9 | .169 | 2.58 |
| 38.b | 9.10 | 40.6 | 31.4 | .108 | 2.59 |
| 38.c | 7.65 | 39.6 | 40.0 | .0825 | 2.58 |
| 40.b | 8.35 | 38.8 | 35.8 | .0903 | 2.53 |
| 40.c | 10.05 | 37.8 | 25.9 | .121 | 2.57 |
| 40.d | 12.30 | 37.2 | 12.6 | .246 | 2.58 |
| 41.a | 9.65 | 28.3 | 28.3 | .0834 | 2.53 |
| 41.b | 11.20 | 26.8 | 19.1 | .117 | 2.58 |
| 41.c | 8.40 | 29.6 | 35.8 | .0687 | 2.58 |
| 43.a | 7.48 | 36.7 | 33.4 | .0915 | 2.48 |
| 43.b | 7.30 | 24.8 | 44.4 | .0464 | 2.59 |
| 43.d | 6.95 | 24.6 | 66.4 | .0311 | 2.56 |
| 43.e | 6.75 | 25.6 | 75.3 | .0284 | 2.54 |
| 45.a | 7.05 | 44.2 | 57.7 | .0639 | 2.58 |
| 45.b | 7.10 | 17.0 | 54.7 | .0260 | 2.58 |
| 45.c | 7.05 | 35.8 | 56.5 | .0529 | 2.58 |
| 49.a | 10.80 | 39.0 | 21.4 | .152 | 2.63 |
| 49.b | 9.40 | 33.8 | 29.8 | .0945 | 2.58 |

Table 11. Transfer Data, III

| Run | $Re_d$ | $Sc_d$ | $We_d x10^6$ | $Pe'_d$ | $Re_c$ |
|---|---|---|---|---|---|
| 31.a | 1047 | .35 | 206 | 8.21 | 59 |
| 31.b | 859 | .34 | 99 | 6.60 | 47 |
| 31.c | 672 | .34 | 50 | 8.67 | 36 |
| 34.a | 991 | .38 | 210 | 7.25 | 59 |
| 34.b | 947 | .36 | 128 | 7.60 | 54 |
| 34.c | 665 | .35 | 50 | 5.23 | 37 |
| 34.d | - | - | - | - | - |
| 34.e | 1045 | .36 | 217 | 8.33 | 60 |
| 34.g | 974 | .35 | 134 | 7.65 | 55 |
| 34.h | 664 | .34 | 49 | 5.14 | 37 |
| 34.i | 657 | .35 | 49 | 5.15 | 37 |
| 36.a | 1011 | .37 | 210 | 8.27 | 59 |
| 36.b | 925 | .37 | 121 | 7.50 | 54 |
| 36.c | 597 | .37 | 52 | 4.85 | 35 |
| 37.a | 780 | .35 | 74 | 6.10 | 44 |
| 37.b | 964 | .35 | 134 | 7.53 | 54 |
| 37.c | 1032 | .36 | 206 | 8.30 | 59 |
| 38.a | 743 | .35 | 65 | 5.85 | 42 |
| 38.b | 970 | .35 | 134 | 7.69 | 54 |
| 38.c | 1038 | .35 | 182 | 8.15 | 58 |
| 40.b | 992 | .37 | 159 | 8.05 | 58 |
| 40.c | 876 | .36 | 101 | 7.03 | 50 |
| 40.d | 526 | .35 | 29 | 4.13 | 29 |
| 41.a | 906 | .37 | 115 | 7.37 | 53 |
| 41.b | 724 | .35 | 61 | 5.67 | 41 |
| 41.c | 1012 | .35 | 160 | 7.95 | 57 |
| 43.a | 817 | .38 | 310 | 6.64 | 48 |
| 43.b | 1100 | .35 | 385 | 8.51 | 62 |
| 43.d | 1546 | .36 | 455 | 12.3 | 88 |
| 43.e | 1695 | .36 | 570 | 13.5 | 97 |
| 45.a | 1382 | .35 | 349 | 10.7 | 77 |
| 45.b | 1318 | .35 | 316 | 10.2 | 74 |
| 45.c | 1345 | .35 | 335 | 10.4 | 75 |
| 49.a | 794 | .34 | 73 | 6.17 | 44 |
| 49.b | 753 | .35 | 124 | 6.05 | 42 |

Table 12. Molecular Diffusivities of Oxygen in Water

| Diffusivity $cm^2/sec \times 10^5$ | Temperature °C | Source |
|---|---|---|
| 1.875 | 16 | Hufner (172) |
| 1.98 | 18 | Carlson (172) |
| 1.99 | 18.2 | Carlson (172) |
| 2.22 | 22 | Birdicka and Wiesner (172) |
| 2.38 | 25 | Kolthoff and Laitinen (172) |
| 2.60 | 25 | Kolthoff and Miller (172) |
| 2.60 | 25 | Wilke (245) |

Table 13. Overall Transfer Characteristics

| Run | $\mu_d/\mu_c$ | $Sh_o$ | $(Re_d Sc_d)^{1/2}$ | $T^* \times 10^2$ |
|---|---|---|---|---|
| 31.a | 43.5 | - | 19.2 | 15.81 |
| 31.b | 43.2 | - | 17.0 | 14.05 |
| 31.c | 42.5 | - | 15.2 | 15.02 |
| 34.a | 46.0 | 10.4 | 19.4 | 10.91 |
| 34.b | 43.9 | 9.44 | 18.5 | 8.20 |
| 34.c | 43.4 | 10.0 | 15.3 | 9.77 |
| 34.e | 44.1 | 7.26 | 19.5 | 6.20 |
| 34.g | 43.5 | 8.34 | 18.4 | 4.46 |
| 34.h | 43.0 | 7.76 | 15.0 | 4.77 |
| 34.i | 43.6 | 9.16 | 15.1 | 4.30 |
| 36.a | 44.2 | 8.82 | 19.4 | 17.20 |
| 36.b | 44.6 | 11.55 | 18.5 | 16.15 |
| 36.c | 44.6 | 12.82 | 14.9 | 16.40 |
| 37.a | 43.7 | 9.16 | 16.5 | 10.82 |
| 37.b | 43.7 | 9.46 | 18.3 | 9.64 |
| 37.c | 43.9 | 7.86 | 19.2 | 11.42 |
| 38.a | 43.5 | 11.4 | 18.2 | 14.29 |
| 38.b | 43.3 | 12.4 | 18.4 | 13.52 |
| 38.c | 43.5 | 12.0 | 19.0 | 14.60 |
| 40.b | 44.6 | 15.2 | 19.2 | 13.10 |
| 40.c | 44.0 | 16.9 | 17.8 | 12.40 |
| 40.d | 43.5 | 8.79 | 13.5 | 16.82 |
| 41.a | 44.5 | - | 18.3 | 8.44 |
| 41.b | 43.6 | 22.2 | 15.9 | 9.64 |
| 41.c | 43.6 | - | 22.4 | 10.06 |
| 43.a | 45.2 | - | - | 16.21 |
| 43.b | 43.7 | - | - | 9.01 |
| 43.d | 43.7 | - | - | 6.59 |
| 43.e | 44.2 | - | - | 6.33 |
| 45.a | 43.7 | - | - | 13.25 |
| 45.b | 43.7 | - | - | 5.32 |
| 45.c | 43.7 | - | - | 10.99 |
| 49.a | 42.7 | 8.53 | 22.2 | 16.00 |
| 49.b | 43.6 | - | 22.1 | 11.02 |

Table 14. Nozzle MX-0 Transfer Efficiencies

| Run | $E_o$ before increase | $E_o$ after increase |
|---|---|---|
| 43.a | 1.22 | .70 |
| 43.b | 1.74 | 1.00 |
| 43.d | 1.83 | 1.09 |
| 43.e | 1.94 | 1.13 |
| 45.a | 1.34 | 0.74 |
| 45.b | 1.65 | 0.96 |
| 45.c | 1.77 | 1.06 |

Table 15. Nozzle MX-00 Transfer Efficiencies

| Run | E | $\overline{k}_d$ (cm/sec)x10$^3$ | $\overline{Sh}_d$ |
|---|---|---|---|
| 31.a | 1.012 | - | - |
| 31.b | 1.007 | - | - |
| 31.c | 1.012 | - | - |
| 34.a | 0.982 | 90.6 | 24.4 |
| 34.b | 0.968 | 54.6 | 19.8 |
| 34.c | 0.976 | 57.0 | 25.4 |
| 34.e | 0.948 | 123.0 | 31.9 |
| 34.g | 0.942 | 119.8 | 42.5 |
| 34.h | 0.942 | 89.8 | 39.6 |
| 34.i | 0.944 | 99.7 | 44.8 |
| 36.a | 0.990 | 33.4 | 8.9 |
| 36.b | 0.994 | 56.3 | 21.1 |
| 36.c | 0.996 | 47.7 | 22.4 |
| 37.a | 0.968 | 65.0 | 27.2 |
| 37.b | 0.974 | 71.5 | 25.2 |
| 37.c | 0.974 | 79.5 | 21.2 |
| 38.a | 0.991 | 51.3 | 22.0 |
| 38.b | 0.992 | 68.0 | 23.8 |
| 38.c | 0.993 | 76.3 | 22.5 |
| 40.b | 0.998 | 78.2 | 25.8 |
| 40.c | 0.996 | 76.1 | 29.9 |
| 40.d | 0.988 | 36.9 | 17.5 |
| 41.a | 1.003 | - | - |
| 41.b | 0.996 | 87.5 | 38.0 |
| 41.c | 1.006 | - | - |
| 49.a | 0.983 | 48.0 | 19.7 |
| 49.b | 1.002 | - | - |

Table 16. Asymptotic Film Coefficients

| Run | $\bar{k}_d$ Stagnant Droplet cm/sec | $\bar{k}_d$ Circulating Droplet cm/sec | $\bar{k}_d$ Turbulent Droplet cm/sec |
|---|---|---|---|
| 31.a | .0157 | .0698 | .1152 |
| 31.b | .0134 | .0529 | .0690 |
| 31.c | .0114 | .0445 | .0446 |
| 34.a | .0191 | .0722 | .1120 |
| 34.b | .0170 | .0561 | .0775 |
| 34.c | .0124 | .0444 | .0437 |
| 34.e | .0289 | .0829 | .1186 |
| 34.g | .0269 | .0655 | .0807 |
| 34.h | .0206 | .0519 | .0439 |
| 34.i | .0220 | .0522 | .0430 |
| 36.a | .0153 | .0701 | .1162 |
| 36.b | .0111 | .0496 | .0735 |
| 36.c | .0088 | .0399 | .0392 |
| 37.a | .0136 | .0477 | .0545 |
| 37.b | .0159 | .0564 | .0802 |
| 37.c | .0188 | .0725 | .1149 |
| 38.a | .0104 | .0441 | .0512 |
| 38.b | .0131 | .0543 | .0811 |
| 38.c | .0148 | .0637 | .1030 |
| 40.b | .0141 | .0578 | .0895 |
| 40.c | .0122 | .0488 | .0658 |
| 40.d | .0086 | .0390 | .0324 |
| 41.a | .0152 | .0524 | .0712 |
| 41.b | .0128 | .0457 | .0489 |
| 41.c | .0166 | .0606 | .0944 |
| 49.a | .0110 | .0456 | .0558 |
| 49.b | .0140 | .0534 | .0765 |

Table 17. Photo Scale Ratios

| Photo No. | Nozzle | Photo Scale Ratio (PSR) | Maximum °/o Error of Notch Scale Ratio from PSR | Number of Notch Scale Ratios Used to Calculate PSR |
|---|---|---|---|---|
| 30 | MX-00 | 1.085 | 2 | 2 |
| 31 | " | 1.014 | 4 | 2 |
| 34 | " | 1.020 | 3 | 2 |
| 35 | " | 0.997 | 4 | 2 |
| 36 | MX-0 | 1.020 | 2 | 2 |
| 37 | " | 1.006 | 2 | 3 |
| 38 | " | 1.000 | 3 | 5 |
| 39 | " | 0.944 | 1 | 2 |

Table 18. Number of Droplets in Photo Class Sizes

| Photo No. | Midpoint Value of Photo Class Size inches x $10^3$ | | | | | | Total No. of Drops Measured |
|---|---|---|---|---|---|---|---|
| | 2 | 3 | 4 | 5 | 6 | 7 | |
| 30 | 1 | 15 | 2 | 8 | 3 | 1 | 48 |
| 31 | 8 | 5 | 2 | - | - | - | 15 |
| 34 | 20 | 16 | 5 | - | 3 | - | 44 |
| 35 | - | 11 | 11 | 5 | 2 | 2 | 31 |
| 36 | 13 | 9 | 2 | - | 1 | - | 25 |
| 37 | 24 | 20 | 16 | - | - | - | 60 |
| 38 | 10 | 16 | 2 | - | - | - | 28 |
| 39 | 13 | 18 | 1 | - | - | - | 32 |

Table 19. Mean Droplet Diameter

| Photo No. | Flowrate gpm | Mean Droplet Diameter in | Nozzle |
|---|---|---|---|
| 30 | 1.030 | 0.0043 | MX-00 |
| 31 | 1.460 | 0.0026 | " |
| 34 | 1.710 | 0.0029 | " |
| 35 | 0.775 | 0.0041 | " |
| 36 | 0.805 | 0.0027 | MX-0 |
| 37 | 0.805 | 0.0029 | " |
| 38 | 1.235 | 0.0027 | " |
| 39 | 1.480 | 0.0025 | " |

# ABBREVIATIONS

B.C. = boundary condition.

cm = centimeter.

eq(s). = equation(s).

Fig. = figure.

ft = feet.

gpm = gallons per minute.

in. = inch.

L.H.S. = left hand side.

mg/l = milligrams per liter.

ml = milliliter.

mm = millimeter.

psi = pounds per square inch.

psia = pounds per square inch absolute.

psig = pounds per square inch gage.

PSR = photo scale ratio.

R.H.S. = right hand side.

rpm = revolutions per minute.

sec = second.

## SYMBOLS

$A$ = species A in multicomponent system.

$A_i$ = $i^{\underline{th}}$ constant in various infinite summation expressions for transfer efficiency.

$A_{MAX}$ = maximum surface area of oscillating droplet.

$a$ = radius of spherical droplet.

$a'$ = radius of circulation zone in turbulent droplet; general coefficient or proportionality constant.

$a_m$ = major droplet radius of oscillating droplet.

$a_p$ = oscillation amplitude of oscillating droplet.

$B$ = species B in multicomponent system.

$b$ = general coefficient, exponent, or proportionality constant.

$b_m$ = minor droplet radius of oscillating droplet.

$C$ = species C in multicomponent system; degrees centigrade when preceded by $^{o}$.

$C^*$ = dimensionless concentration ratio.

$c_D$ = constant of proportionality.

$D$ = diffusivity.

$D_{AB}$ = diffusivity of A in B.

$D_E$ = effective diffusivity in oscillating droplet system.

$D_{xy}$ = diffusivity in x direction for concentration gradient existing in y direction.

$d$ = diameter.

$d_d$ = droplet diameter.

$d_{dc}$ = critical droplet diameter for droplet circulation.

$E$ = transfer efficiency.

$E'$ = 1- transfer efficiency.

$E_D$ = eddy diffusivity.

$E_o$ = overall transfer efficiency.

$e$ = base of natural logarithm.

$F_A(t)$ = total amount of A absorbed at time t.

$f$ = film thickness.

$f(\ )$ = function of.

$f_D$ = diffusion layer thickness.

$f_n(\ )$ = function of, n any number.

$Gr = L^3 g \Delta\rho/\rho \nu^2$, Grashof number.

$g$ = acceleration of gravity; general coefficient, exponent, or proportionality constant.

$g'$ = general coefficient, exponent, or proportionality constant.

$H$ = Henry's constant.

$h$ = general coefficient, exponent, or proportionality constant.

$I$ = inlet run datum.

$\vec{i}$ = unit vector in x direction.

$J_A$ = mass diffusive flux of A.

$J_{A_x}$ = mass diffusive flux of A in x direction.

$J_x(t)$ = turbulent mass flux in x direction.

$\vec{j}$ = unit vector in y direction.

$K$ = combined liquid and gas phase mass transfer coefficient; general mass transfer coefficient.

$K_G$ = mass transfer coefficient expressed in terms of gas phase parameters.

$K_L$ = mass transfer coefficient expressed in terms of liquid phase parameters.

$k$ = mass transfer (or film) coefficient of single phase.

$\vec{k}$ = unit vector in z direction.

$k_v$ = ratio of actual interfacial velocity to value predicted by potential theory.

$L$ = characteristic length.

$M$ = total mass.

$M_A$ = mass of A.

Mf = mole fraction.

$M(t)$ = mass parameter at time t.

$M'(t)$ = mass deficiency parameter at time t.

$m$ = general coefficient, exponent, or proportionality constant.

$m_A$ = molecular weight of A.

$N_A$ = total mass flux of A.

$N_{A_x}$ = total mass flux of A in x direction.

$N_{G_x}$ = total mass flux in gas phase in x direction.

$n$ = number of species in multicomponent system; general coefficient, exponent, or proportionality constant.

$n_i$ = oscillation index of oscillating droplet.

O = outlet run datum.

Pe = LV/D, mass transfer Peclet number.

Pe' = modified mass transfer Peclet number.

$p$ = partial pressure; general coefficient, exponent, or proportionality constant.

$p'$ = general coefficient, exponent, or proportionality constant.

$p(\ )$ = elliptic integral function.

$p_{AB}$ = partial pressure of A in B.

Q = flowrate.

q( ) = elliptic integral function.

R = universal gas constant; r/a.

$R^*$ = effective diffusivity ratio.

Re = $VL/\nu$ , Reynolds number.

r = radial distance; general coefficient, exponent, or proportionality constant.

r' = radial distance in circulation zone in turbulent droplet.

S( ) = equilibrium solubility relationship.

S' = oscillation function of oscillating droplet.

Sc = $\nu/D$, Schmidt number.

Sh = KL/D, Sherwood number.

$Sh^*$ = $k_c d_d/D_d$, continuous phase transfer parameter.

$Sh_o$ = overall Sherwood number.

$Sh_s$ = stagnant droplet Sherwood number.

s = general coefficient, exponent, or proportionality constant; orthogonal curvilinear co-ordinate.

T = temperature.

$T_m$ = mean temperature.

t = time; general coefficient or exponent.

$t_{ct}$ = contact time.

$T^*$ = $D_d t/a^2$ , dimensionless time parameter.

U = droplet fall velocity; free stream velocity.

u = velocity in x direction.

$u^*$ = u/U, dimensionless velocity in x direction.

$V$ = mass average velocity; characteristic velocity.

$V_A$ = mass average velocity of A.

$V_{dr}$ = velocity in circulating droplet.

$V_w$ = velocity at wall or boundary.

$v$ = velocity in y direction.

$v^*$ = $v/U$, dimensionless velocity in y direction.

$W^2$ = oscillation frequency of oscillating droplet.

$We$ = $fV^2L/\sigma$ , Weber number.

$W_f(\ )$ = frequency function of oscillating droplet.

$y^*$ = $y/x$, dimensionless y direction.

Greek Letter Symbols

$\Delta\rho$ = characteristic change in mass concentration.

$\delta$ = hydrodynamic boundary layer thickness.

$\delta^*$ = $\delta/x$, dimensionless hydrodynamic boundary layer thickness.

$\delta_c$ = concentration boundary layer thickness.

$\delta_c^*$ = $\delta_c/x$, dimensionless concentration boundary layer thickness.

$\varepsilon$ = eddy viscosity.

$\mathcal{f}$ = dimensionless equipotential lines in circulating droplet.

$\theta$ = polar angle in spherical co-ordinates.

$\mathcal{K}_c$ = boundary curvature.

$\lambda_i$ = $i^{\underline{th}}$ eigenvalue in various infinite summation expressions for transfer efficiency.

$\mu$ = viscosity.

$\nu$ = kinematic viscosity.

$\xi$ = dimensionless streamline in circulating droplet.

$\rho$ = mass concentration; mass density.

$\rho^*$ = dimensionless mass concentration.

$\rho_{AB}$ = mass concentration of A in B.

$\rho_{SB}$ = mass density of solution in which B occurs.

$\sigma$ = surface tension.

$\tau$ = shear stress.

$\tau_t$ = Reynolds shear stress.

$\phi$ = Meridional angle in spherical co-ordinates.

$\varnothing$ = sensitivity.

$\varnothing'$ = adjusted sensitivity.

$\varnothing^*$ = $\delta_c/\delta$.

$\Psi$ = stream function.

$\Omega$ = $(\varnothing^*)^3$.

Other Symbols

$\Psi$ = volume.

$\mu a$ = microampheres.

Superscripts

$*$ = dimensionless quantity.

o = degrees temperature.

$\rightarrow$ = vector quantity.

$-$ = time average value.

$'$ = fluctuating component, when used with velocity, pressure, or concentration symbol.

General Subscripts

A = component A in multicomponent system.

B = component B in multicomponent system.

b = bulk portion of phase.

C = component C in multicomponent system.

c = continuous phase.

ct = contact time.

d = discontinuous phase; droplet.

e = equilibrium conditions.

G = gas phase.

i = interface; general summation index.

L = liquid phase.

$\ell$ = component $\ell$ of n component system.

o = overall; initial; boundary.

p = pipe.

s = stagnant droplet; solution.

x = x direction.

y = y direction.

z = z direction.

1 = position 1.

2 = position 2.

3 = position 3.

4 = position 4.

$\gamma$ = orthogonal to equipotential lines.

$\xi$ = orthogonal to streamlines.

$\phi$ = orthogonal to equipotential lines and streamlines.

# LITERATURE CITED

(1) Neil K. Adam, The Physics and Chemistry of Surfaces, Clarendon Press, London, England, 1930, pp. 7-10.

(2) Harold E. Babbitt and E. Robert Baumann, Sewerage and Sewage Treatment, eighth ed., second printing, John Wiley and Sons, New York, N.Y., 1958, p. 387.

(3) Byron R. Bird, Warren E. Stewart, and Edwin N. Lightfoot, Transport Phenomena, fourth printing. John Wiley and Sons, New York, N.Y., 1960, chapter 16.

(4) Ibid., p. 303.

(5) Ibid., p. 409.

(6) Ibid., p. 496.

(7) Ibid., p. 497.

(8) Ibid., p. 539.

(9) Ibid., p. 629.

(10) Ibid., p. 639.

(11) Ibid., pp. 639, 640.

(12) Ibid., p. 646.

(13) Ibid., pp. 652, 653.

(14) W. N. Bond and D. A. Newton, "Bubbles, Drops, and Stokes' Law," Philosophical Magazine, series 7, vol. 5, no. 30 (1928), pp. 794-800.

(15) C. W. Bowman and A. I. Johnson, "Mass Transfer from Carbon Dioxide Bubbles Rising in Water," Canadian Journal of Chemical Engineering, vol. 40 (August 1962), pp. 139-147.

(16) Ibid., p. 139.

(17) Ibid., p. 146.

(18) Erich Brunner, "Reaktionsgeschwindigkeit in Heterogenen Systemen," Zeitschrift fur Physikalische Chemie, vol. 47 (1904), p. 56.

(19) P. H. Calderbank and I. J. O. Korchinski, "Circulation in Liquid Drops," Chemical Engineering Science, vol. 6 (1956), pp. 65-78.

(20) Ibid., p. 67.

(21) Ibid., p. 74.

(22) P. V. Danckwerts, "Kinetics of the Absorption of Carbon Dioxide in Water," Research (London), vol. 2 (1949), pp. 494-495.

(23) P. V. Danckwerts, "Significance of Liquid-Film Coefficients in Gas Absorption," Industrial and Engineering Chemistry, vol. 43, no. 6 (June 1951), pp. 1460-1467.

(24) E. D. Eastman and G. K. Rollerson, Physical Chemistry, first edition, McGraw-Hill Book Company, New York, N.Y., 1947, p. 485.

(25) F. H. Garner and A. H. P. Skelland, "Mechanism of Solute Transfer from Droplets," Industrial and Chemical Engineering Chemistry, vol. 46, no. 6 (June 1954), p. 1260.

(26) Ibid., p. 1262.

(27) Ibid., p. 1263.

(28) T. H. Chilton and A. P. Colburn, "Mass Transfer (Absorption) Coefficients," Ind. Eng. Chem., vol. 26 (1934), no. 11, pp. 1183-1187.

(29) A. P. Colburn, "Relation Between Mass Transfer (Absorption) and Fluid Friction," Ind. Eng. Chem., vol. 22 (1930), pp. 967-970.

(30) A. P. Colburn and O. A. Hougen, "Studies in Heat Transmission, II. Dehumidification," Ind. Eng. Chem., vol. 22, no. 5 (May 1930), p. 525.

(31) A. P. Colburn and D. G. Welsh, "Experimental Study of Individual Transfer Resistances in Countercurrent Liquid-Liquid Extraction," Transactions, American Institute of Chemical Engineers, vol. 38 (1942), p. 179.

(32) J. Crank, The Mathematics of Diffusion, Oxford University Press, London, England, 1956, p. 1.

(33) Ibid., pp. 1, 2.

(34) Ibid., p. 2.

(35) Ibid., p. 4.

(36) Ibid., p. 5.

(37) Ibid., p. 84.

(38) Harold S. Davis and George S. Crandell, "The Role of the Liquid Stationary Film in Batch Absorption of Gases, I. Absorptions Involving No Reversible Chemical Reactions," Journal of the American Chemical Society, vol. 52, no. 10 (October 1930), pp. 3757-3767.

(39) Ibid., p. 3764.

(40) J. Dlouchy and W. H. Gauvin, "Evaporation Rates in Spray Drying," Can. J. Chem. Eng., vol. 38 (August 1960), p. 113.

(41) F. G. Donnan and Irvine Masson, "The Theory of Gas Scrubbing Towers with Internal Packing," Journal of the Society of Chemical Industry, vol. 39, no. 14 (July 31, 1920), p. 236T.

(42) E. R. G. Eckert, Introduction to Transfer of Heat and Mass, McGraw-Hill Book Company, New York, N.Y., 1950.

(43) Ibid., p. 69.

(44) Ibid., p. 71.

(45) Ibid., pp. 128, 249.

(46) Ibid., p. 129.

(47) Ibid., p. 238.

(48) Ibid., p. 251.

(49) Ibid., p. 253.

(50) E. R. Elzinga, Jr. and J. T. Banchero, "Mass Transfer Coefficients for Heat Transfer to Liquid Drops," Chemical Engineering Process Symposium Series (Heat Transfer, Chicago), vol. 55, no. 29, pp. 149-161.

(51) Ibid., p. 149.

(52) Ibid., p. 151.

(53) Ibid., p. 152.

(54) Ibid., p. 154.

(55) Ibid., p. 155.

(56) Encyclopedia Britannica, 1962 ed. "Nernst, Walther Hermann," vol. 16, p. 229.

(57) A. Fage and H. C. H. Townend, "An Examination of Turbulent Flow with an Ultramicroscope," Proceedings, Royal Society, series A, vol. 135 (1935), p. 656.

(58) Gordon M. Fair and John C. Geyer, Elements of Water Supply and Water Waste Disposal, John Wiley and Sons, New York, N.Y., 1958, p. 504.

(59) Adolf Fick, "Ueber Diffusion," Annalen der Physik und Chemie, series 2, vol. 94 (1855), pp. 59-86.

(60) Adolf Eck, "On Liquid Diffusion," Phil. Mag., series 4, vol. 10 (July-December, 1855), pp. 30-39.

(61) S. K. Friedlander, "Mass and Heat Transfer to Single Spheres and Cylinders at Low Reynolds Numbers," Journal of the American Institute of Chemical Engineers, vol. 3, no. 1 (March 1957), pp. 43-48.

(62) N. Frossling, "Uber die Verdunstung Fallender Tropfen," Gerlands Beitrage fur Geophysik, vol. 52 (1938), pp. 170-216.

(63) Benjamin Gal-Or and H. E. Hoelscher, "A Mathematical Treatment on the Effect of Particle Size Distribution on Mass Transfer in Dispersions," J. Am. Inst. Chem. Engrs., vol. 12, no. 3 (May 1966), p. 499.

(64) W. H. Gauvin and L. B. Torobin, "Fundamental Aspects of Solid-Gas Flow. Part I: Introductory Concepts and Idealized Sphere Motion in Viscous Regime," Can. J. Chem. Eng., vol. 37 (August 1959), p. 129.

(65) W. H. Gauvin and L. B. Torobin, "Fundamental Aspects of Solid-Gas Flow. Part II: The Sphere Wake in Steady Laminar Fluids," Can. J. Chem. Eng., vol. 37 (October 1959), p. 167.

(66) W. H. Gauvin and L. B. Torobin, "Fundamental Aspects of Solid-Gas Flow. Part III: Accelerated Motion of a Particle in a Fluid," Can. J. Chem. Eng., vol. 37 (December 1959), p. 224.

(67) W. H. Gauvin and L. B. Torobin, "Fundamental Aspects of Solid-Gas Flow. Part IV: The Effects of Particle Rotation, Roughness and Shape," Can. J. Chem. Eng., vol. 38 (October 1960), p. 142.

(68) W. H. Gauvin and L. B. Torobin, "Fundamental Aspects of Solid-Gas Flow. Part V: The Effects of Fluid Turbulence on the Particle Drag Coefficient," Can. J. Chem. Eng., vol. 38 (December 1960), p. 189.

(69) S. Goldstein, ed. Modern Developments in Fluid Dynamics, (2 volumes), Oxford University Press, London, England, 1938.

(70) Ibid., pp. 50-54.

(71) Ibid., p. 120.

(72) Ibid., p. 132.

(73) Ibid., pp. 646, 647.

(74) R. M. Griffith, "Mass Transfer from Drops and Bubbles," Chem. Eng. Sci., vol. 12 (1960), pp. 198-213.

(75) Ibid., p. 198.

(76) Ibid., p. 202.

(77) Ibid., p. 203.

(78) Ibid., p. 204.

(79) Ibid., p. 208.

(80) E. A. Guggenhiem, "Surface Thermodynamics Progress Since Willard Gibbs," Surface Chemistry, special supplement to Research, Interscience Publishers, New York, N.Y., 1949.

(81) M. J. Hadamard, "Mouvement Permanent Lent D'une Sphere Liquide et Visqueuse Dans un Liquide Visqueux," Comptes Rendus, vol. 152 (1911), part 1, pp. 1735-1738.

(82) Handbook of Chemistry and Physics, forty fourth ed., Chemical Rubber Publishing Company, Cleveland, Ohio, 1963, p. 1708.

(83) A. E. Handlos and T. Baron, "Mass and Heat Transfer from Drops in Liquid-Liquid Extraction," J. Am. Inst. Chem. Engrs., vol. 3, no. 1 (March 1957), pp. 127-132.

(84) Ibid., p. 128.

(85) Ibid., p. 129.

(86) T. J. Hanratty, "Turbulent Exchange of Mass and Momentum with a Boundary, " J. Am. Inst. Chem. Engrs., vol. 2 (1956), no. 3, pp. 359-362.

(87) William D. Harkins, The Physical Chemistry of Surface Films, Reinhold Publishing Corporation, New York, N.Y., 1952, p. 8.

(88) Ibid., p. 94.

(89) Donald R. F. Harleman, "The Significance of Longitudinal Dispersion in the Analysis of Pollution in Estuaries," Proceedings of the Second International Water Pollution Research Conference, Tokyo, 1964, pp. 279-306.

(90) Peter Harriott, "A Review of Mass Transfer to Interfaces," Can. J. Chem. Eng., vol. 40 (April 1962), pp. 61-68.

(91) Ibid., p. 63.

(92) Ibid., p. 64.

(93) Ibid., p. 66.

(94) Ibid., pp. 66, 67.

(95) Ibid., p. 67.

(96) Ibid., p. 68.

(97) R. T. Haslam, R. L. Hershey, and R. H. Keen, "Effect of Gas Velocity and Temperature on Rate of Absorption," Industrial and Engineering Chemistry, vol. 16, no. 12 (December 1924), p. 1227.

(98) P. M. Heertjes, W. A. Holve, and H. Talsma, "Mass Transfer Between Isobutanol and Water in a Spray-Column," Chem. Eng. Sci., vol. 3 (1954), pp. 122-142.

(99) Ibid., p. 131.

(100) Ibid., p. 132.

(101) Ibid., p. 138.

(102) J. C. Henniker, "The Depth of the Surface Zone of a Liquid," Reviews of Modern Physics, vol. 21, no. 2 (April 1949), pp. 322-341.

(103) Ralph Higbie, "The Rate of Absorption of a Pure Gas Into a Still Liquid During Short Periods of Exposure," Trans., Am. Inst. Chem. Engrs., vol. 31, no. 2 (June 1935), pp. 365-389.

(104) T. W. Hoffman and W. H. Gauvin, "Evaporation of Stationary Droplets in High Temperature Surroundings," Can. J. Chem. Eng., vol. 38 (October 1960), pp. 129-131.

(105) Ibid., pp. 129, 130.

(106) Ibid., p. 130.

(107) T. J. Horton, T. R. Fritsch, and R. C. Kintner, "Experimental Determination of Circulation Velocities Inside Drops." Can. J. Chem. Eng., vol. 43 (June 1965), pp. 143-146.

(108) Ibid., p. 143.

(109) Ibid., p. 145.

(110) R. R. Hughes and E. R. Gilliland, "The Mechanics of Drops," Chemical Engineering Progress, vol. 48, no. 10 (October 1952), pp. 147-504.

(111) Ibid., p. 502.

(112) Ferdinand Hurter, "The Comparative Efficiency of Various Modes of Treating Liquids with Gases," J. Soc. Chem. Ind., vol. 4 (November 30, 1885), p. 639.

(113) Ferdinand Hurter, "The Comparative Efficiency of Various Modes of Treating Liquids with Gases," J. Soc. Chem. Ind., vol. 6 (November 30, 1887), p. 707.

(114) Ferdinand Hurter, "Coke Towers and Similar Apparatus," J. Soc. Chem. Ind., vol. 12 (March 31, 1893), p. 227.

(115) International Critical Tables, first ed., 1928, McGraw-Hill Book Company, New York, N.Y., vol. 3, p. 257.

(116) International Encyclopedia of Chemical Science, "Phase," Van Nostrand Company, Princeton, N.J., 1964, p. 888.

(117) L. E. Johns, Jr. and R. B. Beckmann, "Mechanism of Dispersed-Phase Mass Transfer in Viscous Single-Drop Extraction Systems," J. Am. Inst. Chem. Engrs., vol. 12, no. 1 (January 1966), pp. 10-16.

(118) Ibid., p. 10.

(119) Ibid., p. 11.

(120) Ibid., p. 12.

(121) A. I. Johnson and A. E. Hamielec, "Mass Transfer Inside Drops," J. Am. Inst. Chem. Engrs., vol. 6, no. 1 (March 1960), pp. 145-149.

(122) Ibid., p. 145.

(123) Ibid., p. 146.

(124) Ibid., pp. 146, 147.

(125) A. I. Johnson and A. E. Hamielec, "Viscous Flow Around Fluid Spheres at Intermediate Reynolds Numbers," Can. J. Chem. Eng., vol. 40 (April 1962), pp. 41-45.

(126) Ibid., p. 41.

(127) A. I. Johnson, D. M. Ward, O. Trass, and C. W. Bowman, "Mass Transfer from Fluid and Solid Spheres at Low Reynolds Numbers, Part I," Can. J. Chem. Eng., vol. 39 (February 1961), pp. 9-13.

(128) Ibid., p. 9.

(129) A. I. Johnson, D. M. Ward, and O. Trass, "Mass Transfer from Fluid and Solid Spheres at Low Reynolds Numbers, Part II," Can. J. Chem. Eng., vol. 40 (August 1962), pp. 164-168.

(130) Ibid., p. 164.

(131) R. B. Keey and J. B. Glen, "Mass Transfer from Solid Spheres," Can. J. Chem. Eng., vol. 42 (October 1964), pp. 227-232.

(132) Ibid., p. 227.

(133) Ibid., p. 228.

(134) R. C. Kintner, T. J. Horton, R. E. Graumann, and S. Amberkar, "Photography in Bubble and Drop Research," Can. J. Chem. Eng., vol. 39 (December 1961) pp. 235-241.

(135) Ibid., p. 237.

(136) M. Kishinevski and L. A. Mochalova, "Surface Resistance in Absorption Processes," Journal of Applied Chemistry of the U.S.S.R. (English translation), vol. 32 (May-August, 1959), p. 1039.

(137) R. Kronig and J. C. Brink, "On the Theory of Extraction from Falling Drops," Applied Scientific Research, vol. A2 (1950), pp. 142-154.

(138) Ibid., p. 154.

(139) Ibid., p. 144.

(140) Horace Lamb, Hydrodynamics, sixth ed., Dover Publications, New York, N.Y., 1945.

(141) Ibid., pp. 450-455, 473-475.

(142) Ibid., p. 590.

(143) Ibid., p. 600.

(144) J. Otis Laws, "Measurements of the Fall-Velocities of Water-Drops and Raindrops," Transactions, American Geophysical Union, (1941), pp. 709-721.

(145) J. B. Lewis, "The Mechanism of Mass Transfer of Solutes Across Liquid-Liquid Interfaces, Part I: The Determination of Individual Transfer Coefficients for Binary Systems," Chem. Eng. Sci., vol. 3 (1954), pp. 248-259.

(146) Ibid., p. 248.

(147) Ibid., p. 249.

(148) J. B. Lewis, "The Mechanism of Mass Transfer of Solutes Across Liquid-Liquid Interfaces, Part II: The Transfer of Organic Solutes Between Solvent and Aqeous Phases," Chem. Eng. Sci., vol. 3 (1954), pp. 260-278.

(149) J. B. Lewis, "The Mechanism of Mass Transfer of Solutes Across Liquid-Liquid Interfaces, Part III," Chem. Eng. Sci., vol. 8 (1958), pp. 295-308.

(150) J. B. Lewis and H. R. C. Pratt, "Oscillating Droplets," Nature, vol. 171 (June 27, 1953), p. 1155.

(151) W. K. Lewis, "The Principles of Counter-Current Extraction," J. Ind. Eng. Chem., vol. 8 (September 1916), p. 825.

(152) W. K. Lewis and W. G. Whitman, "Principles of Gas Absorption," Ind. Eng. Chem., vol. 16, no. 12 (December 1924), pp. 1215-1220.

(153) Ibid., pp. 1217, 1218.

(154) Ibid., p. 1219.

(155) C. S. Lin, R. W. Moulton, and G. L. Putnam, "Mass Transfer Between Solid Wall and Fluid Streams," Ind. Eng. Chem., vol. 45, no. 3 (March 1953), pp. 636-646.

(156) Ibid., p. 637.

(157) William O. Lynch and Clair N. Sawyer, "Effects of Detergents on Oxygen Transfer in Bubble Aeration," Journal of the Water Pollution Control Federation, vol. 32, no. 1 (January 1960), pp. 25-40.

(158) K. H. Mancy, J. J. McKeown, and D. A. Okun, "Effects of Surface-Active Agents on Bubble Aeration," Conference on Biological Waste Treatment, no. 12 (April 20-22, 1960).

(159) K. H. Mancy, D. A. Okun, and C. N. Reilley, "A Galvanic Cell Oxygen Analyzer," Journal of Electro-analytical Chemistry, vol. 4 (1962), pp. 65-92.

(160) Ibid., pp. 67, 68.

(161) Ibid., pp. 76-78.

(162) K. H. Mancy and W. C. Westgarth, "A Galvanic Cell Oxygen Analyzer," J.W.P.C.F., vol. 34 (1962), pp. 1037-1051.

(163) Ibid., pp. 1040-1045.

(164) Ibid., p. 1045.

(165) J. Marangozis and A. I. Johnson, "Mass Transfer With and Without Chemical Reaction," Can. J. Chem. Eng., vol. 39 (August 1961), pp. 152-158.

(166) James C. Maxwell, "Illustrations of the Dynamical Theory of Gases, Part II: On the Process of Diffusion of Two or More Kinds of Moving Particles Among One Another," Phil. Mag., series 4, vol. 20 (1860), pp. 21-33.

(167) Ibid., p. 22.

(168) James C. Maxwell, "Diffusion," The Scientific Papers of James Clark Maxwell, vol. 2 (2 volumes), W. D. Niven, ed., Dover Publications, New York, N.Y., pp. 625-646.

(169) Ibid., p. 627.

(170) Ibid., p. 628.

(171) McGraw-Hill Encyclopedia of Science and Technology, 1966 ed.,"Interface of Phases," vol. 7.

(172) R. J. Millington, "Diffusion Constant and Diffusion Coefficient," Science, vol. 122 (December 1955), pp. 1090, 1091.

(173) Walther H. Nernst, "Theorie der Reaktionsgeschwindigkeit in Heterogenen Systemen," Z. Physik. Chem. (Leipzig), vol. 47 (1904), p. 52.

(174) Albert B. Newman, "The Drying of Porous Solids: Diffusion and Surface Emission Equations," Trans. Am. Inst. Chem. Engrs., vol. 27 (1931), pp. 203-211.

(175) Arthur Noyes and Willis R. Whitney, "Ueber die Auflosungsgeschwindigkeit von Festen Stoffen in Ihren Eigenen Losungen," Z. Physik. Chem., vol. 23 (1897), p. 689.

(176) Wilhelm Nusselt, "Warmeubergang Diffusion und Verdunstung," Zeitschrift fur Angewandte Mathematik und Mechanic, vol. 10, no. 2 (April 1930), pp. 105-121.

(177) Clyde Orr, Jr., Particulate Technology, MacMillan Company, New York, N.Y., 1966, p. 457.

(178) J. H. Perry, ed., Chemical Engineer's Handbook, chapter 14, McGraw-Hill Book Company, New York, N.Y., 1942, p. 6-14.

(179) C. V. Raman and L. A. Ramdas, "On the Thickness of the Optical Transition Layer in Liquid Surfaces," Phil. Mag. and Journal of Science, series 7, vol. 3 (January-June 1927), p. 220.

(180) P. M. Rose and R. C. Kintner, "Mass Transfer from Large Oscillating Drops," J. Am. Inst. Chem. Engrs., vol. 12, no. 3 (May 1966), pp. 530-534.

(181) Ibid., p. 530.

(182) Ibid., pp. 530, 531.

(183) Ibid., p. 531.

(184) Hunter Rouse, Elementary Mechanics of Fluids, John Wiley and Sons, New York, N.Y., 1964, pp. 183-200.

(185) Ibid., p. 185.

(186) Hunter Rouse, ed., Advanced Mechanics of Fluids, John Wiley and Sons, New York, N.Y., 1959.

(187) R. S. Schechter and R. W. Farley, "Interfacial Tension Gradients and Droplet Behavior," Can. J. Chem. Eng., vol. 41 (June 1963), pp. 103-107.

(188) Ibid., p. 103.

(189) Ibid., p. 104.

(190) Ibid., pp. 103, 104.

(191) Ibid., p. 105.

(192) Ibid., p. 106.

(193) Hermann Schlichting, Boundary Layer Theory, Translated from German by J. Kestin, fourth ed., McGraw-Hill Book Company, 1960.

(194) Ibid., pp. 137-139.

(195) Ibid., p. 458.

(196) Ibid., p. 475.

(197) Ibid., p. 462.

(198) Ibid., p. 476.

(199) Ernst Schmidt, "Verdunstung und Warmeubergang," Gesundheits Ingenieur, vol. 52, no. 29 (July 20, 1929), pp. 525-529.

(200) K. L. Schulze, "Can Fish Farms Clean Our Polluted Waters?" Saturday Review, June 4, 1966, pp. 62-63.

(201) Thomas K. Sherwood, Absorption and Extraction, first ed., McGraw-Hill Book Company, New York, N.Y., 1937.

(202) Ibid., p. 3.

(203) Ibid., p. 5.

(204) Ibid., p. 7.

(205) Ibid., p. 189.

(206) Thomas K. Sherwood, "Mass Transfer and Friction in Turbulent Flow," Trans. Am. Inst. Chem. Engrs., vol. 36, (1940), p. 821.

(207) Thomas K. Sherwood and H. S. Bryant, Jr., "Mass Transfer Through Compressible Turbulent Boundary Layers," Can. J. Chem. Eng., vol. 35 (August 1957), p. 51

(208) S. Sideman and H. Shabtai, "Direct-Contact Heat Transfer Between a Single Drop and an Immiscible Liquid Medium," Can. J. Chem. Eng., vol. 42 (June 1964), pp. 107-117.

(209) Ibid., p. 107.

(210) Ibid., p. 108.

(211) Ibid., p. 109, 110.

(212) Ibid., p. 110.

(213) Ibid., p. 111.

(214) Ibid., p. 112.

(215) Ibid., p. 113.

(216) Ibid., p. 114.

(217) Standard Methods for the Examination of Water and Waste Water, eleventh ed., American Public Health Association, New York, N.Y., 1961, pp. 309-311.

(218) T. Takamatsu, M. Hiraoka, and K. Tanaka, "Simultaneous Heat and Mass. Transfer Between Gas and Liquid Phases, Part I: Analysis of Unsteady State Transfer," International Journal of Heat and Mass Transfer, vol. 7 (June 1964), pp. 621-630.

(219) G. Temple and W. G. Bickley, Rayleigh's Principle and Its Applications to Engineering, Oxford University Press, London, England, 1933, pp. 150-152.

(220) H. L. Toor and J. M. Marchello, "Film Penetration Model for Mass and Heat Transfer," J. Am. Inst. Chem. Engrs., vol. 4 (1958), no. 1, pp. 97-101.

(221) Robert E. Treybal, Liquid Extraction, second ed., McGraw-Hill Book Company, New York, N.Y., 1963.

(222) Ibid., p. 150.

(223) Ibid., p. 151.

(224) Ibid., p. 170.

(225) Ibid., p. 171.

(226) Ibid., p. 173.

(227) Ibid., p. 174.

(228) Ibid., p. 176.

(229) Ibid., p. 177.

(230) Ibid., p. 178.

(231) Ibid., p. 179.

(232) Ibid., p. 183.

(233) Ibid., pp. 183-186.

(234) Ibid., p. 186.

(235) Ibid., p. 188.

(236) Ibid., p. 189.

(237) W. B. VanArsdel, "The Theory of Gas-Scrubbing Towers with Internal Packing," Chemical and Metallurgical Engineering, vol. 23, no. 23 (December 8, 1920), pp. 1115, 1116.

(238) W. B. VanArsdel, "An Extension of the Theory of Gas Absorption Towers," Ch. Met. Eng., vol. 28, no. 20 (May 21, 1923), pp. 889-892.

(239) Van Nostrand's Scientific Encyclopedia, third ed., "Absorption," Van Nostrand Company, Princeton, N.J., 1958, p. 5.

(240) Ibid., "Solution(s) and Solubility," p. 1528.

(241) Walther G. Whitman, "A Preliminary Experimental Confirmation of the Two-Film Theory of Gas Absorption," Ch. Met. Eng., vol. 29 (1923), no. 4, pp. 146-148.

(242) Walther G. Whitman and D. S. Davis, "Comparative Absorption Rates for Various Gases," Ind. Eng. Chem., vol. 16, no. 12 (December 1924), p. 1235.

(243) Walther G. Whitman and J. C. Keats, "Rates and Absorption and Heat Transfer Between Gases and Liquids," J. Ind. Eng. Chem., vol. 14, no. 3 (March 1922), p. 186.

(244) C. R. Wilke, "Estimation of Liquid Diffusion Coefficients," Chem. Eng. Prog., vol. 45, no. 3 (March 1949), pp. 218-224.

(245) Ibid., p. 220.

(246) R. S. Willows and E. Hatschek, Surface Tension and Surface Energy and Their Influence on Chemical Phenomena, third ed., P. Blakiston's Son and Company, Philadelphia, Penn., 1923, p. 200.